# VAPB mediated Lipid Dysregulation and its role in the pathogenesis of Amyotrophic Lateral Sclerosis

विद्या वाचस्पति की
उपाधि की अपेक्षाओं की आंशिक पूर्ति में प्रस्तुत शोध प्रबंध

A thesis submitted in partial fulfillment of the requirements of the degree of Doctor of Philosophy

द्वारा / By
**लवलीन कुमार गर्ग / Lovleen Kumar Garg**

पंजीकरण सं. / Registration No.:
**२०१८२००४ / 20182004**

शोध प्रबंध पर्यवेक्षक / Thesis Supervisor:
**प्रोफेसर गिरीश रत्नपारखी / Professor Girish Ratnaparkhi**




भारतीय विज्ञान शिक्षा एवं अनुसंधान संस्थान पुणे
INDIAN INSTITUTE OF SCIENCE EDUCATION AND RESEARCH PUNE
**2026**

# CERTIFICATE

Certified that the work incorporated in the thesis entitled “VAPB mediated Lipid Dysregulation and its role in the pathogenesis of Amyotrophic Lateral Sclerosis”, submitted by Lovleen Kumar Garg was carried out by the candidate, under my supervision. The work presented here or any part of it has not been included in any other thesis submitted previously for the award of any degree or diploma from any other University or institution.

G S Ratnaparkhi

Prof. Girish Ratnaparkhi

Date: Feb 04, 2026

# DECLARATION

| | | |
|---|---|---|
| Name of Student | : | Lovleen Kumar Garg |
| Reg. No. | : | 20182004 |
| Thesis Supervisor | : | Prof. Girish Ratnaparkhi |
| Department | : | Biology |
| Date of joining program | : | August 01, 2018 |
| Date of Pre-Synopsis Seminar | : | November 26, 2025 |

Title of Thesis: **VAPB mediated Lipid Dysregulation and its role in the pathogenesis of Amyotrophic Lateral Sclerosis**

I declare that this written submission represents my idea in my own words and where others' ideas have been included; I have adequately cited and referenced the original sources. I declare that I have acknowledged collaborative work and discussions wherever such work has been included. I also declare that I have adhered to all principles of academic honesty and integrity and have not misrepresented or fabricated or falsified any idea/data/fact/source in my submission. I understand that violation of the above will be cause for disciplinary action by the Institute and can also evoke penal action from the sources which have thus not been properly cited or from whom proper permission has not been taken when needed.

The work reported in this thesis is the original work done by me under the guidance of **Prof. Girish Ratnaparkhi.**

Date: Feb 04, 2026



Signature of the student

**Dedicated to the loving memory of my sister**

**Shilpa Garg (1989-2013)**

# Acknowledgements

I am grateful to my Ph.D. supervisor, Prof. Girish Ratnaparkhi for giving me the opportunity to pursue research in his lab. His constant support, encouragement and the academic freedom he provided, helped me in developing independent thinking and intellectual growth. His scientific insights, critical thinking were crucial for shaping the thesis work. I have deepest gratitude for him to allow me pursuing the lipid metabolism project and his constructive feedback was instrumental in completion of the thesis. Also, I would like to acknowledge that he gave me the opportunity to explore national and international conferences which were independent of *Drosophila* field that widened my knowledge for the metabolism field. I would like to thank him that he put me on different projects which led me to contribute in different fields and enhanced my knowledge in various aspects of the neurodegeneration field.

I sincerely thank my Research Advisory Committee members, Prof. Siddhesh Kamat and Dr. Raghav Rajan for their valuable guidance and constant support throughout the journey. Their insightful comments and critical evaluations significantly strengthened the scientific rigor of this work. I also would like to mention that Prof. Siddhesh was involved in establishing this project in the lab as a collaborator for which I am really grateful. I express my gratitude to Prof. Raghu Padinjat, NCBS Bangalore as my external examiner during the comprehensive seminar and I would like to thank him also for providing the reagents when needed.

I am deeply grateful from the bottom of heart to my official mentor Kriti Chaplot and unofficial mentor Shweta Tendulkar for their dedicated mentoring, guidance and unwavering support during my journey. They played a crucial role in the initial training, introduction to *Drosophila* genetics, data analysis and scientific thinking. Their patience, approachability, and willingness to engage in detailed discussions greatly enhanced my confidence and independence as a researcher. I am really thankful to them as they established the platform for the lipid project which made my journey fruitful and exciting. Also, they were always there for me whenever I needed their guidance even after leaving the lab that helped me in the completion of my Ph.D. I also sincerely thank Senthil for his meticulous preparation of fly reagents. I would like to thank Kundan, Shweta and Kriti for suggesting the changes in the thesis.

I humbly acknowledge Dr. Jomon Joseph and Dr. Gaurav Das from NCCS, Pune for their collaboration and contributions to my work. Their expertise, discussions and scientific thinking helped me in the interpretation of the study. I also thank Prof. Richa Rikhy, Dr. Anuradha Ratnaparkhi and Dr. Girish Deshpande for their valuable inputs and constructive suggestions at various stages of this research. I am particularly thankful to Dr. Girish Deshpande for his presence in the lab meetings and engaging in informal discussions, which provided clarity, motivation, and critical perspectives that strengthened this work. I want to specifically thank Prof. Thomas Pucadyil who introduced me to the field of lipids. His way of thinking and precise observations helped me in developing the mindset which is required for research. He also helped me in developing a habit of constant reading about the field which strengthened my work to next level. I would like to thank Dr. Suhita Nadkarni for allowing me to work in her lab as semester project student. I learnt a lot about computational work during my time which helped me in developing the skills for image analysis later.

I acknowledge all the funding agencies which supported my academic and research journey. I extend my gratitude to IISER Pune, CSIR for providing the fellowship in a timely manner and EMBO, ANRF-SERB, Infosys for providing the travel grants which enabled me to attend international conferences, present my research and engage with the scientific community.

The support of the Biology Office and the Biology Department for providing a conducive academic and administrative environment has been instrumental throughout my dual degree program. I am grateful to the fly facility staff, especially Yashwant, Snehal, and Ashwini, for their technical assistance and consistent support. I also thank the microscopy facility, particularly Santosh and Vijay, for their help with imaging and instrumentation. I extend my appreciation to the IISER academic staff and the housekeeping staff for their essential contributions in maintaining a smooth, efficient, and supportive research environment.

I would like to thank my current lab members—Namrata, Sanhita, Alex, Amrita, Kanika, Saubhagya, Adheena and Karthik—for their support, engaging discussions during lab meetings, and for creating a positive work environment. I am also grateful to the past lab members—Bhagyashree, Amar, Kriti, Shweta, Prajna, Sushmitha, Aparna, Kundan, Subhradip, Neel, Jyothish, Aarti, Akshata, Vidyadheesh and Pulkit—for their valuable inputs, informal scientific discussions, and for making the lab a lively space through lab parties and chai-time

conversations that made both masters and Ph.D. journey enjoyable. I would like to specially mention Shweta, Prajna and Kundan for all the fun parties that created some wonderful moments during the initial years of the lab.

I thank the members of Richa's lab—Bhavin, Dnayanesh, Debasmita, Sameer, Somya, Harsh, Rahul, and Shashwat—and Siddhesh's lab—Karthik, Arnab, Ojal, Aakash, Kaveri, and Sonali—for making my time memorable during New Year parties. I am especially grateful to the members of Thomas's lab, with Soumya as a mentor, along with Megha, Sukrut and Gregor, for their help with experiments, insightful discussions, and for fostering a friendly environment through informal interactions.

I sincerely thank my batchmates—Dhruv, Saurabh, Ritwik, Sajid, Megha, Shikha, Karthik, Rathi, Sandra, Anant, and Subhayan—for making this journey memorable. Their companionship, encouragement, and camaraderie during trips, birthday celebrations, and other shared experiences have made the MS and PhD experience not only rewarding academically but also rich with friendship and lasting memories. The laughter, support, and shared adventures with them have been an integral and cherished part of this journey.

I would like to express my heartfelt gratitude to Team Lohri and the Punjabi community at IISER, which we started in 2021, for their enthusiasm, dedication, and collaborative spirit. Special thanks to Priya, Anant, Dhruv, Saurabh, Piyush, Chitvan, Pujith, Shivesh, Ajay, Arnav and Khushi for their help in organizing the events and for keeping the Punjabi spirit alive on campus. Your energy, teamwork, and creativity made these celebrations memorable and fostered a sense of community. I sincerely hope that this tradition continues to thrive in the coming years, inspiring future students to participate and carry forward this vibrant legacy.

I am deeply grateful to my friends—Dhruv, Saurabh, Priya, Bhoomi, and Sushant—for their constant support, companionship, and many unforgettable moments we shared throughout my PhD journey. Their presence during trips, hostel parties, and birthday celebrations added immense joy and balance to the rigorous demands of research. Beyond the celebrations, their encouragement, understanding, and willingness to listen during challenging times provided me with emotional strength and motivation. The laughter, shared experiences, and candid conversations with them created memories that I will cherish forever. Their friendship has truly enriched both my personal life and this academic journey.

Big shoutout for my hostel friends—Dhruv, Pranjal, Praghal, Darshan, Ajinkya, Arnab, Hitendra, Prajjwal, and Saurabh—for their constant support and companionship throughout my PhD journey. Their presence made hostel life enjoyable and helped me navigate challenging times, including the quarantines, by keeping spirits high and making every moment memorable. Their readiness to help, share experiences, and stand by me in both difficult and joyful moments has been a source of strength and comfort. I deeply cherish their friendship and the positive impact they have had on my personal and academic life. I am especially grateful to Dhruv for providing the display screen which played a huge role in the analysis of my work and writing papers along with thesis.

I am deeply grateful to my Bachelor's friends Rahul, Digvijay, Rishabh for their unwavering support, and friendship throughout my Integrated PhD journey. I especially thank Simran for always being there for me, for the countless trips we took together, and for exploring cafes and new experiences, making even ordinary days memorable. Lavleen deserves my heartfelt thanks for always being just a call away whenever I needed guidance, encouragement, or simply someone to talk to; her constant support has been a source of immense comfort. I am also thankful to Nikita for being a supportive and understanding friend, for sharing laughter, and for always being willing to listen. Vaishali has been incredibly helpful both academically and personally—assisting with reagents, supporting experiments, and always being ready to help whenever required. The friendships I have built with them have provided balance, joy, and a sense of belonging, enriching my life beyond the academic realm.

I am sincerely thankful to my school principal, late Mr. Mehta, for his guidance and encouragement during my formative years, which laid the foundation for my academic pursuits. I also extend my heartfelt gratitude to Prof. Kashmir Singh and Prof. Deshdeepak Singh at the Panjab University for their constant guidance, mentorship, and for providing recommendations whenever required. Their support has been invaluable in shaping both my academic and professional journey.

I am profoundly grateful to my family—my mother and father along with elder sister moniya—for their patience, understanding, and unwavering support throughout this long and challenging journey. Their constant encouragement and belief in me have been a source of strength and motivation, helping me overcome both academic and personal challenges. I also wish to

acknowledge my relatives and friends who generously supported me financially whenever needed, ensuring that I could focus on my research without worry. Finally, I am deeply thankful to my beloved Lucy, whose smile and presence have been a constant source of joy, comfort, and inspiration, reminding me to keep moving forward even in difficult times. The love, support, and care from all of them have been invaluable, and I dedicate this achievement to their unwavering presence in my life.

Finally, I would like to acknowledge myself for persevering through moments of sorrow, struggle, and uncertainty, for finding the courage to keep moving forward even when the path seemed unclear and hope seemed distant. I am grateful for the resilience, patience, and determination that allowed me to continue despite challenges and setbacks. I also wish to express my gratitude to Lord Shiva and Guru Nanak for providing me with inner strength, guidance, and the faith to endure difficulties, inspiring me to remain steadfast and committed throughout this journey. Their blessings have been a constant source of courage and motivation.

During the struggles of my Ph.D. journey, I gained a talent of writing which helped me remain calm and composed. Here, I am writing one of those poems which may inspire coming students as well when their crosses may not work, their blots might fail or they may not get the results what they wished for, but in the end everything falls into the right place as Girish says.

**वक्त तो दे वक्त को गु.जरने के लिए , धीरे धीरे बीत जाएगा।**

**तू सबर् तो रख मेरे दोस्त, तेरा बुरा वक्त भी एक पल में बीत जाएगा।।**

**~Lovleen Garg**

# Table of Contents

*List of Figures*…….…….....(i)

*List of Tables*……(iv)

*Abbreviations*…….……...(v)

*Synopsis*……...…..……..(viii)

*Publications*/Manuscripts...……..(xi)

***Chapter I*: Lipid metabolism at the crossroads of neurodegeneration?**

1.1 ABSTRACT……..……....…….……...1

1.2 INTRODUCTION……..……..……..……..……...1

**1.2.1 Lipids- Classification, Structure and Functions…….....……...….1**

**1.2.2 Lipid Droplets (LDs)-Structure and Functions…….……..…….……....6**

**1.2.3 Role of lipids in neurodegeneration…….……...…..……7**

**1.2.4 Amyotrophic Lateral Sclerosis (ALS)…….…….……8**

**1.2.5 Lipid homeostasis in ALS……10**

**1.2.6 *Drosophila* models of ALS disease...……13**

1.3 OPEN QUESTIONS…….……...14

1.4 REFERENCES…….…….……...…16

***Chapter II*: Introduction to VAPB and In Silico Prediction of *Drosophila* VAP interactors**

2.1 ABSTRACT……..……..…….30

2.2 INTRODUCTION……..……..……31

**2.2.1 VAPB- Structure and Functions…….31**

**2.2.2 VAPA and VAPB physical interactors……...31**

**2.2.3 VAP roles in *Drosophila*……...…...33**

2.3 RESULTS……...……..……...…….……35

**2.3.1 *Drosophila* homologs of Human VAPA and VAPB interactors……...….35**

**2.3.2 *Drosophila* VAP interactors……...……..40**

**2.3.3 Prediction of *Drosophila* VAP interactome……..…..…….42**

2.4 DISCUSSION……...……..…….……45

**2.4.1 *Drosophila* as a model to study VAP roles…….……...….45**

**2.4.2 *Drosophila* VAP roles in the nervous system…….…45**

2.5 LIMITATIONS AND CONCLUSION……...…….45

2.6 MATERIALS AND METHODS……..……...…46

**2.6.1 Database and websites……46**

2.7 REFERENCES……...……...……...…47

***Chapter III*: Lipid imbalance in Amyotrophic Lateral Sclerosis 8/*ALS8* model uncovers VAPB role in LD homeostasis**

3.1 ABSTRACT……...…….……...…..52

3.2 INTRODUCTION……..……...…….…….52

**3.2.1 Role of VAPB in lipid transport……...……...52**

**3.2.2 *VAPB* as an *ALS8* locus……53**

**3.2.3 LDs in cellular homeostasis and disease…….……..…54**

**3.2.4 Lipid homeostasis in *Drosophila ALS8* model……54**

3.3 RESULTS……...……..……56

**3.3.1 Age dependent LC-MS based lipid profiling of *ALS8* flies' brain……56**

**3.3.2 Age dependent LD distribution in *ALS8* model…….……58**

**3.3.3 Rescue of LD homeostasis with *VAP*$^{WT}$ in *ALS8* model…….62**

**3.3.4 Role of VAP in LD homeostasis……...……65**

**3.3.5 *VAP*$^{P58S}$ affects glial LD homeostasis in a genomic model of *ALS8*……...69**

**3.3.6 Removal of *VAP*$^{P58S}$ from glia rescues *ALS8* climbing ability……71**

**3.3.7 Lowering CE levels in neurons improves motor function of *ALS8* flies……..…74**

3.4 DISCUSSION……..…76

**3.4.1 Cholesterol imbalance in *Drosophila ALS8* adult brains……..76**

**3.4.2 VAP role in LD homeostasis……76**

**3.4.3 *VAP* knockdown positively regulates LDs……..……77**

**3.4.4 *VAP* overexpression negatively affects LD homeostasis……77**

**3.4.5 *Drosophila VAP*$^{P58S}$ negatively regulates LDs……..……..77**

3.5 CONCLUSION……78

3.6 MATERIALS AND METHODS…….79

**3.6.1 *Drosophila* husbandry, fly stocks and reagents……..79**

**3.6.2 Lipid extraction and targeted LC-MS lipidomics……..…79**

**3.6.3 Lipid Droplet staining for larval and adult brains……....……79**

**3.6.4 Microscope imaging and analysis……....80**

**3.6.5 Climbing Assay……..…81**

**3.6.6 Software/Applications……..82**

3.7 CONTRIBUTIONS…….82

3.8 ACKNOWLEDGEMENTS…….82

3.9 REFERENCES……83

***Chapter IV*: Sphingolipid dysregulation and Ceramide Transfer role in *ALS8* pathogenesis**

4.1 ABSTRACT…….90

4.2 INTRODUCTION……..……...90

**4.2.1 Introduction to Sphingolipids…….90**

**4.2.2 Sphingolipids in the nervous system……...…91**

**4.2.3 Introduction to CERT……..91**

**4.2.4 Sphingolipids role in *ALS8 Drosophila* model……92**

4.3 RESULTS……...……93

**4.3.1 Sphingolipids are altered in a *Drosophila* model of *ALS8*…….…93**

**4.3.2 Generation and validation of *CERT* transgenic lines……93**

**4.3.3 Tissue specific modulation of *CERT* in *ALS8* flies……96**

**4.3.4 Impact of blocking ceramide synthesis on motor function in *ALS8* males…….98**

**4.3.5 Blocking ceramide synthesis or transfer in adult stage delays progression of *ALS8*……100**

**4.3.6 Reducing Fatty acyl CoA availability in neurons improves *ALS8* motor function……..……..102**

4.4 DISCUSSION……104

**4.4.1 Ceramides and its derivatives are elevated in *ALS8* model…….....104**

**4.4.2 Reducing sphingolipid levels in the neurons improve motor function of *VAP$^{P58S}$* animals……104**

**4.4.3 Increased lipid production in neurons contribute to the progression of ALS disease……..…105**

4.5 CONCLUSION……..……..…106

4.6 MATERIALS AND METHODS…….....107

**4.6.1 *Drosophila* husbandry, fly stocks and reagents……107**

**4.6.2 Lipid extraction and targeted LC-MS lipidomics……107**

**4.6.3 Cloning and generation of *CERT* transgenic lines……...…107**

**4.6.4 Real Time PCR……...108**

**4.6.5 Drug feeding…….....…108**

**4.6.6 Statistical tests…….……...108**

**4.6.7 Software/ Applications……..108**

4.7 CONTRIBUTIONS……...108

4.8 ACKNOWLEDGEMENTS……...…108

4.9 REFERENCES……...…109

***Chapter V*: Glial ceramide orchestrates LD homeostasis and motor function of *Drosophila***

5.1 ABSTRACT……...…116

5.2 INTRODUCTION…….……116

**5.2.1 Ceramides and their roles……..……116**

**5.2.2 Ceramide dysregulation in the brain……..……..117**

**5.2.3 CERT role in *Drosophila* physiology……117**

5.3 RESULTS……..119

**5.3.1 A reverse genetic screen for motor function in the Ceramide pathway……119**

**5.3.2 LD homeostasis in Glia is sensitive to ceramide levels…….……121**

**5.3.3 Lack of Ceramide Transfer leads to age-dependent motor dysfunction……123**

**5.3.4 Lack of Ceramide Transfer perturbs LD homeostasis……124**

**5.3.5 Lack of glial *CERT* leads to age-dependent motor defects in *Drosophila*……..126**

**5.3.6 Lack of glial Ceramide Transfer leads to LD defects in the adult brain……129**

**5.3.7 Motor function can be rescued by transgenic glial CERT……..……131**

**5.3.8 LD dynamics can be rescued by glial expression of CERT……..…132**

**5.3.9 Glial ceramide in *Drosophila* development regulates adult motor function……...134**

5.4 DISCUSSION……136

**5.4.1 Lipid homeostasis in Motor neuron disorders…….…….136**

**5.4.2 Differential role of ceramides in neurons and glia…….……..136**

**5.4.3 CERT function in the glia……...…137**

**5.4.4 Ceramide connection to LD homeostasis……...…138**

5.5 CONCLUSION……...…139

5.6 MATERIALS AND METHODS……...…140

**5.6.1 *Drosophila* husbandry, fly stocks and reagents……140**

**5.6.2 Statistical tests……140**

**5.6.3 Software/ Applications……...140**

5.7 CONTRIBUTIONS……...140

5.8 ACKNOWLEDGEMENTS……...140

5.9 REFERENCES……..141

***FUTURE DIRECTIONS*.....147**

*Appendix I:* **Balancing and validation of fly reagents**

I.1 INTRODUCTION…….……149

I.2 RESULTS AND DISCUSSION……..……...150

**I.2.1 Addition of balancers and tissue specific Gal4s in CRISPR *VAP$^{P58S}$* fly line……...150**

**I.2.2 Recombination of *Gal80$^{ts}$* to the *VAP$^{P58S}$* line and its validation…….…….152**

**I.2.3 Addition of Tissue specific Gal4 lines to *Gal80$^{ts}$, VAP$^{P58S}$ Drosophila*…….…...…153**

I.3 REFERENCES……...…158

*Appendix II:* **Role of Peptidyl Prolyl Isomerases in the aggregate dynamics of *ALS8* model**

II.1 INTRODUCTION…….160

II.2 RESULTS AND DISCUSSION……161

**II.2.1 Differential aggregate dynamics of *cis-trans* Proline present in VAP protein…….161**

**II.2.2 PPIase screening for identifying potential modifiers involved in $VAP^{P58S}$ folding…….162**

II.3 MATERIALS AND METHODS…….…….....165

**II.3.1 Fluorescent Recovery After Photobleaching……..165**

**II.3.2 Larval brain immunostaining and aggregate analysis……..…165**

II.4 CONTRIBUTIONS……...166

II.5 REFERENCES……..166

*Appendix III:* **Role of autophagy in the pathogenesis of *ALS8* model of *Drosophila***

III.1 INTRODUCTION……...168

III.2 RESULTS AND DISCUSSION……..169

**III.2.1 *ALS14/TER94* modulation in neurons enhances the motor phenotype of *ALS8*…….169**

**III.2.2 *TER94* KD in neurons shows a novel upward halt wing phenotype in *Drosophila*…….170**

**III.2.3 *Atg1* KD in neurons impairs motor function of rescued *ALS8* flies……..171**

III.3 REFERENCES……172

# List of Figures

*Chapter I:* **Lipid metabolism at the crossroads of neurodegeneration**

1.1: Molecular structure of different lipid species which play major roles in the brain…….5

1.2: Pathological hallmarks and Genes associated with Amyotrophic Lateral Sclerosis……....10

*Chapter II:* **Introduction to VAPB and In Silico Prediction of *Drosophila* VAP interactors**

2.1: Schematic diagram of VAPB roles in the cellular homeostasis…….……33

2.2: *Drosophila* VAP roles in lipid transfer at ER-Golgi network……34

*Chapter III:* **Lipid imbalance in ALS8 model uncovers VAPB role in LD homeostasis**

3.1: Age dependent lipid profiling of *Drosophila* adult brains……57

3.2: BODIPY stained LD distribution in the adult brain of *Drosophila*……..58

3.3: Perturbation of LD homeostasis in the adult brain of *ALS8* model…….....60

3.4: Quantitation of LDs present in the adult brain of *ALS8* flies……61

3.5: Single copy of $VAP^{WT}$ partially restores LD homeostasis in *ALS8* flies……..63

3.6: Quantitation of LDs restoration by $VAP^{WT}$ in ALS8 flies……64

3.7: Glial *VAP* modulation affects LD homeostasis in *Drosophila* larval brain…….65

3.8: Glial loss of *VAP* leads to more LDs with smaller size in the *Drosophila* adult brain……67

3.9: More *VAP* in glia negatively affects LD homeostasis in the adult brain…….68

3.10: *VAP* KD rescues LD homeostasis in the glia of *ALS8* flies……..70

3.11: *VAP* modulation in glia at adult stage affects LDs in *ALS8* brains…….72

3.12: $VAP^{P58S}$ removal in adult glia rescues *ALS8* climbing ability……...73

3.13: Genetic KD of *CG8112* in neurons improves motor function in *ALS8* model……..75

3.14: Schematic model of VAP role in LD homeostasis…….78

*Chapter IV:* **Sphingolipid dysregulation and Ceramide Transfer role in ALS8 pathogenesis**

4.1: Age dependent sphingolipid profiling of *ALS8* brains……94

4.2: Validation of *CERT* transgenic fly lines……..95

4.3: Motor function of *ALS8* flies after *CERT* modulation in neurons, glia and muscles……97

4.4: Tissue specific role of ceramide synthesis in *ALS8* motor dysfunction……99

4.5: Lowering ceramides in the neurons at adult stage delays $VAP^{P58S}$ motor defects……...101

4.6: KD of *bmm and ACAT1* in the neurons at adult stage rescues motor dysfunction of *ALS8*…103

4.7: Lipid accumulation in neurons contributes to the progression of ALS disease……....106

*Chapter V:* **Glial ceramide orchestrates Lipid Droplet homeostasis and motor function of *Drosophila***

5.1: Motor assay screen for enzymes involved in *de novo* ceramide synthesis……..120

5.2: Effect of glial ceramide pathway gene KD on LD distribution in the *Drosophila* adult brain…….122

5.3: C*ERT* loss in *Drosophila* has age dependent motor dysfunction……..124

5.4: *CERT* loss in *Drosophila* perturbs LD homeostasis in the adult brain ……125

5.5: Tissue-specific *CERT* role in motor function……127

5.6: $CERT^{EAAD}$ OE in neurons and glia does not affect motor function of *Drosophila*…….128

5.7: Glial *CERT* affects LD dynamics in the *Drosophila* adult brain……130

5.8: Glial expression of *CERT* rescues motor dysfunction in $CERT^{\Delta}$……..132

5.9: Glial expression of *CERT* rescues LD defects seen in $CERT^{\Delta}$…….133

5.10: Developmental role of glial ceramide is crucial for motor activity of *Drosophila*……..135

5.11: Schematic model of ceramide and CERT roles in neurons and glia…….139

*Appendix- I:* **Balancing and validation of fly reagents**

I.1: Schematic diagram of adding balancer chromosomes to the CRISPR *VAP$^{P58S}$*……150

I.2: Schematic diagram of adding tissue specific Gal4 drivers to the CRISPR *VAP$^{P58S}$*……151

I.3: Validation of CRISPR *VAP$^{P58S}$* fly line containing tissue specific Gal4 drivers…….151

I.4: Schematic diagram of recombining *Gal80$^{ts}$* to the CRISPR *VAP$^{P58S}$*…….152

I.5: Validation of CRISPR *VAP$^{P58S}$* fly line recombined with *Gal80$^{ts}$*…….153

I.6: Schematic diagram of adding tissue specific Gal4 drivers to the *VAP$^{P58S}$*, *Gal80$^{ts}$*…….154

*Appendix- II:* **Role of Peptidyl Prolyl Isomerases in the aggregate dynamics of *ALS8* model**

II.1: FRAP experiment for understanding protein movement in VAP proline mutations..……..162

II.2: Modulating PPIase affects VAP$^{P58S}$ aggregates in 3$^{rd}$ instar larval brain……..….163

II.3: Quantitation for aggregate density on modulation of PPIases in *VAP$^{P58S}$*……...…..…163

*Appendix- III:* **Role of autophagy in the pathogenesis of *ALS8* model of *Drosophila***

III.1 Impact of modulating *TER94* in the neurons on the motor function of *ALS8* flies……...169

III.2 Knockdown of *TER94* in neurons of *ALS8* shows upward halt wing phenotype……170

III.3 Removal of Atg1 in the neurons of rescued *ALS8* females leads to motor impairment……...171

# List of Tables

*Chapter I:* **Lipid metabolism at the crossroads of neurodegeneration**

1.1: Lipid levels detected in various samples of ALS patients or animal models……..…12

*Chapter II:* **Introduction to VAPB and In Silico Prediction of *Drosophila* VAP interactors**

2.1: List of VAPA/B interactors in *Homo sapiens* and their orthologs in *Drosophila*……..….35

2.2: *Drosophila* VAP interactors and their homologs in *Homo sapiens*……40

2.3: List of VAP interactors representing Type I FFAT motif prediction……...…43

2.4: List of VAP interactors representing Type II FFAT motif prediction…….43

2.5: List of VAP interactors representing Type III FFAT motif prediction…….44

2.6: List of VAP interactors representing Type IV FFAT motif prediction……44

*Chapter V:* **Glial ceramide orchestrates Lipid Droplet homeostasis and motor function of *Drosophila***

5.1 Genes of the *Drosophila* Ceramide pathway screened for adult motor function…….119

*Appendix- I:* **Balancing and validation of fly reagents**

I.1: List of the fly lines balanced and recombined in the lab……..154

*Appendix- II:* **Role of Peptidyl Prolyl Isomerases in the aggregate dynamics of *ALS8* model**

II.1: List of PPIases along with Gene ID and KD/OE line used for the study……164

# Abbreviations

AA- Amino acid

ACAT1/2- Acetyl-CoA acetyltransferase 1/2

ACAT-Acetyl-CoA: Cholesterol acyl transferase

ACBD4/5- Acyl-CoA Binding Domain Containing 4/5

AGPAT- 1-acyl-sn-glycerol-3-phosphate acyltransferase

AL- Antennal Lobe

ALS- Amyotrophic Lateral Sclerosis

ALS8- Amyotrophic Lateral Sclerosis 8

ApoE- Apolipoprotein E

APP- Amyloid Precursor Protein

Atg1- Autophagy Intiation factor 1

ATGL- Adipocyte Triglyceride Lipase

BDSC- Bloomington *Drosophila* Stock Center

Bmm- Brummer

BSA- Bovine Serum Albumin

C-1-P- Ceramide -1-Phosphate

C9ORF72- Chromosome 9 Open Reading Frame 72

CCD- Coiled Coil Domain

CERS- Ceramide Synthase

CERT1- Ceramide Transfer 1

CEs- Cholesterol Esters

CHCl3- Choloroform

CPE- Ceramide Phosphoethanolamine

CPES- Ceramide Phosphoethanolamine Synthase

CsA- Cyclosporin A

CSF- Cerebrospinal Fluid

Cyp-1- Cyclophillin 1

DAGs- Diacylglycerols

DGATs-Diacylglycerol Acyltransferases

DMSO- Dimethyl Sulfoxide

EAAT2- Excitatory Amino Acid Transporter 2

Elav- Embryonic Lethal, Abnormal Vision

ER- Endoplasmic Reticulum

FAF1- Fas Associated Factor 1

fALS- Familial ALS

FAPP2- Four Adaptor Phosphate Protein 2

FASN-Fatty Acid Synthase

FDA- Food and Drug Administration

FDR- False Discovery Rate

FFAs- Free Fatty Acids

FFAT- Phe-Phe Acidic Tract

FKBP- FK506 Binding Protein

FRAP- Fluorescence Recovery After Photobleaching

FUS- Fused in Sarcoma

GBA1- Glucocerebrosidase

GFP –Green Fluorescent Protein

GPAT- Glycerol-3-phosphate acyltransferase

GPLs- Glycerophospholipids

GSLs- Glycosphingolipids

*gVAP*$^{P58S}$- *VAP*$^{P58S}$ allele under genomic promotor of endogenous *VAP*

*gVAP*$^{WT}$- *VAP*$^{WT}$ allele under genomic promotor of endogenous *VAP*

HSAN1- Hereditary Sensory and Automatic Neuropathy 1

HSP- Hereditary Spastic Paraplegia

IFC- Infertile crescent

iPSCs- Induced Pluripotent Stem Cells

JNK- c-Jun N-terminal Kinase

KD- Knockdown

KDSR- 3-ketodihydrosphingosine reductase

LC-MS- Liquid Chromatography- Mass Spectrometry

LDs- Lipid Droplets

LTPs- Lipid Transfer Proteins

MAGs- Monoacylglycerols

MAM- Membrane Associated Mitochondria

MCS- Membrane:membrane contact site

Me-OH- Methanol

MHC- Myosin Heavy Chain

MIGA2- Mitoguardian 2

MIP- Maximum Intensity Projection

MNDs- Motor neuron disorders

MOSPD1/2/3- Motile Sperm Containing Domain Protein 1/2/3

MSP- Major Sperm Protein

NFkB- Nuclear Factor kappa-light chaini enhancer of activated B cells

NMJ- Neuro muscular junction

nSyb- Neuronal Synaptobrevin

OE- Overexpression

ORP2- OSBP Related Protein 2

ORP8- OSBP Related Protein 8

OSBP- Oxysterol Binding Protein

PA- Phosphatidic Acid

PBS- Phosphate Buffer Saline

PC- Phosphatidylcholine

PE- Phosphatidylethanolamine

PFA- Paraformaldehyde

PGC-1α- Peroxisome proliferator –activated receptor gamma coactivator 1- alpha

PG-Phosphatidylglycerol

PI- Phosphatidylinositol

PI4P- Phosphatidylinositol-4-Phosphate

PITPNM1/2/3- Phosphatidylinositol Transfer Protein, Membrane-Associated 1/2/3

PLs- Phospholipids

PS- Phosphatidylserine

PSLs- Phosphosphingolipids

PTPIP51- Protein Tyrosine Phosphatase Interacting Protein 51

PPIases – Peptidyl Prolyl Isomerases

PUFAs- Poly Unsaturated Fatty Acids

RdgB- Retinal degeneration B

Repo- reverse polarity

ROI- Region of Interest

ROS- Reactive Oxygen Species

RT-PCR- Real time Polymerase Chain Reaction

S1P-Sphingosine-1-Phosphate

Sac1- Suppressor of Actin 1

sALS- Sporadic ALS

SEM- Standard Error Mean

SEZ- Suboesophageal zone

SING- Startle Induced Negative Geotaxis

SLs- Sphingolipids

SMs- Sphingomyelins

SOAT- Sterol O-Acyltransferase

SOD1- Superoxide Dismutase 1

Spen- split ends

SPT-1/II- Serine Palmitoyltransferase- I/II

SREBPs-Sterol regulatory element-binding proteins

STARD3- StAR Related Lipid Transfer Domain 3

STING- Stimulator of Interferon Genes

SVZ- Sub-ventricular zone

TAGs- Triacylglycerols/Triglycerides

TCA-Tri Carboxylic Acid

TDP43- TAR DNA binding Protein 43

TMD- Transmembrane Domain

TOR- Target of Rapamycin

TER94- Transitional Endoplasmic Reticulum 94

UAS- Upstream Activated Sequence

ULK1- Unc-51-Like autophagy activating Kinase 1

UPR- Unfolded Protein Response

VAMP- Vesicle Associated Membrane Protein

VAP-33/VAP- *Drosophila* VAP-33

VAPA- VAMP Associated Protein A

VAPB- VAMP Associated Protein B

$VAP^{P56S}$- Human *VAPB* allele, *ALS8*

$VAP^{P58S}$- *Drosophila ALS8* allele

$VAP^{WT}$- *Drosophila* wildtype VAP

VCP- Valosin Containing Protein

VDRC- Veinna *Drosophila* Resource Center

VPS13A/B/C/D- Vacuolar Protein Sorting A/B/C/D

## Synopsis

Lipids play an indispensable role in the cellular architecture and signaling via membrane organization, intracellular trafficking, energy metabolism and regular organelle maintenance. In the central nervous system, lipid metabolism is crucial due to high metabolic demand, constant membrane reorganization and limited neuronal regenerative capacity. Also, neurotransmission requires myelination of the axons for the fast neurotransmission. Major lipid classes like sterols, sphingolipids and phospholipids govern synaptic transmission, neuron-glia cross talk and vesicle trafficking. Emerging evidence from the past two decades has established lipid dysregulation as a major contributor to the neurodegenerative disorders where altered lipid species, defective lipid transport and lipid accumulation intersect with mitochondrial dysfunction, ER stress, neuroinflammation and unfolded protein response (UPR).

Amyotrophic Lateral Sclerosis (ALS) is a fatal late onset motor neurodegenerative disease characterized by the loss of both upper and lower motor neurons leading to gradual paralysis due to the weakening of muscles. Most of the ALS patients die within 3-5 years after the diagnosis because of respiratory failure. Around ~10% of the cases belong to familial inheritance while the rest of cases are sporadic in nature. General pathological hallmarks of ALS include protein aggregation, inflammation, oxidative stress and glutamate excitotoxicity whereas metabolic alterations have recently gained attention. Clinical and experimental studies reveal significant changes in sterols, sphingolipids and lipid droplet (LD) dynamics in ALS patients or rat models specifically for *SOD1/ALS1* (Superoxide dismutase 1). However, other ALS loci have not been well studied in the context of lipid metabolism. Moreover, understanding of lipid imbalance in the progression of ALS pathogenesis is quite ambiguous and more studies need to be done to comment on its roles.

VAPB (Vesicle Associated Membrane Protein-Associated Protein B), is a resident of endoplasmic reticulum (ER) membrane which is known to be the $8^{th}$ locus of ALS (ALS8) disease due to point mutation from Proline to Serine at $56^{th}$ position in human patients. VAPB is involved in organelle tethering via membrane-membrane contact sites and interacts with a diverse group of proteins. This mutation leads to perturbation of VAPB functions and affects cellular homeostasis, thus affecting the overall physiology of human patients. Animal models such as *Drosophila* shares a conserved protein sequence for VAPB where the *ALS8* model has been replicated and shows similar phenotypes of ALS disease. This thesis investigates VAPB mediated lipid dysregulation in

the pathogenesis of ALS using *D. melanogaster* as model organism. Using the combination of lipidomics, genetic tools and microscopy, I have uncovered VAPB specific roles in lipid metabolism, LD regulation and how sphingolipid species such as ceramide play differential roles in neurons or glia which ultimately regulates motor function of *Drosophila* and contribute to ALS disease.

In the first chapter, I have reviewed the roles of lipid metabolism with primary focus on neurodegenerative disorders and introduced major lipid classes like sterols, sphingolipids, phospholipids and fatty acids. I have also given separate attention to the lipid droplets as emerging studies suggest their importance in the other cellular functions and organelle communication apart from just lipid storage. Then, I have tried to explain how lipid perturbation at the cellular level can influence the neuronal functions via affecting different organelles and contributing to the neurological disorders such as Alzheimer's, Parkinson's and motor neuron disorders. Next, I have introduced ALS as a motor neuron disorder where different genetic loci affect lipid homeostasis and how it may contribute to the disease progression. Finally, I have suggested *Drosophila melanogaster* as a powerful model system to study lipid dysregulation in ALS because of the simplistic maintenance, conserved genome and lipid species. Also, tissue specific modulation in flies gives it an extra advantage to understand the lipid metabolism in the neurodegenerative disorders.

Chapter II is majorly focused on VAPB/VAP structure and its functions. I have firstly described VAPB as a crucial protein involved in various cellular processes and how it interacts with a large pool of proteins present in humans but *Drosophila* VAP still has not been well studied in terms of its physical interactions with other proteins. Using bioinformatics and in silico predictions, this chapter tries to identify the putative *Drosophila* homologs of human VAP interactors and predict novel *Drosophila* VAP interacting partners based on FFAT motif analysis. Looking at the predictions of potential interactors, it becomes quite clear that *Drosophila* is an ideal organism to study VAP related functions. However, limitations are discussed at the end emphasizing the need for in vivo validations.

In the third chapter, I have focused on the *ALS8* mutant in *Drosophila* and showed how cholesterol homeostasis is completely perturbed in the brain of $VAP^{P58S}$ ALS disease mutant. Using LC-MS based lipid profiling, age dependent changes are visible in the lipid species particularly neutral lipids which are core components of LDs. Furthermore, a single copy of *VAP* is sufficient

to rescue these levels. Parallel microscopy imaging revealed defects in LD homeostasis which uncovered a novel role for VAP in glia specific LD regulation. Interestingly, *VAP*$^{P58S}$ seems to be playing a negative regulator for LD growth in the glia and its removal not only restores LD homeostasis but also improves motor performance of *ALS8* diseased flies. This chapter clearly shows LD dysregulation as a key pathological hallmark of ALS8 and positions VAPB as a regulator of lipid storage and its dynamics in the cell.

Chapter IV explores sphingolipid metabolism in ALS8 mainly focusing towards ceramides and sphingomyelins. Lipidomic analysis revealed elevated sphingolipid levels in the brains of *VAP*$^{P58S}$ males implicating disrupted lipid homeostasis in the disease. Then, I introduced Ceramide Transfer (CERT) as a protein of interest because of its interaction with VAPB and give a brief description about its roles and the generation of transgenic lines. Interestingly, tissue specific modulation of ceramide synthesis and transfer demonstrates their differential role in neurons and glia where reducing ceramide/sphingomyelin levels in neurons can delay the progression of the disease. Additionally, I found out reducing fatty acyl-CoA availability in the neurons for the production of CEs and ceramides improves motor function of the *ALS8* flies. This chapter establishes ceramide accumulation in neurons as a pathogenic driver in ALS8 model and CERT as a modifier of *ALS8* loci.

The final chapter shifts the study towards the glial role of ceramides/sphingomyelins in maintaining brain lipid homeostasis and *Drosophila* motor function. In chapter IV, I discovered the differential role of ceramides in neurons and glia which I pursued further by performing a reverse genetic screen of enzymes involved in ceramide synthesis and identified their roles in the motor behavior of the flies. Further, I showed ceramide transfer is crucial for glia functioning, in the absence of which it can cause motor impairment. Interestingly, these defects are in direct correlation with LD dysregulation in the glia of the adult brain and shows ceramide presence at the ER of glial cells directly influences LD homeostasis as well as motor function. This chapter highlights unexplored areas of sphingolipids in the field of LD homeostasis and glia specific roles in the locomotion of *Drosophila.*

Appendix I is focused towards fly reagent making for the experiments performed in the lab and balancing of *VAP*$^{P58S}$ CRISPR mutant generated in the lab with tissue specific Gal4 for the future studies. One of the limitations of genomic model of ALS was complicated genetics and unavailability of chromosomes for balancing *Gal80*$^{ts}$, which is a better tool for temperature shift

experiments. I have recombined *Gal80$^{ts}$* with the *VAP$^{P58S}$* CRISPR line which can be used for future experiments. In Appendix II, I have tried to understand the role of protein folding in aggregation dynamics in the brain of overexpression model of *ALS8* and performed a reverse genetic screen to identify the chaperone proteins which may influence mutant protein aggregates. Appendix III is focused on the role of autophagy in *ALS8* disease where I showed how *ALS14* can influence motor function of *ALS8* flies. During these experiments, I identified a novel phenotype of VCP protein in flies where its knockdown in the neurons shows upward halt wing phenotype.

In summary, I have tried to address the role of lipid metabolism in ALS8 disease and during the course of experiments, I have identified unexplored areas of lipid specific functions as well as LD roles in the flies which establishes a strong platform for the future studies.

In addition to this, I have significantly contributed to two research articles from the lab. In the first study, we found a role for Caspar/FAF1 (VAPB interactor) in the glial cells of *ALS8* mutant where it was regulating neuroinflammation via IMD/NFkB pathway. In the second study, I was involved in the standardization of aggregate analysis and performing motor assays.

## Publications/Manuscripts

1. Garg, L., Karthik, H., Deivasigamani, S., Ratnaparkhi, A., & Ratnaparkhi, G.S. (2026). Glial ceramide orchestrates Lipid Droplet homeostasis and motor function of *Drosophila. DMM,* (under review).

2. Thulasidharan, A., Garg, L., Tendulkar, S., & Ratnaparkhi, G. S. (2024). Age-dependent dynamics of neuronal VAPB(ALS) inclusions in the adult brain. *Neurobiol Dis*, *196*, 106517. https://doi.org/10.1016/j.nbd.2024.106517

3. Tendulkar, S., Hegde, S., Garg, L., Thulasidharan, A., Kaduskar, B., Ratnaparkhi, A., & Ratnaparkhi, G. S. (2022). Caspar, an adapter for VAPB and TER94, modulates the progression of ALS8 by regulating IMD/NFkappaB-mediated glial inflammation in a Drosophila model of human disease. *Hum Mol Genet*, *31*(17), 2857-2875. https://doi.org/10.1093/hmg/ddac076

4. Garg, L., Chaplot, K., Tendulkar, S., Kamat, S., & Ratnaparkhi, G.S. (2026). Perturbation of lipid homeostasis in Amyotrophic Lateral Sclerosis 8 uncovers glial specific VAPB role in Lipid Droplet regulation. *(Manuscript in preparation)*.

5. Garg, L., Chaplot, K., Karthik, H. & Ratnaparkhi, G.S. (2026). Role of Peptidyl Prolyl Isomerases in aggregation dynamics of a *Drosophila* model of Amyotrophic Lateral Sclerosis. *(Manuscript in preparation)*.

# Chapter I

# Lipid metabolism at the crossroads of neurodegeneration?

## 1.1 Abstract

Lipids are the essential building blocks of cellular system that play fundamental roles in membrane organization, cell signaling and energy metabolism. Lipid homeostasis is tightly regulated in the central nervous system due to high metabolic demand and limited regenerative capacity of neurons. Major lipid classes like sterols, sphingolipids, phospholipids and fatty acids play crucial roles in the synaptic transmission, intracellular trafficking and organelle functioning. Since the past two decades, multiple studies point toward the contribution of lipid dysregulation in the progression of neurodegenerative disorders by affecting different cellular processes such as mitochondrial activity, vesicle trafficking, oxidative stress etc.

Amyotrophic Lateral Sclerosis (ALS) is a late onset neurodegenerative disease characterized by the loss of motor neurons resulting in gradual paralysis due to weakening of muscles. Around ~10% of the cases belong to familial ones where point mutation in the ALS locus can induce disease and can be passed through familial inheritance. There are a number of pathological hallmarks associated with the disease like endoplasmic reticulum (ER) stress, inflammation and protein degradation however lipid disruption has not been studied thoroughly. *Drosophila melanogaster* is an ideal model system to understand the pathogenesis of ALS due to its conserved genome. This chapter highlights the contribution of lipid homeostasis in neurodegenerative disorders particularly ALS and emphasizes the utility of *Drosophila* as a model organism for studying lipid signaling pathways in *ALS* mutants.

## 1.2 Introduction

**1.2.1 Lipids- Classification, Structure and Functions**: Lipids constitute a major class of macromolecules that are quite diverse in nature and serve essential biological functions (Gunay et al., 2021; Schmitt et al., 2014; Tracey et al., 2021; Tracey et al., 2018; Yang et al., 2022). They are the integral components of membranes and act as signaling molecules within the cell. In addition, lipids can act as reservoir of energy and metabolic substrates for the cell functioning and its maintenance (Bezawork-Geleta et al., 2025; Carreira et al., 2019; Cockcroft & Raghu, 2018; Hannun & Obeid, 2018; Mejhert et al., 2022; Rickman et al., 2020; Teixeira et al., 2021; Yang et

al., 2020). Lipid homeostasis is crucial for organismal well-being and any perturbation can affect their physiology. Primarily, three major classes of lipids- sterols, sphingolipids (SLs) and phospholipids (PLs) are important for these functions (Fig. 1.1) (Carreira et al., 2019; Hannun & Obeid, 2018; Hussain et al., 2019; Kraut, 2011; Raghu et al., 2021; Tracey et al., 2018; Vance, 2015; Walther & Farese, 2012; Yang et al., 2022).

Cholesterol, a key lipid hydrocarbon, is usually present in membranes with approx. 25% of the body total cholesterol present only in the brain (Chang et al., 2006; Ikonen, 2008). 75% of total brain cholesterol is used for making myelin and rest is utilized for membrane maintenance of neurons and astrocytes (Morell & Jurevics, 1996). It plays a critical role in synaptogenesis, synaptic transmission and membrane fluidity (Linetti et al., 2010; Yang et al., 2022). Cholesterol synthesis peaks during the early brain development and remains relatively stable in adulthood (Hussain et al., 2019; Ikonen, 2008; Kim et al., 2023; Schmitt et al., 2014). In mature brains, neurons exhibit reduced cholesterol synthetic capacity and heavily depends on the astrocyte derived cholesterol supplied through Apo lipoprotein E (ApoE) containing lipoproteins (Ferris et al., 2017; Karten et al., 2006). Decrease in cholesterol levels in the neurons can lead to decreased synaptic transmission and impaired synaptic plasticity (Gunay et al., 2021; Hartmann et al., 2022; Linetti et al., 2010). Excess free cholesterol is esterified by Acyl-CoA: Cholesterol acyltransferase (ACAT) to form cholesterol esters which accumulate in lipid droplets (Mathiowetz & Olzmann, 2024; Schmitt et al., 2014; Tracey et al., 2018; Zhang et al., 2025). Also, dysregulation of cholesterol metabolism has been associated with a number of neurological disorders with Alzheimer's being the most studied one (Kozlova et al., 2024; Moulton et al., 2021; Rachakonda et al., 2004; Sultana et al., 2013).

Sphingolipids are another major class of membrane lipids which is highly conserved and found in all eukaryotes and some prokaryotes (Bartke & Hannun, 2009; Hannun & Obeid, 2018). They are defined as class of lipids consisting of one polar head group and two non-polar tails (Bartke & Hannun, 2009; Carreira et al., 2019). Ceramides lie at the center of sphingolipid pathway serving as precursor of all other sphingolipids (McCluskey et al., 2022; Mencarelli & Martinez-Martinez, 2013). In the nervous system, sphingolipids are particularly abundant and play crucial roles in the brain development, neuronal differentiation, synaptic transmission and myelin stability (Bartke & Hannun, 2009; Carter et al., 1947; Goyal et al., 2019; Hannun & Obeid, 2018; Henriques et al., 2017; Islam et al., 2025; Pan et al., 2023). They also behave as dynamic signaling molecules

capable of organizing lipid rafts and these rafts serve as platform for signal transduction, protein sorting and cell-cell communication which is critical for synaptic plasticity (Crivelli et al., 2022; He et al., 2010; Hussain et al., 2019; Kim et al., 2023; McCluskey et al., 2022; Tracey et al., 2021; Yuyama et al., 2012). They are broadly classified into ceramides, sphingomyelins and glycosphingolipids (Carreira et al., 2019; Carter et al., 1947). Ceramides are de novo synthesized at ER membrane through a series of enzymes and transfer to Golgi for certain modifications, leading to the formation of complex SLs like sphingomyelins, and glycosphingolipids (Mencarelli & Martinez-Martinez, 2013; Pant et al., 2020; Voelzmann & Bauer, 2010). They play crucial role in signal transduction pathways, intracellular trafficking and lysosome function (Tracey *et al.*, 2018; McCluskey *et al.*, 2022; Pan *et al.*, 2023). One important feature of sphingolipid biology is the antagonism between ceramide and sphingosine-1-phosphate also referred to as Cer-S1P rheostat (de Wit et al., 2019; Filippov et al., 2012; Pant et al., 2020; Pinto et al., 2011). Ceramides are generally associated with growth arrest, inflammation and apoptosis under specific conditions like oxidative and metabolic stress (de Wit et al., 2019; Vos et al., 2021). Ceramide accumulation is known to promote mitochondrial dysfunction, through transport from ER to mitochondria where it incorporates into mitochondrial membranes (Amatruda et al., 2025; Wang et al., 2009). This disruption affects mitochondrial activity which have implications in neurological disorders. On the other hand, S1P regulates neuroimmune interactions, oligodendrocyte survival and remyelination. Reduced S1P levels have been detected in neurodegenerative disorders (Choi et al., 2011; He et al., 2010; Pan et al., 2023).

Phospholipids represent structurally diverse and fundamental architecture of the cellular membranes. Phospholipids help in the formation of membrane bilayer and protects cell from the outside environment (Li et al., 2015; Vance, 2015). Most of the organelles present in the cell are also covered with bilayer of phospholipids like ER, Golgi, mitochondria and endosomes etc. (Fagone & Jackowski, 2009; Kuge et al., 1986; Li et al., 2015; Ross et al., 1997; Vance et al., 1977; Vance, 2015). They are classified into two major categories, Glycerophospholipids (GPLs) and Phosphosphingolipids (PSLs) (Ross et al., 1997; Vance et al., 1977). GPLs is the dominant class of lipids in the brain consisting of a glycerol backbone esterified to two hydrophobic fatty acid chains and hydrophilic phosphate containing head group (Tracey et al., 2018). Phosphatidylcholine (PC) is the most abundant one due to its molecular geometry providing symmetry to the bilayer. In addition to this, choline is a neurotransmitter present in neurons which

comes from PC (Weiss et al., 1958). Another phospholipid, Phosphatidylethanolamine (PE) plays role in membrane fluidity which may facilitate vesicular budding and membrane fusion (Wright & McMaster, 2002). Both lipids are synthesized at ER membrane through Kennedy pathway or can be alternatively synthesized involving mitochondria (Cockcroft & Raghu, 2018; Fagone & Jackowski, 2009; Vance et al., 1977). Other phospholipids like Phosphatidylserine (PS), Phosphatidylinositol (PI), Phosphatidic acid (PA) and Phosphatidylglycerol (PG) play various roles in terms of vesicle trafficking, lysosome functioning, synaptic transmission and membrane plasticity (Cockcroft et al., 2016; Cockcroft & Raghu, 2018; Kuge et al., 1986; Li et al., 2015; Mesmin et al., 2019; Raghu et al., 2021; Ross et al., 1997; Vance et al., 1977).

Fatty acids are a diverse class of lipids classified according to carbon chain lengths and degree of saturation (Fig. 1.1) (Ebert et al., 2003; Hamilton et al., 2007; Mathiowetz & Olzmann, 2024). They act as substrates for energy production as well as structural components of the membranes (Hamilton et al., 2007). De novo fatty acid synthesis in the brain generally involves acetyl-CoA primarily from tricarboxylic acid (TCA) cycle in mitochondria. Fatty acid synthase (FASN) catalyzes the condensation of acetyl CoA to generate saturated fatty acids which may be converted to unsaturated ones also (Tracey et al., 2021; Zhang et al., 2025). However, polyunsaturated fatty acids (PUFAs) requirement is dependent on peripheral supply because of absence of n-3 and n-6 desaturases (Rickman et al., 2020; Tracey et al., 2018; Yang et al., 2022). Apart from providing structural integrity to the cells, lipids are also used for brain energy requirements through fatty acid β-oxidation. Although glucose remains the primary energy resource for the brain, fatty acid oxidation can contributes upto 20% of total cerebral energy consumption under physiological conditions (Ebert et al., 2003). Lipid metabolism is tightly regulated between neurons and astrocytes where neurons rely heavily on glial cells for lipid stores under stress (Byrns et al., 2024; Goodman et al., 2024; Haynes et al., 2024; Ilieva et al., 2009; Liping Wang, 2022; Zhao et al., 2025). Moreover, under stress conditions, neurons are prone to oxidation of lipids and thus transfer oxidative lipid species to astrocytes. Astrocytes act as hub of lipid droplets in the brain which mainly contains neutral lipids and interact with different organelles in the cell. In the past decade, alteration in lipid metabolism have been linked to multiple neurodegenerative diseases like Alzheimer's, Parkinson's, Huntington's and other neurodegenerative disorders (Lee et al., 2011) (Liu *et al.*, 2015, 2017; Ioannou *et al.*, 2019; Moulton *et al.*, 2021; Haynes *et al.*, 2024).

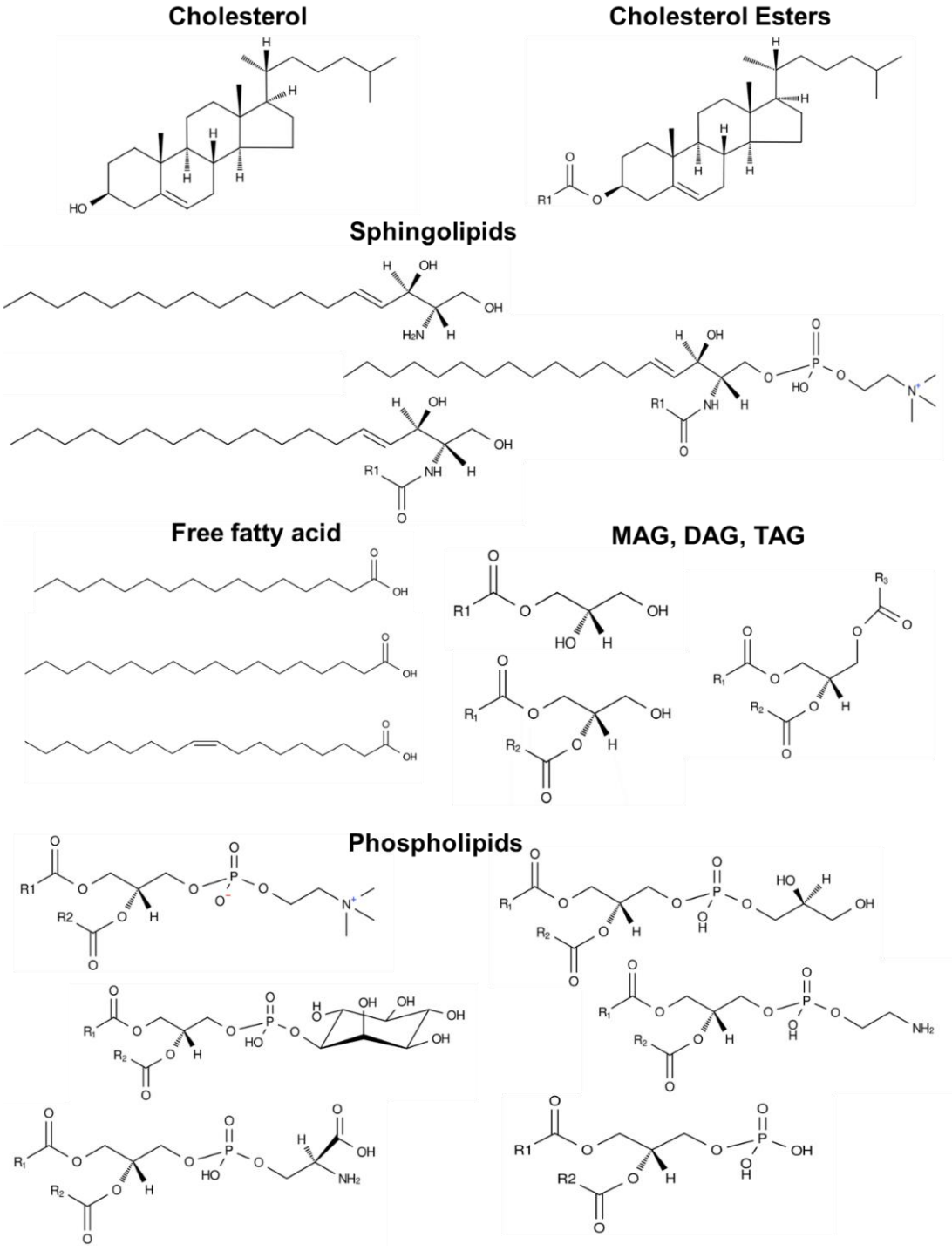



**Figure 1.1: Molecular structure of different lipid species that play major roles in the brain.** Schematic representation of chemical structures of lipids like Cholesterol, Cholesterol Esters, Sphingolipids (Sphingosine, Ceramides, Sphingomyelin), Free Fatty Acid (Palmitic Acid, Stearic Acid, Oleic Acid), Monoacylglycerol (MAG), Diacylglycerol (DAG), Triacylglycerol (TAG) and Phospholipids (PC, PG, PI, PE, PS, PA) are shown. (Source: www.lipidmaps.org)

**1.2.2 Lipid Droplets (LDs) -Structure and functions:** Lipid droplets (LDs) are considered as important cellular organelles consisting of lipophilic neutral lipid core mainly Triacylglycerols (TAGs) and cholesterol esters (CEs), enclosed by a monolayer of phospholipids (Walther & Farese, 2012). Initially, treated as storage house of lipids, LDs are now recognized as dynamic organelles involved in lipid homeostasis, inflammation and mitochondrial functioning (Mejhert et al., 2022). Interestingly, presence of proteins on the surface of droplets makes it more complex organelles which is still in exploration phase (Bohnert & Schrul, 2024). Majorly, LDs have been associated with liver or fat body where they play active role in metabolism and lipid storage (Mathiowetz & Olzmann, 2024). Two core components of LDs are synthesized at ER membrane through set of enzymes. Diacylglycerol acyltransferases (DGATs) leads to the formation of TAGs using DAGs and fatty acyl CoA as substrates. Similarly, ACAT synthesize cholesterol esters from cholesterol and fatty acyl CoA (Henne et al., 2025). LD formation and growth occurs via incorporation of these lipids and fusion events regulated by LD associated proteins (Robenek et al., 2006). Perilipin family of proteins play key role in controlling lipid storage and LD mobilization by regulating access of lipases on LD surface (Farmer et al., 2020).

LD degradation can happen through multiple ways such as lipase mediated lipolysis, lipophagy or mitochondrial fatty acid oxidation (Bezawork-Geleta et al., 2025; Girard et al., 2020). LD formation has been observed in multiple brain cell types. However, their presence in the central nervous system have recently gained attention which is being studied in context of neurodegeneration (Farmer et al., 2020; Moulton et al., 2021). LD accumulation has been well characterized in sub ventricular zone (SVZ) which demands high metabolic activity. LDs increase in SVZ with age and reported to be altered in neurodegenerative disorders (Zhang et al., 2025). Other regions such as cortex, hippocampus, hypothalamus and olfactory bulb also have been reported to contain LDs (Farmer et al., 2020). LD accumulation along with altered lipid metabolism is documented in diseases such as Alzheimer's, Parkinson's, Huntington's and motor neuron disorders as well (Teixeira et al., 2021). Generally, other cellular processes like inflammation, oxidative stress and autophagy have been linked to LD accumulation which collectively contribute to the pathogenesis of the disease (Chen et al., 2022; Freyre et al., 2019; Girard et al., 2020; Goodman et al., 2024; Nguyen & Olzmann, 2017; Smolic et al., 2021; Tokutake et al., 2015; Weber-Boyvat et al., 2015; Yang et al., 2020).

**1.2.3 Role of lipids in neurodegeneration:** Neurodegenerative disorders are recently being recognized as disorders of metabolic imbalance where lipid homeostasis is completely perturbed (Filippov et al., 2012; Jana et al., 2009; Schmitt et al., 2014; Sultana et al., 2013; Yang et al., 2022; Zhu et al., 2025). Alterations in cholesterol, fatty acids, glycerophospholipids, sphingolipids and TAGs have been observed to interact with protein aggregates present in the cells (Ruipérez et al., 2010; Yuyama et al., 2012). Dementia associated disorders such as Alzheimer's or Huntington's shows cognitive impairment driven by synaptic loss, neuronal death and chronic neuroinflammation (Lee et al., 2011; Sultana et al., 2013). Primarily, cholesterol, phospholipids and sphingolipids are severally affected (de Wit et al., 2019; Filippov et al., 2012; He et al., 2010; Long et al., 2026; Moulton et al., 2021; Zhao et al., 2025). Cholesterol metabolism is one of the major factors in dementia pathology. Excess neuronal cholesterol promotes amyloidogenic processing of amyloid precursor protein (APP) and stabilize β-secretase activity which enhances Amyloid-β production in Alzheimer's (Bryleva et al., 2010). In Huntington's disease, aberrant activation of sterol regulatory element-binding proteins (SREBPs) alters cholesterol biosynthesis and oxysterol signaling, whereas elevation in ceramide levels exacerbates mitochondrial energy deficits and oxidative stress (Lee et al., 2011; Long et al., 2026).

Seizure disorders such as epilepsy and multiple sclerosis are generally occurred due to pathological neuronal hyper-excitability which is extremely sensitive to lipid metabolism (Amatruda et al., 2025; Pant et al., 2020; Tracey et al., 2018; Zhang et al., 2025). Membrane cholesterol modulates the activity and localization of voltage gated ion channels and neurotransmitter receptors (Butchbach et al., 2004). Altered cholesterol and sphingolipid levels completely disrupts the synaptic plasticity (Hussain et al., 2019). Moreover, disruption of neuronal ceramide synthesis leads to spontaneous seizures (Anna B. Ziegler 2025). Lipid droplets serve as adaptive buffers during seizure activity (Farmer et al., 2020). Excess free fatty acids (FFAs) or lipid peroxidation products are exported from neurons to glia due to intense neuron firing which are then stored in LDs (Hamilton et al., 2007; Yang et al., 2020).However, accumulation of LDs can contribute to neuroinflammation and thus epileptogenesis (Zhang et al., 2025).

Motor neuron disorders share selective neuronal populations with high energy demand and limited regenerative capacity (McCluskey et al., 2022; Rickman et al., 2020; Schmitt et al., 2014; Zhai et al., 2009). In these circumstances, mainly fatty acid, sphingolipid turnover and LD dynamics are affected leading to mitochondrial dysfunction and impaired proteostasis (Browne et

al., 2006; Chaves-Filho et al., 2019; Dupuis et al., 2004; Henriques et al., 2015; Jang et al., 2021). In Parkinson's, α-synuclein comes directly in contact with membrane lipids and lipid droplets. Physiological binding to phospholipid surface regulates lipid turnover whereas pathogenic mutant protein disrupt LD interactions and results in excessive FFA accumulation and lipotoxic stress (Ruipérez et al., 2010). Elevated cholesterol and oxysterols further enhance α-synuclein aggregation and oxidative damage (Cheng et al., 2011; Girard et al., 2020). Mutations in glucocerebrosidase (GBA1) reduce lysosomal ceramide production which affects autophagic flux and stabilize these aggregates contributing to the pathogenesis of the disease (Liping Wang, 2022). Particularly in ALS, disruption in the delicate balance of lipids can lead to significant dysfunction in lipid dependent pathways and contribute to pathology of the disease (González De Aguilar, 2019; Liu *et al.*, 2020; Sol *et al.*, 2021; Agrawal *et al.*, 2022).

**1.2.4 Amyotrophic Lateral Sclerosis (ALS):** ALS also known as Lou Gehrig's disease is an adult onset progressive neurodegenerative disease characterized by the loss of both upper and lower motor neurons (Alsultan et al., 2016; Genge et al., 2024; van Es et al., 2017). It is the one of the most common motor neuron disorder with 2 per 1,00,000 individuals affected with average onset of 65 years old (Sanhueza et al., 2015). The neuronal degeneration cause the weakening of the muscles, voluntary movement loss and thus paralysis in the patient (Sanhueza *et al.*, 2015; Kirby *et al.*, 2016; Stump *et al.*, 2023). Early symptoms of ALS are muscle cramps, spasticity and localized muscle weakness in the limbs or neck. As the disease progresses, patients suffer through slurred speech, difficulty in swallowing food, sialorrhea, shortness of breath and respiratory failure (Genge, Wainwright and Vande Velde, 2023; Kour *et al.*, 2023; Mcbenedict *et al.*, 2025). Most of the patients die within 2-5 years after diagnosis however the exact cause of ALS still remains unknown and poorly understood with no effective cure (Genge et al., 2024; Murage et al., 2024; Sanhueza et al., 2015). Till now, FDA (Food and Drug Administration) approved drugs like Riluzole and Edaravone shows mild improvement in some patients and generally more effective during the early stages of the disease (McBenedict et al., 2025). Riluzole suppresses glutamate release via acting on voltage dependent sodium channels whereas Edaravone acts as free radical scavenger and leads to reduction in oxidative stress (Carrì et al., 2015; Ilieva et al., 2009; Rachakonda et al., 2004; Wiedau-Pazos et al., 1996)

Most of the ALS cases are sporadic in nature (sALS), where the underlying cause is unknown, while ~10% of the cases belong to familial ones termed as fALS known to transmit within families (Ajroud-Driss & Siddique, 2015; Borgese et al., 2021). Although fALS cases are quite low compared to sALS, their studies have been instrumental in identifying genetic causes and disease mechanisms (McBenedict et al., 2025; Sanhueza et al., 2015). The antioxidant enzyme superoxide dismutase also known as SOD1 was the first one to be linked with familial ALS in 1993. The gene encodes SOD1 whose function is to convert toxic reactive oxygen species (ROS) to dioxides (Ferrante et al., 1997; Wiedau-Pazos et al., 1996). Recently, Tofersen (approved by FDA) is being used to treat ALS patients with point mutations in *SOD1* which is somewhat proved to be effective (Genge et al., 2024; van Es et al., 2017). Till now, more than 30 genes have been associated with disease with 18 being definitive loci. Interestingly, any point mutations in these genes can induce ALS symptoms and affect the physiology (Tracey et al., 2021). These loci are classified into various functional categories like RNA metabolism, mitochondria function, proteostasis, ER stress, cytoskeleton dynamics and protein quality control (Fig. 1.2) (Layalle et al., 2021). Given the molecular heterogeneity, multiple mechanisms likely to converge to produce common clinical and pathological phenotypes characteristic of ALS (Teuling *et al.*, 2007; Sanhueza *et al.*, 2015; Masrori and Van Damme, 2020; Borgese, Navone, *et al.*, 2021; Layalle *et al.*, 2021). Out of all the known ALS causing loci, the occurrence rate of *SOD1, C9ORF72,* TAR DNA-binding protein 43 *(TARDBP/TDP43)* and Fused in sarcoma (*FUS)* mutant variants is around 50% of all cases whereas other loci come under rare genetic disorders although those proteins have been to be modified in these mutants as well (Ajroud-Driss & Siddique, 2015).

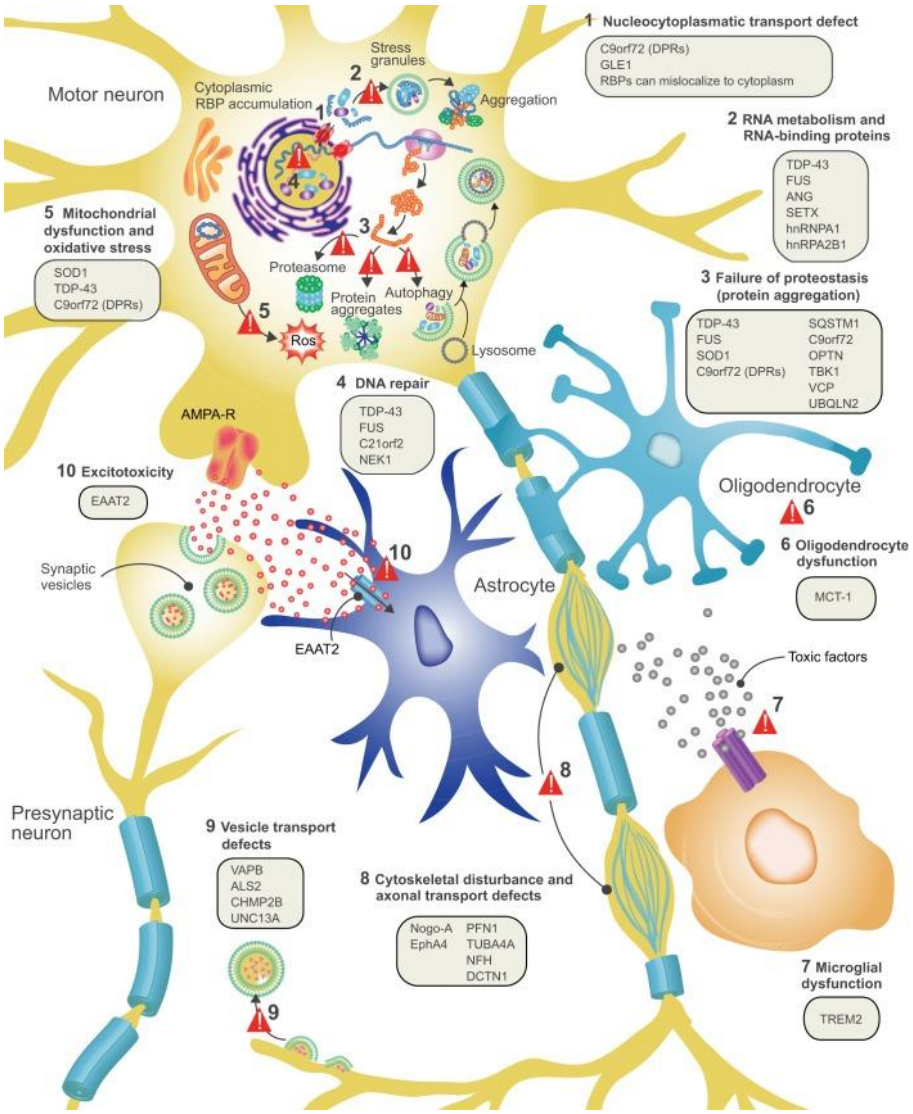



**Figure 1.2: Pathological hallmarks and Genes associated with Amyotrophic Lateral Sclerosis.** Schematic diagram of ALS associated genetic loci and pathological hallmarks visible in those mutants. These loci share some of the common cellular dysfunctions as shown in each box marked by that particular function. Figure is adapted from (Van Damme et al., 2017)

**1.2.5 Lipid homeostasis in ALS**: Emerging evidence from the past two decades highlights systemic metabolic dysfunction as an important factor in ALS pathogenesis (Agrawal et al., 2022; Browne et al., 2006). Many ALS patients have shown symptoms of hyper-metabolism and in some cases it may occur before the onset of motor symptoms (Liu et al., 2020; Robelin & Gonzalez De Aguilar, 2014; Sol et al., 2021; Tracey et al., 2021). Clinically, it is generally associated with weight loss, reduced adiposity and poorer prognosis. Patients who lose 5% of their body mass till the diagnosis have increased risk of death which makes it crucial to study its underlying causes

(Dupuis et al., 2004; Dupuis et al., 2011; Huang et al., 2015; Jésus et al., 2018; Paganoni et al., 2011). ALS loci like *SOD1, FUS* and *TARDBP* have been shown to play important roles in lipid metabolism (Alsultan et al., 2016; Carrì et al., 2015; Cutler et al., 2002; Zhan et al., 2015). Knockout of *TARDBP* in mouse models results in significantly reduced fat deposition and increased lipid oxidation. Moreover, genes associated with obesity and metabolic control are also altered (Iguchi et al., 2012). In the healthy brain, oxidative and metabolic stress is generally at low levels however hypermetabolism in ALS leads to increased demand for energy and scarcity of nutrient availability (Desport et al., 2006; Desport et al., 2001; Jésus et al., 2018). A significant decrease in membrane fluidity of the brain and spinal cord also has been observed as the disease progress in ALS mouse models possibly due to lipid peroxidation (Agrawal et al., 2022; Schmitt et al., 2014). Alterations in polyunsaturated/saturated lipid ratio can decrease membrane fluidity and promotes lipid-lipid and lipid-protein cross-linking. These changes can thus affect the function of motor neurons in ALS (Cutler *et al.*, 2002; Chaves-Filho *et al.*, 2019; González De Aguilar, 2019; Jang *et al.*, 2021; Layalle *et al.*, 2021; Sol *et al.*, 2021; Le *et al.*, 2023). Elevated ketone bodies have been detected in the cerebrospinal fluid (CSF) of ALS patients which point towards lipid derived energy metabolism. Increased lipid utilization leads to oxidative stress which leads to peroxidation of lipids and can enhance ketone bodies formation (Sol et al., 2021).

One of the most prominent alterations observed in ALS patients is the increased amount of cholesterol esters in the spinal cord (Browne et al., 2006; Chaves-Filho et al., 2019). In *SOD1*$^{G93A}$ mouse model of ALS, six fold of CEs is seen compared to age matched controls and generally these esters include fatty acids which are not synthesized in the body and depends on dietary sources (Chaves-Filho et al., 2019; Cutler et al., 2002; Ferrante et al., 1997). Proteomic analysis has revealed substantial changes in the neuronal lipid rafts where cytoskeletal elements and inflammatory elements are upregulated but proteins regulating metabolism, vesicular transport and neurotransmitters are downregulated. Proteins affected in metabolic process is indicative of decreased production of lactate, and suggest a potential defect in astrocyte metabolic support to neurons (Chaplot et al., 2019; Chaves-Filho et al., 2019; Thau et al., 2012; Zhai et al., 2009). Astrocytes in ALS spinal cord are shown to have higher LD accumulation that may be sequestering peroxidation prone fatty acids away from membrane bilayers under oxidative stress. Lipid peroxidation products can impair astrocyte glutamate transporter EAAT2 (Excitatory Amino acid

Transporter 2) which is normally localized to lipid raft domains. Reduced EAAT2 activity can contribute to glutamate-mediated excitotoxicity (Bristol & Rothstein, 1996; Yang et al., 2022).

Mitochondrial dysfunction is one of the hallmarks of ALS pathology and closely associated with lipid metabolism (Shi et al., 2010). Neuronal mitochondria exhibit abnormal morphology such as swelling, clustering and formation of vacuoles in ALS patients or animal models. These phenotypes are accompanied by impaired mitochondrial bioenergetics and increased ROS species (Browne et al., 2006; Carrì et al., 2015; Wong et al., 2024).

Mitochondrial biogenesis regulator PGC-1α is found to be downregulated in the skeletal muscles leading to altered lipid metabolism in ALS patients. However, upregulation in CNS improves mitochondrial function and improves survival along with motor performance (Eschbach et al., 2013; Thau et al., 2012). Lipid species such as cardiolipin, resident of inner mitochondrial membrane play essential role in ATP production and mitochondrial structure dynamicity (de Kroon et al., 1997). Interestingly, in *SOD1*$^{G93A}$ rodents, cardiolipin levels are significantly reduced in spinal cord tissue consistent with structural degeneration (Chaves-Filho et al., 2019).

**Table 1.1: Lipid levels detected in various samples of ALS patients or animal models**

| S.No. | Lipid class | Blood | CSF | Human spinal cord | Animal models |
|---|---|---|---|---|---|
| 1 | Sphingomyelins | Higher | Higher | Higher | Mixed |
| 2 | Ceramides | Higher | n.d. | Higher | Mixed |
| 3 | Glucosylceramides | Higher | higher | Mixed | Mixed |
| 4 | Gangliosides | n.d. | n.d. | n.d. | Higher |
| 5 | Triglycerides | Higher | Lower | Higher | n.s. |
| 6 | Diglycerides | Higher | Lower | Mixed | Mixed |
| 7 | Phosphatidylcholine | Mixed | Higher | Higher | Mixed |
| 8 | Phosphatidylethanolamine | Mixed | n.s. | Higher | Mixed |
| 9 | Phosphatidylinositol | n.s. | n.s. | n.s. | Mixed |
| 10 | Lysophospholipids | Higher | Higher | Higher | Higher |
| 11 | Saturated fatty acids | Mixed | n.d. | n.d. | n.d. |
| 12 | Monounsaturated FA | Higher | n.d. | n.d. | n.d. |
| 13 | Polyunsaturated FA | Higher | n.d. | n.d. | n.d. |
| 14 | Cholesterol esters | Higher | n.s. | Higher | Higher |
| 15 | Cholesterol | Higher | n.d. | n.d. | n.d. |

n.d. not detected, n.s. non-significant, mixed- variability in different published results, Source (Agrawal et al., 2022)

**1.2.6 *Drosophila* models of ALS disease:** *Drosophila melanogaster* is one of the powerful experimental models for studying neurodegenerative disorders due to genetic tractability, short lifespan and high degree of similarity between fly and human disease associated genes (Casci & Pandey, 2015; Reiter et al., 2001). Around 77% of known human disease genes have orthologs in *Drosophila* genome and different genetic tools such as UAS-Gal4 system, MiMIC transposons and CRISPR/Cas9 genomic editing has facilitated precise manipulation of gene expression in tissue or stage specific manner (Duffy, 2002; Gratz et al., 2015; Venken et al., 2011). These features of *Drosophila* makes the flies an ideal model system to study ALS linked mutations for dissecting pathogenic pathways and identify their genetic modifiers.

*SOD1/ALS1*, first gene linked to ALS has been extensively studied in fly model system (Chaplot et al., 2019; Deivasigamani et al., 2014). Early studies using mutagenesis approach showed that missense mutations in the gene affect protein function and compromise the survival (Zhou & Xu, 2024). Further experiments revealed that tissue specific expression of mutant gene in motor neurons induce motor defects, protein accumulation and electrophysiological abnormalities. Knock-in models of *SOD1* mutant in the flies recapitulated key disease phenotypes sharing similarities with human symptoms (Hegde & Srivastava, 2022). Genetic models of flies expressing *G85R, H71Y* and *H48R* mutations have shortened lifespan, developmental defects and adult dyskinesia due to muscle axon contraction (Braems et al., 2021). Moreover, antioxidant compounds have been proven to be neuroprotective by improving motor performance, increasing survival rate and reducing cytoplasmic inclusion bodies of *hSOD1* mutants (Liguori et al., 2021). *Alsin* is the ALS loci which encodes for Alsin protein and functions as guanine exchange factor for Rab5 and perform specific roles in endosomal trafficking. Loss of *ALS2* have been linked to juvenile form of ALS and *ALS2* null mutants shows marked reduction in lifespan which can be rescued by wildtype expression (Chandran et al., 2007; Hegde & Srivastava, 2022).

TARDBP is one of the major pathological hallmarks of ALS with aggregates present in a large proportion of the human patients (Layalle et al., 2021). *Drosophila* models with human TDP-43 in neurons leads to age dependent neurodegeneration, axonal loss, motor neuron death (Iguchi et al., 2012; Zhan et al., 2015). Mitochondria abnormalities have also been observed in these models representing observations found in human ALS tissues (Braun et al., 2011). FUS is another RNA binding protein linked to ALS with point mutations found in both familial and sporadic cases (Zhou & Xu, 2024). Expressing human mutant copy shows similar phenotypes of

ALS which correlates with the human counterpart. Moreover, disruption in NMJ (neuromuscular junction) architecture, glutamate receptor composition, mitochondrial activity act as contributors to FUS toxicity (Steyaert et al., 2018). Different fly models of *FUS* mutants such as *R521C, R521H, R518K, R524S* and *P525L* shows severe retinal neurodegeneration. Also, *FUS* expression can induce Hippo pathway and c-Jun-N-terminal kinase (JNK) signaling pathway leading to neurodegeneration in transgenic fly models (Casci & Pandey, 2015; Steyaert et al., 2018; Tendulkar et al., 2022). Most common genetic contributor of ALS identified is hexanucleotide (GGGGCC) repeat in C9orf72 gene which induce developmental lethality, eye degeneration, locomotor impairment and neuronal morphological defects on expressing long repeats (Jang et al., 2021). VAPB (Vesicle Associated Membrane Protein –Associated Protein B) is another ALS loci also known as ALS8 found in familial ALS patients (Nishimura et al., 2004). *VAP33-A*, fly ortholog of *VAPB,* regulates synaptic bouton formation, glutamate receptor clustering at the NMJ junctions which gets altered due to disruption in its activity (Ratnaparkhi et al., 2008). Further studies have identified VAPB roles in endosomal trafficking, autophagy, ER-Golgi network and membrane-membrane contact sites (Kors et al., 2022). Interestingly, few studies have been focused on lipid metabolism in the pathogenesis of ALS which have been modelled in *Drosophila.* My thesis work will be focused on VAPB as protein of interest and how its functions are affected in ALS disease with respect to lipid metabolism and cellular homeostasis

### 1.3 Open questions

**Connection between lipid homeostasis and ALS:** Multiple evidence from recent LC_MS (Liquid chromatography-Mass spectrometry) lipid profiling of different ALS patients hint towards complete lipid dysregulation in the tissue samples. However, the contribution of lipid dysregulation in the pathogenesis of the disease is still unclear. Also, studies from different ALS loci suggests different pattern of lipid species levels in the samples. Does that mean different loci affect particular lipid signaling pathways or change in any specific lipid pathways can lead to same ALS like symptoms?

**Cell specific lipid dysregulation in ALS:** Majority of the studies point towards lipid imbalance and hypermetabolism in the neurons of ALS mutants, however contribution from non-neuronal cells like glia and muscle is still lacking. Glial cells have been always looked from the angle of storehouse of lipid droplets but is there more to that, which may be playing a contributing factor

in the disease. Recent studies have reported importance of different lipid species in neurons and glia so it becomes crucial to study lipid metabolism of ALS mutant in cell specific manner. Also, is there any tissue specific role for the same set of genes involved in lipid synthesis or signaling which may lead to different phenotypes in the animal model?

**Role of Lipid droplets in glial cells:** Glia is known to be the hub of lipid droplets in the brain. Most of the neurodegenerative models reports accumulation of LDs in the glia of the brain. However, what is the impact of LD accumulation on the behavior of ALS patients is still not completely understood. Also, most of ALS mutants show accumulation of LDs but is that applicable for all type of loci needs to be studied. Secondly, there are very few studies which reports reduction of LDs in neurodegenerative models so what will happen if there is reduction in LDs?

**Temporal dynamics of lipid imbalance:** There are number of studies which has shown changes in the lipid levels of asymptomatic ALS patients. So, the question arises if these changes can be seen as biomarkers of the disease. Also, most of the neurodegenerative disorders show lipid dysregulation so is there specific pattern to these lipids with respect to each neurodegenerative disorder. Secondly, do these changes in lipids occurs at same time in different ALS models or depends on individual loci?

**Impact of diet on ALS pathogenesis:** Although human body is capable of synthesizing various lipids but a number of lipid species are obtained from diet which body is unable to produce. Moreover, the effect of diet on the symptoms and progression of the disease is still unclear. It becomes quite important to study the impact of different lipids such as fatty acids on the ALS phenotypes for which *Drosophila* is an excellent model.

## 1.4 References:

Agrawal, I., Lim, Y. S., Ng, S. Y., & Ling, S. C. (2022). Deciphering lipid dysregulation in ALS: from mechanisms to translational medicine. *Transl Neurodegener*, *11*(1), 48. https://doi.org/10.1186/s40035-022-00322-0

Ajroud-Driss, S., & Siddique, T. (2015). Sporadic and hereditary amyotrophic lateral sclerosis (ALS). *Biochimica et Biophysica Acta (BBA) - Molecular Basis of Disease*, *1852*(4), 679–684. https://doi.org/https://doi.org/10.1016/j.bbadis.2014.08.010

Alsultan, A. A., Waller, R., Heath, P. R., & Kirby, J. (2016). The genetics of amyotrophic lateral sclerosis: current insights. *Degener Neurol Neuromuscul Dis*, *6*, 49–64. https://doi.org/10.2147/DNND.S84956

Amatruda, M., Marechal, D., Gacias, M., Wentling, M., Turpin-Nolan, S., Morstein, J., Moniruzzaman, M., Bruning, J. C., Haughey, N. J., Trauner, D. H., & Casaccia, P. (2025). Neuroprotective effect of neuron-specific deletion of the C16 ceramide synthetic enzymes in an animal model of multiple sclerosis. *Glia*, *73*(2), 271–290. https://doi.org/10.1002/glia.24631

Anna B. Ziegler , C. W., Konstantin Beckschäfer,Anna-Lena Wulf,Neena Dhiman,Peter Soba,Christoph Thiele,Reinhard Bauer,Gaia Tavosanis (2025). Individual lipid alterations at the origin of neuronal Ceramide Synthase defects. *PloS Genetics*, *21*(9). https://doi.org/https://doi.org/10.1371/journal.pgen.1011880

Bartke, N., & Hannun, Y. A. (2009). Bioactive sphingolipids: metabolism and function. *Journal of Lipid Research*, *50*, S91–S96. https://doi.org/https://doi.org/10.1194/jlr.R800080-JLR200

Bezawork-Geleta, A., Devereux, C. J., Keenan, S. N., Lou, J., Cho, E., Nie, S., De Souza, D. P., Narayana, V. K., Siddall, N. A., Rodrigues, C. H. M., Portelli, S., Zheng, T., Nim, H. T., Ramialison, M., Hime, G. R., Dodd, G. T., Hinde, E., Ascher, D. B., Stroud, D. A., & Watt, M. J. (2025). Proximity proteomics reveals a mechanism of fatty acid transfer at lipid droplet-mitochondria- endoplasmic reticulum contact sites. *Nat Commun*, *16*(1), 2135. https://doi.org/10.1038/s41467-025-57405-5

Bohnert, M., & Schrul, B. (2024). Lipid droplets in health and disease. *FEBS Lett*, *598*(10), 1113–1115. https://doi.org/10.1002/1873-3468.14900

Borgese, N., Navone, F., Nukina, N., & Yamanaka, T. (2021). Mutant VAPB: Culprit or Innocent Bystander of Amyotrophic Lateral Sclerosis? *Contact*, *4*. https://doi.org/10.1177/25152564211022515

Braems, E., Tziortzouda, P., & Van Den Bosch, L. (2021). Exploring the alternative: Fish, flies and worms as preclinical models for ALS. *Neuroscience Letters*, *759*, 136041. https://doi.org/https://doi.org/10.1016/j.neulet.2021.136041

Braun, R. J., Sommer, C., Carmona-Gutierrez, D., Khoury, C. M., Ring, J., Büttner, S., & Madeo, F. (2011). Neurotoxic 43-kDa TAR DNA-binding Protein (TDP-43) Triggers Mitochondrion-

dependent Programmed Cell Death in Yeast. *Journal of Biological Chemistry*, *286*(22), 19958–19972. https://doi.org/https://doi.org/10.1074/jbc.M110.194852

Bristol, L. A., & Rothstein, J. D. (1996). Glutamate transporter gene expression in amyotrophic lateral sclerosis motor cortex. *Annals of Neurology*, *39*(5), 676–679. https://doi.org/https://doi.org/10.1002/ana.410390519

Browne, S. E., Yang, L., DiMauro, J.-P., Fuller, S. W., Licata, S. C., & Beal, M. F. (2006). Bioenergetic abnormalities in discrete cerebral motor pathways presage spinal cord pathology in the G93A SOD1 mouse model of ALS. *Neurobiology of Disease*, *22*(3), 599–610. https://doi.org/https://doi.org/10.1016/j.nbd.2006.01.001

Bryleva, E. Y., Rogers, M. A., Chang, C. C. Y., Buen, F., Harris, B. T., Rousselet, E., Seidah, N. G., Oddo, S., LaFerla, F. M., Spencer, T. A., Hickey, W. F., & Chang, T.-Y. (2010). ACAT1 gene ablation increases 24(S)-hydroxycholesterol content in the brain and ameliorates amyloid pathology in mice with AD. *Proceedings of the National Academy of Sciences*, *107*(7), 3081–3086. https://doi.org/10.1073/pnas.0913828107

Butchbach, M. E. R., Tian, G., Guo, H., & Lin, C.-l. G. (2004). Association of Excitatory Amino Acid Transporters, Especially EAAT2, with Cholesterol-rich Lipid Raft Microdomains: IMPORTANCE FOR EXCITATORY AMINO ACID TRANSPORTER LOCALIZATION AND FUNCTION. *Journal of Biological Chemistry*, *279*(33), 34388–34396. https://doi.org/https://doi.org/10.1074/jbc.M403938200

Byrns, C. N., Perlegos, A. E., Miller, K. N., Jin, Z., Carranza, F. R., Manchandra, P., Beveridge, C. H., Randolph, C. E., Chaluvadi, V. S., Zhang, S. L., Srinivasan, A. R., Bennett, F. C., Sehgal, A., Adams, P. D., Chopra, G., & Bonini, N. M. (2024). Senescent glia link mitochondrial dysfunction and lipid accumulation. *Nature*, *630*(8016), 475–483. https://doi.org/10.1038/s41586-024-07516-8

Carreira, A. C., Santos, T. C., Lone, M. A., Zupančič, E., Lloyd-Evans, E., de Almeida, R. F. M., Hornemann, T., & Silva, L. C. (2019). Mammalian sphingoid bases: Biophysical, physiological and pathological properties. *Progress in Lipid Research*, *75*(100988). https://doi.org/10.1016/j.plipres.2019.100988

Carrì, M. T., Valle, C., Bozzo, F., & Cozzolino, M. (2015). Oxidative stress and mitochondrial damage: importance in non-SOD1 ALS [Mini Review]. *Frontiers in Cellular Neuroscience, Volume 9 - 2015*.

Carter, H. E., Haines, W. J., Ledyard, W. E., & Norris, W. P. (1947). Biochemistry of the sphingolipides: i. Preparation of sphingolipides from beef brain and spinal cord. *Journal of Biological Chemistry*, *169*(1), 77–82. https://doi.org/https://doi.org/10.1016/S0021-9258(17)35063-9

Casci, I., & Pandey, U. B. (2015). A fruitful endeavor: Modeling ALS in the fruit fly. *Brain Research*, *1607*, 47–74. https://doi.org/https://doi.org/10.1016/j.brainres.2014.09.064

Chandran, J., Ding, J., & Cai, H. (2007). Alsin and the Molecular Pathways of Amyotrophic Lateral Sclerosis. *Molecular Neurobiology*, *36*(3), 224–231. https://doi.org/10.1007/s12035-007-0034-x

Chang, T.-Y., Chang, C. C. Y., Ohgami, N., & Yamauchi, Y. (2006). Cholesterol Sensing, Trafficking, and Esterification. *Annual Review of Cell and Developmental Biology*, *22*(Volume 22, 2006), 129–157. https://doi.org/https://doi.org/10.1146/annurev.cellbio.22.010305.104656

Chaplot, K., Pimpale, L., Ramalingam, B., Deivasigamani, S., Kamat, S. S., & Ratnaparkhi, G. S. (2019). SOD1 activity threshold and TOR signalling modulate VAP(P58S) aggregation via reactive oxygen species-induced proteasomal degradation in a Drosophila model of amyotrophic lateral sclerosis. *Dis Model Mech*, *12*(2). https://doi.org/10.1242/dmm.033803

Chaves-Filho, A. B., Pinto, I. F. D., Dantas, L. S., Xavier, A. M., Inague, A., Faria, R. L., Medeiros, M. H. G., Glezer, I., Yoshinaga, M. Y., & Miyamoto, S. (2019). Alterations in lipid metabolism of spinal cord linked to amyotrophic lateral sclerosis. *Sci Rep*, *9*(1), 11642. https://doi.org/10.1038/s41598-019-48059-7

Chen, S., Roberts, M. A., Chen, C. Y., Markmiller, S., Wei, H. G., Yeo, G. W., Granneman, J. G., Olzmann, J. A., & Ferro-Novick, S. (2022). VPS13A and VPS13C Influence Lipid Droplet Abundance. *Contact (Thousand Oaks)*, *5*, 25152564221125613. https://doi.org/10.1177/25152564221125613

Cheng, D., Jenner, A. M., Shui, G., Cheong, W. F., Mitchell, T. W., Nealon, J. R., Kim, W. S., McCann, H., Wenk, M. R., Halliday, G. M., & Garner, B. (2011). Lipid Pathway Alterations in Parkinson's Disease Primary Visual Cortex. *PLoS One*, *6*(2), e17299. https://doi.org/10.1371/journal.pone.0017299

Choi, J. W., Gardell, S. E., Herr, D. R., Rivera, R., Lee, C.-W., Noguchi, K., Teo, S. T., Yung, Y. C., Lu, M., Kennedy, G., & Chun, J. (2011). FTY720 (fingolimod) efficacy in an animal model of multiple sclerosis requires astrocyte sphingosine 1-phosphate receptor 1 (S1P1) modulation. *Proceedings of the National Academy of Sciences*, *108*(2), 751–756. https://doi.org/10.1073/pnas.1014154108

Cockcroft, S., Garner, K., Yadav, S., Gomez-Espinoza, E., & Raghu, P. (2016). RdgBalpha reciprocally transfers PA and PI at ER-PM contact sites to maintain PI(4,5)P2 homoeostasis during phospholipase C signalling in Drosophila photoreceptors. *Biochem Soc Trans*, *44*(1), 286–292. https://doi.org/10.1042/BST20150228

Cockcroft, S., & Raghu, P. (2018). Phospholipid transport protein function at organelle contact sites. *Curr Opin Cell Biol*, *53*, 52–60. https://doi.org/10.1016/j.ceb.2018.04.011

Crivelli, S. M., Giovagnoni, C., Zhu, Z., Tripathi, P., Elsherbini, A., Quadri, Z., Pu, J., Zhang, L., Ferko, B., Berkes, D., Spassieva, S. D., Martinez-Martinez, P., & Bieberich, E. (2022). Function of ceramide transfer protein for biogenesis and sphingolipid composition of extracellular vesicles. *J Extracell Vesicles*, *11*(6), e12233. https://doi.org/10.1002/jev2.12233

Cutler, R. G., Pedersen, W. A., Camandola, S., Rothstein, J. D., & Mattson, M. P. (2002). Evidence that accumulation of ceramides and cholesterol esters mediates oxidative stress-induced death of motor neurons in amyotrophic lateral sclerosis. *Ann Neurol*, *52*(4), 448–457. https://doi.org/10.1002/ana.10312

de Kroon, A. I. P. M., Dolis, D., Mayer, A., Lill, R., & de Kruijff, B. (1997). Phospholipid composition of highly purified mitochondrial outer membranes of rat liver and Neurospora crassa. Is cardiolipin present in the mitochondrial outer membrane? *Biochimica et Biophysica Acta (BBA) - Biomembranes*, *1325*(1), 108–116. https://doi.org/https://doi.org/10.1016/S0005-2736(96)00240-4

de Wit, N. M., den Hoedt, S., Martinez-Martinez, P., Rozemuller, A. J., Mulder, M. T., & de Vries, H. E. (2019). Astrocytic ceramide as possible indicator of neuroinflammation. *Journal of Neuroinflammation*, *16*(1), 48. https://doi.org/10.1186/s12974-019-1436-1

Deivasigamani, S., Verma, H. K., Ueda, R., Ratnaparkhi, A., & Ratnaparkhi, G. S. (2014). A genetic screen identifies Tor as an interactor of VAPB in a Drosophila model of amyotrophic lateral sclerosis. *Biol Open*, *3*(11), 1127–1138. https://doi.org/10.1242/bio.201410066

Desport, J.-C., Torny, F., Lacoste, M., Preux, P.-M., & Couratier, P. (2006). Hypermetabolism in ALS: Correlations with Clinical and Paraclinical Parameters. *Neurodegenerative Diseases*, *2*(3-4), 202–207. https://doi.org/10.1159/000089626

Desport, J. C., Preux, P. M., Magy, L., Boirie, Y., Vallat, J. M., Beaufrère, B., & Couratier, P. (2001). Factors correlated with hypermetabolism in patients with amyotrophic lateral sclerosis. *The American Journal of Clinical Nutrition*, *74*(3), 328–334. https://doi.org/https://doi.org/10.1093/ajcn/74.3.328

Duffy, J. B. (2002). GAL4 system in Drosophila: a fly geneticist's Swiss army knife. *Genesis*, *34*(1-2), 1–15. https://doi.org/10.1002/gene.10150

Dupuis, L., Oudart, H., René, F., de Aguilar, J.-L. G., & Loeffler, J.-P. (2004). Evidence for defective energy homeostasis in amyotrophic lateral sclerosis: Benefit of a high-energy diet in a transgenic mouse model. *Proceedings of the National Academy of Sciences*, *101*(30), 11159–11164. https://doi.org/10.1073/pnas.0402026101

Dupuis, L., Pradat, P.-F., Ludolph, A. C., & Loeffler, J.-P. (2011). Energy metabolism in amyotrophic lateral sclerosis. *The Lancet Neurology*, *10*(1), 75–82. https://doi.org/https://doi.org/10.1016/S1474-4422(10)70224-6

Ebert, D., Haller, R. G., & Walton, M. E. (2003). Energy Contribution of Octanoate to Intact Rat Brain Metabolism Measured by 13C Nuclear Magnetic Resonance Spectroscopy. *The Journal of Neuroscience*, *23*(13), 5928. https://doi.org/10.1523/JNEUROSCI.23-13-05928.2003

Eschbach, J., Schwalenstöcker, B., Soyal, S. M., Bayer, H., Wiesner, D., Akimoto, C., Nilsson, A.-C., Birve, A., Meyer, T., Dupuis, L., Danzer, K. M., Andersen, P. M., Witting, A., Ludolph, A. C., Patsch, W., & Weydt, P. (2013). PGC-1α is a male-specific disease modifier of human and

experimental amyotrophic lateral sclerosis. *Human Molecular Genetics*, *22*(17), 3477–3484. https://doi.org/10.1093/hmg/ddt202

Fagone, P., & Jackowski, S. (2009). Membrane phospholipid synthesis and endoplasmic reticulum function. *Journal of Lipid Research*, *50*, S311–S316. https://doi.org/https://doi.org/10.1194/jlr.R800049-JLR200

Farmer, B. C., Walsh, A. E., Kluemper, J. C., & Johnson, L. A. (2020). Lipid Droplets in Neurodegenerative Disorders. *Front Neurosci*, *14*, 742. https://doi.org/10.3389/fnins.2020.00742

Ferrante, R. J., Browne, S. E., Shinobu, L. A., Bowling, A. C., Baik, M. J., MacGarvey, U., Kowall, N. W., Brown Jr, R. H., & Beal, M. F. (1997). Evidence of Increased Oxidative Damage in Both Sporadic and Familial Amyotrophic Lateral Sclerosis. *Journal of Neurochemistry*, *69*(5), 2064–2074. https://doi.org/https://doi.org/10.1046/j.1471-4159.1997.69052064.x

Ferris, H. A., Perry, R. J., Moreira, G. V., Shulman, G. I., Horton, J. D., & Kahn, C. R. (2017). Loss of astrocyte cholesterol synthesis disrupts neuronal function and alters whole-body metabolism. *Proceedings of the National Academy of Sciences*, *114*(5), 1189–1194. https://doi.org/10.1073/pnas.1620506114

Filippov, V., Song, M. A., Zhang, K., Vinters, H. V., Tung, S., Kirsch, W. M., Yang, J., & Duerksen-Hughes, P. J. (2012). Increased Ceramide in Brains with Alzheimer's and Other Neurodegenerative Diseases. *Journal of Alzheimer's Disease*, *29*(3), 537–547. https://doi.org/10.3233/JAD-2011-111202

Freyre, C. A. C., Rauher, P. C., Ejsing, C. S., & Klemm, R. W. (2019). MIGA2 Links Mitochondria, the ER, and Lipid Droplets and Promotes De Novo Lipogenesis in Adipocytes. *Mol Cell*, *76*(5), 811–825 e814. https://doi.org/10.1016/j.molcel.2019.09.011

Genge, A., Wainwright, S., & Vande Velde, C. (2024). Amyotrophic lateral sclerosis: exploring pathophysiology in the context of treatment. *Amyotroph Lateral Scler Frontotemporal Degener*, *25*(3-4), 225–236. https://doi.org/10.1080/21678421.2023.2278503

Girard, V., Goubard, V., Querenet, M., Seugnet, L., Pays, L., Nataf, S., Dufourd, E., Cluet, D., Mollereau, B., & Davoust, N. (2020). Spen modulates lipid droplet content in adult Drosophila glial cells and protects against paraquat toxicity. *Sci Rep*, *10*(1), 20023. https://doi.org/10.1038/s41598-020-76891-9

Goodman, L. D., Ralhan, I., Li, X., Lu, S., Moulton, M. J., Park, Y. J., Zhao, P., Kanca, O., Ghaderpour Taleghani, Z. S., Jacquemyn, J., Shulman, J. M., Ando, K., Sun, K., Ioannou, M. S., & Bellen, H. J. (2024). Tau is required for glial lipid droplet formation and resistance to neuronal oxidative stress. *Nat Neurosci*, *27*(10), 1918–1933. https://doi.org/10.1038/s41593-024-01740-1

Goyal, G., Zheng, J., Adam, E., Steffes, G., Jain, M., Klavins, K., & Hummel, T. (2019). Sphingolipid-dependent Dscam sorting regulates axon segregation. *Nat Commun*, *10*(1), 813. https://doi.org/10.1038/s41467-019-08765-2

Gratz, S. J., Rubinstein, C. D., Harrison, M. M., Wildonger, J., & O'Connor-Giles, K. M. (2015). CRISPR-Cas9 Genome Editing in Drosophila. *Current Protocols in Molecular Biology*, *111*(1), 31.32.31–31.32.20. https://doi.org/https://doi.org/10.1002/0471142727.mb3102s111

Gunay, A., Shin, H. H., Gozutok, O., Gautam, M., & Ozdinler, P. H. (2021). Importance of lipids for upper motor neuron health and disease. *Semin Cell Dev Biol*, *112*, 92–104. https://doi.org/10.1016/j.semcdb.2020.11.004

Hamilton, J. A., Hillard, C. J., Spector, A. A., & Watkins, P. A. (2007). Brain Uptake and Utilization of Fatty Acids, Lipids and Lipoproteins: Application to Neurological Disorders. *Journal of Molecular Neuroscience*, *33*(1), 2–11. https://doi.org/10.1007/s12031-007-0060-1

Hannun, Y. A., & Obeid, L. M. (2018). Sphingolipids and their metabolism in physiology and disease. *Nat Rev Mol Cell Biol*, *19*(3), 175–191. https://doi.org/10.1038/nrm.2017.107

Hartmann, H., Ho, W. Y., Chang, J. C., & Ling, S. C. (2022). Cholesterol dyshomeostasis in amyotrophic lateral sclerosis: cause, consequence, or epiphenomenon? *FEBS J*, *289*(24), 7688–7709. https://doi.org/10.1111/febs.16175

Haynes, P. R., Pyfrom, E. S., Li, Y., Stein, C., Cuddapah, V. A., Jacobs, J. A., Yue, Z., & Sehgal, A. (2024). A neuron-glia lipid metabolic cycle couples daily sleep to mitochondrial homeostasis. *Nat Neurosci*, *27*(4), 666–678. https://doi.org/10.1038/s41593-023-01568-1

He, X., Huang, Y., Li, B., Gong, C.-X., & Schuchman, E. H. (2010). Deregulation of sphingolipid metabolism in Alzheimer's disease. *Neurobiology of Aging*, *31*(3), 398–408. https://doi.org/https://doi.org/10.1016/j.neurobiolaging.2008.05.010

Hegde, K. N., & Srivastava, A. (2022). Drosophila melanogaster as a Tool for Amyotrophic Lateral Sclerosis Research. *J Dev Biol*, *10*(3). https://doi.org/10.3390/jdb10030036

Henne, W. M., Reynolds, E., & Prinz, W. A. (2025). Lipid droplets: Open questions and conceptual advances around a unique organelle. *J Cell Biol*, *224*(10). https://doi.org/10.1083/jcb.202406019

Henriques, A., Croixmarie, V., Bouscary, A., Mosbach, A., Keime, C., Boursier-Neyret, C., Walter, B., Spedding, M., & Loeffler, J. P. (2017). Sphingolipid Metabolism Is Dysregulated at Transcriptomic and Metabolic Levels in the Spinal Cord of an Animal Model of Amyotrophic Lateral Sclerosis. *Front Mol Neurosci*, *10*, 433. https://doi.org/10.3389/fnmol.2017.00433

Henriques, A., Croixmarie, V., Priestman, D. A., Rosenbohm, A., Dirrig-Grosch, S., D'Ambra, E., Huebecker, M., Hussain, G., Boursier-Neyret, C., Echaniz-Laguna, A., Ludolph, A. C., Platt, F. M., Walther, B., Spedding, M., Loeffler, J.-P., & Gonzalez De Aguilar, J.-L. (2015). Amyotrophic lateral sclerosis and denervation alter sphingolipids and up-regulate glucosylceramide synthase. *Human Molecular Genetics*, *24*(25), 7390–7405. https://doi.org/10.1093/hmg/ddv439

Huang, R., Guo, X., Chen, X., Zheng, Z., Wei, Q., Cao, B., Zeng, Y., & Shang, H. (2015). The serum lipid profiles of amyotrophic lateral sclerosis patients: A study from south-west China and a meta-analysis. *Amyotrophic Lateral Sclerosis and Frontotemporal Degeneration*, *16*(5-6), 359–365. https://doi.org/10.3109/21678421.2015.1047454

Hussain, G., Wang, J., Rasul, A., Anwar, H., Imran, A., Qasim, M., Zafar, S., Kamran, S. K. S., Razzaq, A., Aziz, N., Ahmad, W., Shabbir, A., Iqbal, J., Baig, S. M., & Sun, T. (2019). Role of cholesterol and sphingolipids in brain development and neurological diseases. *Lipids Health Dis*, *18*(1), 26. https://doi.org/10.1186/s12944-019-0965-z

Iguchi, Y., Katsuno, M., Takagi, S., Ishigaki, S., Niwa, J.-i., Hasegawa, M., Tanaka, F., & Sobue, G. (2012). Oxidative stress induced by glutathione depletion reproduces pathological modifications of TDP-43 linked to TDP-43 proteinopathies. *Neurobiology of Disease*, *45*(3), 862–870. https://doi.org/https://doi.org/10.1016/j.nbd.2011.12.002

Ikonen, E. (2008). Cellular cholesterol trafficking and compartmentalization. *Nature Reviews Molecular Cell Biology*, *9*(2), 125–138. https://doi.org/10.1038/nrm2336

Ilieva, H., Polymenidou, M., & Cleveland, D. W. (2009). Non-cell autonomous toxicity in neurodegenerative disorders: ALS and beyond. *J Cell Biol*, *187*(6), 761–772. https://doi.org/10.1083/jcb.200908164

Islam, M. N., Mandal, N., Khanom, N. I., Spivey, A. L., Patel, A. S., Ahmed, T., Islam, R., & Bhuiyan, M. I. H. (2025). Sphingolipid Signaling and Metabolism in Neuronal and Glial Cells: Implications for Cerebrovascular and Neurodegenerative Disorders. *Aging Dis*. https://doi.org/10.14336/AD.2025.1024

Jana, A., Hogan, E. L., & Pahan, K. (2009). Ceramide and neurodegeneration: Susceptibility of neurons and oligodendrocytes to cell damage and death. *Journal of the Neurological Sciences*, *278*(1), 5–15. https://doi.org/https://doi.org/10.1016/j.jns.2008.12.010

Jang, H. J., Le, M. U. T., Park, J. H., Chung, C. G., Shon, J. G., Lee, G. S., Moon, J. H., Lee, S. B., Choi, J. S., Lee, T. G., & Yoon, S. (2021). Matrix-Assisted Laser Desorption/Ionization Mass Spectrometry Imaging of Phospholipid Changes in a Drosophila Model of Early Amyotrophic Lateral Sclerosis. *J Am Soc Mass Spectrom*, *32*(10), 2536–2545. https://doi.org/10.1021/jasms.1c00167

Jésus, P., Fayemendy, P., Nicol, M., Lautrette, G., Sourisseau, H., Preux, P. M., Desport, J. C., Marin, B., & Couratier, P. (2018). Hypermetabolism is a deleterious prognostic factor in patients with amyotrophic lateral sclerosis. *European Journal of Neurology*, *25*(1), 97–104. https://doi.org/https://doi.org/10.1111/ene.13468

Karten, B., Campenot, R. B., Vance, D. E., & Vance, J. E. (2006). Expression of ABCG1, but Not ABCA1, Correlates with Cholesterol Release by Cerebellar Astroglia*. *Journal of Biological Chemistry*, *281*(7), 4049–4057. https://doi.org/https://doi.org/10.1074/jbc.M508915200

Kim, Y., Mavodza, G., Senkal, C. E., & Burd, C. G. (2023). Cholesterol-dependent homeostatic regulation of very long chain sphingolipid synthesis. *J Cell Biol*, *222*(12). https://doi.org/10.1083/jcb.202308055

Kors, S., Costello, J. L., & Schrader, M. (2022). VAP Proteins - From Organelle Tethers to Pathogenic Host Interactors and Their Role in Neuronal Disease. *Front Cell Dev Biol*, *10*, 895856. https://doi.org/10.3389/fcell.2022.895856

Kozlova, A., Zhang, S., Sudwarts, A., Zhang, H., Smirnou, S., Sun, X., Stephenson, K., Zhao, X., Jamison, B., Ponnusamy, M., He, X., Pang, Z. P., Sanders, A. R., Bellen, H. J., Thinakaran, G., & Duan, J. (2024). Alzheimer's disease risk allele of PICALM causes detrimental lipid droplets in microglia. *Res Sq*. https://doi.org/10.21203/rs.3.rs-4407146/v1

Kraut, R. (2011). Roles of sphingolipids in Drosophila development and disease. *J Neurochem*, *116*(5), 764–778. https://doi.org/10.1111/j.1471-4159.2010.07022.x

Kuge, O., Nishijima, M., & Akamatsu, Y. (1986). Phosphatidylserine biosynthesis in cultured Chinese hamster ovary cells. III. Genetic evidence for utilization of phosphatidylcholine and phosphatidylethanolamine as precursors. *Journal of Biological Chemistry*, *261*(13), 5795–5798. https://doi.org/https://doi.org/10.1016/S0021-9258(17)38452-1

Layalle, S., They, L., Ourghani, S., Raoul, C., & Soustelle, L. (2021). Amyotrophic Lateral Sclerosis Genes in Drosophila melanogaster. *Int J Mol Sci*, *22*(2). https://doi.org/10.3390/ijms22020904

Lee, J., Kosaras, B., Del Signore, S. J., Cormier, K., McKee, A., Ratan, R. R., Kowall, N. W., & Ryu, H. (2011). Modulation of lipid peroxidation and mitochondrial function improves neuropathology in Huntington's disease mice. *Acta Neuropathologica*, *121*(4), 487–498. https://doi.org/10.1007/s00401-010-0788-5

Li, J., Wang, X., Zhang, T., Wang, C., Huang, Z., Luo, X., & Deng, Y. (2015). A review on phospholipids and their main applications in drug delivery systems. *Asian Journal of Pharmaceutical Sciences*, *10*(2), 81–98. https://doi.org/https://doi.org/10.1016/j.ajps.2014.09.004

Liguori, F., Amadio, S., & Volonté, C. (2021). Where and Why Modeling Amyotrophic Lateral Sclerosis. *International Journal of Molecular Sciences*, *22*(8), 3977.

Linetti, A., Fratangeli, A., Taverna, E., Valnegri, P., Francolini, M., Cappello, V., Matteoli, M., Passafaro, M., & Rosa, P. (2010). Cholesterol reduction impairs exocytosis of synaptic vesicles. *Journal of Cell Science*, *123*(4), 595–605. https://doi.org/10.1242/jcs.060681

Liping Wang, G. L., Zhongyuan Zuo, Yarong Li, Seul Kee Byeon, Akhilesh Pandey, Hugo J. Bellen. (2022). Neuronal activity induces glucosylceramide that is secreted via exosomes for lysosomal degradation in glia. *Science Advances*.

Liu, J., Luo, X., Chen, X., & Shang, H. (2020). Lipid Profile in Patients With Amyotrophic Lateral Sclerosis: A Systematic Review and Meta-Analysis. *Front Neurol*, *11*, 567753. https://doi.org/10.3389/fneur.2020.567753

Long, J., Liu, S., Shi, Y., Zhang, C., Qin, L., & Ai, Q. (2026). Targeting lipid metabolism in neurodegenerative diseases: From experimental to clinical. *Metabolism*, *175*, 156436. https://doi.org/10.1016/j.metabol.2025.156436

Mathiowetz, A. J., & Olzmann, J. A. (2024). Lipid droplets and cellular lipid flux. *Nat Cell Biol*, *26*(3), 331–345. https://doi.org/10.1038/s41556-024-01364-4

McBenedict, B., Hauwanga, W. N., Nezam, U., Ko Oo, A., Eapi, S., Pradhan, S., Dang, N. B., Cher, P. W., Orsini, M. A., & Lima Pessoa, B. (2025). Amyotrophic Lateral Sclerosis (ALS) Type 8: A Narrative Review. *Cureus*, *17*(1), e76717. https://doi.org/10.7759/cureus.76717

McCluskey, G., Donaghy, C., Morrison, K. E., McConville, J., Duddy, W., & Duguez, S. (2022). The Role of Sphingomyelin and Ceramide in Motor Neuron Diseases. *J Pers Med*, *12*(9). https://doi.org/10.3390/jpm12091418

Mejhert, N., Gabriel, K. R., Frendo-Cumbo, S., Krahmer, N., Song, J., Kuruvilla, L., Chitraju, C., Boland, S., Jang, D. K., von Grotthuss, M., Costanzo, M. C., Ryden, M., Olzmann, J. A., Flannick, J., Burtt, N. P., Farese, R. V., Jr., & Walther, T. C. (2022). The Lipid Droplet Knowledge Portal: A resource for systematic analyses of lipid droplet biology. *Dev Cell*, *57*(3), 387–397 e384. https://doi.org/10.1016/j.devcel.2022.01.003

Mencarelli, C., & Martinez-Martinez, P. (2013). Ceramide function in the brain: when a slight tilt is enough. *Cell Mol Life Sci*, *70*(2), 181–203. https://doi.org/10.1007/s00018-012-1038-x

Mesmin, B., Kovacs, D., & D'Angelo, G. (2019). Lipid exchange and signaling at ER-Golgi contact sites. *Curr Opin Cell Biol*, *57*, 8–15. https://doi.org/10.1016/j.ceb.2018.10.002

Morell, P., & Jurevics, H. (1996). Origin of cholesterol in myelin. *Neurochemical Research*, *21*(4), 463–470. https://doi.org/10.1007/BF02527711

Moulton, M. J., Barish, S., Ralhan, I., Chang, J., Goodman, L. D., Harland, J. G., Marcogliese, P. C., Johansson, J. O., Ioannou, M. S., & Bellen, H. J. (2021). Neuronal ROS-induced glial lipid droplet formation is altered by loss of Alzheimer's disease-associated genes. *Proc Natl Acad Sci U S A*, *118*(52). https://doi.org/10.1073/pnas.2112095118

Murage, B., Tan, H., Mashimo, T., Jackson, M., & Skehel, P. A. (2024). Spinal cord neurone loss and foot placement changes in a rat knock-in model of amyotrophic lateral sclerosis Type 8. *Brain Commun*, *6*(3), fcae184. https://doi.org/10.1093/braincomms/fcae184

Nguyen, T. B., & Olzmann, J. A. (2017). Lipid droplets and lipotoxicity during autophagy. *Autophagy*, *13*(11), 2002–2003. https://doi.org/10.1080/15548627.2017.1359451

Nishimura, A. L., Mitne-Neto, M., Silva, H. C. A., Richieri-Costa, A., Middleton, S., Cascio, D., Kok, F., Oliveira, J. R. M., Gillingwater, T., Webb, J., Skehel, P., & Zatz, M. (2004). A Mutation in the Vesicle-Trafficking Protein VAPB Causes Late-Onset Spinal Muscular Atrophy and Amyotrophic Lateral Sclerosis. *The American Journal of Human Genetics*, *75*(5), 822–831. https://doi.org/10.1086/425287

Paganoni, S., Deng, J., Jaffa, M., Cudkowicz, M. E., & Wills, A.-M. (2011). Body mass index, not dyslipidemia, is an independent predictor of survival in amyotrophic lateral sclerosis. *Muscle & Nerve*, *44*(1), 20–24. https://doi.org/https://doi.org/10.1002/mus.22114

Pan, X., Dutta, D., Lu, S., & Bellen, H. J. (2023). Sphingolipids in neurodegenerative diseases. *Front Neurosci*, *17*, 1137893. https://doi.org/10.3389/fnins.2023.1137893

Pant, D. C., Aguilera-Albesa, S., & Pujol, A. (2020). Ceramide signalling in inherited and multifactorial brain metabolic diseases. *Neurobiol Dis*, *143*, 105014. https://doi.org/10.1016/j.nbd.2020.105014

Pinto, S. N., Silva, L. C., Futerman, A. H., & Prieto, M. (2011). Effect of ceramide structure on membrane biophysical properties: The role of acyl chain length and unsaturation. *Biochimica et Biophysica Acta (BBA) - Biomembranes*, *1808*(11), 2753–2760. https://doi.org/https://doi.org/10.1016/j.bbamem.2011.07.023

Rachakonda, V., Pan Th Fau - Le, W. D., & Le, W. D. (2004). Biomarkers of neurodegenerative disorders: how good are they? *Cell research*, *14*(5), 349–360.

Raghu, P., Basak, B., & Krishnan, H. (2021). Emerging perspectives on multidomain phosphatidylinositol transfer proteins. *Biochim Biophys Acta Mol Cell Biol Lipids*, *1866*(9), 158984. https://doi.org/10.1016/j.bbalip.2021.158984

Ratnaparkhi, A., Lawless, G. M., Schweizer, F. E., Golshani, P., & Jackson, G. R. (2008). A Drosophila model of ALS: human ALS-associated mutation in VAP33A suggests a dominant negative mechanism. *PLoS One*, *3*(6), e2334. https://doi.org/10.1371/journal.pone.0002334

Reiter, L. T., Potocki, L., Chien, S., Gribskov, M., & Bier, E. (2001). A Systematic Analysis of Human Disease-Associated Gene Sequences In Drosophila melanogaster [10.1101/gr.169101]. *Genome Research*, *11*(6), 1114–1125. https://doi.org/10.1101/gr.169101

Rickman, O. J., Baple, E. L., & Crosby, A. H. (2020). Lipid metabolic pathways converge in motor neuron degenerative diseases. *Brain*, *143*(4), 1073–1087. https://doi.org/10.1093/brain/awz382

Robelin, L., & Gonzalez De Aguilar, J. L. (2014). Blood Biomarkers for Amyotrophic Lateral Sclerosis: Myth or Reality? *BioMed Research International*, *2014*(1), 525097. https://doi.org/https://doi.org/10.1155/2014/525097

Robenek, H., Hofnagel, O., Buers, I., Robenek, M. J., Troyer, D., & Severs, N. J. (2006). Adipophilin-enriched domains in the ER membrane are sites of lipid droplet biogenesis. *Journal of Cell Science*, *119*(20), 4215–4224. https://doi.org/10.1242/jcs.03191

Ross, B. M., Moszczynska, A., Blusztajn, J. K., Sherwin, A., Lozano, A., & Kish, S. J. (1997). Phospholipid biosynthetic enzymes in human brain. *Lipids*, *32*(4), 351–358. https://doi.org/https://doi.org/10.1007/s11745-997-0044-x

Ruipérez, V., Darios, F., & Davletov, B. (2010). Alpha-synuclein, lipids and Parkinson's disease. *Progress in Lipid Research*, *49*(4), 420–428. https://doi.org/https://doi.org/10.1016/j.plipres.2010.05.004

Sanhueza, M., Chai, A., Smith, C., McCray, B. A., Simpson, T. I., Taylor, J. P., & Pennetta, G. (2015). Network analyses reveal novel aspects of ALS pathogenesis. *PLoS Genet*, *11*(3), e1005107. https://doi.org/10.1371/journal.pgen.1005107

Schmitt, F., Hussain, G., Dupuis, L., Loeffler, J. P., & Henriques, A. (2014). A plural role for lipids in motor neuron diseases: energy, signaling and structure. *Front Cell Neurosci*, *8*, 25. https://doi.org/10.3389/fncel.2014.00025

Shi, P., Gal, J., Kwinter, D. M., Liu, X., & Zhu, H. (2010). Mitochondrial dysfunction in amyotrophic lateral sclerosis. *Biochimica et Biophysica Acta (BBA) - Molecular Basis of Disease*, *1802*(1), 45–51. https://doi.org/https://doi.org/10.1016/j.bbadis.2009.08.012

Smolic, T., Tavcar, P., Horvat, A., Cerne, U., Haluzan Vasle, A., Tratnjek, L., Kreft, M. E., Scholz, N., Matis, M., Petan, T., Zorec, R., & Vardjan, N. (2021). Astrocytes in stress accumulate lipid droplets. *Glia*, *69*(6), 1540–1562. https://doi.org/10.1002/glia.23978

Sol, J., Jove, M., Povedano, M., Sproviero, W., Dominguez, R., Pinol-Ripoll, G., Romero-Guevara, R., Hye, A., Al-Chalabi, A., Torres, P., Andres-Benito, P., Area-Gomez, E., Pamplona, R., Ferrer, I., Ayala, V., & Portero-Otin, M. (2021). Lipidomic traits of plasma and cerebrospinal fluid in amyotrophic lateral sclerosis correlate with disease progression. *Brain Commun*, *3*(3), fcab143. https://doi.org/10.1093/braincomms/fcab143

Steyaert, J., Scheveneels, W., Vanneste, J., Van Damme, P., Robberecht, W., Callaerts, P., Bogaert, E., & Van Den Bosch, L. (2018). FUS-induced neurotoxicity in Drosophila is prevented by downregulating nucleocytoplasmic transport proteins. *Human Molecular Genetics*, *27*(23), 4103–4116. https://doi.org/10.1093/hmg/ddy303

Sultana, R., Perluigi, M., & Butterfield, D. A. (2013). Lipid peroxidation triggers neurodegeneration: A redox proteomics view into the Alzheimer disease brain. *Free Radical Biology and Medicine*, *62*, 157–169. https://doi.org/https://doi.org/10.1016/j.freeradbiomed.2012.09.027

Teixeira, V., Maciel, P., & Costa, V. (2021). Leading the way in the nervous system: Lipid Droplets as new players in health and disease. *Biochim Biophys Acta Mol Cell Biol Lipids*, *1866*(1), 158820. https://doi.org/10.1016/j.bbalip.2020.158820

Tendulkar, S., Hegde, S., Garg, L., Thulasidharan, A., Kaduskar, B., Ratnaparkhi, A., & Ratnaparkhi, G. S. (2022). Caspar, an adapter for VAPB and TER94, modulates the progression of ALS8 by regulating IMD/NFkappaB-mediated glial inflammation in a Drosophila model of human disease. *Hum Mol Genet*, *31*(17), 2857–2875. https://doi.org/10.1093/hmg/ddac076

Thau, N., Knippenberg, S., Körner, S., Rath, K. J., Dengler, R., & Petri, S. (2012). Decreased mRNA Expression of PGC-1α and PGC-1α-Regulated Factors in the SOD1G93A ALS Mouse Model and in Human Sporadic ALS. *Journal of Neuropathology & Experimental Neurology*, *71*(12), 1064–1074. https://doi.org/10.1097/NEN.0b013e318275df4b

Tokutake, Y., Gushima, K., Miyazaki, H., Shimosato, T., & Yonekura, S. (2015). ALS-associated P56S-VAPB mutation restrains 3T3-L1 preadipocyte differentiation. *Biochem Biophys Res Commun*, *460*(3), 831–837. https://doi.org/10.1016/j.bbrc.2015.03.118

Tracey, T. J., Kirk, S. E., Steyn, F. J., & Ngo, S. T. (2021). The role of lipids in the central nervous system and their pathological implications in amyotrophic lateral sclerosis. *Semin Cell Dev Biol*, *112*, 69–81. https://doi.org/10.1016/j.semcdb.2020.08.012

Tracey, T. J., Steyn, F. J., Wolvetang, E. J., & Ngo, S. T. (2018). Neuronal Lipid Metabolism: Multiple Pathways Driving Functional Outcomes in Health and Disease. *Front Mol Neurosci*, *11*, 10. https://doi.org/10.3389/fnmol.2018.00010

Van Damme, P., Robberecht, W., & Van Den Bosch, L. (2017). Modelling amyotrophic lateral sclerosis: progress and possibilities. *Dis Model Mech*, *10*(5), 537–549. https://doi.org/10.1242/dmm.029058

van Es, M. A., Hardiman, O., Chio, A., Al-Chalabi, A., Pasterkamp, R. J., Veldink, J. H., & van den Berg, L. H. (2017). Amyotrophic lateral sclerosis. *The Lancet*, *390*(10107), 2084–2098. https://doi.org/https://doi.org/10.1016/S0140-6736(17)31287-4

Vance, D. E., Choy, P. C., Farren, S. B., Lim, P. H., & Schneider, W. J. (1977). Asymmetry of phospholipid biosynthesis. *Nature*, *270*(5634), 268–269. https://doi.org/10.1038/270268a0

Vance, J. E. (2015). Phospholipid Synthesis and Transport in Mammalian Cells. *Traffic*, *16*(1), 1–18. https://doi.org/https://doi.org/10.1111/tra.12230

Venken, K. J. T., Schulze, K. L., Haelterman, N. A., Pan, H., He, Y., Evans-Holm, M., Carlson, J. W., Levis, R. W., Spradling, A. C., Hoskins, R. A., & Bellen, H. J. (2011). MiMIC: a highly versatile transposon insertion resource for engineering Drosophila melanogaster genes. *Nature Methods*, *8*(9), 737–743. https://doi.org/10.1038/nmeth.1662

Voelzmann, A., & Bauer, R. (2010). Ceramide synthases in mammalians, worms, and insects: emerging schemes. *Biomol Concepts*, *1*(5-6), 411–422. https://doi.org/10.1515/bmc.2010.028

Vos, M., Dulovic-Mahlow, M., Mandik, F., Frese, L., Kanana, Y., Haissatou Diaw, S., Depperschmidt, J., Bohm, C., Rohr, J., Lohnau, T., Konig, I. R., & Klein, C. (2021). Ceramide accumulation induces mitophagy and impairs beta-oxidation in PINK1 deficiency. *Proc Natl Acad Sci U S A*, *118*(43). https://doi.org/10.1073/pnas.2025347118

Walther, T. C., & Farese, R. V., Jr. (2012). Lipid droplets and cellular lipid metabolism. *Annu Rev Biochem*, *81*, 687–714. https://doi.org/10.1146/annurev-biochem-061009-102430

Wang, X., Rao, R. P., Kosakowska-Cholody, T., Masood, M. A., Southon, E., Zhang, H., Berthet, C., Nagashim, K., Veenstra, T. K., Tessarollo, L., Acharya, U., & Acharya, J. K. (2009). Mitochondrial degeneration and not apoptosis is the primary cause of embryonic lethality in ceramide transfer protein mutant mice. *J Cell Biol*, *184*(1), 143–158. https://doi.org/10.1083/jcb.200807176

Weber-Boyvat, M., Kentala, H., Peranen, J., & Olkkonen, V. M. (2015). Ligand-dependent localization and function of ORP-VAP complexes at membrane contact sites. *Cell Mol Life Sci*, *72*(10), 1967–1987. https://doi.org/10.1007/s00018-014-1786-x

Weiss, S. B., Smith, S. W., & Kennedy, E. P. (1958). The enzymatic formation of lecithin from cytidine diphosphate choline and D-1,2-diglyceride. *Journal of Biological Chemistry*, *231*(1), 53–64. https://doi.org/https://doi.org/10.1016/S0021-9258(19)77284-6

Wiedau-Pazos, M., Goto, J. J., Rabizadeh, S., Gralla, E. B., Roe, J. A., Lee, M. K., Valentine, J. S., & Bredesen, D. E. (1996). Altered Reactivity of Superoxide Dismutase in Familial Amyotrophic Lateral Sclerosis. *Science*, *271*(5248), 515–518. https://doi.org/10.1126/science.271.5248.515

Wong, H. C., Lang, A. E., Stein, C., & Drerup, C. M. (2024). ALS-Linked VapB P56S Mutation Alters Neuronal Mitochondrial Turnover at the Synapse. *J Neurosci*, *44*(35). https://doi.org/10.1523/JNEUROSCI.0879-24.2024

Wright, M. M., & McMaster, C. R. (2002). PC and PE synthesis: Mixed micellar analysis of the cholinephosphotransferase and ethanolaminephosphotransferase activities of human choline/ethanolamine phosphotransferase 1 (CEPT1). *Lipids*, *37*(7), 663–672. https://doi.org/https://doi.org/10.1007/s11745-002-0947-6

Yang, D., Wang, X., Zhang, L., Fang, Y., Zheng, Q., Liu, X., Yu, W., Chen, S., Ying, J., & Hua, F. (2022). Lipid metabolism and storage in neuroglia: role in brain development and neurodegenerative diseases. *Cell Biosci*, *12*(1), 106. https://doi.org/10.1186/s13578-022-00828-0

Yang, L., Liang, J., Lam, S. M., Yavuz, A., Shui, G., Ding, M., & Huang, X. (2020). Neuronal lipolysis participates in PUFA-mediated neural function and neurodegeneration. *EMBO Rep*, *21*(11), e50214. https://doi.org/10.15252/embr.202050214

Yuyama, K., Sun, H., Mitsutake, S., & Igarashi, Y. (2012). Sphingolipid-modulated Exosome Secretion Promotes Clearance of Amyloid-β by Microglia. *Journal of Biological Chemistry*, *287*(14), 10977–10989. https://doi.org/https://doi.org/10.1074/jbc.M111.324616

Zhai, J., Ström, A.-L., Kilty, R., Venkatakrishnan, P., White, J., Everson, W. V., Smart, E. J., & Zhu, H. (2009). Proteomic characterization of lipid raft proteins in amyotrophic lateral sclerosis mouse spinal cord. *The FEBS Journal*, *276*(12), 3308–3323. https://doi.org/https://doi.org/10.1111/j.1742-4658.2009.07057.x

Zhan, L., Xie, Q., & Tibbetts, R. S. (2015). Opposing roles of p38 and JNK in a Drosophila model of TDP-43 proteinopathy reveal oxidative stress and innate immunity as pathogenic components of neurodegeneration. *Human Molecular Genetics*, *24*(3), 757–772. https://doi.org/10.1093/hmg/ddu493

Zhang, L., Zhou, Y., Yang, Z., Jiang, L., Yan, X., Zhu, W., Shen, Y., Wang, B., Li, J., & Song, J. (2025). Lipid droplets in central nervous system and functional profiles of brain cells containing lipid droplets in various diseases. *J Neuroinflammation*, *22*(1), 7. https://doi.org/10.1186/s12974-025-03334-5

Zhao, X., Li, Y., Zhang, S., Sudwarts, A., Zhang, H., Kozlova, A., Moulton, M. J., Goodman, L. D., Pang, Z. P., Sanders, A. R., Bellen, H. J., Thinakaran, G., & Duan, J. (2025). Alzheimer's disease protective allele of Clusterin modulates neuronal excitability through lipid-droplet-

mediated neuron-glia communication. *Mol Neurodegener*, *20*(1), 51. https://doi.org/10.1186/s13024-025-00840-1

Zhou, L., & Xu, R. (2024). Invertebrate genetic models of amyotrophic lateral sclerosis [Review]. *Frontiers in Molecular Neuroscience*, *Volume 17 - 2024*.

Zhu, Y., Cho, K., Lacin, H., Zhu, Y., DiPaola, J. T., Wilson, B. A., Patti, G., & Skeath, J. B. (2025). Loss of dihydroceramide desaturase drives neurodegeneration by disrupting endoplasmic reticulum and lipid droplet homeostasis in glial cells. *Elife*, *13*. https://doi.org/10.7554/eLife.99344

# Chapter II

# Introduction to VAPB and In Silico Prediction of *Drosophila* VAP interactors

## 2.1 Abstract

VAPB is an evolutionarily conserved ER membrane protein that plays a central role in the maintenance of cellular functions through interacting with diverse range of proteins. VAPB belongs to the family of VAP proteins and contains three functional domains. Out of these, Major Sperm Protein (MSP) domain faces towards the cytosol which interacts with more than 250 proteins in the mammalian cell and helps in membrane-membrane contact site formation. By tethering the organelles to ER membrane, VAPB helps in lipid transfer, mitochondrial functioning, autophagy and calcium homeostasis. Interestingly, in *Drosophila* only 36 proteins have been discovered so far which is quite surprising as it shares similar domains and structure to the mammalian VAPB. Previous studies have mostly focused towards *ALS8* allele whereas endogenous role of VAPB has not been explored well in *Drosophila.* To address this gap, a comprehensive database is generated compiling human VAMP Associated Protein A and B (VAPA/B) physical interactors through available databases and identifying their *Drosophila* homologs. This revealed a substantial number of conserved proteins between both species highlighting the potential for undiscovered VAP interactors in *Drosophila.*

Since a number of VAPA and VAPB physical interactors contain FFAT (two phenylalanines in an acidic tract) motif that interact with MSP domain, in silico prediction was performed to predict the potential interactors of *Drosophila* VAP which may bind through canonical or non-canonical FFAT motif. Using sequence based screening, predicted interactors are classified into four FFAT motif types. Some of interactors were correctly predicted proved by individual studies whereas uncharacterized proteins containing potential FFAT motifs have also been identified in the study. Although the predictions are based solely on sequence analysis and require further validations, these findings offer an organized framework for future proteomic and genetic studies at understanding the conserved and context dependent roles of VAP proteins in cellular homeostasis.

## 2.2 Introduction

**2.2.1 VAPB- Structure and Functions:** VAPB belongs to the family of VAP proteins and has different isoforms such as VAPA, MOSPD1/2/3 (Motile Sperm Domain-Containing Protein 1/2/3) (James & Kehlenbach, 2021). It is named as VAPB because of its ability to interact with VAMP protein and initially cloned from the marine mollusk *Aplysia californica* (Kors, Costello, et al., 2022). VAPB is conserved across all eukaryotic species and known to interact with a large pool of proteins (James & Kehlenbach, 2021). VAPB is a type II integral ER membrane protein with three domains namely Major Sperm Protein (MSP) domain, Coiled-Coil Domain (CCD) and Trans-Membrane Domain (TMD) (Wyles & Ridgway, 2004). The N terminal MSP domain faces towards the cytosol consisting immunoglobin like β sheet and share similarity with MSP protein of *Ascaris suum.* The VAP family proteins is known to dimerize through their CCD domain and also known to interact with SNARE proteins. VAP family proteins are single pass membrane proteins inserted into the ER membrane through their TMD domain with short C-terminus tail inside the ER lumen (Mesmin et al., 2019). VAPA and VAPB has around 63% sequence similarity and share huge number of common binding partners (Kamemura & Chihara, 2019). VAPB is ubiquitously expressed and known to form membrane-membrane contact sites (MCS) with proteins from other organelles and helps in performing variety of functions (Alpy et al., 2013; Chen et al., 2022; Cockcroft & Raghu, 2018; Freyre et al., 2019; Kumagai & Hanada, 2019; Mesmin et al., 2019; Weber-Boyvat et al., 2015; Xu et al., 2020). VAPB has been associated with a number of cellular processes such as vesicle trafficking, calcium homeostasis, lipid transfer, membrane tethering, autophagy, unfolded protein response and mitochondrial functioning (Tendulkar et al., 2022). Moreover, they have been shown to perform non-cell autonomous functions by cleaving and releasing MSP domain outside the cell which act as ligand for receptors on the receiving end (Tsuda et al., 2008).

**2.2.2 VAPA and VAPB physical interactors:** Mammalian VAPB is known to interact with more than 250 proteins (www.thebiogrid.org) which are involved in various cellular processes. Around 50 proteins are experimentally proved to be in physical interaction with VAP proteins {Kors, 2022 #39}. Many of these proteins interact with the MSP domain of the VAP with FFAT motif (two phenylananines in an acidic tract) (Slee & Levine, 2019). Conventional FFAT motif consists of the core sequence "EFFDA-E" surrounded by acidic amino acid residues. Initially, acidic AA sequence upstream of the core sequence binds to the basic electropositive surface of MSP after which the

motif binds to K87 and M89 to form a stable complex (Murphy & Levine, 2016). The variability in FFAT sequence can affect the affinity for protein binding and some of these interactors may contain one or no phenylalanine at all (Di Mattia et al., 2020; Slee & Levine, 2019). Also, major portion of VAPB interactors do not contain FFAT motif suggesting other regions maybe involved in the interaction (Kors, Schrader, et al., 2022). These interactions are important for performing several functions. One of these examples is organelle tethering where proteins like PTPIP51, MIGA2 (Mitoguardian 2) are involved in ER-mitochondria tethering (Gomez-Suaga et al., 2017; Kors, Schrader, et al., 2022; Xu et al., 2020). OSBP (Oxysterol Binding Protein), CERT1 (Ceramide Transfer 1), PITPNM1/2/3 (Phosphatidylinositol Transfer Protein, Membrane-Associated 1/2/3), FAPP2 (Four-Phosphate Adaptor Protein 2), STARD3 (StAR-related lipid transfer domain 3) are active in ER-Golgi and ER-PM contact sites where they play crucial role in lipid transport (Alpy et al., 2013; Cockcroft et al., 2016; Di Mattia et al., 2020; Kumagai & Hanada, 2019; Olkkonen, 2015; Xu et al., 2020). VPS13A/D (Vacuolar Protein Sorting 13 A/D) are important for lipid transport between ER to mitochondria whereas VPS13A/C (Vacuolar Protein Sorting 13 A/C) are important for ER-LD contact sites (Chen et al., 2022; Yeshaw et al., 2019). Recently, VAPB has been shown to interact with ACBD4/5 (Acyl-CoA Binding Domain 4/5) to establish ER-peroxisome contact sites (Costello et al., 2017). VAPB plays an important role in autophagy as well where it interacts with ULK1 (Unc-51-Like autophagy activating Kinase 1) complex (Zhao et al., 2018). But not all proteins are involved in organelle tethering. For example, VAPB interacts with FAF1 which makes complex with VCP/p97 (Valosin Containing Protein), involved in proteosomal degradation (Baron et al., 2014; Tendulkar et al., 2022). VAPB is shown to interact with STING (Stimulator of Interferon Genes) in the ER membrane which is one of the regulators of inflammation via NFkB pathway (Ji et al., 2025). Also, Nup358 (Nucleoporin 358) interacts with VAPB which mediates ER-mitochondria contact sites (Kalarikkal et al., 2024). Thus, VAPB seems to be the central player in the cell which is quite important for normal functioning of the cell and its loss can have drastic effect on cellular health (Borgese et al., 2021)(Fig. 2.1).

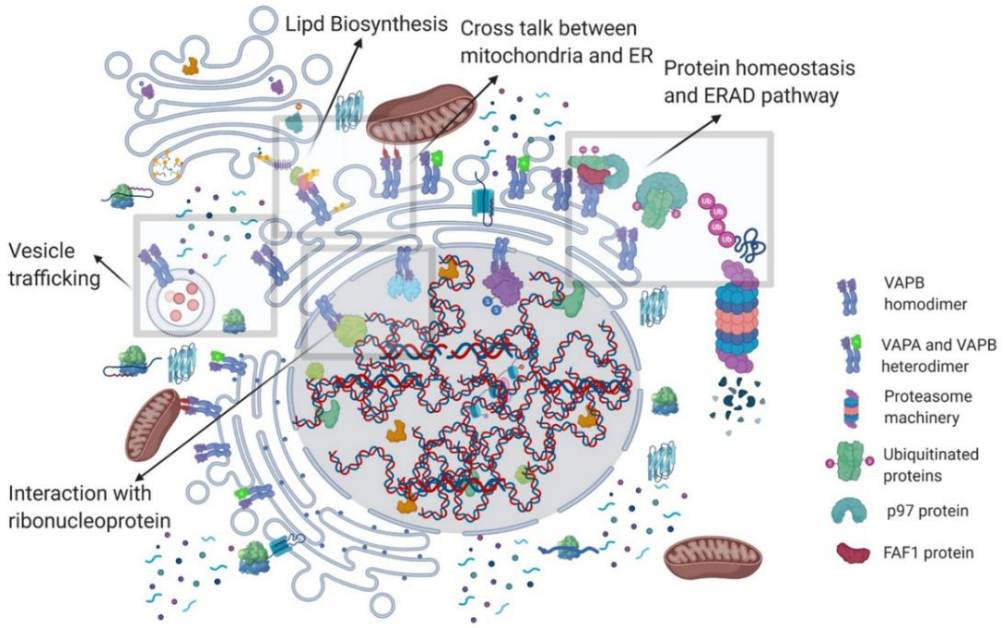



**Figure 2.1: Schematic diagram of VAPB roles in the cellular homeostasis.**

Cellular functions involving VAPA and VAPB are shown in the above figure where both are present at ER membrane and interacts with different proteins and organelles. Some of the major functions are shown in a box. (Biorender.com)

**2.2.3 VAP roles in *Drosophila:*** Unlike mammals, *Drosophila* has single isoform of VAPB also known as VAP-33A (Tsuda et al., 2008). VAP is quite important in terms of axonal growth, dendritic arborization and overall brain function (Deivasigamani et al., 2014; Han et al., 2012; Kamiyama et al., 2024; Moustaqim-Barrette et al., 2014; Ratnaparkhi et al., 2008; Tsuda et al., 2008; Xu et al., 2020). *VAP* null has been found to be pupal lethal and neuronal knockdown of *VAP* also leads to the lethality (Kamiyama et al., 2024; Ratnaparkhi et al., 2008; Tsuda et al., 2008). In terms of VAP functions, *Drosophila* VAP has always been studied from the lens of *ALS8* mutant as it shares conserved sequence in terms of domains and functions (Chaplot et al., 2019; Han et al., 2012; McBenedict et al., 2025; Ratnaparkhi et al., 2008; Tendulkar et al., 2022; Thulasidharan et al., 2024; Tsuda et al., 2008). But VAP endogenous roles have not been explored very well. Till now, 36 proteins are known to physically interact with VAP (http://flybase.org). Interestingly, most of these proteins have been shown to play an important role in the brain development and NMJ architecture (Deivasigamani et al., 2014; Han et al., 2012; Ratnaparkhi et al., 2008). Some of these functions are synapse formation, bouton size regulation, axonal guidance and retinal degeneration (Cockcroft et

al., 2016; Han et al., 2012; Mishra et al., 2024; Tsuda et al., 2008). Also, VAP interaction with proteins such as OSBP, CG9205, RdgB (Retinal degeneration B), CERT, Sac1 is crucial for maintaining ER-Golgi lipid homeostasis (Kumagai & Hanada, 2019; Mishra et al., 2024; Sanhueza et al., 2015)(Fig. 2.2). Similarly, VAP interaction with Miga (Mitoguardian) has been shown to play important role in ER-mitochondria network (Xu et al., 2020). Recent study highlights VAP role in cell growth and proliferation where it interacts with l(2)gl and hpo to play essential role in Notch signaling (Portela et al., 2024). VAP interaction with Acbp7 which is homolog of ACBD4/5 shows that *Drosophila* VAP is quite conserved in terms of its functions as it is important for peroxisome functioning (Kors et al., 2024). In case of *ALS8* mutant, *Drosophila* model has been extensively studied where it is shown to be genetic interactor of other ALS loci such as *SOD1/*ALS1, *VCP/ALS14 (Chaplot et al., 2019; Tendulkar et al., 2022).* Atg1 which is homolog of ULK1 has reported to be affected in *ALS8* suggesting VAP plays an important role in autophagy as well (Zhao et al., 2018). As *Drosophila* VAP shares conserved sequence with the mammalian VAPB and common interacting partners. *Drosophila* becomes an ideal organism to study VAP functions in the flies and looking for new interacting partners of VAP which may be characterized in the flies also.

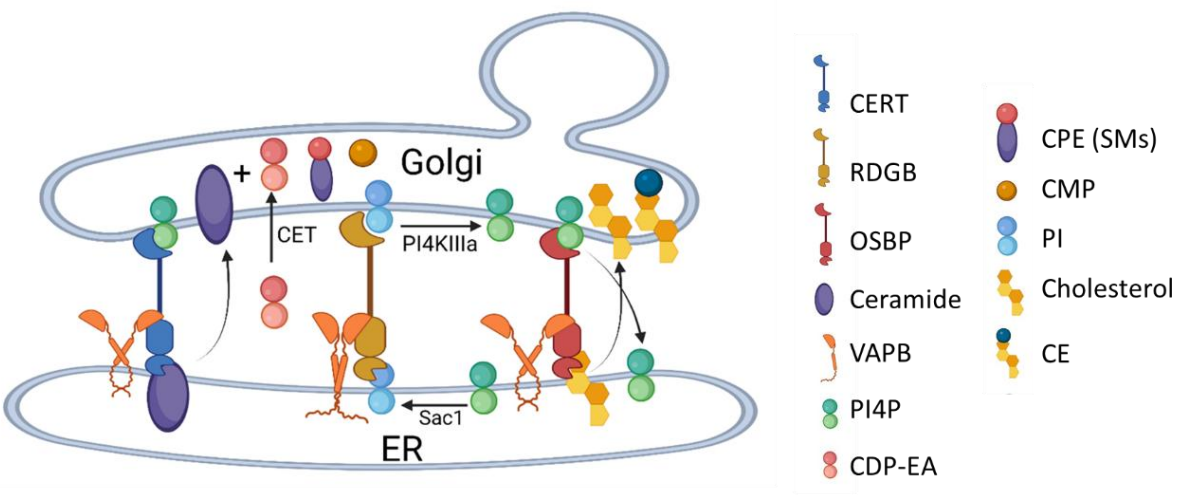



**Figure 2.2: *Drosophila* VAP roles in lipid transfer at ER-Golgi network.**

*Drosophila* VAP plays an important role at ER-Golgi network where it interacts with various proteins to transfer lipids from the ER membrane. Proteins listed here are shown to interact with VAP and perform their functions. (Biorender.com)

## 2.3 Results

**2.3.1 *Drosophila* homologs of Human VAPA and VAPB interactors:** From mammalian studies, using various techniques such as immunoprecipitation, mass spectrometry, affinity based experiments, different databases have been generated which are publicly available such as bioplex network, string network as described in Materials and Methods to find VAPA or VAPB interactors. More than 400 proteins have been found to interact with VAPs in mammals whereas in *Drosophila* around 36 proteins have been discovered to physically interact with VAP (*Drosophila* homolog of human VAPA and VAPB). This huge lack of information is quite important to study so firstly I have made a database listing all the orthologs of physical interactors of human VAPA/B which are present in flies (Table 2.1). This database clearly shows there is significant number of proteins conserved between humans and flies. So, it becomes quite important to find the *Drosophila* interactors which still have not been discovered. I also found that around 150 proteins were physically interacting with both VAPA and VAPB. However, a large pool of proteins specifically interacts with either VAPB or VAPA. Like there are 107 proteins which have been found to interact with VAPB although their binding to VAPA is still unknown. Similarly, around 203 proteins have been shown to be interacting partners of VAPA alone. In the following table, *Drosophila* orthologs have been mentioned on the right side of mammalian protein and if multiple isoforms are present, all are mentioned in the linear sequence. Blank space represents absence of the homolog in flies.

**Table 2.1: List of VAPA/B interactors in *Homo sapiens* and their orthologs in *Drosophila.***

| Human Symbol | Fly Symbol | Human Symbol | Fly Symbol | Human Symbol | Fly Symbol |
|---|---|---|---|---|---|
| VAPB and VAPA | | VAPB | | VAPA | |
| 1. ABCE1 | Pix | 1. AGR2 | | 1. ABCD1 | ABCD |
| 2. ACBD4 | CG8814 | 2. AIG1 | CG3625 | 2. ABCD3 | Pmp70 |
| 3. ACBD5 | CG8814 | 3. AQP2 | Drip | 3. ACO2 | mAcon1 |
| 4. AFTPH | Afti | 4. ARF6 | Arf51F | 4. ADCY6 | CG43373 |
| 5. AHCTF1 | Elys | 5. ARHGEF5 | Exn | 5. ADGRG7 | CG11318 |
| 6. AKAP11 | | 6. GET3 | CG1598 | 6. ADRB2 | Octbeta2R |
| 7. AQP6 | Eglp4 | 7. ATL3 | atl | 7. AP2B1 | AP-1-2beta |
| 8. ARHGEF12 | RhoGEF2 | 8. ATP5PB | ATPsynB | 8. APOD | NLaz |
| 9. BET1 | Bet1 | 9. ATP5PD | ATPsynD | 9. APP | Appl |
| 10. BIRC3 | Diap2 | 10. BAG6 | CG7546 | 10. ARF4 | Arf102F |
| 11. CANX | Cnx14D | 11. BCL10 | | 11. ASB14 | nompC |
| 12. CCDC40 | l(2)41Ab | 12. BICD2 | BicD | 12. ASB17 | stops |
| 13. CCNB2 | CycB | 13. BMPR1A | tkv | 13. ATAD1 | nmd |
| 14. CD79A | | 14. BRIP1 | CG4078 | 14. ATF2 | Atf-2 |
| 15. CDH1 | CadN2 | 15. CAND1 | Cand1 | 15. ATG16L1 | Atg16 |
| 16. CFTR | CG10505 | 16. CEBPZ | CG7839 | 16. ATP2A2 | SERCA |

| | | | | | |
|---|---|---|---|---|---|
| 17. CFTR | rdog | 17. CELSR2 | stan | 17. ATP6V0D1 | VhaAC39-1 |
| 18. CFTR | CG4562 | 18. COA3 | Ccdc56 | 18. ATP6V1A | Vha68-2 |
| 19. CFTR | CG31792 | 19. CERT1 | cert | 19. ATP6V1A | Vha68-1 |
| 20. CFTR | CG9270 | 20. COX7C | COX7C | 20. ATP6V1B2 | Vha55 |
| 21. CFTR | Mrp4 | 21. CTU2 | CG10189 | 21. ATP6V1E1 | Vha26 |
| 22. CFTR | CG7627 | 22. CYP3A7 | Cyp9f2 | 22. ATP6V1G1 | Vha13 |
| 23. CFTR | CG11898 | 23. CYP3A7 | Cyp9b1 | 23. BCS1L | CG4908 |
| 24. CFTR | l(2)03659 | 24. CYP3A7 | Cyp6a17 | 24. CACNG1 | |
| 25. CLUAP1 | Cluap1 | 25. DDOST | Ost48 | 25. CAV1 | |
| 26. COX14 | | 26. DOP1A | CG15099 | 26. CAV2 | |
| 27. COX4I1 | COX4L | 27. ELOVL4 | Elo68beta | 27. CCDC127 | tbrd-1 |
| 28. COX5B | COX5B | 28. EMD | CG3748 | 28. CCDC127 | tbrd-3 |
| 29. COX6C | cype | 29. EPHA4 | Eph | 29. CCDC127 | fs(1)h |
| 30. CYB561 | CG1275 | 30. EYA2 | eya | 30. CD81 | Tsp96F |
| 31. CYBRD1 | CG1275 | 31. FAF2 | Faf2 | 31. CDC42 | Cdc42 |
| 32. DUSP15 | CG10089 | 32. FAM118B | | 32. CDK9 | Cdk9 |
| 33. DUSP9 | Mkp3 | 33. FAM174A | CG12159 | 33. CEP83 | Rilpl |
| 34. EBAG9 | CG32536 | 34. FIS1 | Fis1 | 34. CEPT1 | bbc |
| 35. EBP | | 35. NIPSNAP2 | Nipsnap | 35. CERKL | Cerk |
| 36. ERBB2 | Egfr | 36. GET4 | CG9853 | 36. CHCHD3 | Chchd3 |
| 37. ESR2 | ERR | 37. GLP1R | Pdfr | 37. CHCHD6 | Chchd3 |
| 38. ESRRB | ERR | 38. GPN3 | CG2656 | 38. CKAP4 | SMC3 |
| 39. FAF1 | casp | 39. GPR25 | moody | 39. CLN8 | CG17841 |
| 40. OTULINL | | 40. GPR25 | CG4313 | 40. CMTR1 | CG6379 |
| 41. RETREG3 | | 41. GPR25 | Tre1 | 41. COX6B1 | COX6B |
| 42. FAM170A | | 42. HNRNPC | CG42458 | 42. CTHRC1 | |
| 43. MIGA2 | Miga | 43. HNRNPH1 | glo | 43. CTSA | CG4572 |
| 44. FAM83G | | 44. IL18R1 | otk | 44. CYB5R3 | CG5946 |
| 45. FKBP8 | zda | 45. IL18R1 | CG13506 | 45. DCAF5 | CG42233 |
| 46. GOLT1B | CG32576 | 46. IL18R1 | Toll-4 | 46. DDX46 | CG6227 |
| 47. HACD3 | Hacd2 | 47. IL18R1 | Fas2 | 47. DDX58 | Dcr-2 |
| 48. HEATR5B | CG2747 | 48. IL18R1 | Dscam2 | 48. DDX58 | Dcr-1 |
| 49. HIST1H4A | His4:CG33887 | 49. IL18R1 | sns | 49. DDX58 | Fancm |
| 50. HSD17B13 | CG15629 | 50. IL18R1 | CG45263 | 50. DYRK1A | mnb |
| 51. INSIG1 | | 51. INTU | in | 51. EED | escl |
| 52. JAGN1 | jagn | 52. KPNA2 | Pen | 52. EED | esc |
| 53. JMY | Root | 53. KTN1 | CG43755 | 53. EFTUD2 | CG4849 |
| 54. KCNB1 | Shab | 54. KTN1 | CG31797 | 54. EGFR | Egfr |
| 55. KRAS | Ras85D | 55. MAD2L2 | rev7 | 55. EGLN3 | Hph |
| 56. LAMP1 | Lamp1 | 56. MAP4K3 | hppy | 56. EIF2AK3 | PEK |
| 57. LMBR1L | lili | 57. MARCHF5 | CG9855 | 57. EIF3B | eIF3b |
| 58. LMNA | LamC | 58. MORF4L2 | MRG15 | 58. EIF3K | eIF3k |
| 59. LMNA | Lam | 59. MPST | | 59. EIF5A | eEF5 |
| 60. LSG1 | Ns3 | 60. MTCH2 | Mtch | 60. EIF6 | eIF6 |
| 61. LTBR | | 61. MTNR1A | Tre1 | 61. EMC2 | CG17556 |
| 62. MAPK3 | rl | 62. NBR1 | ref(2)P | 62. ERLIN1 | IKKbeta |
| 63. MGST1 | Mgstl | 63. NBR1 | mib1 | 63. ERLIN2 | |
| 64. MICAL3 | Mical | 64. NBR1 | mib2 | 64. FANCD2 | Fancd2 |
| 65. MORF4L1 | MRG15 | 65. NBR1 | CG5445 | 65. FBXO6 | |
| 66. MPRIP | osp | 66. ND5 | ND5 | 66. FBXW11 | slmb |
| 67. MTMR12 | CG14411 | 67. NDUFB3 | ND-B12 | 67. FLOT1 | Flo1 |
| 68. NACAD | Nacalpha | 68. NDUFB9 | ND-B22 | 68. FLOT2 | Flo2 |
| 69. NDUFA12 | ND-B17.2 | 69. OXCT1 | SCOT | 69. FN1 | sca |
| 70. NDUFA7 | ND-B14.5A | 70. PITRM1 | CG3107 | 70. FN1 | CG41520 |
| 71. NDUFB8 | ND-ASHI | 71. PKN2 | Pkn | 71. FNDC3A | mtgo |
| 72. NDUFS4 | ND-18 | 72. PLEKHA4 | CG34383 | 72. GABARAPL2 | Atg8a |
| 73. NDUFS6 | ND-13A | 73. POTEF | Act88F | 73. GBE1 | AGBE |

| | | | | | |
|---|---|---|---|---|---|
| 74. NDUFV3 | CG11752 | 74. PPT1 | Ppt1 | 74. GKN1 | |
| 75. NFATC2 | NFAT | 75. PRKACG | Pka-C1 | 75. GLB1 | Ect3 |
| 76. NFKB1 | Rel | 76. PRKAR2B | Pka-R2 | 76. GOLIM4 | CG12213 |
| 77. NGB | glob1 | 77. PTGES | CG33178 | 77. GOSR1 | Gos28 |
| 78. NOL11 | CG9300 | 78. PTGES | CG33177 | 78. GOSR2 | Membrin |
| 79. NTRK1 | CG1440 | 79. PTGES | Mgstl | 79. GPR89A | GPHR |
| 80. NTRK1 | CG13423 | 80. REEP4 | ReepA | 80. HELLS | Iswi |
| 81. NTRK1 | otk | 81. RFT1 | CG3149 | 81. HIF1AN | HSPBAP1 |
| 82. NTRK1 | Ror | 82. RHBDD3 | | 82. HIF1AN | JMJD5 |
| 83. NTRK1 | Nrk | 83. RNASEK | RNASEK | 83. HSD17B10 | scu |
| 84. OSBP | Osbp | 84. RNF111 | CG6923 | 84. HSD17B11 | CG9265 |
| 85. OSBP2 | Osbp | 85. S100A16 | | 85. HSD17B11 | CG15629 |
| 86. OSBPL10 | CG1513 | 86. SCAF4 | CG4266 | 86. IMMT | Mitofilin |
| 87. OSBPL10 | CG42668 | 87. SCD | Desat2 | 87. ISLR | haf |
| 88. OSBPL11 | CG1513 | 88. SEC22B | Sec22 | 88. ISLR | kek2 |
| 89. OSBPL11 | CG42668 | 89. SEPTIN9 | septin2 | 89. ISLR | hfw |
| 90. OSBPL1A | CG3860 | 90. SLC22A1 | CG6356 | 90. ISLR | kek1 |
| 91. OSBPL2 | CG3860 | 91. SLC22A1 | CG7458 | 91. ISLR | kek6 |
| 92. OSBPL3 | Osbp | 92. SLC22A1 | CG4462 | 92. ISLR | Lapsyn |
| 93. OSBPL6 | Osbp | 93. SLC22A1 | SLC22A | 93. ISLR | swi2 |
| 94. OSBPL9 | CG1513 | 94. SLC22A1 | Orct | 94. ISLR | CG7896 |
| 95. PHB | l(2)37Cc | 95. SLC22A1 | Orct2 | 95. ISLR | kek3 |
| 96. PITPNM1 | rdgB | 96. SLC22A1 | CG4459 | 96. ISLR | CG16974 |
| 97. PITPNM2 | rdgB | 97. SLC22A1 | CG4465 | 97. ISLR | Lrt |
| 98. PITPNM3 | rdgB | 98. SLC22A1 | CG4630 | 98. ISLR | CG1504 |
| 99. PRKACA | Pka-C1 | 99. SLC22A1 | CG44098 | 99. ITGA4 | ItgaPS4 |
| 100. PRKACB | Pka-C1 | 100. SLC25A24 | SCaMC | 100. ITGA4 | ItgaPS5 |
| 101. PRKAR1A | Pka-R1 | 101. SLC25A35 | CG18327 | 101. ITGA4 | scb |
| 102. PRKAR1B | Pka-R1 | 102. SLC25A35 | CG8323 | 102. ITPR3 | Itp-r83A |
| 103. PTPN1 | Ptp61F | 103. SLC26A2 | Prestin | 103. JTB | JTBR |
| 104. PTPN12 | CG42327 | 104. SLC35C2 | CG14971 | 104. JUN | Jra |
| 105. PTPN12 | Ptp61F | 105. SLC39A8 | Zip71B | 105. VIRMA | vir |
| 106. PTPN12 | Ptp99A | 106. SLC39A9 | Zip102B | 106. KIDINS220 | CG42672 |
| 107. PTPN12 | mop | 107. SLC6A15 | CG43066 | 107. KIF14 | neb |
| 108. PTPN12 | PTP-ER | 108. SLC7A2 | slif | 108. KLRD1 | rgn |
| 109. PTPN5 | PTP-ER | 109. SNX2 | Snx1 | 109. LEPROTL1 | CG30423 |
| 110. PTRH2 | CG1307 | 110. SNX25 | snz | 110. LGALS3BP | Tango10 |
| 111. RAB3GAP1 | CG31935 | 111. SNX5 | Snx6 | 111. LPGAT1 | CG34348 |
| 112. RAB3GAP2 | Rab3-GAP | 112. SNX6 | Snx6 | 112. LPGAT1 | Agpat3 |
| 113. RAB5C | Rab5 | 113. SPEG | Unc-89 | 113. LPGAT1 | Agpat1 |
| 114. RAB9A | Rab9 | 114. SSR4 | Tapdelta | 114. LPGAT1 | Agpat4 |
| 115. RAI14 | | 115. STX1B | Syx1A | 115. LPGAT1 | CG15450 |
| 116. RASSF1 | Rassf | 116. STX2 | Syx1A | 116. LPGAT1 | LPCAT |
| 117. RASSF3 | Rassf | 117. STX4 | Syx1A | 117. LPGAT1 | Gpat4 |
| 118. RB1CC1 | Atg17 | 118. STX5 | Syx5 | 118. LPGAT1 | Agpat2 |
| 119. RECQL4 | RecQ4 | 119. SYNE4 | | 119. LRRK1 | Lrrk |
| 120. RHBDD1 | | 120. SYVN1 | sip3 | 120. MBOAT7 | frj |
| 121. RHBDF2 | rho-5 | 121. TMEM101 | | 121. MCM2 | Mcm2 |
| 122. RHOT2 | Miro | 122. TOMM20 | Tom20 | 122. MCU | MCU |
| 123. RMDN2 | | 123. TOMM22 | mge | 123. METTL14 | Mettl14 |
| 124. RMDN3 | | 124. TPTE | Pten | 124. MGST3 | |
| 125. RNF4 | dgrn | 125. TTC39B | | 125. MMGT1 | CG15168 |
| 126. RPN2 | OstDelta | 126. UBC | Ubi-p63E | 126. MRTO4 | RpLP0-like |
| 127. RTN1 | Rtnl1 | 127. UBE4A | CG11070 | 127. MTMR14 | EDTP |
| 128. SCN3B | | 128. UBL4A | CG7215 | 128. MTMR4 | CG3632 |
| 129. SLC22A15 | CG6356 | 129. VAPA | Vap33 | 129. NANP | CG15771 |
| 130. SLC22A15 | Orct | 130. VCL | Vinc | 130. NDUFA10 | ND-42 |

| | | | | | |
|---|---|---|---|---|---|
| 131. SLC22A15 | Orct2 | 131. VHL | Vhl | 131. NDUFA13 | ND-B16.6 |
| 132. SLC25A46 | Slc25A46a | 132. YBX1 | yps | 132. NDUFA2 | ND-B8 |
| 133. SLC25A46 | Slc25A46b | 133. ZDHHC15 | CG1407 | 133. NDUFA5 | ND-13B |
| 134. ST7 | CG3634 | | | 134. NDUFA6 | ND-B14 |
| 135. STARD3 | Start1 | | | 135. NDUFA9 | ND-39 |
| 136. STARD3NL | Start1 | | | 136. NDUFB11 | NP15.6 |
| 137. STK3 | hpo | | | 137. NDUFB4 | ND-B15 |
| 138. STK4 | hpo | | | 138. NDUFS1 | ND-75 |
| 139. STOM | CG42540 | | | 139. NDUFS2 | ND-49 |
| 140. STX1A | Syx1A | | | 140. NDUFS5 | ND-15 |
| 141. SURF6 | Surf6 | | | 141. NDUFS8 | ND-23 |
| 142. SYNE2 | Msp300 | | | 142. NDUFV1 | ND-51 |
| 143. SYNRG | Eps-15 | | | 143. NDUFV2 | ND-24 |
| 144. TACC1 | tacc | | | 144. NEU1 | |
| 145. TCTN2 | tctn | | | 145. NFATC1 | NFAT |
| 146. TGOLN2 | | | | 146. NSF | Nsf2 |
| 147. TJP1 | pyd | | | 147. NSF | comt |
| 148. TMEM216 | CG11760 | | | 148. OPRD1 | AstC-R2 |
| 149. TMEM216 | TMEM216 | | | 149. OPRK1 | AstC-R2 |
| 150. TMX2 | CG11007 | | | 150. OPRM1 | AstC-R2 |
| 151. TRIOBP | osp | | | 151. OPRM1 | AstC-R1 |
| 152. TTC1 | CG14894 | | | 152. OPRM1 | Rh7 |
| 153. UNC93B1 | CG3078 | | | 153. ORC3 | Orc3 |
| 154. UQCRC2 | UQCR-C2 | | | 154. PARD3 | baz |
| 155. UQCRFS1 | RFeSP | | | 155. PCTP | CG6565 |
| 156. USP20 | Usp20-33 | | | 156. PEX14 | Pex14 |
| 157. USP33 | Usp20-33 | | | 157. PGRMC2 | MSBP |
| 158. VAMP1 | Syb | | | 158. PHB2 | Phb2 |
| 159. VAMP2 | nSyb | | | 159. PHGDH | CG6287 |
| 160. VAMP8 | Syb | | | 160. PHTF2 | phtf |
| 161. VCP | TER94 | | | 161. PIEZO1 | Piezo |
| 162. VDAC3 | porin | | | 162. PITPNA | vib |
| 163. VKORC1 | Vkor | | | 163. POR | Cpr |
| 164. VPS13A | Vps13 | | | 164. CAVIN3 | |
| 165. VPS13C | Vps13 | | | 165. PRNP | AnxB10 |
| 166. WDR44 | CG34133 | | | 166. PRNP | CrebB |
| 167. YIF1A | Yif1 | | | 167. PSTPIP2 | CG8176 |
| 168. YIPF5 | Yip1d1 | | | 168. PTAR1 | temp |
| 169. YWHAB | 14-3-3zeta | | | 169. PTRF | |
| 170. ZBTB22 | ab | | | 170. RAB1A | Rab1 |
| 171. ZBTB22 | CG6654 | | | 171. RAB1B | Rab1 |
| 172. ZDBF2 | | | | 172. RAB5B | Rab5 |
| 173. ZFYVE27 | | | | 173. RAB8A | Rab8 |
| 174. ZNF598 | CG11414 | | | 174. ROBO2 | robo1 |
| | | | | 175. RPL5 | RpL5 |
| | | | | 176. RPLP0 | RpLP0 |
| | | | | 177. RPS15A | RpS15Aa |
| | | | | 178. RPS15A | RpS15Ab |
| | | | | 179. RPS16 | RpS16 |
| | | | | 180. RPS26 | RpS26 |
| | | | | 181. RSAD2 | |
| | | | | 182. RTN3 | Rtnl1 |
| | | | | 183. RTN4 | Rtnl1 |
| | | | | 184. SACM1L | Sac1 |
| | | | | 185. SCRN1 | CG10098 |
| | | | | 186. SEC11C | twr |
| | | | | 187. SERPINB9 | Spn55B |

| | | | | | |
|---|---|---|---|---|---|
| | | | | 188. SERPINB9 | Spn42Dc |
| | | | | 189. SF3B4 | Spx |
| | | | | 190. SIK1 | Sik2 |
| | | | | 191. SIN3A | Sin3A |
| | | | | 192. SLC16A7 | Mct1 |
| | | | | 193. SLC25A1 | sea |
| | | | | 194. SLC25A12 | aralar1 |
| | | | | 195. SLC35B1 | meigo |
| | | | | 196. SLC39A4 | foi |
| | | | | 197. SMARCA4 | brm |
| | | | | 198. SOAT1 | CG8112 |
| | | | | 199. SOD2 | Sod2 |
| | | | | 200. SRI | CG17765 |
| | | | | 201. STOML2 | Stoml2 |
| | | | | 202. STT3B | Stt3B |
| | | | | 203. SURF4 | Surf4 |
| | | | | 204. TAP1 | CG1824 |
| | | | | 205. TAP1 | CG3156 |
| | | | | 206. TCIRG1 | Vha100-4 |
| | | | | 207. TKT | CG8036 |
| | | | | 208. TKT | CG5103 |
| | | | | 209. TMED1 | opm |
| | | | | 210. TMEM229B | |
| | | | | 211. TMEM35A | CG13920 |
| | | | | 212. TMEM38B | CG4239 |
| | | | | 213. TMEM43 | CG8111 |
| | | | | 214. TMEM63B | CG11210 |
| | | | | 215. TMEM86B | CG7582 |
| | | | | 216. TMIE | CG15130 |
| | | | | 217. TOMM40 | Tom40 |
| | | | | 218. TOMM6 | |
| | | | | 219. TRPM7 | Trpm |
| | | | | 220. TUBA1C | alphaTub84B |
| | | | | 221. UBAC2 | rngo |
| | | | | 222. UBAP2L | lig |
| | | | | 223. UBE3A | Ube3a |
| | | | | 224. UQCRB | UQCR-14L |
| | | | | 225. UQCRB | UQCR-14 |
| | | | | 226. UQCRC1 | UQCR-C1 |
| | | | | 227. UTP4 | l(3)72Dn |
| | | | | 228. VAMP3 | Syb |
| | | | | 229. VAMP5 | Syb |
| | | | | 230. VAPB | Vap33 |
| | | | | 231. VAV1 | Vav |
| | | | | 232. VCAM1 | |
| | | | | 233. VDAC1 | porin |
| | | | | 234. VDAC2 | porin |
| | | | | 235. VMP1 | Tango5 |
| | | | | 236. XPR1 | CG10483 |
| | | | | 237. YWHAE | 14-3-3epsilon |
| | | | | 238. ZFPL1 | CG5382 |
| | | | | 239. ZMYM1 | woc |
| | | | | 240. ZNF318 | CG9776 |

First column shares common interactors of both VAPA and VAPB in humans. Third column shows interactors specific to VAPB so far. Fifth column shows VAPA specific interactors. Second, fourth and sixth columns represent *Drosophila* homologs. For more information about the listed proteins

information is available at http://genenames.org (*H. sapiens)* and http://flybase.org (*D. melanogaster).*

**2.3.2 *Drosophila* VAP interactors:** From Table 2.1 it is quite clear that VAPA/B interacts with a large number of mammalian proteins but the question arises, do all proteins share similar sequence which is involved in the physical interaction. Multiple studies have reported that VAPA/B interactors have conserved FFAT motif sequence which binds to MSP domain and it is important for the functioning of the protein as well. However, out of 460 mammalian proteins only few proteins have been shown to contain FFAT motif such as OSBP, CERT, FAF1, PTPIP51 and Nir etc (Kors, Costello, et al., 2022). Tim Levine group have published studies which predicts the proteins that may contain FFAT motif (Mikitova & Levine, 2012; Murphy & Levine, 2016; Slee & Levine, 2019). What have been known so far that proteins may contain canonical or non-canonical FFAT motif. Also, recent studies have suggested phosphorylation of FFAT motif can influence protein activity as well (Di Mattia et al., 2020). In our study, we used the two sequences from (Mikitova & Levine, 2012). First one represents conserved FFAT motif where sequence starts with acidic amino acid residue Aspartate or Glutamate then after 0-5 amino acid sequence following sequence is present [DE]-[FY]-[FY]-[DEST]-[ACST]-X-[DEST] named as Type I. In the second case, interactors was identified using non-canonical sequence [DE]-X(0,5)-X-[FY]-[FYCILMVWH]-[DEST]-[ACST]-X-[DESTGNQ] which was named Type II. However, after the discovery of FAF1 which interacts with VAP have been shown to contain Glutamate instead of Phenylalanine in the second position of FFAT (Baron et al., 2014; Tendulkar et al., 2022), we introduced that also in the first two sequences named them Type III, Type IV and came with a list of interactors.

Firstly, we checked the *Drosophila* database to make a list of known VAP-33 interactors and then checked which proteins may have these FFAT sequences along with their human counterpart (Table 2.2). We found 13 proteins out of 36 which may have canonical or non-canonical FFAT motif present in the protein. Also, 9 human proteins shared similar sequence with the *Drosophila* ones.

**Table 2.2: *Drosophila* VAP interactors and their homologs in *Homo sapiens*.**

| S. No. | Name | Flybase | Type | Sequence | Function | Location | *H. sapiens* | Sequence |
|---|---|---|---|---|---|---|---|---|
| 1 | OSBP | CG6708 | I | DEEMEFFDAEE | sterol transporter | intracellular membrane bound organelle | OSBP, OSBP2, OSBP3 | DEDDENEFFDAPE, EEDEDTEYFDAME, DSLSEFFDAQE |

| | | | | | | | | |
|---|---|---|---|---|---|---|---|---|
| 2 | CERT | CG7207 | I | EDEFFDAVE | Ceramide transfer | Intracellular ER-Golgi interface | CERT1 | EEEFFDAVE |
| 3 | Acbp7 | CG8814 | III | YDDPYD | Lipid transfer | ER-Peroxisome | ACBD4 ACBD5 | EVFCDSLE EYCDSME |
| 4 | AGPAT3 | CG4729 | II | DKIIDSFLETGS | acyltransferase activity | endomembrane system | AGPAT3 | |
| 5 | Casp | CG8400 | III | ESSTDEFEDATD | protein metabolism | | FAF1 | DSDGDDFEDATE |
| 6 | ft | CG3352 | II | DEVPVFISANE, ELVHGRAYFSSGG | protein binding | plasma membrane | FAT4 | ENEPGGSYITTVS |
| 7 | l(2)gl | CG2671 | II | EDGSVKFWDCTG | syntaxin binding | plasma membrane | LLGL1 | EDGTVRFWDASG |
| 8 | Miga | CG12125 | III | DPNFDSAES | | mitochondria | MIGA2 | DSLTEDSFFSATE |
| 9 | NF-YA | CG3891 | II | EGGRFHSAQE | DNA binding (RNA polII specific) | CCAAT binding factor complex | NFYA | |
| 10 | Rictor | CG8002 | II | DDYIERFYETGS | protein serine/threonine kinase activator | TORC2 complex | RICTOR | DASLFLESTE |
| 11 | Sac1 | CG9128 | II | EQGHVANFVETEQ | PI4P phosphatase | ER membrane | SACM1L | EKFYVEACD, EGHAANFVETEQ |
| 12 | Vha68-2 | CG3762 | III | DMATIQVYEETSG | ATP binding | plasma membrane | ATP6V1A | DMATIQVYEETSG |
| 13 | Vha68-3 | CG5075 | III | DMATIQVYEDTSG | ATP binding | plasma membrane | ATP6V1A | DMATIQVYEETSG |
| 14 | CCT2 | CG7033 | | | ATP binding | cytoplasm | CCT2 | |
| 15 | CG13220 | CG13220 | | | | | | |
| 16 | CG1513 | CG1513 | | | sterol transporter | cytosol | OSBPL10 | |
| 17 | CG2064 | CG2064 | | | NADP retinol dehydrogenase | ER membrane | RDH11 | |
| 18 | CG33523 | CG33523 | | | | Endomembrane system | MOSPD2 | |
| 19 | CG5742 | CG5742 | | | signaling receptor binding I | cytoplasm | ANKRD13C | |
| 20 | CG8188 | CG8188 | | | ubiquitin protein transferase I | nucleus | UBE2S | |
| 21 | CG8765 | CG8765 | | | MADF-BESS domain transcription regulator | nucleus | | |
| 22 | CG9205 | CG9205 | | | sterol transporter | cytosol | | |

| | | | | | | | | |
|---|---|---|---|---|---|---|---|---|
| 23 | d | CG42840 | | | motor activity | myosin complex | RASIP1 | |
| 24 | dachs | | | | | | | |
| 25 | DL | CG3619 | | | calcium ion binding | plasma membrane | DLL1 | |
| 26 | Dscam1 | CG17800 | | | antigen binding | plasma membrane | DSCAML1 | |
| 27 | git | CG16728 | | | Muscle morphogenesis, synaptic vesicle recycling | Presynaptic active zone | GIT2, GIT1 | |
| 28 | hpo | CG11228 | | | Cell growth, proliferation, apoptosis | cytoplasm | STK3, STK4 | |
| 29 | kek6 | Cg1804 | | | neurotrophin binding | type I terminal bouton I | LRFN1 | |
| 30 | LFG | CG3814 | | | | | TMBIM4 | |
| 31 | MRG15 | CG6363 | | | Cap-H2 enzyme regulator | NuA4 histone acetyltransferase complex | MORF4L1 | |
| 32 | Nemp | CG9723 | | | | nuclear inner membrane I | NEMP1 | |
| 33 | Pcyt2 | CG18330 | | | choline-phosphate cytidylyltransferase | cytoplasm | PCYT1A | |
| 34 | ReepA | CG42678 | | | microtubule binding | ER, cytoplasmic microtubule, presynapse | REEP2 | |
| 35 | Rel | CG11992 | | | DNA binding transcription factor | cytoplasm | NFKB1 | |
| 36 | Vha44 | CG8048 | | | proton transmembrane transporter | plasma membrane | ATP6V1C1 | |

More information about the role of individual proteins is available at listed websites: http://flybase.org, http://thebiogrid.org

**2.3.3 Prediction of *Drosophila* VAP interactome:** Based on human VAP interactors and FFAT sequence, we looked for their homologs in *Drosophila* which may contain similar sequence and come up with a list of proteins using "genome.jp" database. We used similar sequences as described in earlier results and named as Type I (Table 2.3), II (Table 2.4), III (Table 2.5) and IV (Table 2.6). We came up with a list of predicted interactors out of which some are already shown to be physical interactors in *Drosophila* marked by * in the tables.

**Table 2.3: List of VAP interactors representing Type I FFAT motif prediction**

| S.No. | *H.sapiens* | *Drosophila* | Protein Name | *Drosophila* Sequence |
|---|---|---|---|---|
| 1* | CERT1 | Cert | Ceramide transfer protein | EDEFFDAVE |
| 2 | MICAL3 | Mical | Molecule interacting with CasL, isoform C | DSDDSDDFYDSSE |
| 3* | OSBP | Osbp | oxysterol binding protein | DEEMEFFDAEE |
| 4* | PITPNM2 | rdgB | retinal degeneration B, isoform D | DEEFFDCLD |
| 5 | WDR44 | CG34133 | | DSDSSEEFFDAED |

***** represents known physical interactor of *Drosophila* VAP.

**Table 2.4: List of VAP interactors representing Type II FFAT motif prediction**

| S.No. | *H.sapiens* | *Drosophila* | Protein Name | *Drosophila* Sequence |
|---|---|---|---|---|
| 1* | ABCE1 | Pixie | Pixie | DEPSAYLDSEQ |
| 2* | ACBD4/5 | Acbp7 | Acyl-CoA Binding Protein 7 | EEAMQRYVESLQ |
| 3* | AGPAT3 | AGPAT3 | 1-acyl-sn-glycerol-3-phosphate acyltransferase gamma | DKIIDSFLETGS |
| 4 | AHCTF1 | Elys | Elys isoform B | DGNLYFVSSEE |
| 5 | AQP6 | Eglp4 | entomoglyceroporin 4, isoform E | DPRNSKFHDSVG |
| 6 | ATP5F1D | CG2968 | ATP synthase, δ subunit | DGKTLKFFVSSGS |
| 7 | BICD2 | Bicd | Bicaudal D | DSVEIKKYVDTVS |
| 8 | BMPR1A | Tkv | thickveins, isoform A | ERVAVKTFFTTEE |
| 9 | BRIP1 | CG4078 | | DNPKYISSLG |
| 10 | CDH1 | CadN2 | Cadherin-N2 isoform C | DIFWDTEN |
| 11 | CAND1 | Cand1 | Cullin-associated and neddylation-dissociated 1 | DTEDDEYVDSEE |
| 12 | CFTR | Cftr | CF transmembrane conductance regulator | DCVSCIFLTSVT |
| 13 | DOP1A | CG15099 | Protein dopey-1 | DIIRAMYISSGN ELYAFFTTLG |
| 14* | FAF1 | Casp | Caspar | DLTEDGFMDTEQ ESNKDMFLSSLT DLLNFVTANG |
| 15* | FAT4 | Ft | Fat | DEVPVFISANE ELVHGRAYFSSGG |
| 16 | HEATR5B | CG2747 | | DRFVEAIE DGGAFYTTDT |
| 17 | INTU | CG16993/in | inturned | DLANWEEYVSTDG |
| 18 | KCNB1 | Shab | Shaker cognate b, isoform A | DIGDNQPYYDTSG EFECCFCTTKG |
| 19* | LLGL1 | l(2) | lethal (2) giant larvae | EDGSVKFWDCTG |
| 20 | MICAL3 | Mical | Molecule interacting with CasL, isoform C | DIDDIEFMDTGS |
| 21 | MTMR12 | CG14411 | | EPYYSTLG |
| 22 | NFATC2 | Nfat | Nfat nuclear factor, isoform B | ETKFISARN DVSGFMDTTS |
| 23 | PPT1 | Ppt1 | Palmitoyl-protein thioesterase 1, isoform B | ESQWFQYYTTGQ |
| 24 | RASSF1/3 | Rassf | Ras association family member | DDFMTATG |

| | | | | |
|---|---|---|---|---|
| 25* | RICTOR | Rictor | rapamycin-insensitive companion of Tor, isoform B | DDYIERFYETGS |
| 26 | RPN2 | Ostdelta | oligosaccharide transferase delta subunit, isoform B | DLQSIFFSSLN |
| 27 | RTN1 | Rtnl1 | Reticulon-like1, isoform H | DQDNEKFISSED |
| 28* | SACM1L | Sac1 | Sac1 phosphatase, isoform B | EQGHVANFVETEQ |
| 29 | SNX2 | Snx1 | Sorting nexin 1, isoform B | DRNESDLFVSALS DLDFMNFLESDQ |
| 30 | SPEG | Unc-89 | Unc-89, isoform C | DNRFLSSIE DICHAELFYDSLD |
| 31 | TJP1 | Pyd | Polychaetoid, isoform G | EAGIFVTAVQ |
| 32 | TTC1 | CG14894 | | DDEFHDAIG |
| 33 | USP20/33 | Usp20-33 | Ubiquitin specific protease 20/33 | DCMASFFSADE |
| 34 | ZNF598 | CG11414 | | EHYFCHFCDADG |

***** represents known physical interactor of *Drosophila* VAP.

**Table 2.5: List of VAP interactors representing Type III FFAT motif prediction**

| S.No. | *H. sapiens* | *Drosophila* | Protein name | *Drosophila* Sequence |
|---|---|---|---|---|
| 1* | FAF1 | Casp | Caspar | ESSTDEFEDATD |
| 2 | STARD3 | Start1 | Start1, isoform C | DQDEFEDAKD |
| 3 | USP20/33 | Usp20-33 | Ubiquitin specific protease 20/33 | ESEYDTCES |

***** represents known physical interactor of *Drosophila* VAP.

**Table 2.6: List of VAP interactors representing Type IV FFAT motif prediction**

| S.No. | *H. sapiens* | *Drosophila* | Protein name | *Drosophila* Sequence |
|---|---|---|---|---|
| 1* | ATP6V1A | Vha68-2 | Vacuolar H+ ATPase 68 kDa subunit 2 | DMATIQVYEETSG |
| 2* | ATP6V1A | Vha68-3 | Vacuolar H+ ATPase 68 kDa subunit 3 | DMATIQVYEDTSG |
| 3 | BAG6 | CG7546 | | DPTFEESDT |
| 4 | BMPR1A | Tkv | Thickveins, isoform A | EGYEDADN |
| 5 | MICAL3 | Mical | Molecule interacting with CasL, isoform C | ESDSEMFEEADD |
| 6* | MIGA2 | Miga | Mitoguardian, isoform B | DPNFDSAES |
| 7 | PLEKHA4 | Kmr | Kraamer, isoform 1 | ESLSEQFEETLS |
| 8 | PTPN5 | Ptp-ER | protein tyrosine phosphatase-ERK/Enhancer of Ras1 | ESEFDIYDDTRS |
| 9 | RASSF1/3 | Rassf | Ras association family member | ETSLDNFETCDD |
| 10 | SPEG | Unc-89 | Unc-89, isoform C | DYDRGTSYDSTVE |
| 11 | TPTE | Pten | Phosphatase and tensin homolog, isoform G | DIVTKIQYDTSTN |
| 12 | VPS13A/C | Vps13 | Vacuolar protein sorting 13, isoform B | DVTLSKFEDAAS |
| 13 | WDR44 | CG34133 | | DDFVMEFESSLN |

***** represents known physical interactor of *Drosophila* VAP.

## 2.4 Discussion

**2.4.1 *Drosophila* as a model to study VAP roles:** Based on Table 2.1, it is quite clear that *Drosophila* genome shares a large pool of conserved proteins which may perform similar functions like *H. sapiens* proteins which are known to interact with VAP family of proteins. It becomes quite important to perform *Drosophila* VAP specific proteomics to find its interacting partners and check the similarity among their homologs in other species. As *Drosophila* contains only one VAP protein instead of two isoforms, it becomes an excellent model to study the genetic interactions between VAP and its binding partners. For example, VAP has been shown to affect Miga function in *Drosophila (Xu et al., 2020).* Similarly, Sac1 activity is affected in *Drosophila ALS8* overexpression model (Sanhueza et al., 2015). The conserved nature of FFAT motif among VAP interactors of *H. sapiens* and *D. melanogaster* provides additional benefit to study these interactions and study its impact on the cellular functioning (Murphy & Levine, 2016). One study from our lab has shown *Caspar,* FAF1 homolog, roles in primordial germ cells where FFAT motif is not required for its performance (Das et al., 2024). In Chapter V, we have tried to look at another protein function i.e. Ceramide Transfer (CERT) where we have mutated CERT FFAT motif and study its roles in *Drosophila.*

**2.4.2 *Drosophila* VAP roles in the nervous system:** Although VAP express ubiquitously, it seems to be quite important in the nervous system (Borgese et al., 2021; Moustaqim-Barrette et al., 2014; Portela et al., 2024; Wong et al., 2024). Majority of the studies have been focused towards brain development and only limited research is done on VAP roles in adults. Also, VAP interacts with variety of proteins which performs diverse roles in the cell such as lipid homeostasis, autophagy and mitochondrial functioning (Bezawork-Geleta et al., 2025; Di Mattia et al., 2020; Freyre et al., 2019; Han et al., 2012; Thulasidharan et al., 2024; Yamanaka et al., 2020). So, the question arises, if one function is affected will that affect other cellular processes as well. Also, VAP is known to be cleaved and secrete outside the cell where it binds to the receptors as the receiving end. But the roles of extracellular VAP in the nervous system still need to be studied further (Han et al., 2012; Kamemura & Chihara, 2019; Tsuda et al., 2008).

**2.5 Limitations and Conclusion:** The FFAT motif predictions are completely theoretical based on the sequence used. In some circumstances, it is possible it may predict false FFAT motifs. There are few examples like Miga, Acbp7 which have been shown to contain different FFAT motif than

predicted ones. However, proteins like Caspar has conserved FFAT like motif as predicted and proved to be physically interact with VAP via its FFAT motif in *Drosophila* (Tendulkar et al., 2022). Interestingly, Vha68-2 and Vha68-3 which are *Drosophila* VAP interactors contain Type III FFAT motif and play crucial role in lysosome functioning (Guruharsha et al., 2011). So, it is important to check if the interaction is dependent on FFAT motif. Proteins like Mical, Wdr44, Start1, Usp20/33 seems to be promising candidate of VAP interactors containing FFAT motif and should be studied thoroughly.

## 2.6 Materials and Methods

**2.6.1 Database and websites:** To create the list of human VAPA and VAPB interactors, multiple databases were used such as Biogrid (www.thebiogrid.org), STRING (www.string-db.org), Bioplex network. DAVID (https://davidbioinformatics.nih.gov/summary_new.jsp) and Gene ontology (https://geneontology.org/) were used to find the functions, location of the proteins. The list of table with individual information about the proteins is deposited in the lab group google drive with the name of FFAT folder. To find the orthologs of *Drosophila* proteins, (http://flybase.org) was used. To predict the FFAT motifs, sequence were picked up from (Mikitova & Levine, 2012). For the prediction of FFAT motifs, (http://www.genome.jp) was used for both *H. sapiens* and *D. melanogaster*.

## References

Alpy, F., Rousseau, A., Schwab, Y., Legueux, F., Stoll, I., Wendling, C., Spiegelhalter, C., Kessler, P., Mathelin, C., Rio, M. C., Levine, T. P., & Tomasetto, C. (2013). STARD3 or STARD3NL and VAP form a novel molecular tether between late endosomes and the ER. *J Cell Sci*, *126*(Pt 23), 5500-5512. https://doi.org/10.1242/jcs.139295

Baron, Y., Pedrioli, P. G., Tyagi, K., Johnson, C., Wood, N. T., Fountaine, D., Wightman, M., & Alexandru, G. (2014). VAPB/ALS8 interacts with FFAT-like proteins including the p97 cofactor FAF1 and the ASNA1 ATPase. *BMC Biol*, *12*, 39. https://doi.org/10.1186/1741-7007-12-39

Bezawork-Geleta, A., Devereux, C. J., Keenan, S. N., Lou, J., Cho, E., Nie, S., De Souza, D. P., Narayana, V. K., Siddall, N. A., Rodrigues, C. H. M., Portelli, S., Zheng, T., Nim, H. T., Ramialison, M., Hime, G. R., Dodd, G. T., Hinde, E., Ascher, D. B., Stroud, D. A., & Watt, M. J. (2025). Proximity proteomics reveals a mechanism of fatty acid transfer at lipid droplet-mitochondria-endoplasmic reticulum contact sites. *Nat Commun*, *16*(1), 2135. https://doi.org/10.1038/s41467-025-57405-5

Borgese, N., Navone, F., Nukina, N., & Yamanaka, T. (2021). Mutant VAPB: Culprit or Innocent Bystander of Amyotrophic Lateral Sclerosis? *Contact*, *4*. https://doi.org/10.1177/25152564211022515

Chaplot, K., Pimpale, L., Ramalingam, B., Deivasigamani, S., Kamat, S. S., & Ratnaparkhi, G. S. (2019). SOD1 activity threshold and TOR signalling modulate VAP(P58S) aggregation via reactive oxygen species-induced proteasomal degradation in a Drosophila model of amyotrophic lateral sclerosis. *Dis Model Mech*, *12*(2). https://doi.org/10.1242/dmm.033803

Chen, S., Roberts, M. A., Chen, C. Y., Markmiller, S., Wei, H. G., Yeo, G. W., Granneman, J. G., Olzmann, J. A., & Ferro-Novick, S. (2022). VPS13A and VPS13C Influence Lipid Droplet Abundance. *Contact (Thousand Oaks)*, *5*, 25152564221125613. https://doi.org/10.1177/25152564221125613

Cockcroft, S., Garner, K., Yadav, S., Gomez-Espinoza, E., & Raghu, P. (2016). RdgBalpha reciprocally transfers PA and PI at ER-PM contact sites to maintain PI(4,5)P2 homoeostasis during phospholipase C signalling in Drosophila photoreceptors. *Biochem Soc Trans*, *44*(1), 286-292. https://doi.org/10.1042/BST20150228

Cockcroft, S., & Raghu, P. (2018). Phospholipid transport protein function at organelle contact sites. *Curr Opin Cell Biol*, *53*, 52-60. https://doi.org/10.1016/j.ceb.2018.04.011

Costello, J. L., Castro, I. G., Hacker, C., Schrader, T. A., Metz, J., Zeuschner, D., Azadi, A. S., Godinho, L. F., Costina, V., Findeisen, P., Manner, A., Islinger, M., & Schrader, M. (2017). ACBD5 and VAPB mediate membrane associations between peroxisomes and the ER. *J Cell Biol*, *216*(2), 331-342. https://doi.org/10.1083/jcb.201607055

Das, S., Hegde, S., Wagh, N., Sudhakaran, J., Roy, A. E., Deshpande, G., & Ratnaparkhi, G. S. (2024). Caspar determines primordial germ cell identity in Drosophila melanogaster. *bioRxiv*. https://doi.org/10.1101/2024.04.25.591132

Deivasigamani, S., Verma, H. K., Ueda, R., Ratnaparkhi, A., & Ratnaparkhi, G. S. (2014). A genetic screen identifies Tor as an interactor of VAPB in a Drosophila model of amyotrophic lateral sclerosis. *Biol Open*, *3*(11), 1127-1138. https://doi.org/10.1242/bio.201410066

Di Mattia, T., Martinet, A., Ikhlef, S., McEwen, A. G., Nomine, Y., Wendling, C., Poussin-Courmontagne, P., Voilquin, L., Eberling, P., Ruffenach, F., Cavarelli, J., Slee, J., Levine, T. P., Drin, G., Tomasetto, C., & Alpy, F. (2020). FFAT motif phosphorylation controls formation and lipid transfer function of inter-organelle contacts. *EMBO J*, *39*(23), e104369. https://doi.org/10.15252/embj.2019104369

Freyre, C. A. C., Rauher, P. C., Ejsing, C. S., & Klemm, R. W. (2019). MIGA2 Links Mitochondria, the ER, and Lipid Droplets and Promotes De Novo Lipogenesis in Adipocytes. *Mol Cell*, *76*(5), 811-825 e814. https://doi.org/10.1016/j.molcel.2019.09.011

Gomez-Suaga, P., Paillusson, S., Stoica, R., Noble, W., Hanger, D. P., & Miller, C. C. J. (2017). The ER-Mitochondria Tethering Complex VAPB-PTPIP51 Regulates Autophagy. *Curr Biol*, *27*(3), 371-385. https://doi.org/10.1016/j.cub.2016.12.038

Guruharsha, K. G., Rual, J. F., Zhai, B., Mintseris, J., Vaidya, P., Vaidya, N., Beekman, C., Wong, C., Rhee, D. Y., Cenaj, O., McKillip, E., Shah, S., Stapleton, M., Wan, K. H., Yu, C., Parsa, B., Carlson, J. W., Chen, X., Kapadia, B., . . . Artavanis-Tsakonas, S. (2011). A protein complex network of Drosophila melanogaster. *Cell*, *147*(3), 690-703. https://doi.org/10.1016/j.cell.2011.08.047

Han, S. M., Tsuda, H., Yang, Y., Vibbert, J., Cottee, P., Lee, S. J., Winek, J., Haueter, C., Bellen, H. J., & Miller, M. A. (2012). Secreted VAPB/ALS8 major sperm protein domains modulate mitochondrial localization and morphology via growth cone guidance receptors. *Dev Cell*, *22*(2), 348-362. https://doi.org/10.1016/j.devcel.2011.12.009

James, C., & Kehlenbach, R. H. (2021). The Interactome of the VAP Family of Proteins: An Overview. *Cells*, *10*(7). https://doi.org/10.3390/cells10071780

Ji, W., Zhang, Y., Zhang, L., Liu, Q., Niu, S., Feng, Y., Chen, F., Liu, X., & Li, X. (2025). VAPB is a negative regulator of STING-mediated innate immune signaling. *Science Advances*, *11*(49), eaea3996. https://doi.org/10.1126/sciadv.aea3996

Kalarikkal, M., Saikia, R., Oliveira, L., Bhorkar, Y., Lonare, A., Varshney, P., Dhamale, P., Majumdar, A., & Joseph, J. (2024). Nup358 restricts ER-mitochondria connectivity by modulating mTORC2/Akt/GSK3beta signalling. *EMBO Rep*, *25*(10), 4226-4251. https://doi.org/10.1038/s44319-024-00204-8

Kamemura, K., & Chihara, T. (2019). Multiple functions of the ER-resident VAP and its extracellular role in neural development and disease. *J Biochem*, *165*(5), 391-400. https://doi.org/10.1093/jb/mvz011

Kamiyama, D., Nishida, Y., Kamiyama, R., Sego, A., Vining, G., Bui, K., Fitch, M., Do, H., Avraham, O., & Chihara, T. (2024). The VAPB Axis Precisely Coordinates the Timing of

Motoneuron Dendritogenesis in Neural Map Development. *Res Sq*. https://doi.org/10.21203/rs.3.rs-5684747/v1

Kors, S., Costello, J. L., & Schrader, M. (2022). VAP Proteins - From Organelle Tethers to Pathogenic Host Interactors and Their Role in Neuronal Disease. *Front Cell Dev Biol*, *10*, 895856. https://doi.org/10.3389/fcell.2022.895856

Kors, S., Schrader, M., & Costello, J. L. (2022). Multiple Ways to Keep FFAT Under Control! *Contact (Thousand Oaks)*, *5*, 1-4. https://doi.org/10.1177/25152564221101219

Kors, S., Schuster, M., Maddison, D. C., Kilaru, S., Schrader, T. A., Costello, J. L., Islinger, M., Smith, G. A., & Schrader, M. (2024). New insights into the functions of ACBD4/5-like proteins using a combined phylogenetic and experimental approach across model organisms. *Biochim Biophys Acta Mol Cell Res*, *1871*(8), 119843. https://doi.org/10.1016/j.bbamcr.2024.119843

Kumagai, K., & Hanada, K. (2019). Structure, functions and regulation of CERT, a lipid-transfer protein for the delivery of ceramide at the ER-Golgi membrane contact sites. *FEBS Lett*, *593*(17), 2366-2377. https://doi.org/10.1002/1873-3468.13511

McBenedict, B., Hauwanga, W. N., Nezam, U., Ko Oo, A., Eapi, S., Pradhan, S., Dang, N. B., Cher, P. W., Orsini, M. A., & Lima Pessoa, B. (2025). Amyotrophic Lateral Sclerosis (ALS) Type 8: A Narrative Review. *Cureus*, *17*(1), e76717. https://doi.org/10.7759/cureus.76717

Mesmin, B., Kovacs, D., & D'Angelo, G. (2019). Lipid exchange and signaling at ER-Golgi contact sites. *Curr Opin Cell Biol*, *57*, 8-15. https://doi.org/10.1016/j.ceb.2018.10.002

Mikitova, V., & Levine, T. P. (2012). Analysis of the key elements of FFAT-like motifs identifies new proteins that potentially bind VAP on the ER, including two AKAPs and FAPP2. *PLoS One*, *7*(1), e30455. https://doi.org/10.1371/journal.pone.0030455

Mishra, S., Manohar, V., Chandel, S., Manoj, T., Bhattacharya, S., Hegde, N., Nath, V. R., Krishnan, H., Wendling, C., Di Mattia, T., Martinet, A., Chimata, P., Alpy, F., & Raghu, P. (2024). A genetic screen to uncover mechanisms underlying lipid transfer protein function at membrane contact sites. *Life Sci Alliance*, *7*(6). https://doi.org/10.26508/lsa.202302525

Moustaqim-Barrette, A., Lin, Y. Q., Pradhan, S., Neely, G. G., Bellen, H. J., & Tsuda, H. (2014). The amyotrophic lateral sclerosis 8 protein, VAP, is required for ER protein quality control. *Hum Mol Genet*, *23*(8), 1975-1989. https://doi.org/10.1093/hmg/ddt594

Murphy, S. E., & Levine, T. P. (2016). VAP, a Versatile Access Point for the Endoplasmic Reticulum: Review and analysis of FFAT-like motifs in the VAPome. *Biochim Biophys Acta*, *1861*(8 Pt B), 952-961. https://doi.org/10.1016/j.bbalip.2016.02.009

Olkkonen, V. M. (2015). OSBP-Related Protein Family in Lipid Transport Over Membrane Contact Sites. *Lipid Insights*, *8*(Suppl 1), 1-9. https://doi.org/10.4137/LPI.S31726

Portela, M., Mukherjee, S., Paul, S., La Marca, J. E., Parsons, L. M., Veraksa, A., & Richardson, H. E. (2024). The Drosophila tumour suppressor Lgl and Vap33 activate the Hippo pathway through a dual mechanism. *J Cell Sci*, *137*(4). https://doi.org/10.1242/jcs.261917

Ratnaparkhi, A., Lawless, G. M., Schweizer, F. E., Golshani, P., & Jackson, G. R. (2008). A Drosophila model of ALS: human ALS-associated mutation in VAP33A suggests a dominant negative mechanism. *PLoS One*, *3*(6), e2334. https://doi.org/10.1371/journal.pone.0002334

Sanhueza, M., Chai, A., Smith, C., McCray, B. A., Simpson, T. I., Taylor, J. P., & Pennetta, G. (2015). Network analyses reveal novel aspects of ALS pathogenesis. *PLoS Genet*, *11*(3), e1005107. https://doi.org/10.1371/journal.pgen.1005107

Slee, J. A., & Levine, T. P. (2019). Systematic prediction of FFAT motifs across eukaryote proteomes identifies nucleolar and eisosome proteins with the predicted capacity to form bridges to the endoplasmic reticulum. *Contact (Thousand Oaks)*, *2*, 1-21. https://doi.org/10.1177/2515256419883136

Tendulkar, S., Hegde, S., Garg, L., Thulasidharan, A., Kaduskar, B., Ratnaparkhi, A., & Ratnaparkhi, G. S. (2022). Caspar, an adapter for VAPB and TER94, modulates the progression of ALS8 by regulating IMD/NFkappaB-mediated glial inflammation in a Drosophila model of human disease. *Hum Mol Genet*, *31*(17), 2857-2875. https://doi.org/10.1093/hmg/ddac076

Thulasidharan, A., Garg, L., Tendulkar, S., & Ratnaparkhi, G. S. (2024). Age-dependent dynamics of neuronal VAPB(ALS) inclusions in the adult brain. *Neurobiol Dis*, *196*, 106517. https://doi.org/10.1016/j.nbd.2024.106517

Tsuda, H., Han, S. M., Yang, Y., Tong, C., Lin, Y. Q., Mohan, K., Haueter, C., Zoghbi, A., Harati, Y., Kwan, J., Miller, M. A., & Bellen, H. J. (2008). The amyotrophic lateral sclerosis 8 protein VAPB is cleaved, secreted, and acts as a ligand for Eph receptors. *Cell*, *133*(6), 963-977. https://doi.org/10.1016/j.cell.2008.04.039

Weber-Boyvat, M., Kentala, H., Peranen, J., & Olkkonen, V. M. (2015). Ligand-dependent localization and function of ORP-VAP complexes at membrane contact sites. *Cell Mol Life Sci*, *72*(10), 1967-1987. https://doi.org/10.1007/s00018-014-1786-x

Wong, H. C., Lang, A. E., Stein, C., & Drerup, C. M. (2024). ALS-Linked VapB P56S Mutation Alters Neuronal Mitochondrial Turnover at the Synapse. *J Neurosci*, *44*(35). https://doi.org/10.1523/JNEUROSCI.0879-24.2024

Wyles, J. P., & Ridgway, N. D. (2004). VAMP-associated protein-A regulates partitioning of oxysterol-binding protein-related protein-9 between the endoplasmic reticulum and Golgi apparatus. *Exp Cell Res*, *297*(2), 533-547. https://doi.org/10.1016/j.yexcr.2004.03.052

Xu, L., Wang, X., Zhou, J., Qiu, Y., Shang, W., Liu, J. P., Wang, L., & Tong, C. (2020). Miga-mediated endoplasmic reticulum-mitochondria contact sites regulate neuronal homeostasis. *Elife*, *9*. https://doi.org/10.7554/eLife.56584

Yamanaka, T., Nishiyama, R., Shimogori, T., & Nukina, N. (2020). Proteomics-Based Approach Identifies Altered ER Domain Properties by ALS-Linked VAPB Mutation. *Sci Rep*, *10*(1), 7610. https://doi.org/10.1038/s41598-020-64517-z

Yeshaw, W. M., van der Zwaag, M., Pinto, F., Lahaye, L. L., Faber, A. I., Gomez-Sanchez, R., Dolga, A. M., Poland, C., Monaco, A. P., van, I. S. C., Grzeschik, N. A., Velayos-Baeza, A., & Sibon, O. C. (2019). Human VPS13A is associated with multiple organelles and influences mitochondrial morphology and lipid droplet motility. *Elife*, *8*. https://doi.org/10.7554/eLife.43561

Zhao, Y. G., Liu, N., Miao, G., Chen, Y., Zhao, H., & Zhang, H. (2018). The ER Contact Proteins VAPA/B Interact with Multiple Autophagy Proteins to Modulate Autophagosome Biogenesis. *Curr Biol*, *28*(8), 1234-1245 e1234. https://doi.org/10.1016/j.cub.2018.03.002

# Chapter III

# Lipid imbalance in Amyotrophic Lateral Sclerosis 8/*ALS8* model uncovers VAPB role in LD homeostasis

## 3.1 Abstract

VAPB is an ER resident membrane protein which interacts with a lot of proteins to form membrane:membrane contact sites in the cell and helps in lipid transfer to various organelles. *VAPB/VAP* is the 8th ALS locus discovered, with the *VAPB*$^{P56S}$ mutation being the predominant variant in human patients. An orthologous mutation *VAP*$^{P58S}$ is used in *Drosophila* to study ALS8 pathogenesis. Earlier we showed *VAP*$^{P58S}$ flies develops normally; however, adult animals exhibit a shortened lifespan and age-dependent progressive motor dysfunction. In the adult *VAP*$^{P58S}$ brain, we observe mutant protein inclusions, ER stress and increased inflammation. Expression of *VAP*$^{WT}$ can rescue all disease phenotypes.

In this chapter, we investigated lipid imbalance in the *VAP*$^{P58S}$ brain using a combination of lipid mass spectrometry and genetic analysis. We observed an age dependent accumulation of cholesterol esters, accompanied by a concomitant decrease in cholesterol, all of which can be rescued by *VAP*$^{WT}$. Modulating *VAP* in glia perturbs LD homeostasis of the brain which is also affected in *ALS8* mutant. Removing mutant *VAP*$^{P58S}$ from the glia of adult brain leads to increase in LD density and also significantly delays the motor defects. Our study highlights the importance of *VAP* in lipid homeostasis of the brain and give new insights on its role in LD regulation. Further studies can help understand the precise role of *VAP* in the glial LD homeostasis.

## 3.2 Introduction

**3.2.1 Role of VAPB in lipid transport:** Lipids are transported intracellularly via two mechanisms either vesicular transport which requires ATP or non-vesicular transport generally involving lipid transfer proteins(Jansen et al., 2011; Kawano et al., 2006; Mesmin et al., 2019; Olkkonen, 2015; Weber-Boyvat, Kentala, Peranen, et al., 2015). Majority of the lipids are synthesized at ER membrane and then transferred to the other parts of the cell making its maintenance really crucial. Moreover, contact sites between ER and mitochondria or Golgi are highly significant as lot of lipid exchange happen between these membranes (Cockcroft & Raghu, 2018; Di Mattia et al., 2020; Kors, Costello, et al., 2022; Mesmin et al., 2019; Mishra et al., 2024; Yeshaw et al., 2019). Any

perturbation in these sites affect ER lipid homeostasis and cause cellular dysfunctions (Moustaqim-Barrette et al., 2014; Nhek et al., 2010; Teuling et al., 2007; Weber-Boyvat, Kentala, Peranen, et al., 2015). In several studies, VAPB role is well established in terms of lipid transfer to different organelles. OSBP interact with VAPB at ER and helps in transport of cholesterol from ER to Golgi, plasma membrane and lysosomes (Jansen et al., 2011; Weber-Boyvat, Kentala, Lilja, et al., 2015; Weber-Boyvat, Kentala, Peranen, et al., 2015; Wyles & Ridgway, 2004). Similarly, CERT interacts with VAPB at ER to transfer ceramide from ER to Golgi for the formation of other sphingolipids (Hanada, 2014). Another family of proteins VPS13A/C/D also interacts with VAPB at ER to transfer phospholipids and fatty acids (Slee & Levine, 2019; Yeshaw et al., 2019). VAPB role becomes really important in ER maintenance as a number of lipid transfer proteins interact with VAPB to transfer lipids (James & Kehlenbach, 2021; Kamemura & Chihara, 2019; Kors, Costello, et al., 2022; Neefjes & Cabukusta, 2021).

**3.2.2 *VAPB* as an *ALS8* locus:** In a Brazilian family of 28 affected members distributed across four generations, an autosomal dominant missense mutation was identified as 8$^{th}$ locus of ALS in *VAPB/ALS8* which leads to Proline to Serine substitution at 56$^{th}$ position (P56S) (Nishimura et al., 2004). Patients of *ALS8* generally show symptoms of progressive muscle weakness, cramp, autonomic dysfunction and behavioral impairments. *ALS8* subtype not only differs in terms of symptoms but the onset of the disease also varies along with the progression (Borgese et al., 2021; Nishimura et al., 2004; Qiu et al., 2013). Other mutations identified in *VAPB* and related to ALS are P56H, T46I, A145V and V234I (Kors, Costello, et al., 2022). Proline to Serine mutation in *VAPB* leads to the misfolding of mutant protein and cause disruption in cellular functions like membrane trafficking, ER stress response and activates unfolded protein response (Chaplot et al., 2019; Deivasigamani et al., 2014; Moustaqim-Barrette et al., 2014; Teuling et al., 2007; Thulasidharan et al., 2024). To study the role of *VAPB* (VAP further onwards*)* in context of ALS8, various cellular and animal models are available such as iPSCs, patient's cell lines, *S. cerevisiae*, *M. musculus*, *R. rattus*, *C. elegans* and *D. melanogaster* (Deivasigamani et al., 2014; Han et al., 2012; Kamemura et al., 2021; Qiu et al., 2013; Ratnaparkhi et al., 2008; Teuling et al., 2007; Tokutake et al., 2015; Wong et al., 2024; Zein-Sabatto et al., 2021). Each model has its own advantages and disadvantages. From various studies, ER stress, UPR, mitochondrial functioning and inflammation are some of the common factors which have been shown to be contributing to ALS (Chaplot et al., 2019; Moustaqim-Barrette et al., 2014; Tendulkar et al., 2022; Thulasidharan

et al., 2024). However, role of lipid metabolism in *ALS8* has been poorly understood which is quite surprising as a lot of VAP interactors are lipid transfer proteins (Alpy et al., 2013; Borgese et al., 2021; Cockcroft et al., 2016; Kors, Hacker, et al., 2022; Mikitova & Levine, 2012; Mishra et al., 2024; Perry & Ridgway, 2006; Yamaji et al., 2008).

**3.2.3 LDs in cellular homeostasis and disease:** VAP interactors like Oxysterol Related Protein 2 (ORP2) and VPS13A/C and MIGA2 are known to interact with LDs and helps in LD homeostasis (Bezawork-Geleta et al., 2025; Chen et al., 2022; Freyre et al., 2019; Olkkonen, 2015; Weber-Boyvat, Kentala, Lilja, et al., 2015; Xu et al., 2020; Yeshaw et al., 2019). Whenever, there is excess of TAGs or CEs present in the ER membrane, lipid droplets bud out from ER membrane with the help of protein SEIPIN along with phospholipid containing outer leaflet of ER membrane acting as monolayer of LD. Initially, nascent LDs are formed at ER which are quite small in size and later grows to mature LDs with more neutral lipids stuffed inside it. Some of the mature LDs remains bound to ER and thus interact with other organelles also like mitochondria, peroxisomes and lysosomes (Bohnert & Schrul, 2024; Henne et al., 2025; Mathiowetz & Olzmann, 2024; Mejhert et al., 2022; Walther & Farese, 2012). When energy requirements are not met inside the cell via glucose mediated reactions, lipids from LDs are hydrolyzed with the help of different lipases and used via β-oxidation (Haynes et al., 2024; Ioannou et al., 2019). Earlier LDs were considered to be rare in the brain but with a significant number of studies in the last two decades it is very clear glial cells specially astrocytes have a large pool of neutral lipids stored in the form of LDs. Various studies show LD accumulation in the brain of Alzheimer's, Parkinson's and ALS models (Chaves-Filho et al., 2019; Goodman et al., 2024; Ioannou et al., 2019; Liu et al., 2015; Moulton et al., 2021; Teixeira et al., 2021).

**3.2.4 Lipid Homeostasis in *Drosophila ALS8* model:** In *Drosophila*, Proline is conserved at 58$^{th}$ position of *VAP* protein which is mutated to Serine to mimic ALS like phenotypes (Ratnaparkhi et al., 2008; Tsuda et al., 2008). Previously, our lab have used an overexpression model of *VAP*$^{P58S}$ where we showed *SOD1* and *Tor* as genetic interactors of *VAP* and is involved in the modulation of *VAP* aggregation. Knockdown (KD) of these genes also led to increase in oxidized lipids because of higher ROS levels (Chaplot et al., 2019). Then we used genomic model of *ALS8* where mutant gene *VAP*$^{P58S}$ is expressed under genomic promotor of *VAP* as described earlier in

(Moustaqim-Barrette et al., 2014; Tendulkar et al., 2022; Thulasidharan et al., 2024). (Moustaqim-Barrette et al., 2014) showed that OSBP does not interact with *VAP*$^{P58S}$ which may lead to cholesterol accumulation at ER membrane and gets converted to cholesterol esters. Moreover, when human copy of OSBP i.e. ORP8 (independent of VAP binding for function) was expressed in the motor neurons, ALS defects were partially rescued. But no previous study has been done for the lipid profiling of *ALS8* mutation in human patients. Also, *VAP* role in LD homeostasis is poorly understood and it's role in *ALS8* disease. In this study, we have tried to understand the role of *VAP* in maintaining lipid homeostasis of the brain using *Drosophila* as a model organism. With the combination of genetics and biochemistry, we investigated the effect of *VAP*$^{P58S}$ on *Drosophila* brain lipid levels. Based on lipid profiling results, we explored VAP function in LD homeostasis of glia. Our study uncovers the role of *VAP* in regulating glia LD homeostasis which gets perturbed in *VAP*$^{P58S}$ model of *Drosophila*. This disruption in lipid regulation highlights a previously underexplored function of VAP in the nervous system and underscores the importance of lipid balance in the context of ALS8 pathogenesis.

## 3.3 Results

**3.3.1 Age dependent LC-MS based lipid profiling of *ALS8* flies' brain:** In previous studies (Moustaqim-Barrette et al., 2014; Tendulkar et al., 2022) it is reported that Δ*VAP/Y ;; gVAP*$^{P58S}$ has shortened lifespan and climbing defects. So, we wanted to see if there is an age dependent change in the lipid levels. Intriguingly, we found an age dependent increase in cholesterol levels of wild type flies' brain given to the fact that flies cannot synthesize their own cholesterol and depends on the diet (Fig. 3.1A) (Niwa & Niwa, 2011). However, cholesterol esters were quite low in the wildtype flies (Fig. 3.1B). Interestingly, there was significant reduction in the cholesterol levels of the *VAP*$^{P58S}$ brains from day 5 onwards compared to control. Moreover, only mild increase was detected in *ALS8* model brains as they age (Fig. 3.1A). Furthermore, cholesterol ester levels were significantly higher on 2$^{nd}$ day itself which increased robustly with age in the Δ*VAP/Y ;; gVAP*$^{P58S}$ brains and saturates after day 15 (Fig. 3.1B). In addition to this, we did not see much change in the increased levels of saturated or unsaturated chain lengths of CEs. (Moustaqim-Barrette et al., 2014; Thulasidharan et al., 2024) shows that putting genomic copy of *VAP*$^{WT}$ in the *ALS8* background leads to complete rescue of lifespan and motor defects. So, Kriti from the lab in collaboration with Prof. Siddhesh performed LC-MS for cholesterol and cholesterol ester levels in the same genetic background. She found that both lipid levels were completely back to normal levels at day 15 post eclosion (Fig. 3.1C-D). Similarly, Triacylglycerols (TAGs) were found to be higher on 15$^{th}$ day which was rescued with the genomic copy of *VAP*$^{WT}$ (Fig. 3.1E).

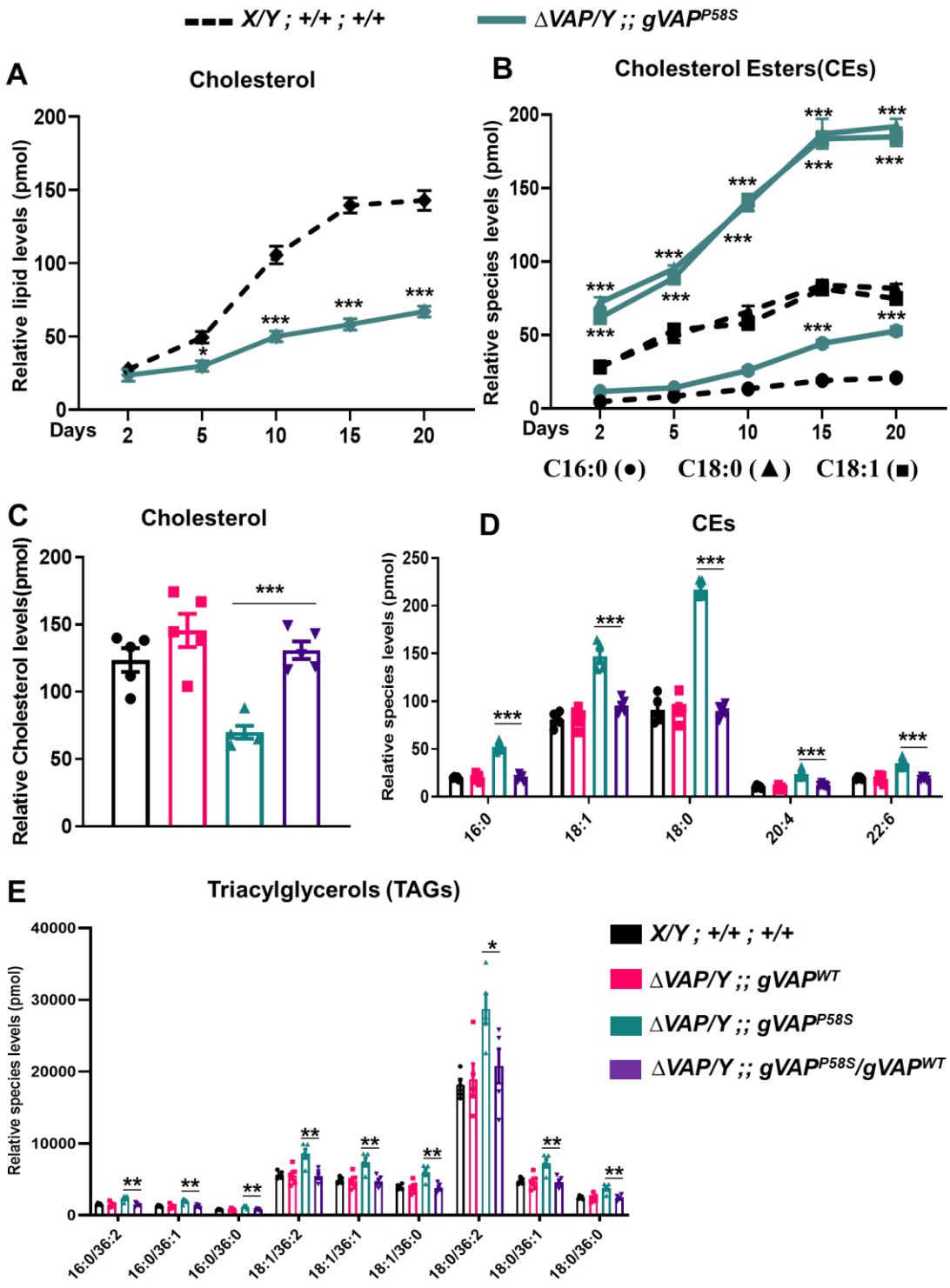



**Figure 3.1: Age dependent lipid profiling of *Drosophila* adult brains.**

(A) Cholesterol levels increase with age in wild-type flies and reach at saturated levels after day 15. Lipid levels are unchanged at 2nd day of mutant flies compared to control but with age these levels are significantly reduced.

(B) Unlike cholesterol, cholesterol esters are increased at 2nd day itself and it increases further with age in ALS8 model. Lipid species for cholesterol esters are presented as C16:0(●), C18:0(▲) and C18:1(■). Mean±Standard Error Mean (SEM) of relative lipid levels are plotted in the graph with number of days on X-axis. Multiple unpaired t-test with FDR approach of Benjamin and Hochberg is used for comparisons between same species of genotypes using APA style for p-values. N=5, n=2 brains for each genotype. Wildtype control shown in black color (---), Δ*VAP/Y ;; gVAP*$^{P58S}$ shown in green color (---).
(C-E) Rescue of cholesterol, cholesterol esters and triacylglycerol levels in the adult brain of 15th day old flies. Data was reproduced from Kriti Chaplot thesis work (Chaplot, 2019).

**3.3.2 Age dependent LD distribution in *ALS8* model:** As suggested in other neurodegeneration models, there is lipid droplet accumulation seen in the glia because of increased lipogenesis in the neurons (Liu et al., 2015). Lipid droplets mainly contain CEs and TAGs as the core component. As we saw in figure 3.1, CEs and TAGs levels were higher at day 15 of *ALS8* flies and these levels were completely rescued after the addition of *VAP*$^{WT}$. Firstly, we decided to probe for age dependent LD distribution using BODIPY in the brain of Δ*VAP/Y ;; gVAP*$^{P58S}$. For quantitation analysis, two zones were selected i.e. Zone 1 with cells around subesophageal region (SEZ) and Zone 2 with cells around antennal lobe (AL) shown in (Fig. 3.2).

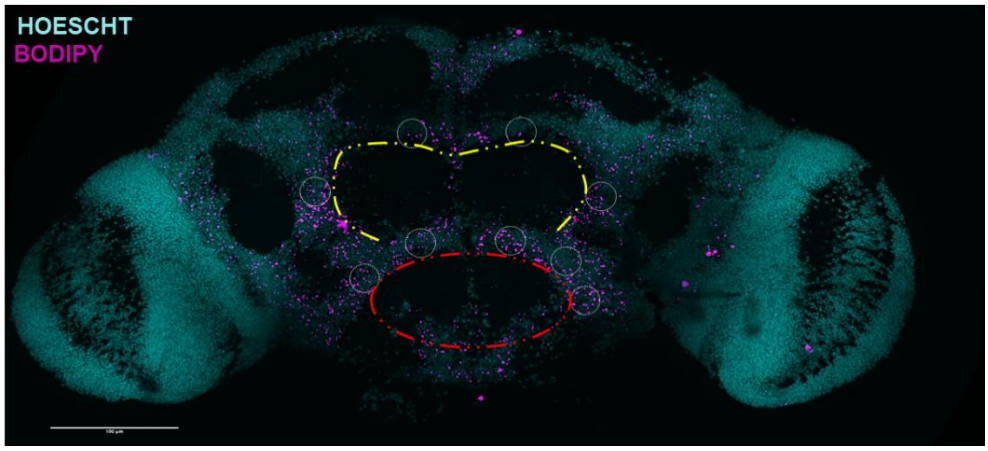



**Figure 3.2: BODIPY stained LD distribution in the adult brain of *Drosophila*.**

Representative maximum intensity projection (MIP) of LD staining in the *Drosophila* male adult brain. Hoescht (cyan) represents nuclei staining, BODIPY (magenta) represents LD staining. Five ROIs are drawn around suboesophageal region (red line) named as zone 1 and four ROIs around antennal lobe (yellow line) named as zone 2 used for LD analysis. Scale bar is shown as 100um. N=1 *CS* adult brain.

We did not see any major changes in the LD distribution of zone 1 and zone 2 in the control brain as they age till 20 days. However, LD size seemed to increase with age (Fig. 3.3A-D). Surprisingly, we saw lesser lipid droplets at the 5$^{th}$ day of Δ*VAP/Y ;; gVAP*$^{P58S}$ brain compared to control (Fig. 3.3A'). Secondly, even CEs and TAGs are higher in *ALS8* model, it is quite puzzling to see less LDs. Next, we looked at LD distribution for 10$^{th}$, 15$^{th}$ and 20$^{th}$ day respt. and did not find any significant decrease further with age in the mutant (Fig. 3.3B'-D'). As shown in (Thulasidharan et al., 2024), two copies of *VAP*$^{P58S}$ in the *ALS8* flies leads to worsened lifespan, motor defects and double aggregation density compared to single dose of *VAP*$^{P58S}$, so we checked its effect on LD distribution. Interestingly, we did not detect major difference compared to single copy of mutant for both zones (Fig.3.3A"-D")

When we quantified LDs for both zones, we found that there was 30-40% decrease in LD density (number of droplets per μm$^3$) of zone 1 in Δ*VAP/Y ;; gVAP*$^{P58S}$ and Δ*VAP/Y ;; gVAP*$^{P58S}$*/gVAP*$^{P58S}$ brains at day 5 which remains constant for other days also with respect to control (Fig. 3.4A). As mentioned earlier, in control we saw age dependent increase in LD size/volume (μm$^3$). However, in the case of single copy and double copy mutants, there was no major change in the median of LD size at day 5 but more fraction of smaller size LDs were found on day 20 suggesting age dependent decrease in LD size in *ALS8* flies (Fig. 3.4B). We found similar results for zone 2 as well where LD density was lower for mutant compared to control but decrease was around 25-30% (Fig. 3.4C). In terms of LD size, we found more droplets of smaller size present out of total fraction in the mutant at day 5 itself (Fig. 3.4D).

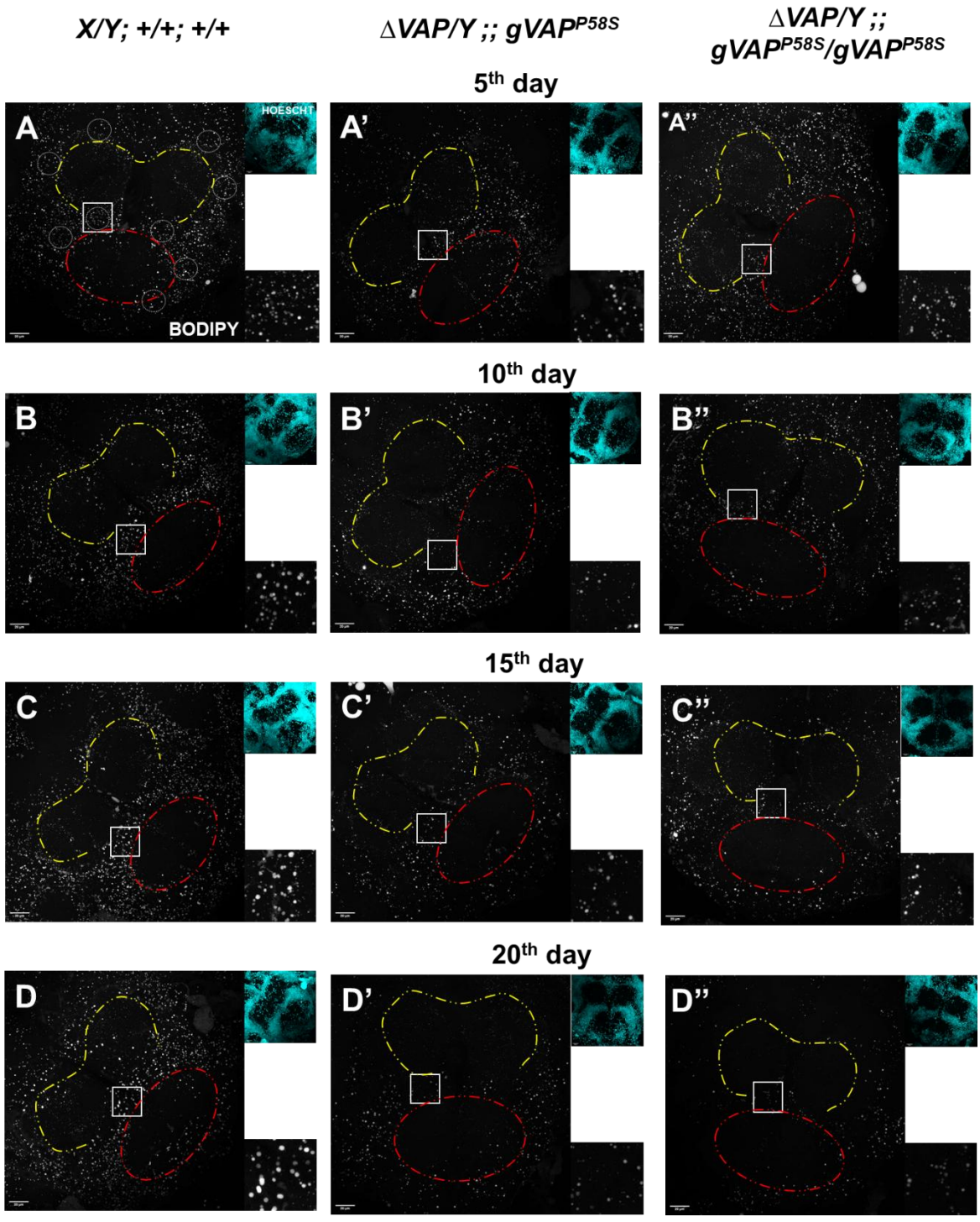



**Figure 3.3: Perturbation of LD homeostasis in the adult brain of *ALS8* model**.

(A-D") Representative MIPs (20% Brightness) of BODIPY (493/503) stained LDs in the *Drosophila* adult brain's central body (0.75X). (A-A") shows 5$^{th}$ day LD distribution for wildtype (A), Δ*VAP/Y ;; gVAP$^{P58S}$* (A') and Δ*VAP/Y ;; gVAP$^{P58S}$/gVAP$^{P58S}$* (A"). Similarly, (B-B"), (C-C") and (D-D") represents distribution for 10$^{th}$, 15$^{th}$ and 20$^{th}$ day respt. Two zones are selected for the

analysis of lipid droplets present in the drawn ROIs as shown in (A) colored by red and yellow lines. Nuclei staining of the adult brain is shown at the right top corner of the LD images. Zoomed image of the inset is shown at the right bottom corner of the individual images. N=5-6 male adult brains per genotype. Scale bar of the image is 20µm.

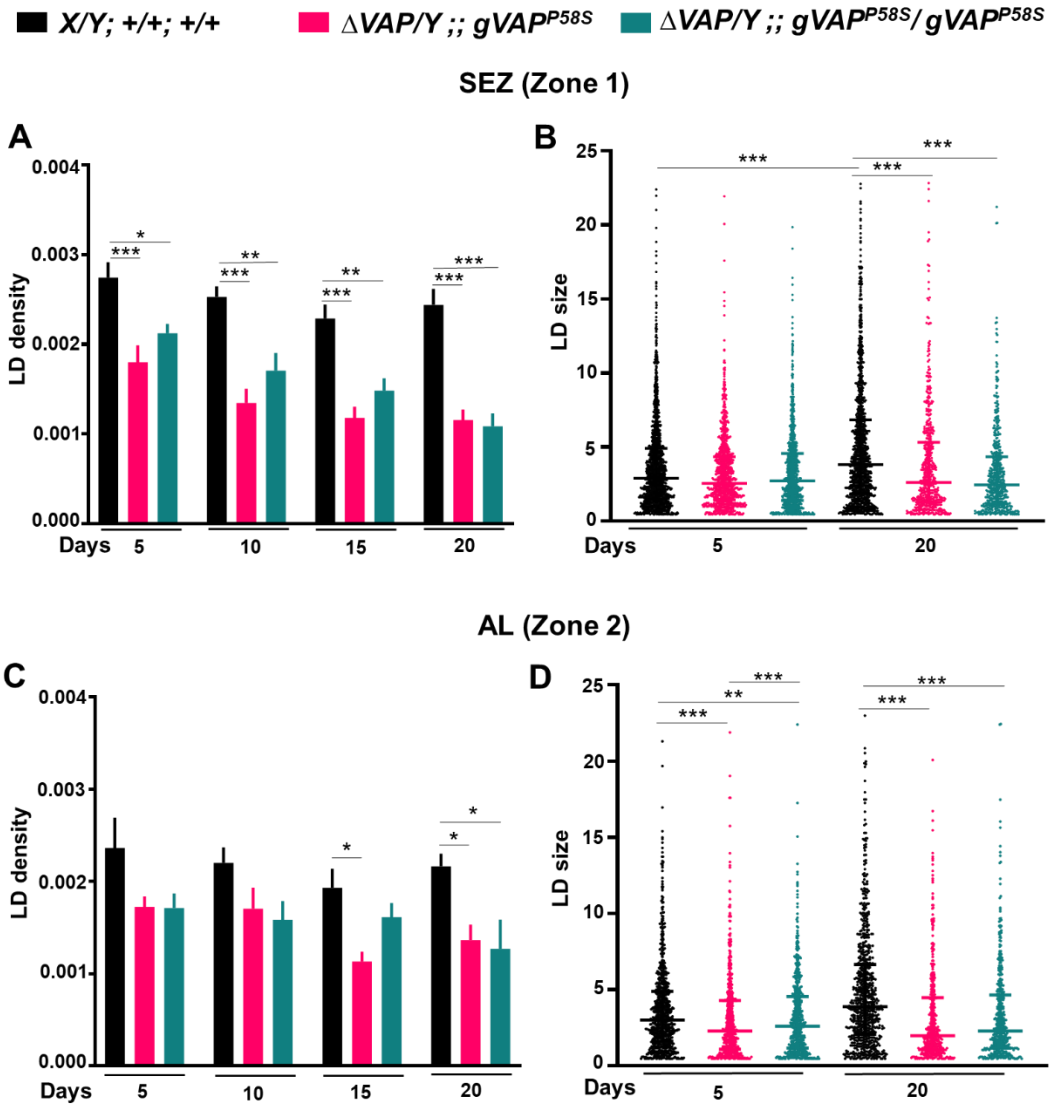



**Figure 3.4: Quantitation of LDs present in the adult brain of *ALS8* flies**.

(A) Quantitative analysis for the LDs in Zone 1(SEZ) is performed using LD density (number of droplets per µm$^3$) as parameter. Around 30% drop in lipid droplets were observed on 5$^{th}$ day only in mutant for both Δ*VAP/Y ;; gVAP*$^{P58S}$ and Δ*VAP/Y ;; gVAP*$^{P58S}$/*gVAP*$^{P58S}$ which remained constant for other days as well. Mean±SEM value of each genotype is plotted in the graph with density on Y axis and number of days on X axis. Two way ANOVA followed by Tukey's test is used for statistical significance using APA style of p values.

(B) Scatter dot plot for LD size/volume (μm$^3$) of zone 1(SEZ) is plotted with the droplets from all ROIs of each genotype taken which was used for LD density. LD size increases with age in control but not for Δ*VAP/Y ;; gVAP*$^{P58S}$ and Δ*VAP/Y ;; gVAP*$^{P58S}$/*gVAP*$^{P58S}$. Median with interquartile range is shown in the graph with size in μm$^3$ on Y-axis and number of days on X-axis. Kruskal-Wallis test followed by Dunn's test for LD size is used for multiple comparisons between genotypes using APA style for showing p-values.
(C) Quantitative analysis for the LD density in Zone 2(AL) of the adult brain for control, Δ*VAP/Y ;; gVAP*$^{P58S}$ and Δ*VAP/Y ;; gVAP*$^{P58S}$/*gVAP*$^{P58S}$ is performed and plotted as Mean±SEM LD density on Y-axis along with number of days on X-axis. Two way ANOVA for LD density followed by Tukey's test for multiple comparisons is used for statistical significance with APA style of p values shown in the graph.
(D) Scatter dot plot for LD size distribution in zone 2(AL) with median and interquartile range is shown for same genotypes. Kruskal-Wallis for LD size followed by Dunn's test is used for multiple comparisons between genotypes using APA style for showing p-values. N=5-6 brains, n= 5 ROIs for Zone 1 of each genotype.

**3.3.3 Rescue of LD homeostasis with *VAP*$^{WT}$ in *ALS8* model:** With single *VAP*$^{WT}$ in the Δ*VAP/Y ;; gVAP*$^{P58S}$ background, we found that CEs and TAGs were completely rescued (Fig. 3.1C-E) so we probed for LD distribution in the similar genetic background in an age dependent manner. Similar changes were seen for LD distribution in the control and Δ*VAP/Y ;; gVAP*$^{P58S}$/*gVAP*$^{P58S}$ flies like in Fig. 3.3 for 5$^{th}$, 10$^{th}$ and 15$^{th}$ day respt. (Fig. 3.5A-C"). In the case of Δ*VAP/Y ;; gVAP*$^{P58S}$/*gVAP*$^{WT}$ flies, initially we did not see rescue in terms of LD density at day 5 but with age LD density was rescued completely for zone 1 (SEZ) (Fig. 3.5A"-C", 3.6A). Interestingly, even after putting *VAP*$^{WT}$ in the Δ*VAP/Y ;; gVAP*$^{P58S}$ background, *VAP*$^{P58S}$ aggregates are still present at day 5 and only with age these aggregates are cleared through autophagy (Thulasidharan et al., 2024). LD density was not restored in Zone 2 (AL) shown in (Fig. 3.6C). Next, we checked for lipid droplet size in the both zones. Unlike LD density, lipid droplet size was reduced in Δ*VAP/Y ;; gVAP*$^{P58S}$/*gVAP*$^{WT}$ compared to control and looks similar to mutant on 5$^{th}$ day (Fig. 3.6B). However, on 15$^{th}$ day, droplet size was significantly bigger than mutant in both zones but not to that control levels (Fig. 3.6B, D).

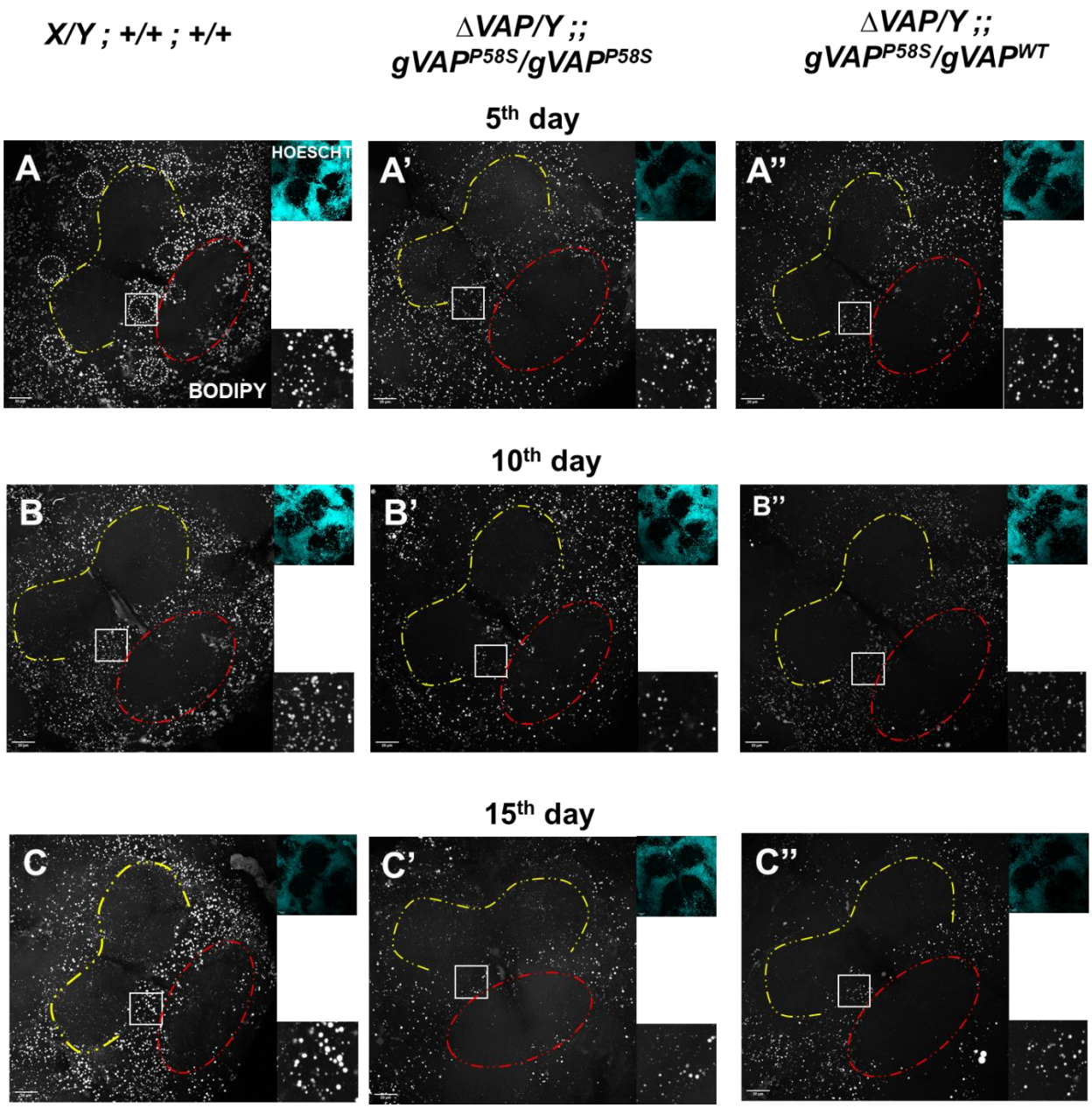



**Figure 3.5: Single copy of *VAP$^{WT}$* partially restores LD homeostasis in *ALS8* flies**.

(A-C") Representative MIP images of BODIPY stained LDs in adult brain's central body (0.80X) for 5$^{th}$, 10$^{th}$, 15$^{th}$ day respt. (A-A") shows 5$^{th}$ day LD distribution for Δ*VAP/Y ;; gVAP$^{P58S}$* and Δ*VAP/Y ;; gVAP$^{P58S}$/gVAP$^{WT}$* compared to control flies. Similarly, (B-B") and (C-C") represents distribution for 10$^{th}$ and 15$^{th}$ days. Two zones are selected for the analysis of lipid droplets present in the drawn ROIs as shown in (A) colored by red and yellow lines. Nuclei staining of the adult brain is shown at the right top corner of the LD images. Zoomed image of the inset is shown at the right bottom corner of the individual images. N=5-6 male adult brains per genotype. Scale bar of the image is 20µm.

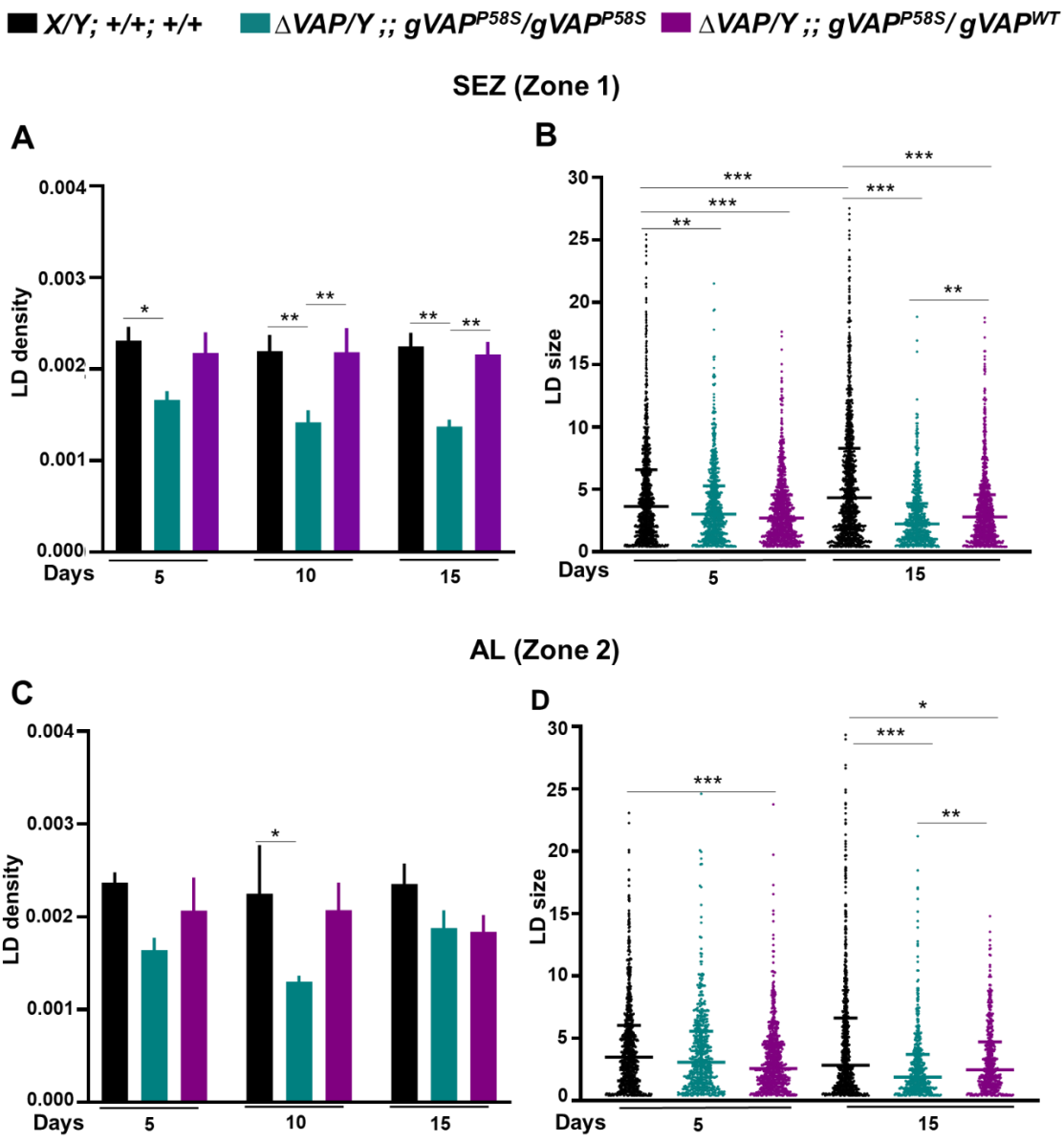



**Figure 3.6: Quantitation of LDs restoration by *VAP$^{WT}$* in ALS8 flies**.

(A) Quantitative analysis for LD density for Zone 1(SEZ) is performed using ImageJ. LD density is reduced by 5$^{th}$ day only in mutant for Δ*VAP/Y ;; gVAP$^{P58S}$/gVAP$^{P58S}$* which did not restores back intially in Δ*VAP/Y ;; gVAP$^{P58S}$/gVAP$^{WT}$* and gradual restores which remains till 15$^{th}$ day also. Mean±SEM value of each genotypes are plotted as LD density (number of droplets per μm$^3$) on Y axis with number of days on X axis. Two way ANOVA is used as statistical test followed by Tukey's test for multiple comparisons using APA style for p values.

(B) Scattered dot plot is shown with median and interquartile range of the LDs from five ROIs of zone 1 (SEZ) of each genotype with LD size on Y axis and number of days on X axis. There was no major change in LD size of mutant and rescue model on day 5 but shows significant rescue at day 15 compared to *ALS8* brains although still lesser than control ones. Kruskal Wallis (Dunn's

test) for LD size is used for multiple comparisons between genotypes using APA style for showing p-values.
(C) LD density is plotted for zone 2 (AL) which showed no significant rescue Δ*VAP/Y ;; gVAP*$^{P58S}$/*gVAP*$^{WT}$ compared to Δ*VAP/Y ;; gVAP*$^{P58S}$/*gVAP*$^{P58S}$ on 5$^{th}$, 10$^{th}$ and 15$^{th}$ days respt. Two way ANOVA is used as statistical test followed by Tukey's test for multiple comparisons using APA style for p values.
(D) Scatter dot plot for LD size distribution is shown for same genotypes. No change was found in the LD size of control, mutant and rescue model at day 5 but significant rescue was there in rescued flies compared to mutant on day 15. Kruskal Wallis followed by Dunn's test for LD size is used for multiple comparisons between genotypes using APA style for showing p-values.
N~5-6 brains, n= 5 ROIs for zone 1 and n= 4 ROIs for Zone 2 of each genotype.

**3.3.4 Role of *VAP* in LD homeostasis:** In various studies, it has been shown that glia is the major hub for the lipid droplets in the brain of *Drosophila* and plays crucial role in LD homeostasis (Byrns et al., 2024; Farmer et al., 2020; Girard et al., 2020; Haynes et al., 2024; Smolic et al., 2021). We modulated *VAP* in the glia of wild type flies and looked at LD distribution in the ventral nerve cord of late 3$^{rd}$ instar larval brain. Interestingly, knockdown of *VAP* in the glia led to higher LD density whereas higher *VAP* levels reduced the density. However, putting more *VAP*$^{P58S}$ showed no change compared to control suggesting partial loss of *VAP* activity (Fig. 3.7A-F). In terms of size, no significant change was observed among the genotypes (Fig. 3.7F).

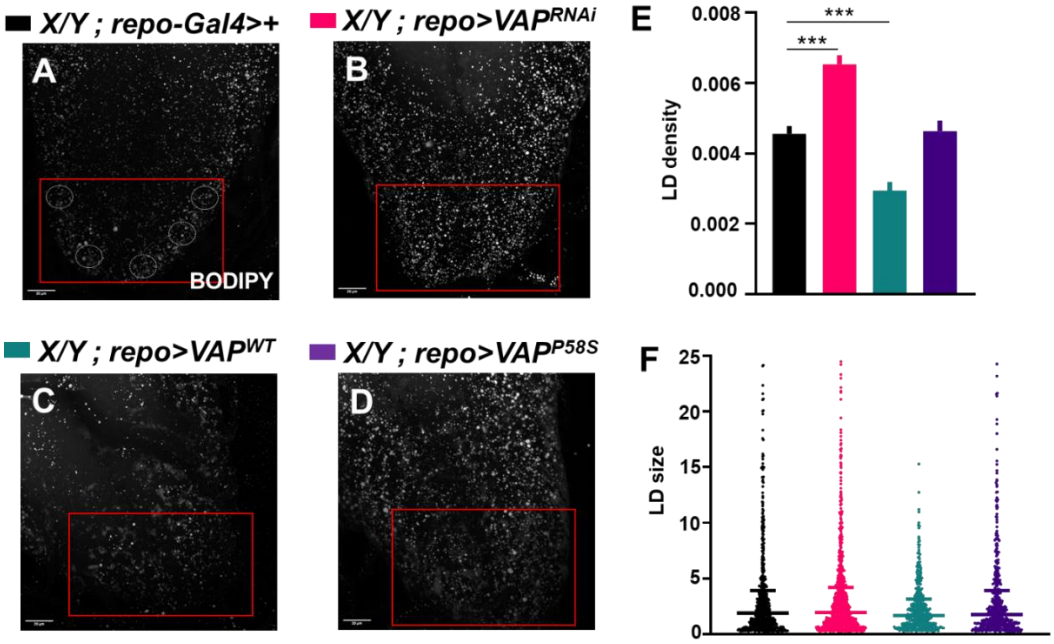


**Figure 3.7: Glial *VAP* modulation affects LD homeostasis in *Drosophila* larval brain**.

(A-D) represents MIP (20% Brightness) of ventral nerve cord of late 3rd instar larval brain stained with BODIPY. *VAP* knockdown in glia increases LDs compared to control (A, B). Overexpression of $VAP^{WT}$ shows decrease in LD density (C) whereas $VAP^{P58S}$ shows no change compared to control (D). Quantitative analysis of LDs in the form of density is presented in (E). LD size is plotted in the form of scattered dot plot showing total droplets accounted for with their size (F). One way ANOVA is used followed by Tukey's test for multiple comparisons with their control, p value is shown in APA style, error bars as SEM. N~4-5 brains, n=5 ROIs. Scale bar is represented as 20µm.

To check if *VAP* shows same affect in adult brain, we modulated *VAP* in the glia and looked at LD distribution in zone 1 (SEZ region) of the adult brain at 5th and 20th day respt. Knockdown of *VAP* in the glia led to marginal increase in LD density on 5th day which significantly increased with age of the flies (Fig. 3.8A-C). However, more number of droplets were of smaller size as shown in (Fig. 3.8D). Then, we increased $VAP^{WT}$ and $VAP^{P58S}$ levels in the glia and looked for LD homeostasis. Interestingly, we found lesser LD density on the 5th day in the case of higher $VAP^{WT}$ levels whereas $VAP^{P58S}$ overexpression showed no change in LD density (Fig. 3.9A-C). For 20th day, we saw the same effect like on 5th day in both cases (Fig. 3.9B). Interestingly, $VAP^{P58S}$ levels in the glia led to more fraction of droplets with smaller size (Fig. 3.9D). These results clearly suggests VAP plays a role in LD homeostasis as knockdown leads to more LDs whereas more VAP reduce LD content. More $VAP^{P58S}$ in the glia shows no change in LD density but in size suggesting mutant VAP behaves like partial loss-of-function allele. From our results, it is observed that *VAP* modulation in the glia regulates LD homeostasis, so we checked it's effect on the climbing activity of flies. No significant change was seen in the flies till 20th day of the wild type flies. However, overexpression of both $VAP^{WT}$ and $VAP^{P58S}$ in the glia showed significant reduction in the motor activity from 25th day onwards (Fig. 3.9E).

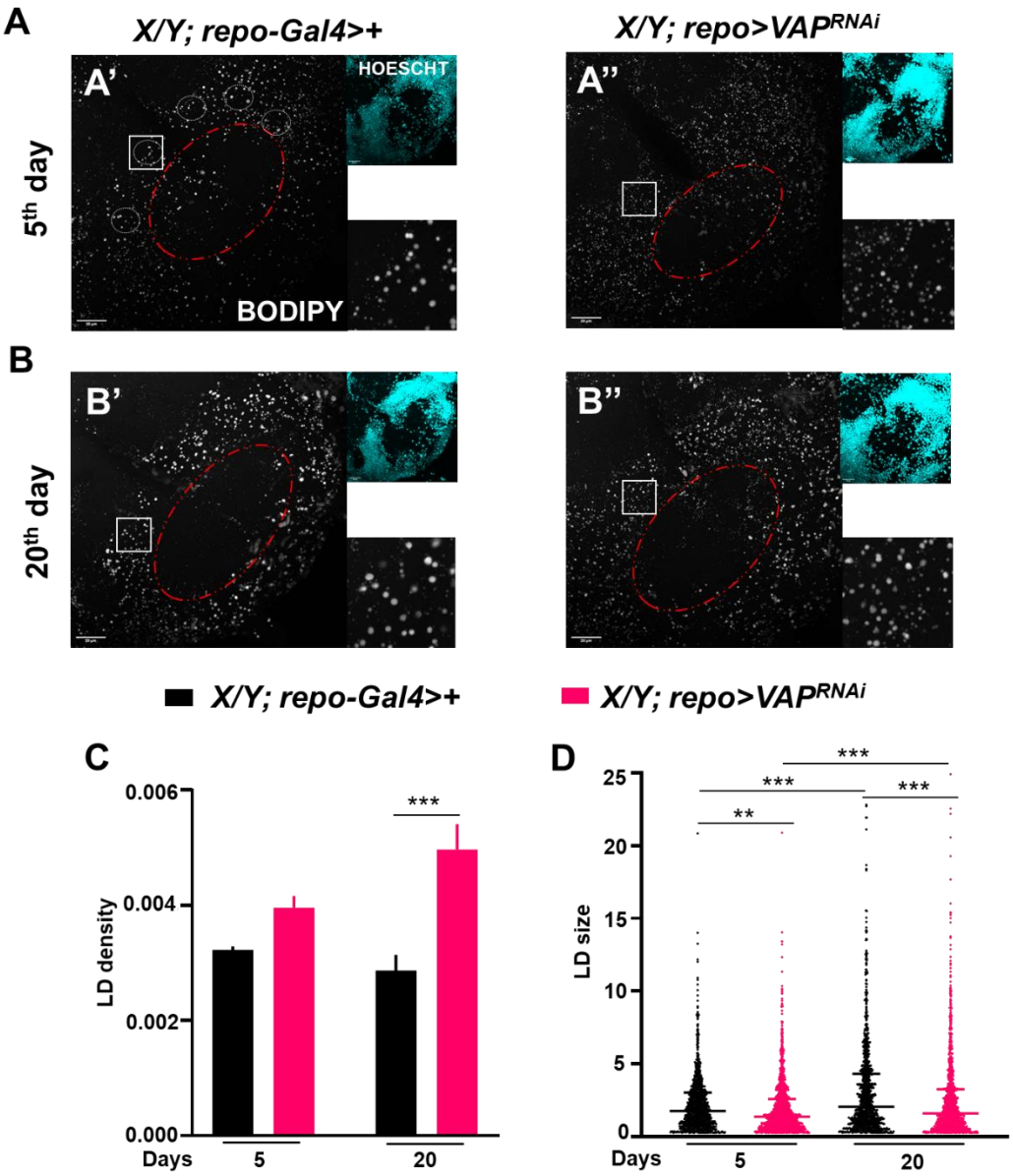



**Figure 3.8: Glial loss of *VAP* leads to more LDs with smaller size in the *Drosophila* adult brain**.

(A-B) shows MIPs (20% Brightness) of age dependent increase in adult brain LDs on *VAP* knockdown in glia. (A', B') are LD stained images for control of day 5 and day 20. (A", B") are LD stained images for *VAP* KD in glia of day 5 and day 20. Five ROIs are marked as circles around SEZ zone outlined with red color as shown in (A). Nuclei staining of the adult brain is shown at the right top corner of the LD images. Zoomed image of the inset is shown at the right bottom corner of the individual images. Scale bar is represented as 20µm.

(C) Mean±SEM is plotted as LD density on Y axis with number of days on X axis where mild increase is visible on 5$^{th}$ day after *VAP* knockdown but on 20$^{th}$ day significant increase can be seen

(B"). Two way ANOVA followed by Tukey's test for multiple comparisons is used for statistical significance with APA style for p values.
(D) LD size is plotted in the form of scatter dot plot for control and *VAP* KD in glia where size is reduced on *VAP* loss in glia. Kruskal Wallis test for LD size is used followed by Dunn's test for comparisons w, p-values are mentioned using APA style.
N=5 brains for each genotypes, n=5 ROIs for LD analysis.

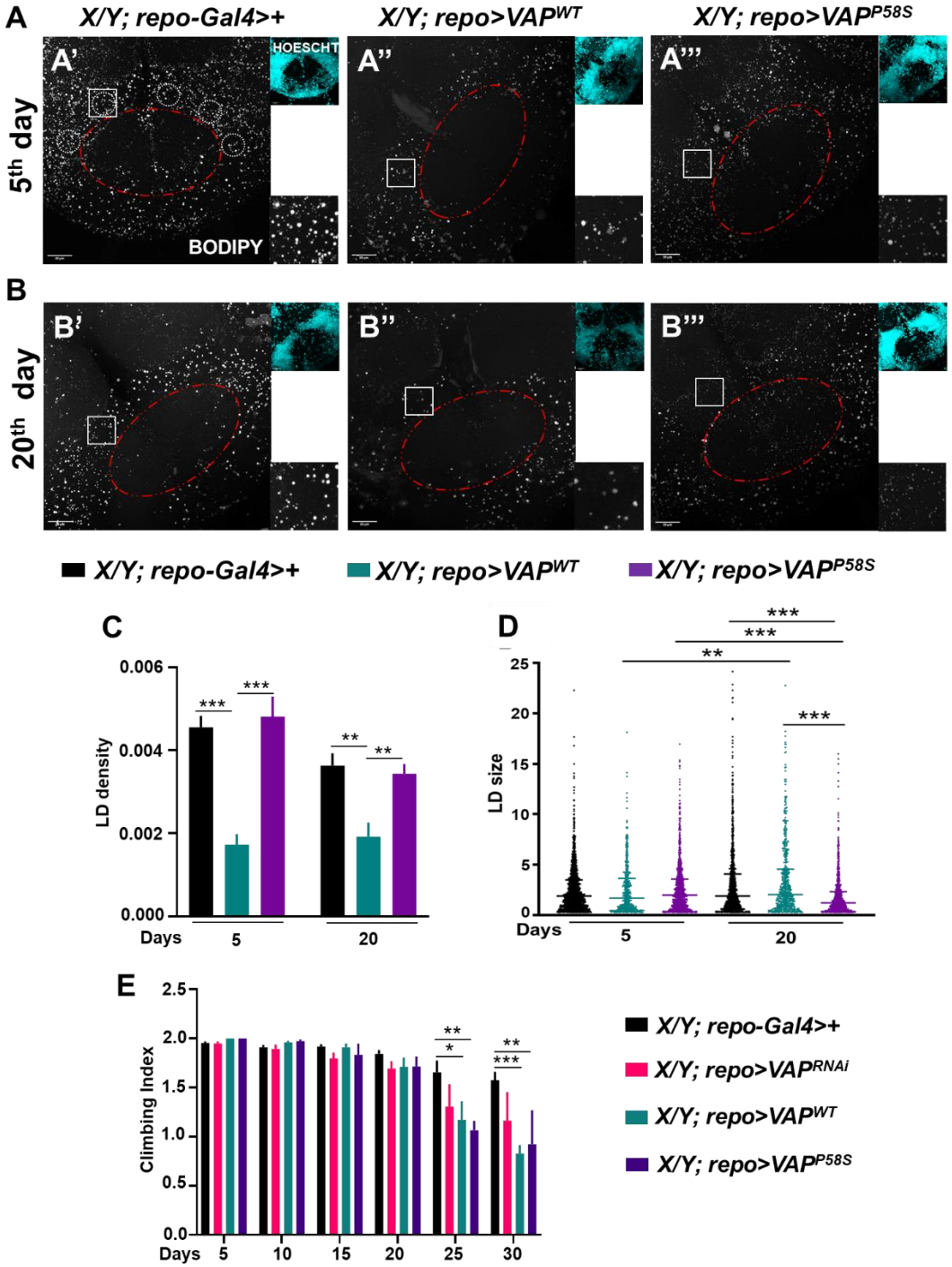


**Figure 3.9: More *VAP* in glia negatively affects LD homeostasis in the adult brain**.

(A-B) are representative images (20% Brightness) of lipid droplets stained in the *Drosophila* adult brain on *VAP* modulation in glia. Five ROIs are marked around SEZ region with red outline as shown in (A') used for analysis. (A'-B') for Gal4 control LD images, (A''-B'') for Glial $VAP^{WT}$ OE, (A'''-B''') for Glial $VAP^{P58S}$ OE is shown for 5$^{th}$ day and 20$^{th}$ day respt. Glial overexpression of $VAP^{WT}$ leads to decrease in LD density on day 5 of flies as shown in (A'') which stays till day 20 as well (B''). $VAP^{P58S}$ OE in glia shows no change in density on day 5 but shows slight increase in density on day 20 (A''', B''', C). Nuclei staining of the adult brain is shown at the right top corner of the LD images. Zoomed image of the inset is shown at the right bottom corner of the individual images. Scale bar is represented as 20µm.
(C) LD density is plotted as Mean±SEM with density on Y axis and number of days on X axis. Two way ANOVA is used followed by Tukey's test followed by multiple comparisons among genotypes with statistical significance shown in APA style for p values.
(D) In terms of LD size, no change was found on day 5 among genotypes but on day 20, $VAP^{P58S}$ OE in glia led to significant decrease in LD size. Kruskal-Wallis for LD size followed by Dunn's test is used for multiple comparisons between genotypes using APA style for showing p-values. N~5-6, brains, n=5 ROIs for each genotype.

**3.3.5 $VAP^{P58S}$ affects glial LD homeostasis in a genomic model of *ALS8*:** As loss of *VAP* in the glia led to more number of LDs, we proposed the question if it shows the same phenotype in *ALS8* model also? We used *split ends* (*spen)* as positive control which is known to regulate LD homeostasis in the glia and on KD, leads to increase in LDs in the adult brain (Girard et al., 2020). We knocked down *VAP* to remove $VAP^{P58S}$ and KD *spen* in the glia of $VAP^{P58S}$ model and looked at LD distribution in the 15 day old male brains. Surprisingly, we saw significant increase in the LD density and size of the droplets for both *VAP* and *spen* shown in (Fig. 3.10A-C). Next, we looked at the climbing activity of the diseased $VAP^{P58S}$ after knocking down both *VAP* and *spen* in the glia. However, we did not see any rescue in their climbing ability (Fig. 3.10D). Interestingly, we found *spen* KD led to worsening of climbing phenotype in *ALS8* suggesting LD accumulation also is bad for flies.

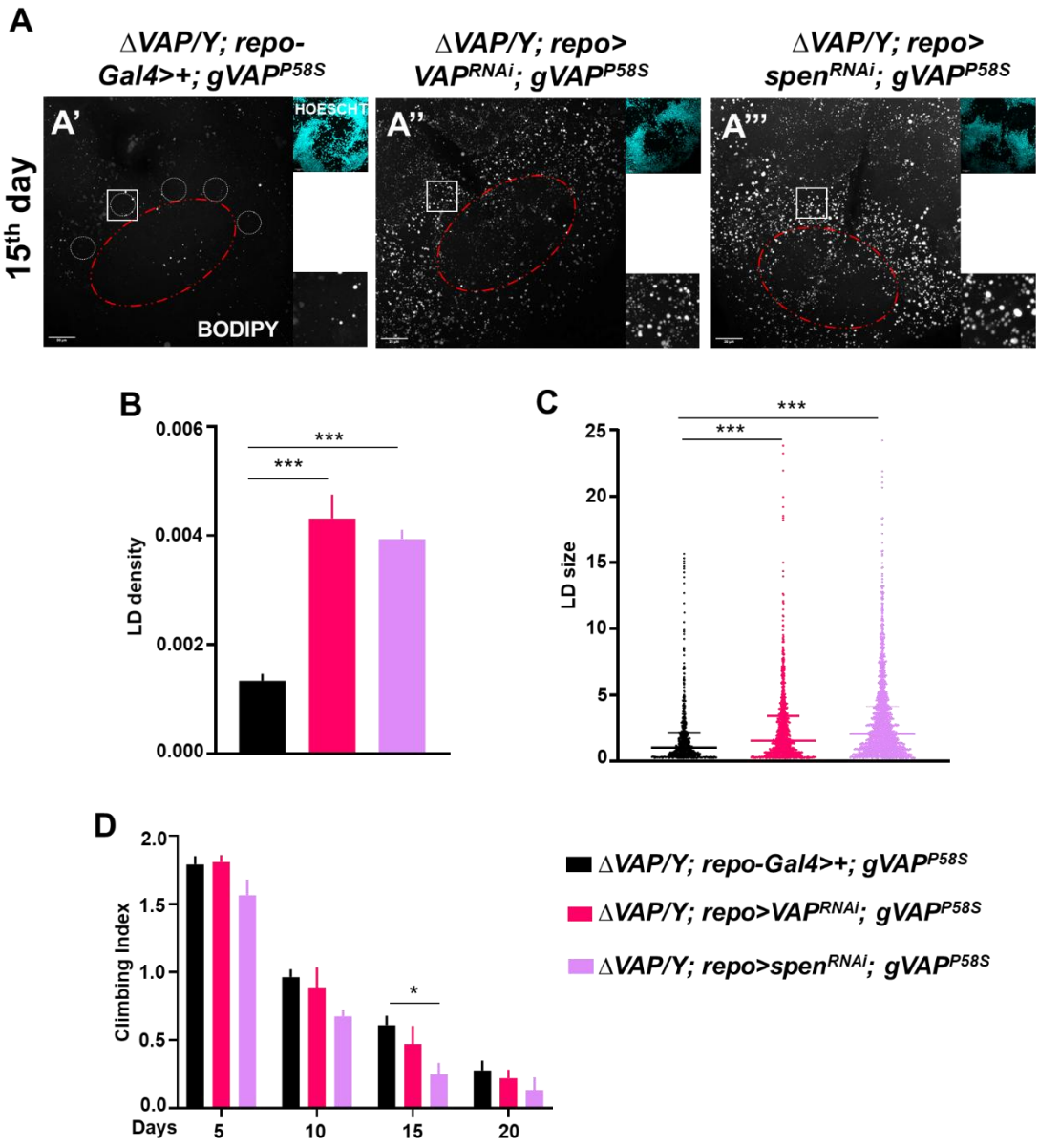



**Figure 3.10: *VAP* KD rescues LD homeostasis in the glia of *ALS8* flies**.

(A) represent MIPs (20%Brightness) of BODIPY stained LDs in the day 15 of adult brain (zone 1) of Δ*VAP/Y ; repo-Gal4>+; gVAP*$^{P58S}$(A'), Δ*VAP/Y ; repo>VAP*$^{RNAi}$*; gVAP*$^{P58S}$ (A") and Δ*VAP/Y ; repo>spen*$^{RNAi}$*; gVAP*$^{P58S}$ (A"'). Both *VAP* and *spen* knockdown in the glia of *VAP*$^{P58S}$ flies lead to significant increase in LD density (B) and size (C). Nuclei staining of the adult brain is shown at the right top corner of the LD images. Zoomed image of the inset is shown at the right bottom corner of the individual images. Scale bar is represented as 20µm.

(B) For LD density, Mean±SEM values are plotted for the mentioned genotypes of day 15. One way ANOVA is used followed by Tukey's test for comparisons with the control using APA style of p values.

(C) For LD size, scatter dot plot is used for the genotypes mentioned with droplets from all five ROIs of each genotype taken into consideration. Kruskal-Wallis followed by Dunn's test is used for statistical significance with APA style p value.
N~5-6, brains, n=5 ROI for each genotype.
(D) represents climbing activity of the flies where both *VAP* and *spen* knockdown in the glia of *ALS8* flies showed no change. Two way ANOVA is used followed by Tukey's test for comparisons with control, p value is shown in APA style.
N=3 biological replicates, n~30 males, error bars as SEM.

**3.3.6 Removal of $VAP^{P58S}$ from glia rescues *ALS8* climbing ability:** From previous studies and our current larval brain experiments it is quite clear that *VAP* plays an important role in the development of flies. Also, *VAP* KD in glia showed changed in LD density of *ALS8* flies but not in motor defects (Fig. 3.10). So, we modulated *VAP* by removing $VAP^{P58S}$ or OE $VAP^{WT}$ and $VAP^{P58S}$ in the glia of *ALS8* flies and kept the eggs at 18°C until the eclosion of flies. After eclosion, we shifted the flies to 25°C for further experiments. We looked at LD distribution of $15^{th}$ day old male brains and found that *VAP* KD was still showing higher LD density as well as bigger size (Fig. 3.11B). However, increasing both $VAP^{WT}$ and $VAP^{P58S}$ in the glia of mutant flies showed no change compared to *ALS8* (Fig. 3.11C-F). Then, we looked at the climbing ability of the flies. As *VAP* was removed from the glia of the mutant, flies showed significant improvement in the climbing ability of the diseased flies till $15^{th}$ day of age post eclosion. However, in the other two cases with more $VAP^{WT}$ and $VAP^{P58S}$ in the glia, it did not affect climbing ability of *ALS8* flies at all (Fig. 3.12A). When we performed the similar experiment with *spen* KD in the glia of the mutant flies, we did not see any rescue and it was worsening the phenotype with age (Fig. 3.12B).

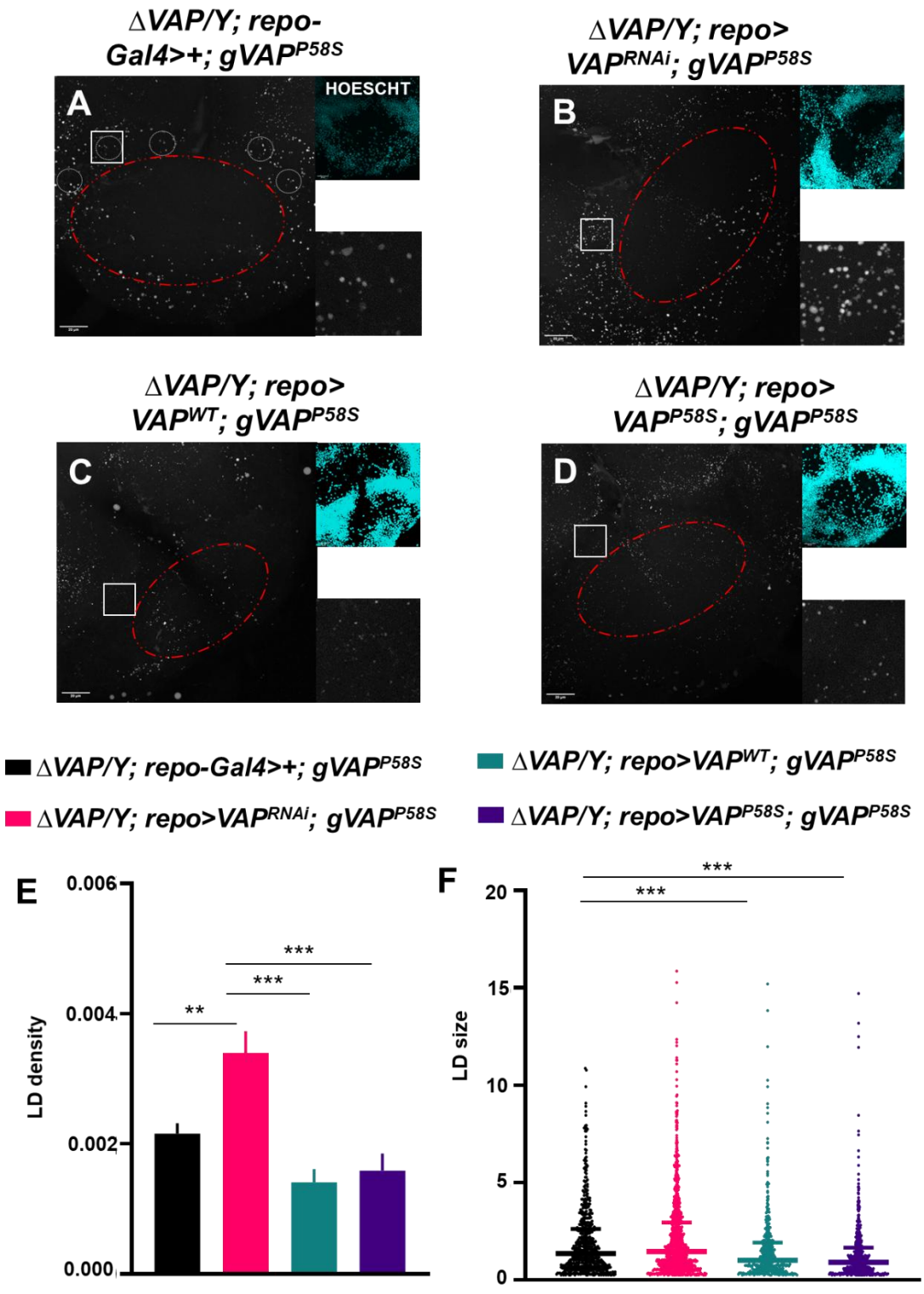



**Figure 3.11: *VAP* modulation in glia at adult stage affects LDs in *ALS8* brains.**

(A-D) are representative MIPs (20% Brightness) of LD distribution in SEZ region of Δ*VAP/Y ; repo-Gal4>+; gVAP*$^{P58S}$ (A), Δ*VAP/Y ; repo>VAP*$^{RNAi}$*; gVAP*$^{P58S}$ (B), Δ*VAP/Y ; repo>VAP*$^{WT}$*;*

*gVAP*$^{P58S}$ (C) and Δ*VAP/Y ; repo>VAP*$^{P58S}$*; gVAP*$^{P58S}$ (D). Removal of VAP$^{P58S}$ in the glia of adult brain increased LD density (E) and LD size (F). Nuclei staining of the adult brain is shown at the right top corner of the LD images. Zoomed image of the inset is shown at the right bottom corner of the individual images. Scale bar is represented as 20µm.

(E) LD density of all genotypes is plotted as Mean±SEM for 15 day old male flies. One way ANOVA is used followed by Tukey's test for multiple comparisons between genotypes with p value shown in APA style.

(F) LD size is plotted as scatter dot plot for all genotypes with all LDs from ROIs. . Kruskal-Wallis followed by Dunn's test is used for statistical significance with APA style p value.

N~5-6 adult brains per genotype, n=5 ROIs of each genotype.

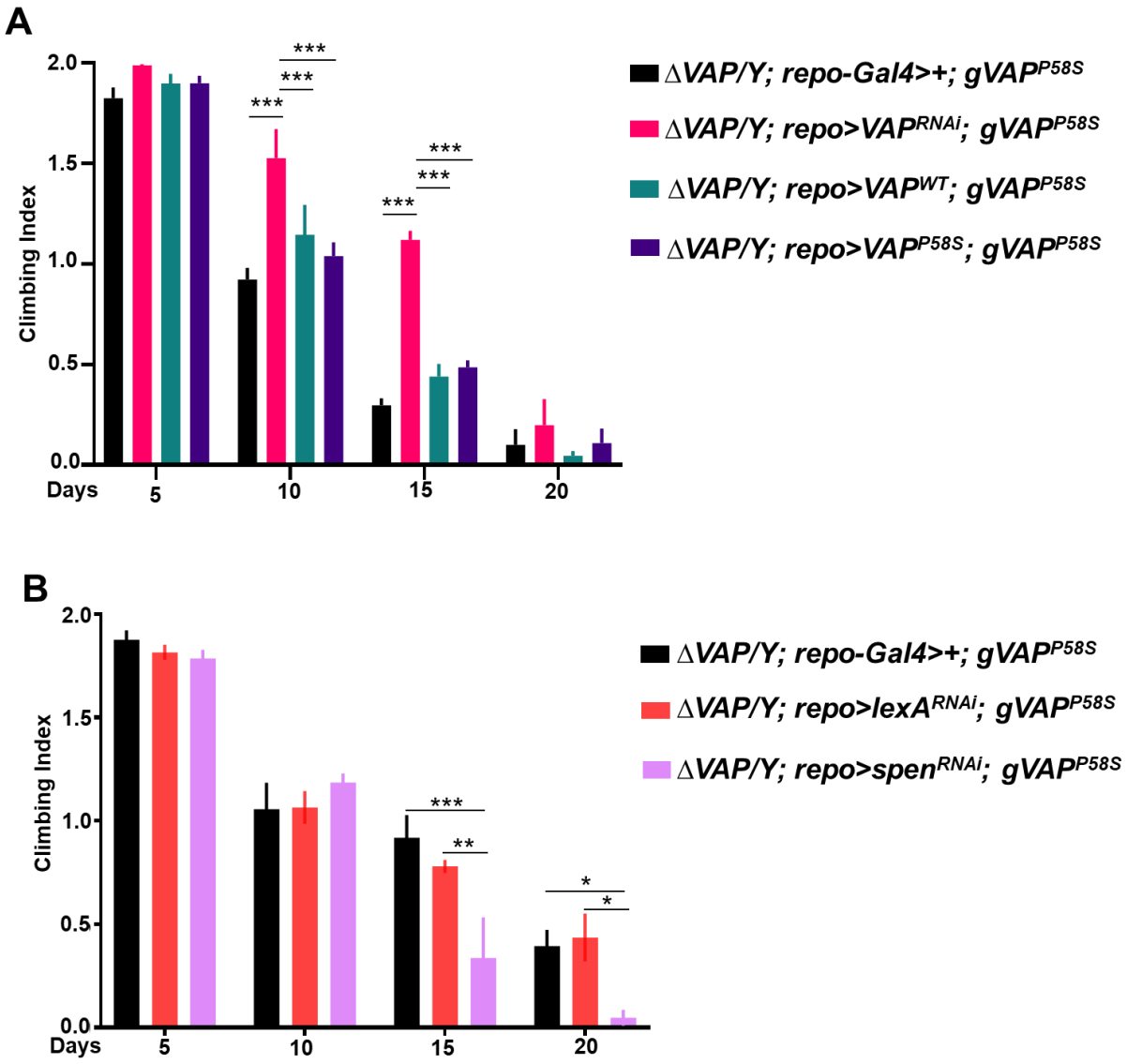


**Figure 3.12: VAP$^{P58S}$ removal in adult glia rescues *ALS8* climbing ability.**

(A) Knockdown of *VAP* in the glia at the adult stage significantly rescued climbing ability of *ALS8* flies whereas putting more *VAP* or *VAP$^{P58S}$* in the glia did not show any change.
(B) Glial *spen* KD in *ALS8* did not rescue climbing even after knocking down at adult stage.
Two way ANOVA is used followed by Tukey's test for multiple comparisons between genotypes, p value is shown in APA style, error bars as SEM. N=3, n~30 males. Experiments are performed at 25°C.

**3.3.7 Lowering CE levels in neurons improves motor ability of *ALS8* flies:** As stated earlier, *Drosophila* cannot make their own cholesterol and depends on the diet. So, cholesterol seems to be coming from the diet only. To negate the possibility that cholesterol changes in the brain of *ALS8* are happening because of different feeding behavior. We performed standardized DIETS assay in Dr. Gaurav Das Lab (Manikrao R. Thakare, 2024) for the 5 day old male flies of control, single copy of *VAP$^{P58S}$* and double copy of *VAP$^{P58S}$*. Interestingly, there was no difference in the feeding of mutants with single copy of *VAP$^{P58S}$* but double copy shows significant decrease suggesting single copy does not affect feeding that much (Fig. 3.13A). Moreover, the lipid changes start happening at 2$^{nd}$ day itself for cholesterol esters which means cholesterol is being converted to CEs. So, we looked for gene known to convert cholesterol to cholesterol esters. *CG8112* is the single homolog of Sterol O-acetyl transferase (SOAT1 and SOAT2 also called as ACATs in mammals). It is known to be active in fat body but some activity is reported in the head also (Schuch, 2021). When we knocked down *CG8112* in the neurons and glia of *ALS8* flies at the adult stage, only neuronal loss showed improvement in the climbing ability (Fig. 3.13B-C). This result supports Tsuda lab observations as well where they suggested cholesterol esters may be accumulated in the neurons.

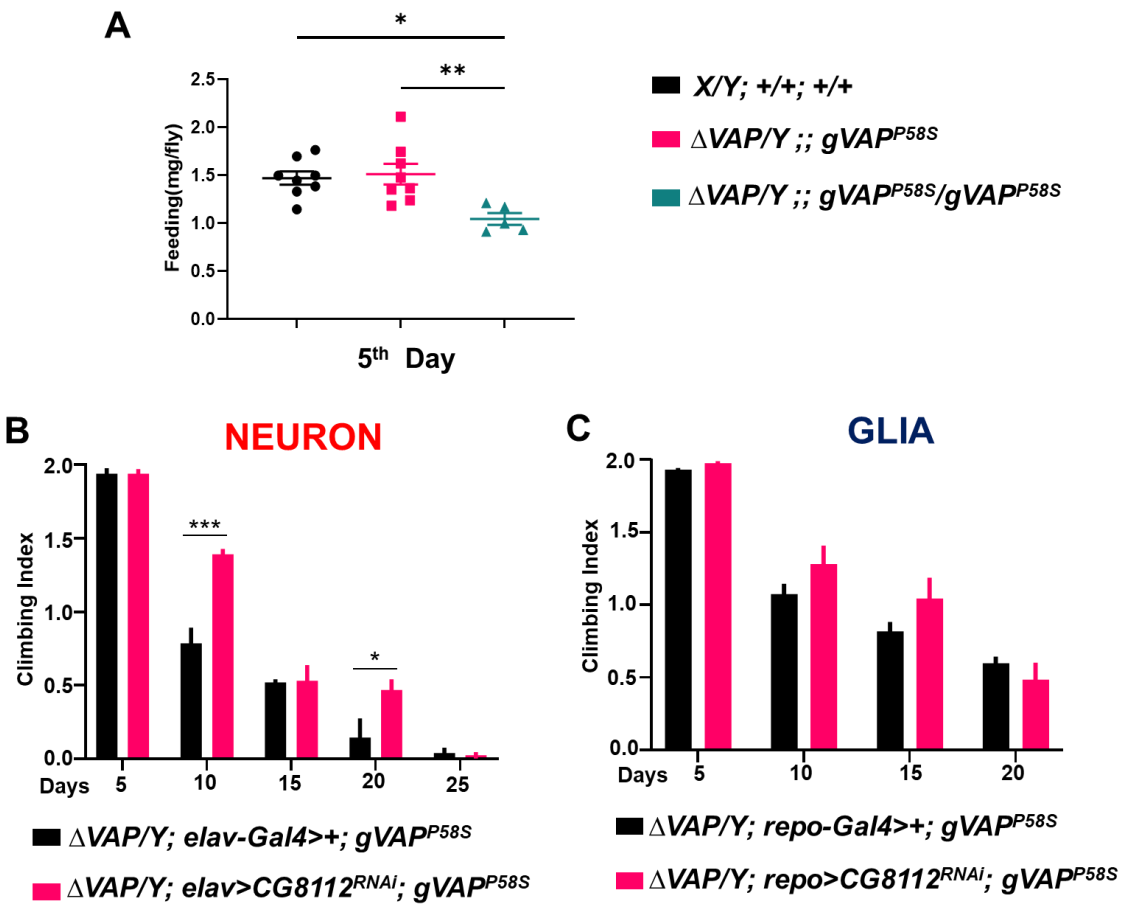



**Figure 3.13: Genetic KD of *CG8112* in neurons improves motor function in *ALS8* model.**

(A) No change was seen in the feeding of Δ*VAP/Y ; repo-Gal4>+; gVAP*$^{P58S}$ compared to control on 5$^{th}$ day but double copy of *VAP*$^{P58S}$ showed decrease in feeding. Flies were kept on regular media till 3$^{rd}$ day, 4$^{th}$ day was kept for adaptation to 5%Yeast-Sugar media for 24 hrs and 5$^{th}$ day was used for the experiment. N=5-8 biological replicates, n=15 male flies for each genotype. One way ANOVA is used followed by Tukey's test for comparisons with APA style of p values.
(B-C) Climbing Assay for neuronal and glial KD of *CG8112* at the adult stage in *ALS8* model. Two way ANOVA is used followed by Tukey's test for multiple comparisons between genotypes, p value is shown in APA style, error bars as SEM. N=3, n~30 males.

## 3.4 Discussion

**3.4.1 Cholesterol imbalance in *Drosophila ALS8* adult brains:** VAP is involved in transfer of different lipid species from ER to various organelles. One such lipid molecule is cholesterol. Cholesterol is quite important in the proper functioning of the brain. Cholesterol helps to make membrane rafts, vesicular formation and maintain plasma membrane fluidity. However, cholesterol is in low amounts at ER membrane which helps in maintaining ER architecture. Any change in cholesterol levels can lead to changes in ER network and affect neuronal functioning (Hartmann et al., 2022; Hussain et al., 2019; Mesmin et al., 2019; Niwa & Niwa, 2011). In the genomic model of *ALS8,* we found low levels of cholesterol in the adult brains in age dependent manner whereas cholesterol ester levels were higher by 2$^{nd}$ itself which was not case for cholesterol. We also checked that feeding was not affected on 5$^{th}$ day post eclosion. It seems during larval development only, CEs are being generated from cholesterol because of inability of OSBP to transfer it from ER membrane (Moustaqim-Barrette et al., 2014). As flies start eating the food post eclosion, cholesterol is converted to cholesterol esters in the mutant flies. This change in cholesterol esters can change ER membrane structure also which then can lead to ER stress (Moustaqim-Barrette et al., 2014; Thulasidharan et al., 2024). When we knocked down the only gene *CG8112* known to convert cholesterol to CEs in flies so far, we observed neuronal loss was showing improvement in the climbing ability of *ALS8* flies. Also, glia did not show any change in the motor activity suggesting CEs maybe toxic in neurons which is known to be the case for other ALS models as well (Ioannou et al., 2019; Liu et al., 2017; Liu et al., 2015). However, *CG8112* is mainly active in fat body and it will be interesting to find the enzymes specific to the brain of the flies (Schuch, 2021).

**3.4.2 VAP role in LD homeostasis:** Interestingly, genomic *ALS8* model had fewer number of LDs compared to control and droplets size was reducing with age which was quite surprising. Another study also confirms these results where they looked at preadipocyte cell line of *VAP$^{P56S}$* and found reduced size of LDs (Tokutake et al., 2015). There are several studies which shows *VAP* involvement in LD regulation however its exact role is still unknown (Henne et al., 2025; Kors, Costello, et al., 2022). There are three stages of LD homeostasis- LD formation, LD growth and LD degradation (Mejhert et al., 2022). Based on earlier studies, it seems VAP may be involved in all stages of LD regulation.

**3.4.3 *VAP* knockdown positively regulates LDs:** Researchers have shown that VAP interaction with ORP2 bring LD near to ER membrane. ORP2 is present at the surface of LD and helps in transport of TAGs. Also, it protects LD from lipolysis (Weber-Boyvat, Kentala, Peranen, et al., 2015). If *VAP* levels are reduced at ER membrane, LDs will move away from ER and thus inhibiting transport of TAGs to the LDs and affect maturation of LDs. This will lead to formation of more LDs with reduced size. Also, because of absence of *VAP*, OSBP will not be able to transfer cholesterol from ER which will lead to its accumulation at ER (Olkkonen, 2015). To prevent the accumulation, it is converted to CEs which may be stored to LDs for stabilizing ER membrane. As VAP levels are low in glia, lipid transfer will be affected which can change ER membrane structure. To prevent ER stress, these lipids are pushed towards lipid droplets so that membrane integrity is maintained. There are other studies which link *VAP* function to the utilization of LDs. Lipases act on LDs for breakdown of TAGs to fatty acids and these fatty acids are transported to mitochondria to be used as energy source (Farmer et al., 2020). Interestingly, VAP helps in making contact site for ER-mitochondria and ER-LDs. So, VAP helps in making a platform which bring LDs near to mitochondria (Bezawork-Geleta et al., 2025). When, *VAP* is knockdown in the glia, it's a possibility, LDs will be away from ER membrane and thus mitochondria will not able to use those lipids.

**3.4.4 *VAP* overexpression negatively affects LD homeostasis:** In the case of *VAP* overexpression, if more lipids are transferred from ER, droplet number may decrease because of less availability of lipids. Also, more VAP can increase ER-mitochondria and ER-LD contact sites which makes LD prone to lipolysis. This can lead to less number of LDs. However, when mutant copy of *VAP* is overexpressed, majority of the protein aggregates but $VAP^{P58S}$ is also known to sequester VAP protein which may reduce its levels in ER membrane. This will lead to small size of LDs in the cell as less VAP will be there for the maturation of LDs.

**3.4.5 $VAP^{P58S}$ as negative regulator of LDs:** In the case of $VAP^{P58S}$ flies, where there is no wild-type VAP present, lipid transfer will be affected as $VAP^{P58S}$ does not interact with LTPs like OSBP and MIGA (Moustaqim-Barrette et al., 2014; Xu et al., 2020). However, the mutant protein is still present in ER membrane which may affect LD maturation and thus the size will keep on reducing

with age. It seems low number of LDs in the mutant is also consequence of defective maturation of LDs. Because nascent LDs size is beyond diffraction limit of microscope, it is quite possible that mature LDs size is reduced in the ALS8 mutant which will not be detected in confocal microscope. This effect is also visible when genomic $VAP^{WT}$ is put back into the *ALS8* mutant. Although LD density is rescued, LD size does not reach up to control levels, however, lipids levels are completely rescued. This shows $VAP^{P58S}$ present at ER is affecting LD maturation. Another possibility is also there where LDs are being utilized for the production of cholesterol esters in the neurons. As VAP mutant copy is present in the glia new LDs are not being produced and the old ones are used leading to reduced LDs with smaller size. It will be interesting to see if higher TAG species detected in lipid profiling are coming from neurons or glia of *ALS8* flies.

A

| Wild-Type | | | | |
|---|---|---|---|---|
| Genotype | Dose | LD density | LD size | LDs |
| Control | 1X | | | |
| $VAP^{RNAi}$ | 0.2X | ↑ | ↓ | |
| $VAP^{WT-OE}$ | 3-5X | ↓ | | |
| $VAP^{P58S-OE}$ | 1X *VAP*<br>3-5X $VAP^{P58S}$ | | ↓ | |

B

| *ALS8/VAP* $^{P58S}$ | | | | |
|---|---|---|---|---|
| Genotype | Dose | LD density | LD size | LDs |
| $VAP^{P58S}$ | 1X | ↓ | ↓ | |
| $VAP^{RNAi}$ | 0.2X | ↑ | ↓ | |
| $VAP^{P58S-OE}$ | 3-5X | ↓ | ↓↓ | |
| $VAP^{WT-OE}$ | 1X $VAP^{P58S}$<br>3-5X $VAP^{WT}$ | ↓ | ↓ | |

Glia

C

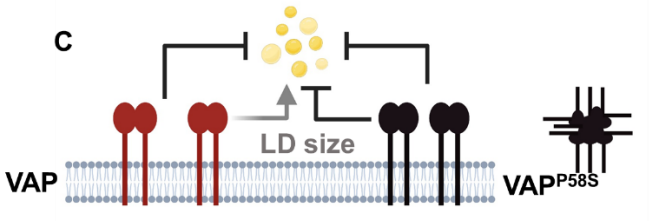



**Figure 3.14: Schematic model of VAP role in LD homeostasis.**

(A) represents tabulated diagram of the effect of glial *VAP* modulation on LD homeostasis in the adult brain. (B) shows tabulated diagram of the effect of glial *VAP* modulation on LD distribution in the brain of *ALS8* flies. (C) Schematic representation of VAP role in LD regulation where less VAP leads to more LDs via increased formation or reduced degradation while VAP positively regulates LD growth. $VAP^{P58S}$ affects both LD formation and degradation along with negatively regulating LD size. (Image credits: Biorender.com)

### 3.5 Conclusion:

*ALS8/VAP*$^{P58S}$ animals show cholesterol imbalance in the adult brain in an age-dependent manner. We hypothesize that this is a direct consequence of the modulation of VAP function in membrane contact sites. We have identified a novel role of VAPB in glia in terms of LD homeostasis which is perturbed in *ALS8* model and need to be studied further.

## 3.6 Materials and Methods

**3.6.1 *Drosophila* husbandry, fly stocks and reagents:** All the experimental stocks are maintained on a standard corn agar media at 25℃ and crosses were set up at 25℃ unless specified. *Canton-S* is used as wild-type control in the experiments. Δ*VAP(Δ166)*, $gVAP^{P58S}$, $gVAP^{WT}$ were kind gifts from Tsuda's lab. Δ*VAP ;; *$gVAP^{P58S}$ is used as *ALS8* model, Δ*VAP ;; *$gVAP^{WT}$*/Tb*, Δ*VAP ; repo-Gal4; *$gVAP^{P58S}$ and Δ*VAP ; elav-Gal4; *$gVAP^{P58S}$ are described in (Tendulkar et al., 2022; Thulasidharan et al., 2024). UAS-Gal4 system is used for the experiments (Duffy, 2002). *repo-Gal4* was a kind gift from Dr. Bradley Jones. *elav-Gal4* is described in (Ratnaparkhi et al., 2008). Bloomington Stocks: *Canton-S* (BL_0001), $VAP^{RNAi}$ (BL_77440), $spen^{RNAi}$ (BL_33398), $CG8112^{RNAi}$ (BL_63035). *UAS-*$VAP^{WT}$ and *UAS-*$VAP^{P58S}$ transgene lines are described in (Chaplot et al., 2019; Ratnaparkhi et al., 2008).

**3.6.2 Lipid extraction and targeted LC-MS lipidomics:** For sample preparation, *Drosophila* adult brains were dissected in ice cold 1X PBS (Phosphate Buffer Saline) with 2 brains in each vial and stored at -80℃ after flash freeze. Then, lipids are extracted with MS grade organic solvents using Folch extraction method as described earlier in (Chaplot et al., 2019; Pathak et al., 2018). Internal standards from Avanti polar lipids were used as follows: 1nmol each of Cholesterol d7, Triacylglycerols, and 100 pmol of 19:0 Cholesterol Ester. After the successful extraction, lipids are resolubilized in 200 µl of 2:1(v/v) of $CHCl_3$, Me-OH and 20 µl is used for injection. All the lipid species were quantified as per protocol described in (Pathak et al., 2018). All the data is acquired and processed through Sciex-OS software. Multiple unpaired t-test comparisons between lipid species followed by False discovery rate (FDR) of Benjamin and Hochberg with p value using APA style. All data represented with Standard Error Mean (SEM).

**3.6.3 Lipid Droplet staining for larval and adult brains:** Late 3$^{rd}$ instar wandering male larvae were selected for the study where brains are dissected in ice cold 1X PBS. Fixation is done for 20 minutes with 4% Paraformaldehyde (PFA with 0.3% Triton-x-100) followed by two immediate washes of 1X PBS and then 3$^{rd}$ wash of 15 minutes with 1X PBS at room temperature. For LD staining, 1:1000 BODIPY$^{TM}$ 493/503 (1mg/ml, Invitrogen, D3922) along with 1:1000 Hoescht (10mg/ml, Invitrogen) in 1X PBS was added to the brains and incubated on rocker for 30 minutes at room temperature under dark conditions. Then, solution is removed and brains are rinsed with 1X PBS. Immediate mounting is done for 5-6 brain samples using slowfade mounting media

(Vectashield S36937, Invitrogen). For adult brains, male flies of required genotype are anesthetized on ice and brains were dissected in ice cold 1X PBS. Similar protocol was used like for larval brain except 4%PFA with 0.5% Triton-x-100 is used and incubated for 30 minutes. Bridge mounting is done for adult brains using slowfade mounting reagent (Vectashield S36937, Invitrogen) and imaging is done within 24 hours of sample preparation.

**3.6.4 Microscope imaging and analysis:** For whole adult brain imaging, Nikon AX scope was used with 60X objective lens and stacked image was acquired at 12 bit depth using tile scanning. For rest of the experiments, mounted samples were imaged on Leica SP8 with 63X objective lens. Z-stacks were acquired with zoom factor of 1X unless specified with 1µm interval at 16-bit depth. Other settings were kept constant across experiments with changes in laser power and gain for individual experiments. For image analysis, Fiji software was used where manual protocol was made for analyzing lipid droplets. Firstly, mean intensity value of each slice was subtracted from that slice of the stack using a macro code. For adult brains, cells surrounding subesophageal zone (SEZ) region with five ROIs as zone 1 and cells surrounding antennal lobe (AL) as zone 2 were taken for LD analysis. A macro code is made which automatically process the ROI and analyze lipid droplets using intensity and size as thresholding parameters. Briefly, an arbitrary constant value was subtracted to reduce the noise and then mean 3D filter was used. Automatic thresholding was done using Otsu method for each slice of stack and then processed through 3D object counter for analyzing the droplets with size filtration of 8-1000. Macro code was able to store each ROI data into excel file where number and volume of droplets can be used for plotting the data. For lipid droplet density, the total number of droplets in each ROI was divided by the volume of the ROI based on the nuclei stack (number of droplets per $\mu m^3$). Lipid droplet size/volume ($\mu m^3$) was plotted in the form of a scattered dot plot by taking the volume of all droplets in the ROIs from all brain samples of each genotype into consideration. Macro code is given below used for analysis.

Mean Intensity subtraction code:

```
// Get the number of slices in the stack
numSlices = nSlices;
// Loop through each slice
for (i = 1; i <= numSlices; i++) {
```

```
    // Set the current slice
    setSlice(i);
    // Measure the current slice to get statistics
    run("Measure");
    // Get the mean intensity from the Results table
    meanValue = getResult("Mean", 0); // Get the mean value from the first row in the Results table
    // Subtract the mean intensity from the current slice
    run("Subtract...", "value=" + meanValue);
    // Clear the Results table for the next iteration
    run("Clear Results");
}
```

For LD analysis:

```
fileName = getTitle();
run("Subtract...", "value=2500 stack");
run("Mean 3D...", "x=2, y=2 z=2");
run("Auto Threshold", "method=Otsu white stack");
run("3D Objects Counter", "threshold=0 slice-0 min.=8 max.=1000 exclude_objects_on_edges objects statistics summary");
run("Summarize");
selectWindow("Results");
path = "location of folder where to store" + fileName + ".csv";
saveAs("Results", path);
close("Results");
close();
close();
```

**3.6.5 Climbing Assay:** Climbing activity of each genotype was observed using the startle-induced negative geotaxis assay (SING) as described (TENDULKAR ET AL., 2022). Three biological replicates of each genotype with 25-30 age-matched male flies were raised at 25 ℃. Each set was transferred to 250ml glass cylinder and allowed to acclimatize for 5 minutes. Then, cylinder was tapped three times to startle the flies and the flies were allowed to climb for 1 minute. After 1

minute, flies were counted based on three classes, non-climbers, poor climbers (0-80ml, 7.5cm) and good climbers (above 80ml or 7.5cm). These classes were given scores of 0, 1 and 2. A 3-minute rest period was given between sets, and the set was repeated twice more. The same protocol was followed for biological replicates and rest of the genotypes. The experiment was done every five days from eclosion, upto 30 days. $CO_2$ was used to anaesthetise the flies after 3 trials, and they were transferred to fresh media vials. Climbing Index was used to represent the motor activity of flies, where the given score was multiplied by the number of flies in that range, and the sum of all three values was averaged with the 3 trial values. Then, the number was divided by the total flies taken for that set.

**3.6.6 Software/Applications:** Graphpad Prism 10.4.1(532) was used for statistical tests and graphs. Image J is used for image analysis and representative images. AI tools have been used for the editing of macro code used for image analysis.

**3.7 Contributions:** Shweta Tendulkar prepared lipid samples from adult brains of different genotypes across different age groups, while Prof. Siddhesh Kamat assisted with LC-MS based lipid profiling and data analysis.

**3.8 Acknowledgements:** Aparna Thulasidharan is acknowledged for her assistance with brain dissections for the LC–MS experiments. We thank Dr. Gaurav Das for permitting me to carry out feeding experiments in his laboratory, and Tanzir, Asmita for providing technical assistance.

## 3.9 References

Alpy, F., Rousseau, A., Schwab, Y., Legueux, F., Stoll, I., Wendling, C., Spiegelhalter, C., Kessler, P., Mathelin, C., Rio, M. C., Levine, T. P., & Tomasetto, C. (2013). STARD3 or STARD3NL and VAP form a novel molecular tether between late endosomes and the ER. *J Cell Sci*, *126*(Pt 23), 5500-5512. https://doi.org/10.1242/jcs.139295

Bezawork-Geleta, A., Devereux, C. J., Keenan, S. N., Lou, J., Cho, E., Nie, S., De Souza, D. P., Narayana, V. K., Siddall, N. A., Rodrigues, C. H. M., Portelli, S., Zheng, T., Nim, H. T., Ramialison, M., Hime, G. R., Dodd, G. T., Hinde, E., Ascher, D. B., Stroud, D. A., & Watt, M. J. (2025). Proximity proteomics reveals a mechanism of fatty acid transfer at lipid droplet-mitochondria- endoplasmic reticulum contact sites. *Nat Commun*, *16*(1), 2135. https://doi.org/10.1038/s41467-025-57405-5

Bohnert, M., & Schrul, B. (2024). Lipid droplets in health and disease. *FEBS Lett*, *598*(10), 1113-1115. https://doi.org/10.1002/1873-3468.14900

Borgese, N., Navone, F., Nukina, N., & Yamanaka, T. (2021). Mutant VAPB: Culprit or Innocent Bystander of Amyotrophic Lateral Sclerosis? *Contact*, *4*. https://doi.org/10.1177/25152564211022515

Byrns, C. N., Perlegos, A. E., Miller, K. N., Jin, Z., Carranza, F. R., Manchandra, P., Beveridge, C. H., Randolph, C. E., Chaluvadi, V. S., Zhang, S. L., Srinivasan, A. R., Bennett, F. C., Sehgal, A., Adams, P. D., Chopra, G., & Bonini, N. M. (2024). Senescent glia link mitochondrial dysfunction and lipid accumulation. *Nature*, *630*(8016), 475-483. https://doi.org/10.1038/s41586-024-07516-8

Chaplot, K. (2019). *Regulation of VAP(P58S) neuroaggregation in a Drosophila model of Amyotrophic Lateral Sclerosis* IISER Pune]. http://dr.iiserpune.ac.in:8080/xmlui/handle/123456789/2922

Chaplot, K., Pimpale, L., Ramalingam, B., Deivasigamani, S., Kamat, S. S., & Ratnaparkhi, G. S. (2019). SOD1 activity threshold and TOR signalling modulate VAP(P58S) aggregation via reactive oxygen species-induced proteasomal degradation in a Drosophila model of amyotrophic lateral sclerosis. *Dis Model Mech*, *12*(2). https://doi.org/10.1242/dmm.033803

Chaves-Filho, A. B., Pinto, I. F. D., Dantas, L. S., Xavier, A. M., Inague, A., Faria, R. L., Medeiros, M. H. G., Glezer, I., Yoshinaga, M. Y., & Miyamoto, S. (2019). Alterations in lipid metabolism of spinal cord linked to amyotrophic lateral sclerosis. *Sci Rep*, *9*(1), 11642. https://doi.org/10.1038/s41598-019-48059-7

Chen, S., Roberts, M. A., Chen, C. Y., Markmiller, S., Wei, H. G., Yeo, G. W., Granneman, J. G., Olzmann, J. A., & Ferro-Novick, S. (2022). VPS13A and VPS13C Influence Lipid Droplet Abundance. *Contact (Thousand Oaks)*, *5*, 25152564221125613. https://doi.org/10.1177/25152564221125613

Cockcroft, S., Garner, K., Yadav, S., Gomez-Espinoza, E., & Raghu, P. (2016). RdgBalpha reciprocally transfers PA and PI at ER-PM contact sites to maintain PI(4,5)P2 homoeostasis during

phospholipase C signalling in Drosophila photoreceptors. *Biochem Soc Trans*, *44*(1), 286-292. https://doi.org/10.1042/BST20150228

Cockcroft, S., & Raghu, P. (2018). Phospholipid transport protein function at organelle contact sites. *Curr Opin Cell Biol*, *53*, 52-60. https://doi.org/10.1016/j.ceb.2018.04.011

Deivasigamani, S., Verma, H. K., Ueda, R., Ratnaparkhi, A., & Ratnaparkhi, G. S. (2014). A genetic screen identifies Tor as an interactor of VAPB in a Drosophila model of amyotrophic lateral sclerosis. *Biol Open*, *3*(11), 1127-1138. https://doi.org/10.1242/bio.201410066

Di Mattia, T., Martinet, A., Ikhlef, S., McEwen, A. G., Nomine, Y., Wendling, C., Poussin-Courmontagne, P., Voilquin, L., Eberling, P., Ruffenach, F., Cavarelli, J., Slee, J., Levine, T. P., Drin, G., Tomasetto, C., & Alpy, F. (2020). FFAT motif phosphorylation controls formation and lipid transfer function of inter-organelle contacts. *EMBO J*, *39*(23), e104369. https://doi.org/10.15252/embj.2019104369

Duffy, J. B. (2002). GAL4 system in Drosophila: a fly geneticist's Swiss army knife. *Genesis*, *34*(1-2), 1-15. https://doi.org/10.1002/gene.10150

Farmer, B. C., Walsh, A. E., Kluemper, J. C., & Johnson, L. A. (2020). Lipid Droplets in Neurodegenerative Disorders. *Front Neurosci*, *14*, 742. https://doi.org/10.3389/fnins.2020.00742

Freyre, C. A. C., Rauher, P. C., Ejsing, C. S., & Klemm, R. W. (2019). MIGA2 Links Mitochondria, the ER, and Lipid Droplets and Promotes De Novo Lipogenesis in Adipocytes. *Mol Cell*, *76*(5), 811-825 e814. https://doi.org/10.1016/j.molcel.2019.09.011

Girard, V., Goubard, V., Querenet, M., Seugnet, L., Pays, L., Nataf, S., Dufourd, E., Cluet, D., Mollereau, B., & Davoust, N. (2020). Spen modulates lipid droplet content in adult Drosophila glial cells and protects against paraquat toxicity. *Sci Rep*, *10*(1), 20023. https://doi.org/10.1038/s41598-020-76891-9

Goodman, L. D., Ralhan, I., Li, X., Lu, S., Moulton, M. J., Park, Y. J., Zhao, P., Kanca, O., Ghaderpour Taleghani, Z. S., Jacquemyn, J., Shulman, J. M., Ando, K., Sun, K., Ioannou, M. S., & Bellen, H. J. (2024). Tau is required for glial lipid droplet formation and resistance to neuronal oxidative stress. *Nat Neurosci*, *27*(10), 1918-1933. https://doi.org/10.1038/s41593-024-01740-1

Han, S. M., Tsuda, H., Yang, Y., Vibbert, J., Cottee, P., Lee, S. J., Winek, J., Haueter, C., Bellen, H. J., & Miller, M. A. (2012). Secreted VAPB/ALS8 major sperm protein domains modulate mitochondrial localization and morphology via growth cone guidance receptors. *Dev Cell*, *22*(2), 348-362. https://doi.org/10.1016/j.devcel.2011.12.009

Hanada, K. (2014). Co-evolution of sphingomyelin and the ceramide transport protein CERT. *Biochim Biophys Acta*, *1841*(5), 704-719. https://doi.org/10.1016/j.bbalip.2013.06.006

Hartmann, H., Ho, W. Y., Chang, J. C., & Ling, S. C. (2022). Cholesterol dyshomeostasis in amyotrophic lateral sclerosis: cause, consequence, or epiphenomenon? *FEBS J*, *289*(24), 7688-7709. https://doi.org/10.1111/febs.16175

Haynes, P. R., Pyfrom, E. S., Li, Y., Stein, C., Cuddapah, V. A., Jacobs, J. A., Yue, Z., & Sehgal, A. (2024). A neuron-glia lipid metabolic cycle couples daily sleep to mitochondrial homeostasis. *Nat Neurosci*, *27*(4), 666-678. https://doi.org/10.1038/s41593-023-01568-1

Henne, W. M., Reynolds, E., & Prinz, W. A. (2025). Lipid droplets: Open questions and conceptual advances around a unique organelle. *J Cell Biol*, *224*(10). https://doi.org/10.1083/jcb.202406019

Hussain, G., Wang, J., Rasul, A., Anwar, H., Imran, A., Qasim, M., Zafar, S., Kamran, S. K. S., Razzaq, A., Aziz, N., Ahmad, W., Shabbir, A., Iqbal, J., Baig, S. M., & Sun, T. (2019). Role of cholesterol and sphingolipids in brain development and neurological diseases. *Lipids Health Dis*, *18*(1), 26. https://doi.org/10.1186/s12944-019-0965-z

Ioannou, M. S., Jackson, J., Sheu, S. H., Chang, C. L., Weigel, A. V., Liu, H., Pasolli, H. A., Xu, C. S., Pang, S., Matthies, D., Hess, H. F., Lippincott-Schwartz, J., & Liu, Z. (2019). Neuron-Astrocyte Metabolic Coupling Protects against Activity-Induced Fatty Acid Toxicity. *Cell*, *177*(6), 1522-1535 e1514. https://doi.org/10.1016/j.cell.2019.04.001

James, C., & Kehlenbach, R. H. (2021). The Interactome of the VAP Family of Proteins: An Overview. *Cells*, *10*(7). https://doi.org/10.3390/cells10071780

Jansen, M., Ohsaki, Y., Rega, L. R., Bittman, R., Olkkonen, V. M., & Ikonen, E. (2011). Role of ORPs in sterol transport from plasma membrane to ER and lipid droplets in mammalian cells. *Traffic*, *12*(2), 218-231. https://doi.org/10.1111/j.1600-0854.2010.01142.x

Kamemura, K., Chen, C. A., Okumura, M., Miura, M., & Chihara, T. (2021). Amyotrophic lateral sclerosis-associated Vap33 is required for maintaining neuronal dendrite morphology and organelle distribution in Drosophila. *Genes Cells*, *26*(4), 230-239. https://doi.org/10.1111/gtc.12835

Kamemura, K., & Chihara, T. (2019). Multiple functions of the ER-resident VAP and its extracellular role in neural development and disease. *J Biochem*, *165*(5), 391-400. https://doi.org/10.1093/jb/mvz011

Kawano, M., Kumagai, K., Nishijima, M., & Hanada, K. (2006). Efficient trafficking of ceramide from the endoplasmic reticulum to the Golgi apparatus requires a VAMP-associated protein-interacting FFAT motif of CERT. *J Biol Chem*, *281*(40), 30279-30288. https://doi.org/10.1074/jbc.M605032200

Kors, S., Costello, J. L., & Schrader, M. (2022). VAP Proteins - From Organelle Tethers to Pathogenic Host Interactors and Their Role in Neuronal Disease. *Front Cell Dev Biol*, *10*, 895856. https://doi.org/10.3389/fcell.2022.895856

Kors, S., Hacker, C., Bolton, C., Maier, R., Reimann, L., Kitchener, E. J. A., Warscheid, B., Costello, J. L., & Schrader, M. (2022). Regulating peroxisome-ER contacts via the ACBD5-VAPB tether by FFAT motif phosphorylation and GSK3beta. *J Cell Biol*, *221*(3). https://doi.org/10.1083/jcb.202003143

Liu, L., MacKenzie, K. R., Putluri, N., Maletic-Savatic, M., & Bellen, H. J. (2017). The Glia-Neuron Lactate Shuttle and Elevated ROS Promote Lipid Synthesis in Neurons and Lipid Droplet Accumulation in Glia via APOE/D. *Cell Metab*, *26*(5), 719-737 e716. https://doi.org/10.1016/j.cmet.2017.08.024

Liu, L., Zhang, K., Sandoval, H., Yamamoto, S., Jaiswal, M., Sanz, E., Li, Z., Hui, J., Graham, B. H., Quintana, A., & Bellen, H. J. (2015). Glial lipid droplets and ROS induced by mitochondrial defects promote neurodegeneration. *Cell*, *160*(1-2), 177-190. https://doi.org/10.1016/j.cell.2014.12.019

Manikrao R. Thakare, P. C., Bhavna Pydah, Suhas Sunke, R Sai Prathap Yadav, Pavan Agrawal, Gaurav Das. (2024). DIETS: a simple and sensitive assay to measure and control the intake of complex solid foods, like high-fat diets, in Drosophila. *Elife*. https://doi.org/10.7554/eLife.97706.1.sa2

Mathiowetz, A. J., & Olzmann, J. A. (2024). Lipid droplets and cellular lipid flux. *Nat Cell Biol*, *26*(3), 331-345. https://doi.org/10.1038/s41556-024-01364-4

Mejhert, N., Gabriel, K. R., Frendo-Cumbo, S., Krahmer, N., Song, J., Kuruvilla, L., Chitraju, C., Boland, S., Jang, D. K., von Grotthuss, M., Costanzo, M. C., Ryden, M., Olzmann, J. A., Flannick, J., Burtt, N. P., Farese, R. V., Jr., & Walther, T. C. (2022). The Lipid Droplet Knowledge Portal: A resource for systematic analyses of lipid droplet biology. *Dev Cell*, *57*(3), 387-397 e384. https://doi.org/10.1016/j.devcel.2022.01.003

Mesmin, B., Kovacs, D., & D'Angelo, G. (2019). Lipid exchange and signaling at ER-Golgi contact sites. *Curr Opin Cell Biol*, *57*, 8-15. https://doi.org/10.1016/j.ceb.2018.10.002

Mikitova, V., & Levine, T. P. (2012). Analysis of the key elements of FFAT-like motifs identifies new proteins that potentially bind VAP on the ER, including two AKAPs and FAPP2. *PLoS One*, *7*(1), e30455. https://doi.org/10.1371/journal.pone.0030455

Mishra, S., Manohar, V., Chandel, S., Manoj, T., Bhattacharya, S., Hegde, N., Nath, V. R., Krishnan, H., Wendling, C., Di Mattia, T., Martinet, A., Chimata, P., Alpy, F., & Raghu, P. (2024). A genetic screen to uncover mechanisms underlying lipid transfer protein function at membrane contact sites. *Life Sci Alliance*, *7*(6). https://doi.org/10.26508/lsa.202302525

Moulton, M. J., Barish, S., Ralhan, I., Chang, J., Goodman, L. D., Harland, J. G., Marcogliese, P. C., Johansson, J. O., Ioannou, M. S., & Bellen, H. J. (2021). Neuronal ROS-induced glial lipid droplet formation is altered by loss of Alzheimer's disease-associated genes. *Proc Natl Acad Sci U S A*, *118*(52). https://doi.org/10.1073/pnas.2112095118

Moustaqim-Barrette, A., Lin, Y. Q., Pradhan, S., Neely, G. G., Bellen, H. J., & Tsuda, H. (2014). The amyotrophic lateral sclerosis 8 protein, VAP, is required for ER protein quality control. *Hum Mol Genet*, *23*(8), 1975-1989. https://doi.org/10.1093/hmg/ddt594

Neefjes, J., & Cabukusta, B. (2021). What the VAP: The Expanded VAP Family of Proteins Interacting With FFAT and FFAT-Related Motifs for Interorganellar Contact. *Contact (Thousand Oaks)*, *4*, 25152564211012246. https://doi.org/10.1177/25152564211012246

Nhek, S., Ngo, M., Yang, X., Ng, M. M., Field, S. J., Asara, J. M., Ridgway, N. D., & Toker, A. (2010). Regulation of oxysterol-binding protein Golgi localization through protein kinase D-mediated phosphorylation. *Mol Biol Cell*, *21*(13), 2327-2337. https://doi.org/10.1091/mbc.E10-02-0090

Nishimura, A. L., Mitne-Neto, M., Silva, H. C. A., Richieri-Costa, A., Middleton, S., Cascio, D., Kok, F., Oliveira, J. R. M., Gillingwater, T., Webb, J., Skehel, P., & Zatz, M. (2004). A Mutation in the Vesicle-Trafficking Protein VAPB Causes Late-Onset Spinal Muscular Atrophy and Amyotrophic Lateral Sclerosis. *The American Journal of Human Genetics*, *75*(5), 822-831. https://doi.org/10.1086/425287

Niwa, R., & Niwa, Y. S. (2011). The Fruit Fly Drosophila melanogaster as a Model System to Study Cholesterol Metabolism and Homeostasis. *Cholesterol*, *2011*, 176802. https://doi.org/10.1155/2011/176802

Olkkonen, V. M. (2015). OSBP-Related Protein Family in Lipid Transport Over Membrane Contact Sites. *Lipid Insights*, *8*(Suppl 1), 1-9. https://doi.org/10.4137/LPI.S31726

Pathak, D., Mehendale, N., Singh, S., Mallik, R., & Kamat, S. S. (2018). Lipidomics Suggests a New Role for Ceramide Synthase in Phagocytosis. *ACS Chem Biol*, *13*(8), 2280-2287. https://doi.org/10.1021/acschembio.8b00438

Perry, R. J., & Ridgway, N. D. (2006). Oxysterol-binding protein and vesicle-associated membrane protein-associated protein are required for sterol-dependent activation of the ceramide transport protein. *Mol Biol Cell*, *17*(6), 2604-2616. https://doi.org/10.1091/mbc.e06-01-0060

Qiu, L., Qiao, T., Beers, M., Tan, W., Wang, H., Yang, B., & Xu, Z. (2013). Widespread aggregation of mutant VAPB associated with ALS does not cause motor neuron degeneration or modulate mutant SOD1 aggregation and toxicity in mice. *Molecular neurodegeneration*, *8*(1). https://doi.org/10.1186/1750-1326-8-1

Ratnaparkhi, A., Lawless, G. M., Schweizer, F. E., Golshani, P., & Jackson, G. R. (2008). A Drosophila model of ALS: human ALS-associated mutation in VAP33A suggests a dominant negative mechanism. *PLoS One*, *3*(6), e2334. https://doi.org/10.1371/journal.pone.0002334

Schuch, K. (2021). *Biochemistry and physiology of*

*sterol esterification in Drosophila melanogaster* University of Graz].

Slee, J. A., & Levine, T. P. (2019). Systematic prediction of FFAT motifs across eukaryote proteomes identifies nucleolar and eisosome proteins with the predicted capacity to form bridges to the endoplasmic reticulum. *Contact (Thousand Oaks)*, *2*, 1-21. https://doi.org/10.1177/2515256419883136

Smolic, T., Tavcar, P., Horvat, A., Cerne, U., Haluzan Vasle, A., Tratnjek, L., Kreft, M. E., Scholz, N., Matis, M., Petan, T., Zorec, R., & Vardjan, N. (2021). Astrocytes in stress accumulate lipid droplets. *Glia*, *69*(6), 1540-1562. https://doi.org/10.1002/glia.23978

Teixeira, V., Maciel, P., & Costa, V. (2021). Leading the way in the nervous system: Lipid Droplets as new players in health and disease. *Biochim Biophys Acta Mol Cell Biol Lipids*, *1866*(1), 158820. https://doi.org/10.1016/j.bbalip.2020.158820

Tendulkar, S., Hegde, S., Garg, L., Thulasidharan, A., Kaduskar, B., Ratnaparkhi, A., & Ratnaparkhi, G. S. (2022). Caspar, an adapter for VAPB and TER94, modulates the progression of ALS8 by regulating IMD/NFkappaB-mediated glial inflammation in a Drosophila model of human disease. *Hum Mol Genet*, *31*(17), 2857-2875. https://doi.org/10.1093/hmg/ddac076

Teuling, E., Ahmed, S., Haasdijk, E., Demmers, J., Steinmetz, M. O., Akhmanova, A., Jaarsma, D., & Hoogenraad, C. C. (2007). Motor neuron disease-associated mutant vesicle-associated membrane protein-associated protein (VAP) B recruits wild-type VAPs into endoplasmic reticulum-derived tubular aggregates. *J Neurosci*, *27*(36), 9801-9815. https://doi.org/10.1523/JNEUROSCI.2661-07.2007

Thulasidharan, A., Garg, L., Tendulkar, S., & Ratnaparkhi, G. S. (2024). Age-dependent dynamics of neuronal VAPB(ALS) inclusions in the adult brain. *Neurobiol Dis*, *196*, 106517. https://doi.org/10.1016/j.nbd.2024.106517

Tokutake, Y., Gushima, K., Miyazaki, H., Shimosato, T., & Yonekura, S. (2015). ALS-associated P56S-VAPB mutation restrains 3T3-L1 preadipocyte differentiation. *Biochem Biophys Res Commun*, *460*(3), 831-837. https://doi.org/10.1016/j.bbrc.2015.03.118

Tsuda, H., Han, S. M., Yang, Y., Tong, C., Lin, Y. Q., Mohan, K., Haueter, C., Zoghbi, A., Harati, Y., Kwan, J., Miller, M. A., & Bellen, H. J. (2008). The amyotrophic lateral sclerosis 8 protein VAPB is cleaved, secreted, and acts as a ligand for Eph receptors. *Cell*, *133*(6), 963-977. https://doi.org/10.1016/j.cell.2008.04.039

Walther, T. C., & Farese, R. V., Jr. (2012). Lipid droplets and cellular lipid metabolism. *Annu Rev Biochem*, *81*, 687-714. https://doi.org/10.1146/annurev-biochem-061009-102430

Weber-Boyvat, M., Kentala, H., Lilja, J., Vihervaara, T., Hanninen, R., Zhou, Y., Peranen, J., Nyman, T. A., Ivaska, J., & Olkkonen, V. M. (2015). OSBP-related protein 3 (ORP3) coupling with VAMP-associated protein A regulates R-Ras activity. *Exp Cell Res*, *331*(2), 278-291. https://doi.org/10.1016/j.yexcr.2014.10.019

Weber-Boyvat, M., Kentala, H., Peranen, J., & Olkkonen, V. M. (2015). Ligand-dependent localization and function of ORP-VAP complexes at membrane contact sites. *Cell Mol Life Sci*, *72*(10), 1967-1987. https://doi.org/10.1007/s00018-014-1786-x

Wong, H. C., Lang, A. E., Stein, C., & Drerup, C. M. (2024). ALS-Linked VapB P56S Mutation Alters Neuronal Mitochondrial Turnover at the Synapse. *J Neurosci*, *44*(35). https://doi.org/10.1523/JNEUROSCI.0879-24.2024

Wyles, J. P., & Ridgway, N. D. (2004). VAMP-associated protein-A regulates partitioning of oxysterol-binding protein-related protein-9 between the endoplasmic reticulum and Golgi apparatus. *Exp Cell Res*, *297*(2), 533-547. https://doi.org/10.1016/j.yexcr.2004.03.052

Xu, L., Wang, X., Zhou, J., Qiu, Y., Shang, W., Liu, J. P., Wang, L., & Tong, C. (2020). Miga-mediated endoplasmic reticulum-mitochondria contact sites regulate neuronal homeostasis. *Elife*, *9*. https://doi.org/10.7554/eLife.56584

Yamaji, T., Kumagai, K., Tomishige, N., & Hanada, K. (2008). Two sphingolipid transfer proteins, CERT and FAPP2: their roles in sphingolipid metabolism. *IUBMB Life*, *60*(8), 511-518. https://doi.org/10.1002/iub.83

Yeshaw, W. M., van der Zwaag, M., Pinto, F., Lahaye, L. L., Faber, A. I., Gomez-Sanchez, R., Dolga, A. M., Poland, C., Monaco, A. P., van, I. S. C., Grzeschik, N. A., Velayos-Baeza, A., & Sibon, O. C. (2019). Human VPS13A is associated with multiple organelles and influences mitochondrial morphology and lipid droplet motility. *Elife*, *8*. https://doi.org/10.7554/eLife.43561

Zein-Sabatto, H., Cole, T., Hoang, H. D., Tiwary, E., Chang, C., & Miller, M. A. (2021). The type II integral ER membrane protein VAP-B homolog in C. elegans is cleaved to release the N-terminal MSP domain to signal non-cell-autonomously. *Dev Biol*, *470*, 10-20. https://doi.org/10.1016/j.ydbio.2020.10.015

# Chapter IV

# Sphingolipid dysregulation and Ceramide Transfer role in *ALS8* pathogenesis

## 4.1 Abstract

Sphingolipids are essential bioactive lipid molecules enriched in the central nervous system defined by sphingoid base backbone. They are quite diverse in nature and play important role in the maintenance of cellular membranes and signaling pathways. Sphingosine serve as the core building block of sphingolipids while its N-acylation generates ceramides that is the heart of all other sphingolipid species. Sphingolipids are known to contribute in lipid raft formation and regulate key cellular processes like growth, differentiation, apoptosis and inflammation.

Sphingolipids play distinct and critical role in the neurons and glial cells by regulating myelination, synaptic function and cell survival. Imbalance in sphingolipid pathway has been implicated in several neurological disorders such as Alzheimer's, Parkinson's and ALS. Ceramide transport from ER membrane to the Golgi is mediated by Ceramide Transfer (CERT), a key step in sphingolipid biosynthesis. In the *ALS8 Drosophila* model, where cholesterol homeostasis is disrupted, this study is focused toward sphingolipid species and tissue specific role of *CERT*. Lipidomics and genetic analysis revealed differential aspect of ceramides in the neurons and glia and demonstrate that limiting neuronal lipid synthesis improves motor function highlighting sphingolipid metabolism as a critical contributor to ALS pathogenesis.

## 4.2 Introduction

**4.2.1 Introduction to Sphingolipids:** Sphingolipids are the bioactive molecules representing a major class of eukaryotic lipids. These lipids are defined by their shared structural backbone known as the sphingoid base, an aliphatic amino alcohol (Carreira et al., 2019). In the early twentieth century, biochemical and chemical investigations led to the elucidation of the chemical structure of most prevalent lipid i.e. sphingosine which act as the foundational building block of all sphingolipids and make them distinguished from all other lipid classes (Hannun & Obeid, 2018). Sphingosine is a monounsaturated amino alcohol (2-amino-4-trans-octadecene-1,3-diol). N-acylation of the sphingoid base with fatty acids of different carbon chain lengths through an amide bond at 2-amino group generates ceramides which occupy a central position in the

sphingolipid pathway (Carter et al., 1947). Further modifications to the ceramides leads to the production of complex sphingomyelins and diverse glycosphingolipids. Sphingolipids are the structural components of the membranes and play crucial role in lipid raft formation. Beyond their structural roles, sphingolipids function as potent signaling molecules (Islam et al., 2025). Lipids like ceramide and sphingosine-1-phosphate are key regulators of growth, proliferation, differentiation and apoptosis. Ceramides are generally elevated in response to factors like oxidative stress, radiation activating multiple downstream signaling pathways (Agrawal et al., 2022; Hannun & Obeid, 2018; Islam et al., 2025; Pan et al., 2023; Pant et al., 2019; Theisen et al., 2025; Tracey et al., 2018).

**4.2.2 Sphingolipids in the nervous system:** The nervous system is highly enriched in lipids relative to other tissues ranging from simple fatty acids to complex glycosphingolipids. In the central nervous system, sphingolipid metabolism play differential roles in neurons and glia by regulating processes such as myelination, synaptic function, neuroinflammation and cell survival (Hannun & Obeid, 2018; Islam et al., 2025; McCluskey et al., 2022; Pan et al., 2023; Pant et al., 2020; Tracey et al., 2021; Tracey et al., 2018; Vaughen et al., 2022). Bioactive sphingolipids are increasingly recognized as mediators of neuron-glia communication, influencing inflammatory responses and neuroprotection. These metabolic pathways are tightly regulated and dysregulation of these pathways contribute to the pathogenesis of several neurological disorders (Hannun & Obeid, 2018; Hussain et al., 2019; McCluskey et al., 2022; McInnis et al., 2024; Pan et al., 2023; Theisen et al., 2025; Tracey et al., 2018; Yang et al., 2022). Significant alterations have been reported in the sphingolipids levels of the patients' brain samples suffering from Alzheimer's, Parkinson's disease (Cheng et al., 2011; He et al., 2010; Jana et al., 2009). Genetic mutations affecting sphingolipid metabolism have been associated with neuromuscular diseases as well such as Hereditary Spastic Paraplegia and ALS (Henriques et al., 2017; Oswald et al., 2015). Accumulation of ceramides and cholesterols esters have been detected in the post mortem spinal cord tissue with subsequent studies confirming widespread dysregulation at both presymptomatic and late disease stages in animal models (Chaplot et al., 2019; Cutler et al., 2002; Henriques et al., 2017; Rachakonda et al., 2004).

**4.2.3 Introduction to CERT**: Ceramides are generally synthesized at ER membrane using a set of enzymes present at the ER membrane (Pant et al., 2020; Voelzmann & Bauer, 2010; Yamaji et

al., 2008). Once formed at the ER membrane, Ceramides are transported to the Golgi through vesicular or non-vesicular means for the production of sphingolipids (KENTARO HANADA, 2003). Vesicular transport generally requires ATP whereas non-vesicular transport occurs with the help of LTPs (Kors, Costello, et al., 2022; Mesmin et al., 2019; Peretti et al., 2008; Slee & Levine, 2019; Weber-Boyvat, Kentala, Peranen, et al., 2015). One such LTP is CERT1/CERT, a cytosolic protein present at the ER-Golgi interface (Kawano et al., 2006; Rao et al., 2007; Wang et al., 2009). CERT transfers ceramide from ER to *trans*-Golgi where sphingomyelin (Ceramide Phosphoethanolamine, CPE in flies) formation takes place. CERT contains a Pleckstrin Homology (PH) domain at its N-terminus, which binds to PI4P present on the Golgi and a START domain at the C terminus that binds to ceramide at ER (Crivelli et al., 2022; Kawano et al., 2006; Kumagai & Hanada, 2019; Rao et al., 2014; Rao et al., 2007; Yamaji et al., 2008). CERT is a physical interactor of VAPB and this interaction assists in the transfer of ceramide from the ER (Hanada, 2014; Kawano et al., 2006; Kumagai et al., 2014; Mishra et al., 2024).

**4.2.4 Sphingolipids role in *ALS8 Drosophila* model:** In other *ALS* models, sphingolipids has been shown to be altered but in the case of *ALS8,* the data is still lacking (Agrawal et al., 2022; Henriques et al., 2017; Hussain et al., 2019; Kors, Costello, et al., 2022). Also, CERT interaction with VAPB may play an important role in *ALS8* as OSBP, another physical interactor, does not interact with the mutant protein (Moustaqim-Barrette et al., 2014). In chapter III, we found that cholesterol homeostasis was completely perturbed in the *ALS8* model (Fig. 3.1). In this chapter, firstly, we focused on the sphingolipids species such as ceramides, sphingomyelins and ceramide-1-phosphate and performed LC-MS based lipid profiling on the *ALS8* brains. Then, we tried to understand effect of CERT function in *ALS8* flies in tissue specific manner. Using motor function as readout for the experiments, we identified differential effect of ceramide and CERT in neurons and glia of *ALS8* model.

Further motor assay experiments revealed that unavailability of fatty acyl CoA in neurons which is used for generation of lipid species such as cholesterol esters and ceramides can improve motor function of the diseased flies. Based on results from chapter III and IV, we have tried to model the neuron-glia connection with respect to LDs, lipid synthesis in a *Drosophila* model of *ALS8.*

## 4.3 Results

**4.3.1 Sphingolipids are altered in a *Drosophila* model of *ALS8*:** In Chapter III, we reported that cholesterol, CEs and TAGs are altered in *ALS8* brains (Fig. 3.1), so we checked the sphingolipid levels in the brains of genomic model of $VAP^{P58S}$ in age dependent manner. Similarly like CEs (Fig. 3.1B), we found that sphingolipids such as ceramides, ceramide-1-phosphate (C-1-P) and sphingomyelins (SMs) were almost the double the amount of the lipids present in the wild-type flies' brain (Fig. 4.1 A-C). Also, in wild-type flies, lipid species of different carbon chain lengths like C(16:0), C(18:0) and C(18:1) were quite lower compared to mutants, however, in both cases these species saturated by day 10. Just like cholesterol, CEs and TAGs, sphingolipids were also completely rescued after putting a genomic copy of $VAP^{WT}$ in the *ALS8* background (Fig. 4.1A'-C'). Interestingly not all sphingolipids are changed in the diseased flies. Lipids like sphingosine and S-1-P were not to be found to be altered at all in the *ALS8* brains as reported in (Chaplot, 2019).

**4.3.2 Generation and validation of *CERT* transgenic lines:** In the earlier section, we found only specific sphingolipids were altered in the *ALS8* model (Fig. 4.1). Ceramides are synthesized at ER membrane and transfer to Golgi with the help of LTPs such as *CERT1* and *FAPP2* for the formation of sphingolipids like SMs/CPE, C-1-P, GSLs (Yamaji et al., 2008). We chose CERT as protein of interest as it is highly conserved and known to modulate ceramide and CPE levels in the flies (Rao et al., 2007). We acquired BDSC RNAi line for the knockdown of *CERT* described in Materials and Methods. To overexpress *CERT*, we generated untagged *UAS-CERT* fly line in the lab and verified through sequencing (Fig. 4.2 A). *CERT* transgenic lines were balanced and transcript levels were checked using RT-PCR. *CERT* KD leads to 76% reduction in the whole body whereas two *CERT* OE lines showed around 15 $\log_2$ fold change of *CERT* mRNA levels in the flies (Fig. 4.2A'). For further experiments, we chose *UAS-CERT4C (UAS-*$CERT^{WT}$ here onwards) to overexpress *CERT*. CERT is known to interact with VAPB through its conserved FFAT motif i.e. EFFDAVE. We mutated FF>AA amino acid at 306-307$^{th}$ position and validated the mutation through sequencing (Fig. 4.2B). A schematic is shown with the mutation present in the sequence (Fig. 4.2B'). We sequenced the whole sequence and named it as *UAS-*$CERT^{EAAD}$ as shown in (Fig. 4.2C). We performed RT-PCR to check the transcript levels of different balanced lines where $CERT^{WT}$ primers were used to confirm the *CERT* levels and *FFAT* motif specific primers were

used which would only bind to *wild-type* CERT sequence but not the mutated one (Fig. 4.2C'). For the experiments, we selected *UAS-CERT4A$^{EAAD}$ (UAS-CERT$^{EAAD}$* here onwards*).*

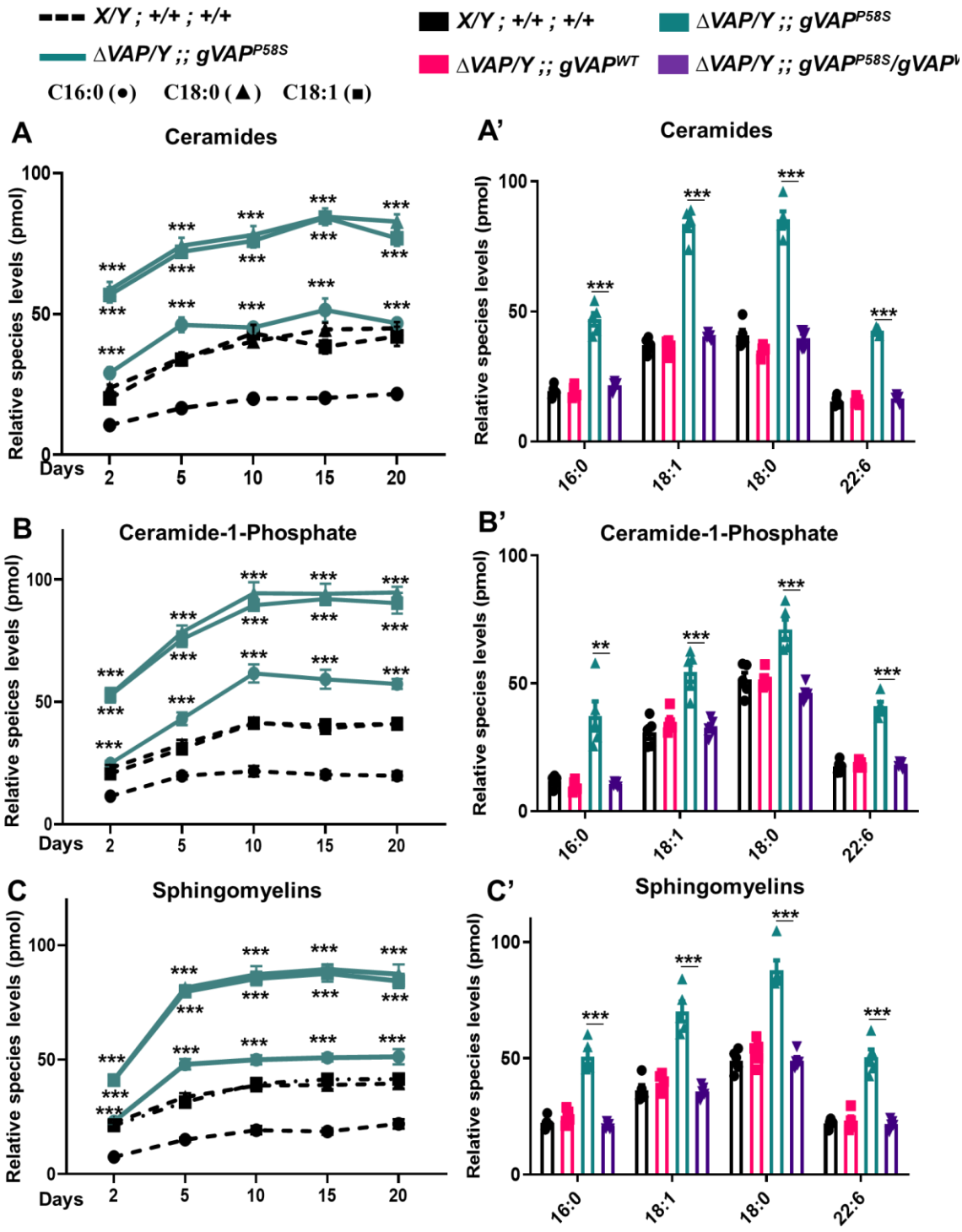



**Figure 4.1: Age dependent sphingolipid profiling of *ALS8* brains.**

(A-C) Sphingolipids like Ceramides (A), C-1-P (B) and Sphingomyelins (C) are increased in *ALS8* brains for different chain lengths (C16:0, C18:0, C18:1) in an age dependent manner and saturates by day 10. Wild-type in black color, genomic $VAP^{P58S}$ in red color. n=2 adult brains, N=5 biological replicates. Multiple unpaired t-test is used for comparison between the genotypes followed by FDR of Benjamin and Hochberg with p value using APA style. Data is represented as Mean±SEM for each lipid species on Y axis with number of days shown on X-axis.
(A'-C') Rescue of sphingolipid levels with genomic copy of $VAP^{WT}$ in *ALS8* brains. Data is reproduced from (Chaplot, 2019).

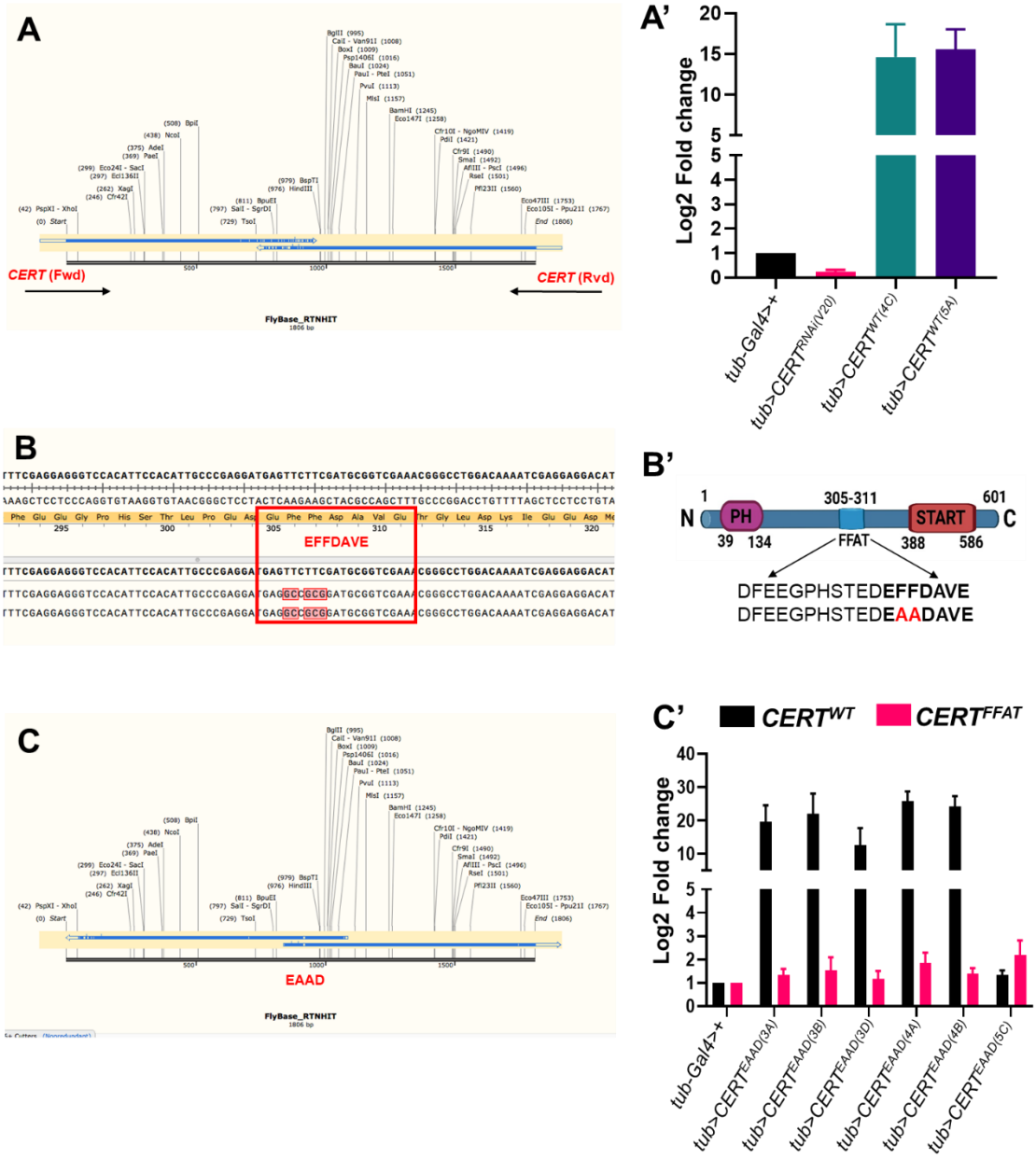
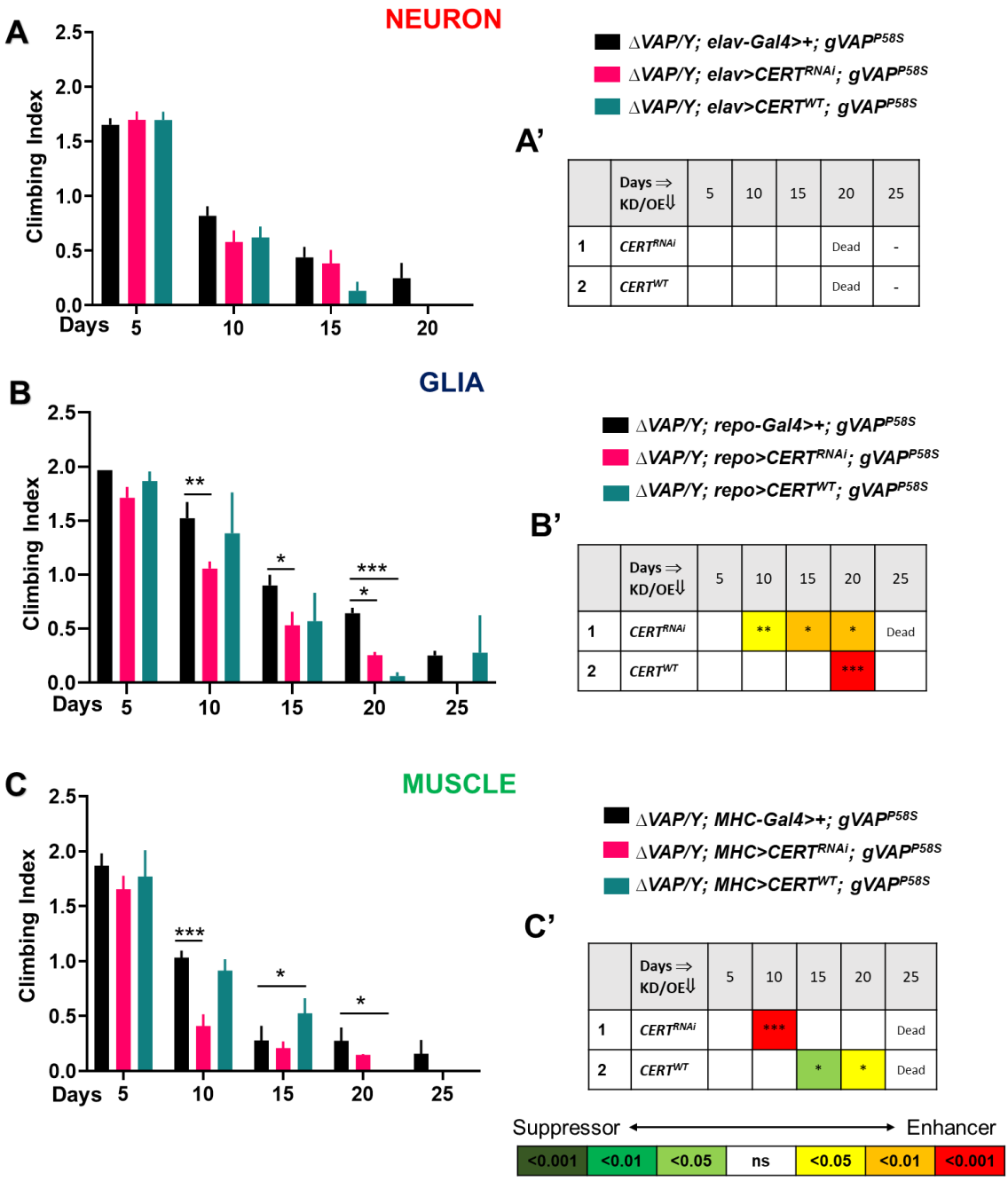


**Figure 4.2: Validation of *CERT* transgenic fly lines.**

(A) shows plasmid DNA sequence of *pUASp-CERT$^{WT}$*. (A') mRNA quantification of *CERT$^{RNAi}$* (BL_60080), *CERT$^{WT(4C)}$*, *CERT$^{WT(5A)}$* using *tub-Gal4* for whole body expression.
(B) (FF>AA) mutation is induced at 306-307$^{th}$ position in the *CERT* gene (*TTCTTC-GCCGCG).*
(B') Domain architecture of *CERT* with (FF>AA) mutation shown.
(C) Sequence result of plasmid DNA sequence of *pUASp-CERT$^{EAAD}$* representing *CERT* is intact except the mutation region. (C') mRNA quantification of different *CERT$^{EAAD}$* fly lines using *tub-Gal4* for whole body expression. *CERT* specific primers show expression of *CERT$^{EAAD}$* transcripts whereas FFAT specific primers does not bind to *CERT$^{EAAD}$* transcripts.
For mRNA quantification, n=10 males of 10 days old, N=3 biological replicates were used.

**4.3.3 Tissue specific modulation of *CERT* in *ALS8* flies:** In our previous studies from the lab, we have found differential role of proteins in tissue specific manner in the *ALS8* background. Also, in chapter III, we found glial specific role of VAP in LD homeostasis (Fig. 3.8 and 3.9), whereas Tsuda lab has showed partial rescue of motor activity by inducing *ORP8* expression in the motor neurons of the diseased flies (Moustaqim-Barrette et al., 2014). So, we KD and OE *CERT* in the neurons, glia and muscles of the *VAP$^{P58S}$* mutant males and performed 'Startle Induced Negative Geotaxis' climbing assay (described in chapter III Materials and Methods) in an age dependent manner. We observed that both KD and OE of *CERT* in the neurons did not show any change in the motor function of the flies (Fig. 4.3 A-A'). In the case of *CERT* KD in the glia, flies showed worsening of the phenotype whereas *CERT$^{WT}$* expression did not alter the motor activity initially but by day 20 they also enhanced the motor phenotype of *ALS8* flies (Fig. 4.3B-B'). Then, we modified *CERT* levels in the muscles using muscle specific *MHC-Gal4* driver in the mutant male flies and found *CERT* KD enhanced the motor phenotype on day 10 whereas *CERT* OE showed no change with mild improvement only on day 15 (Fig. 4.3C-C').




| | Days ⇒ KD/OE⇓ | 5 | 10 | 15 | 20 | 25 |
|---|---|---|---|---|---|---|
| 1 | *CERT^RNAi* | | | | Dead | - |
| 2 | *CERT^WT* | | | | Dead | - |

| | Days ⇒ KD/OE⇓ | 5 | 10 | 15 | 20 | 25 |
|---|---|---|---|---|---|---|
| 1 | *CERT^RNAi* | | ** | * | * | Dead |
| 2 | *CERT^WT* | | | | *** | |

| | Days ⇒ KD/OE⇓ | 5 | 10 | 15 | 20 | 25 |
|---|---|---|---|---|---|---|
| 1 | *CERT^RNAi* | | *** | | | Dead |
| 2 | *CERT^WT* | | | * | * | Dead |

**Figure 4.3: Motor function of *ALS8* flies after *CERT* modulation in neurons, glia and muscles.**

(A) Climbing Index of genomic *ALS8* flies after modulating *CERT* in the neurons of *Drosophila*. (A') Summary of the graph is shown in tabulated form for each interval (5, 10, 15, 20 and 25) where all data points found to be not significant.

(B) Climbing Index of *ALS8* flies on modulating *CERT* in the glia is plotted in the graph with statistical significance. (B') Summary of the climbing index is shown in the tabulated form for each interval (5, 10, 15, 20 and 25) with statistical significance.
(C) Climbing Index is plotted in the form of bar graph after modulation of *CERT* in the muscles of *ALS8* flies with statistical significance. (C') Summary of the graph is shown in the tabulated form for each interval (5, 10, 15, 20 and 25) with statistical significance.
Mean±SEM values are plotted as climbing index on the Y axis with number of days on X axis. n=25-30 males, N=3 biological replicates for each genotype. $p<0.001$(***), $<0.01$(**) and $<0.05$(*).

**4.3.4 Impact of blocking ceramide synthesis on motor function in *ALS8* males:** We did not see any rescue after modulation of *CERT* in the *ALS8* background. Next, we asked if blocking ceramide production will show any improvement in the motor function. So, we selected Schlank as protein of our interest. The reason being *schlank* is the only homolog of six ceramide synthase enzymes present in mammals (Voelzmann & Bauer, 2010). Also, Schlank is the sole protein to generate ceramides either through *de novo* or sphingomyelinase pathway (Pan et al., 2023). So, we knocked down *schlank* in the neurons of the $VAP^{P58S}$ males and looked at the motor activity of the flies (Fig. 4.4A). We observed mild improvement in the motor function but stastically non-significant. Interestingly, in the case of glial knock down of *schlank,* it enhanced the motor defects in *ALS8* flies significantly just like *CERT* (Fig. 4.4 B). Next, we asked the question, if blocking ceramide synthesis through inhibitor can improve the climbing defects as shown in other neurological disorders like Parkinson's in the flies (Vos et al., 2021). Myriocin is a standard ceramide synthesis inhibitor which inhibits the activity of Serine-Palmitoyl Transferase (SPT-I/II), first enzyme of ceramide production (Jana et al., 2009). We also used Avasimibe, reversible inhibitor known to block production of Cholesterol Esters (Hartmann et al., 2022). We fed both drugs (Myriocin 100µM and Avasimibe 20µM) using Dimethylsuphoxide (DMSO) as a solvent to the wild-type and *ALS8* flies post eclosion starting from day 1. Feeding both drugs to the mutant did not show any major change in the flies compared to DMSO fed flies (Fig. 4.4 D) whereas *CS* flies also did not show any significant defect with age (Fig. 4.4 C). Myriocin also known as ISP-1 blocks ceramide at the initial step of its synthesis which will affect sphinganine production as well which is quite important for neurons. This can be one of the reasons that it did not show any rescue in the motor function of ALS8 flies. Avasimibe is a reversible cholesterol ester inhibitor which can explain why it did not show any rescue in the mutant flies.

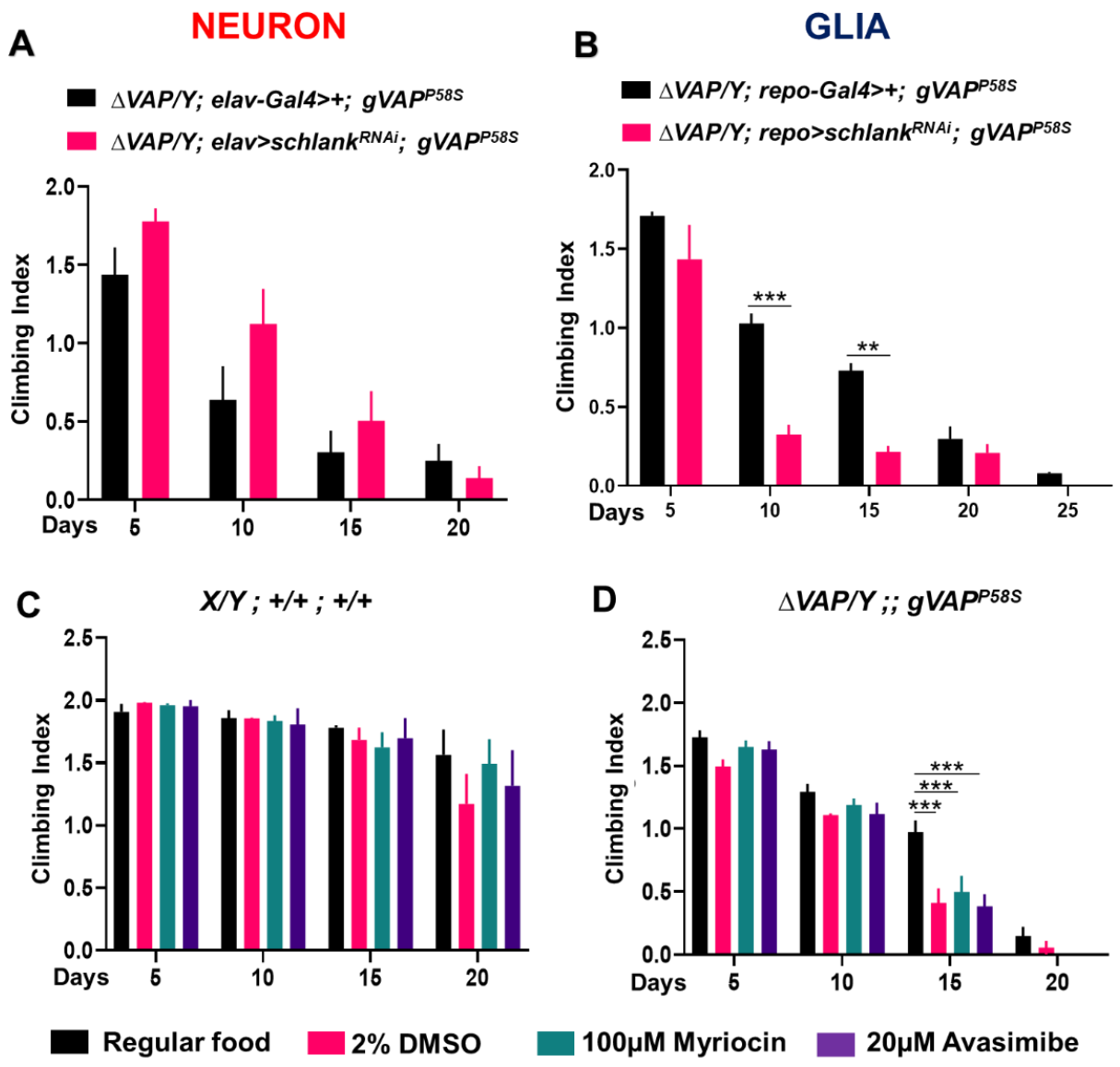



**Figure 4.4: Tissue specific role of ceramide synthesis in *ALS8* motor dysfunction.**

(A) Climbing Index is plotted in form of bar graph for *schlank* KD in the neurons of *ALS8* mutant.
(B) Climbing Index is represented as bar graph after knockdown of *schlank* in the glia of *ALS8* males with their statistical significance.
(C-D) Climbing Index for *CS* flies and *ALS8* flies are plotted in the bar graph form with different drugs as shown in the figure.
Mean±SEM values are plotted in the bar graph with climbing index on Y axis and number of days on X axis with their statistical significance. n=25-30 male flies, N=3 biological replicates of each set. $p<0.001$(***), $<0.01$(**) and $<0.05$(*).

**4.3.5 Blocking ceramide synthesis or transfer in adult stage delays progression of *ALS8*:** Till now, we saw blocking either ceramide synthesis or transfer did not improve motor defects of the $VAP^{P58S}$ flies. Ceramide plays an important role in the development of the nervous system shown by various studies (Anna B. Ziegler 2025; Goyal et al., 2019; Hussain et al., 2019). So, we used the same strategy as used earlier in chapter III for *VAP* modulation and modulated *CERT* at the adult stage of *ALS8* flies by keeping the embryos at 18℃ and shift the F1 progeny to 25℃ after the eclosion (Fig. 3.11). Interestingly, KD of *CERT* in the neurons at the adult stage of the mutant significantly showed improvement in the motor activity on day 10 whereas $CERT^{WT}$ OE showed no change compared to mutant control. When we overexpressed $CERT^{EAAD}$ in the neurons under same conditions, there was significant delay in the motor defects and even at day 15 flies were showing major improvement in climbing. Then, we moved to *schlank* and asked if inhibiting ceramide synthesis will also show improvement? Surprisingly, blocking ceramide synthesis through *schlank* KD in the neurons showed the highest improvement in the motor dysfunction of *ALS8* flies suggesting lowering ceramide levels can improve the climbing activity of the flies (Fig. 4.5A-A').

We performed similar experiment by modulating *CERT* in the glial cells and then looked at the climbing activity of the *ALS8* flies. Unlike neuronal results, KD *CERT* at the adult stage in the glial cells led to the enhancement of motor defects suggesting different roles for *CERT* in the neurons and glia. When we overexpress $CERT^{WT}$ or $CERT^{EAAD}$ in the glial cells, both did not show any improvement, however, $CERT^{WT}$ OE also showed worsening of the phenotype suggesting $VAP^{P58S}$ may be affecting *CERT* functioning. When we used $schlank^{RNAi}$ to reduce the ceramide levels in the glia of $VAP^{P58S}$, it led towards more fraction of poorer climbers than control on day 10 suggesting glial cells are sensitive towards ceramide levels (Fig. 4.5B-B').

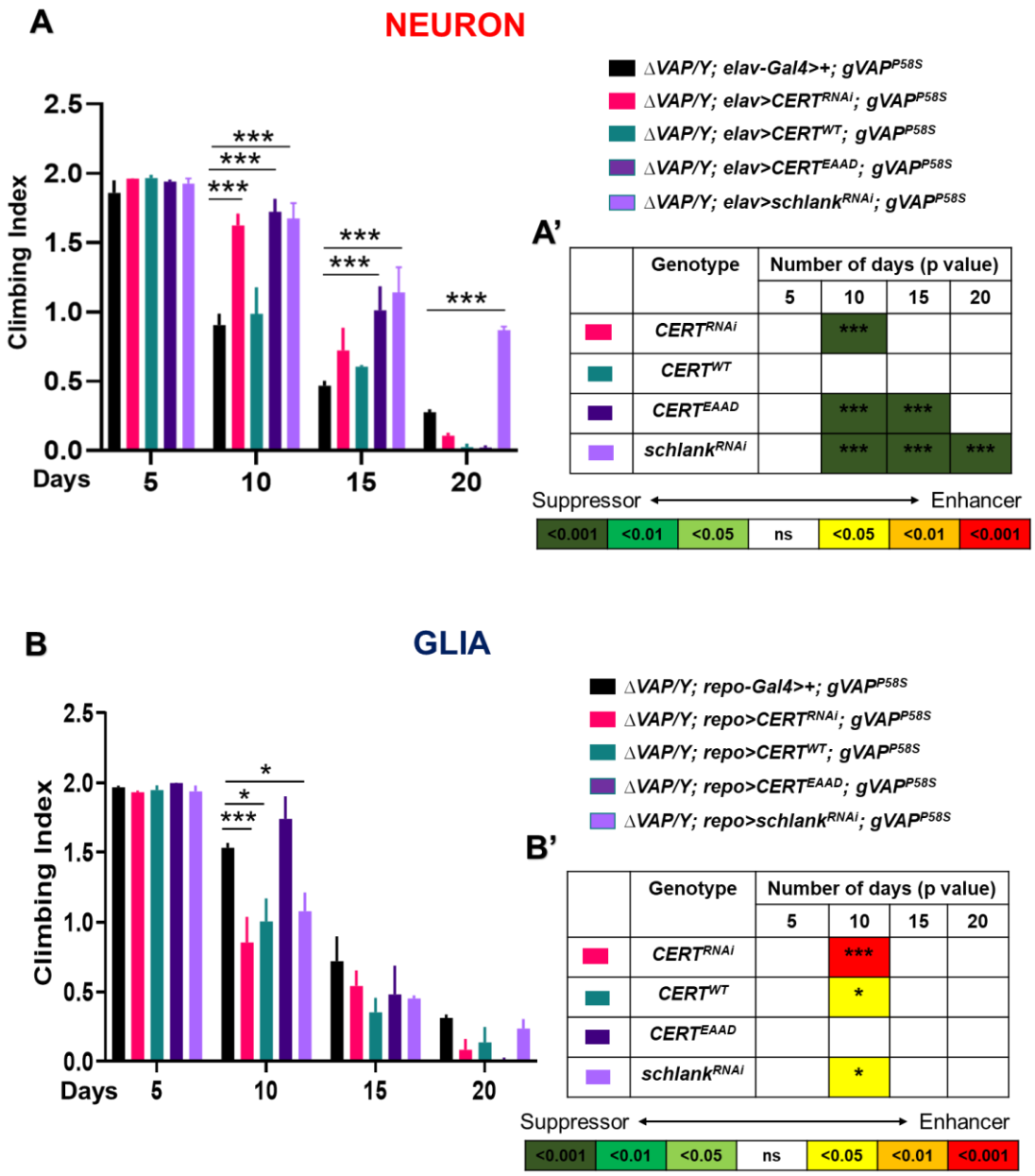



**Figure 4.5: Lowering ceramides in the neurons at adult stage delays *VAP$^{P58S}$* motor defects.**

(A) Perturbing ceramide synthesis or transfer in the neurons during adult stage rescues motor dysfunction of *ALS8* flies. (A') Summary of the bar graph is presented in tabulated form for each interval (5, 10, 15, 20) with their statistical significance.

(B) Climbing Index is plotted for glial modulation of *CERT* and *schlank* at the adult stage in *VAP$^{P58S}$* flies. (B') Summary of the bar graph is shown in tabulated form for each interval (5, 10, 15, 20 and 25) with the statistical significance.

Mean±SEM values are plotted as climbing index in the bar graph on Y axis with number of days on X axis with statistical significance as p<0.001(***), <0.01(**) and <0.05(*). n=25-30 males, N=3 biological replicates per genotype.

**4.3.6 Reducing Fatty acyl CoA availability in neurons improves *ALS8* motor function:** Lipids such as Cholesterol esters, ceramides and TAGs require fatty acyl CoA for their synthesis (Liu et al., 2015). Fatty acyl CoA comes from two components, fatty acid and CoA. Lipases are the enzymes which act on lipids to break them into simpler compounds (Liu et al., 2017; Long et al., 2026). One such lipase is *brummer (bmm),* a homolog of *ATGL* (Adipose Triglyceride Lipase) known to catabolize TAGs into MAGs and DAGs (Bohnert & Schrul, 2024; Walther & Farese, 2012). Interestingly, we did not find any change in the lipid levels of FFAs, MAGs and DAGs (Chaplot, 2019). In the *ALS8* model, more TAGs levels were detected in the lipid profiling (chapter III) so we wanted to see if modulation of *bmm* would have any effect on the motor function of the flies. We used similar strategy like in the case of *VAP, CERT* and *schlank* modulation. We modulated *bmm* in the neurons of *ALS8* flies and kept the embryos at 18℃. After the eclosion, we shifted the flies to 25℃ to perform climbing assay. Interestingly, we found that *bmm* KD in the neurons at the adult stage improved the motor function significantly just like *schlank* whereas $bmm^{WT}$ expression showed no change (Fig. 4.6A-A').

Next, we wanted to see if ketone body production would have any effect on the motor function because under stress conditions fatty acids are used by mitochondria for ATP generation. Acetyl-CoA acetyltransferase (*ACAT1* and *ACAT2*) are two enzymes present in mitochondria which are known to combine two acetyl-CoA to form acetoacetyl-CoA. Interestingly, *ACAT2* KD in neurons led to the first instar larval death. So, we proceeded further with *ACAT1*. Intriguingly, KD of *ACAT1* in the neurons at the adult stage significantly improve the motor function initially and it remain till 15 days compared to control. We used $lexA^{RNAi}$ as a control which did not show any change in motor defects compared to the *ALS8* flies (Fig. 4.6A-A').

Glia is known to contain a lot of lipid droplets so we performed the similar experiment by modulating *bmm* and *ACAT1* in the glia. Both *bmm* KD and OE showed no change at all which was in contrast to the neuronal results and quite unexpected. Next, knocking down of *ACAT1* in the glia cells of $VAP^{P58S}$ flies at 25℃ showed pupal death. However, KD of *ACAT1* in glia at 18℃ leads to eclosion of flies suggesting its crucial role during development. Although, it still did not show any change in the climbing activity of the flies and behaved almost like *ALS8* flies (Fig. 4.6B).

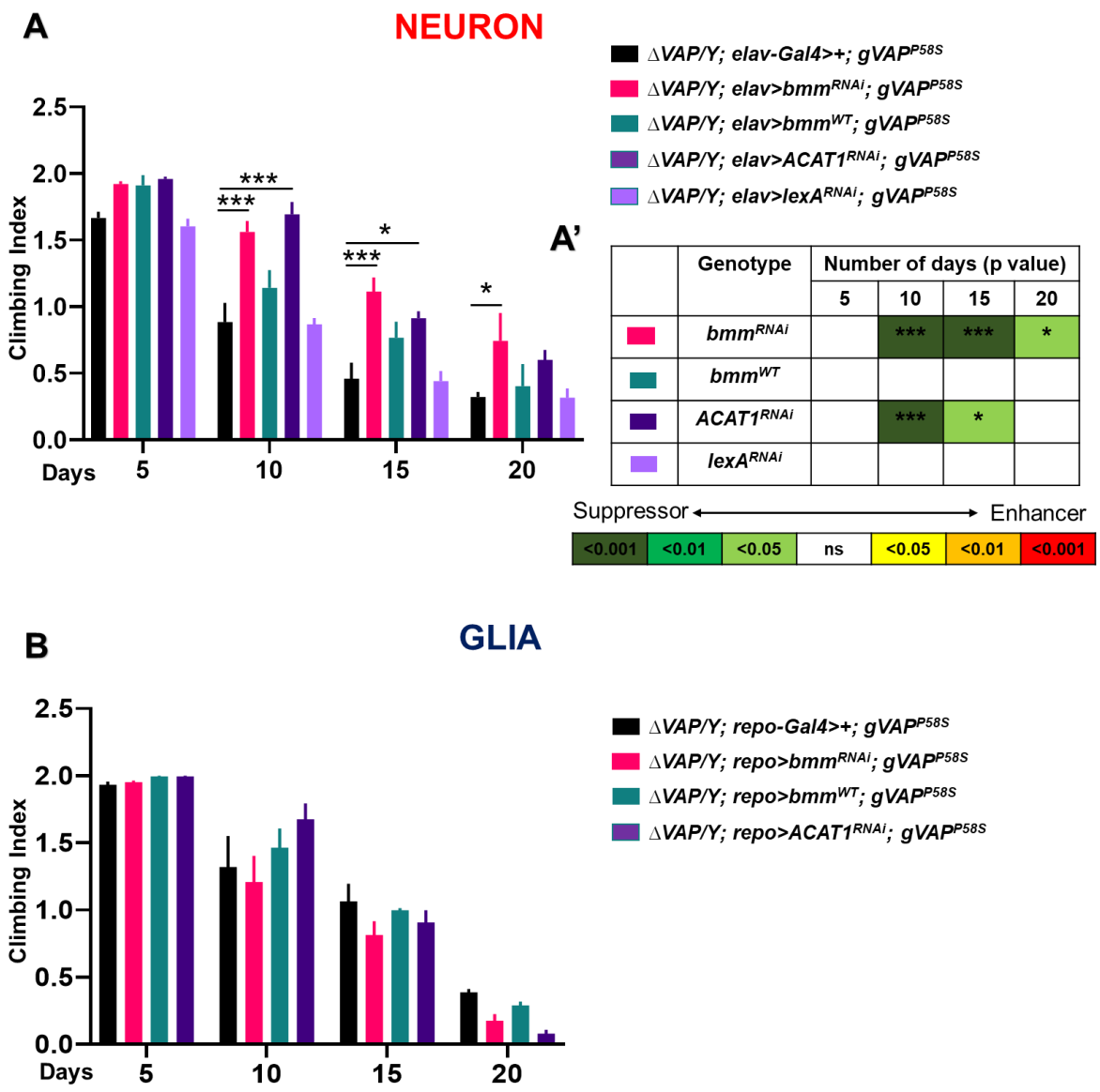



**Figure 4.6: KD of *bmm and ACAT1* in the neurons at adult stage rescues motor dysfunction of *ALS8.***

(A) Climbing Index is plotted in the bar graph representation after modulation of *bmm* and *ACAT1* in the neurons at adult stage of *ALS8* flies with the statistical significance. (A') Summary of the graph is shown in tabulated form with its statistical significance for each interval (5, 10, 15, 20 and 25).

(B) Climbing Index is plotted in the bar graph form after modulation of *bmm* and *ACAT1* in the glia at adult stage of *ALS8* flies where no change was detected.

Mean±SEM values are plotted as climbing index in the bar graph on Y axis with number of days on X axis with statistical significance as p<0.001(***), <0.01(**) and <0.05(*). n=25-30 males, N=3 biological replicates per genotype.

## 4.4 Discussion

**4.4.1 Ceramides and its derivatives are elevated in *ALS8* model:** Multiple evidence from lipid profiling of the ALS patients points toward altered sphingolipid levels in age dependent manner (Agrawal et al., 2022; Cutler et al., 2002; Hannun & Obeid, 2018; Henriques et al., 2017). Specifically, excess ceramides are known to promote accumulate lipids, triggers ER stress and lipotoxic stress (Hebbar et al., 2015; Jana et al., 2009; Mencarelli & Martinez-Martinez, 2013; Vos et al., 2021 ). In our study, we found ceramides and its derivatives such as sphingomyelins and C-1-P are elevated by 2$^{nd}$ itself in the *ALS8* brains. Interestingly, it seems ER-Golgi contact site is severely affected in *ALS8* mutant as Tsuda lab has already shown the inactivity of OSBP protein in the motor neurons of *ALS8* flies (Moustaqim-Barrette et al., 2014). Also, the higher lipid levels are visible much earlier than other phenotypes such as motor function, ER stress and inflammation (Tendulkar et al., 2022; Thulasidharan et al., 2024). This is really important for the presymptomatic ALS patients where lipids can be used as biomarker of the disease (Rachakonda et al., 2004). However, ceramides are elevated in other neurodegenerative disorders as well like Parkinson's and Multiple Sclerosis, so further studies need to be done based on the other derivatives of ceramides such as glycosphingolipids which we could not check in our model system (Cheng et al., 2011; Hebbar et al., 2015; Islam et al., 2025; Long et al., 2026; Rachakonda et al., 2004; Vos et al., 2021). Another interesting fact is the unchanged levels of sphingosine or sphingosine-1-phosphate which shows that particular subtype of sphingolipids are affected where others are completely normal suggest a possibility that only those species are affected where VAPB interactors are involved in sphingolipid transfer such as CERT (Chaplot, 2019). Also, ceramides are known to affect OSBP activity as well. So, it is quite possible that ceramides maybe regulating the increased cholesterol ester levels in *ALS8* model (Henriques et al., 2017; Kumagai & Hanada, 2019; Peretti et al., 2008; Perry & Ridgway, 2006). However, the question still remains why sphingolipids are elevated in *ALS8* flies and what may be causative factor for the increase in these lipid levels?

**4.4.2 Reducing sphingolipid levels in the neurons improve motor function of *VAP$^{P58S}$* animals:** LC-MS lipid profiling of *ALS8* brains showed elevated sphingolipid levels which are generally present at ER-Golgi network. So, we chose CERT as target of interest because of its interaction with VAPB. *CERT* loss of function is known to reduce both ceramide and

sphingomyelin levels (Rao et al., 2014; Rao et al., 2007). Interestingly, we found under normal conditions, blocking CERT in neurons, glia and muscles of *ALS8* did not rescue motor function at all. In addition, blocking ceramide synthesis also did not rescue the phenotype. However, blocking ceramide synthesis as well as transfer in the neurons at the adult stage significantly improved motor function of *ALS8* flies. These results suggest ceramides play quite an important role in the neurodevelopment which is strongly supported by recent studies (Anna B. Ziegler 2025; Goyal et al., 2019; Hussain et al., 2019; Kraut, 2011; Theisen et al., 2025; Zhu et al., 2025). Additionally, when we knocked down *lace* in the neurons, initial gene involved in sphingolipid synthesis, it showed lethality at the pupal stage suggesting increase in ceramides/sphingomyelins can be one of the reasons which is able to push the *ALS8* flies to the eclosion stage. However, after eclosion of the flies, increased ceramides/sphingomyelins in neurons may be contributing to the progression of disease. Interestingly, in glia, reducing ceramide levels were worsening the phenotype that we have tried to address in chapter V.

**4.4.3 Increased lipid production in neurons contribute to the progression of ALS disease:** In other ALS models, lipid levels are known to be increased due to oxidative stress in the neurons. ROS species can lead to oxidation of free fatty acids and affect cellular physiology(Chaplot et al., 2019; Ioannou et al., 2019; Layalle et al., 2021; Liu et al., 2017; Liu et al., 2015; McBenedict et al., 2025; Moulton et al., 2021). To protect these lipids, they are converted to cholesterol esters, TAGs lipids (Chaves-Filho et al., 2019). In our case, we found that CEs, TAGs, ceramides and SMs are increased which need fatty acids as substrate. In other ALS mutants, LDs have been shown to be in abundant amount (Chaves-Filho et al., 2019; Farmer et al., 2020; Girard et al., 2020; Liu et al., 2015; Moulton et al., 2021; Smolic, Tavcar, et al., 2021), whereas in *ALS8* mutant, LDs are less in number and size is reduced with age (chapter III). It seems lipids from LDs of the glia maybe utilized by neurons for the production of cholesterol esters, ceramides and TAGs (Haynes et al., 2024). The reason is inhibition of both *brummer* and *ACAT1* led to improvement of the motor phenotype where fatty acyl CoA production will be affected and also ketone bodies will be reduced in the neurons. This theory is supported by another experiment as well. In chapter III, when we reduced $VAP^{P58S}$ in the glial cells, it led to increase in LDs number in the brain of *ALS8* suggesting its utilization is reduced because of the absence of *VAP* at ER membrane which ultimately will affect lipid production in the neurons and thus rescuing of the motor phenotypes. Another possibility is that blocking *bmm* in neurons will decrease the lipolysis. So, unavailability

of fatty acids in neurons due to *bmm* and *ACAT1* inhibition will lead to less lipogenesis and also ketone bodies which may be responsible for improving motor function. The question arises does TAGs are transported from glia to neurons via some apolipoproteins (Glaz in flies) or LDs can be transported directly?

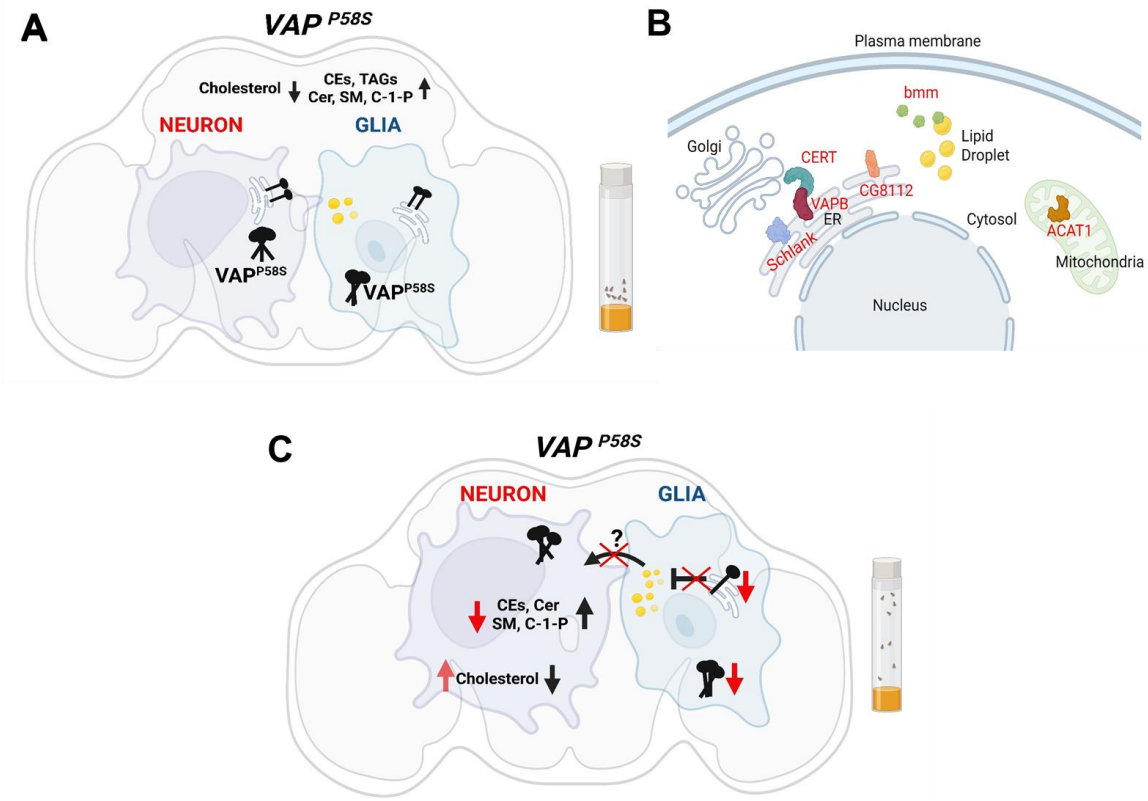



**Figure 4.7: Lipid accumulation in neurons contributes to the progression of ALS disease.**

(A) LC-MS lipid profiling revealed elevated lipid levels in the adult brain of *Drosophila* model of *ALS8* in an age dependent manner whereas LDs are disrupted in the brain.
(B) Genes targeted in the neurons and glia of $VAP^{P58S}$ male flies with their location mentioned.
(C) Reducing lipid levels like CEs, SMs in the neurons leads to improvement in the motor function of *ALS8* flies. Additionally, reducing *VAP* levels in glia increase LD density which may stop the transfer of LDs or TAGs to neurons thus decreasing lipid synthesis in neurons and improving motor performance of the diseased flies.

**4.5 Conclusion:** In summary, LC-MS lipid profiling of *ALS8* model revealed that specific sphingolipid levels are elevated in the brains which may act as contributing factor to the progression of disease. Also, we have identified the differential role of sphingolipids in neurons and glia where reducing lipid production in neurons improves the motor performance of *Drosophila ALS8* flies.

## 4.6 Materials and Methods

**4.6.1 *Drosophila* husbandry, fly stocks and reagents:** All the experimental stocks were maintained and crossed on a standard corn agar media in 12 hr Light: 12hr Dark cycle at 25 ℃ unless specified and F1 male progeny were used for experiments, which were performed at 25℃. *CantonS* was used as wild-type control in the experiments. *UASp-CERT$^{WT}$* and *UASp-CERT$^{EAAD}$* transgenic lines were generated in the lab. *repo-Gal4*, *elav-Gal4*, Δ*VAP ;; gVAP$^{P58S}$*, Δ*VAP ; repo-Gal4; gVAP$^{P58S}$*, Δ*VAP ; elav-Gal4; gVAP$^{P58S}$* and Δ*VAP ; MHC-Gal4,MHC-RFP; gVAP$^{P58S}$* are described in (Tendulkar et al., 2022; Thulasidharan et al., 2024). Bloomington fly Stocks: *CS* (BL_0001), *MHC-Gal4* (BL_38464), *CERT$^{RNAi}$* (BL_60080), *schlank$^{RNAi}$* (BL_29340), *ACAT1$^{RNAi}$* (BL_51785), *bmm$^{RNAi}$* (BL_25926), *UAS-bmm* (BL-76600) were used for experiments.

**4.6.2 Lipid extraction and targeted LC-MS lipidomics:** Sphingolipids were extracted and analyzed using the same protocol as described in chapter III. Internal standards from Avanti polar lipids were used as follows: 100 pmol of 25:0 Ceramide, 12:0 Sphingomyelin, 12:0 Ceramide-1-Phosphate.

**4.6.3 Cloning and generation of *CERT* transgenic lines:** *CERT* cDNA from *Drosophila* Gold collection (https://dgrc.bio.indiana.edu/) was amplified using *CERT* specific primers. Site specific mutagenesis was used to create FF>AA mutation (306-307 AA position) in the *CERT* DNA fragment. The second-chromosome UAS transgenics for *CERT$^{WT}$ and CERT$^{EAAD}$* were generated by targeted insertion at attP40 using the pUASp-attB vector obtained from the *Drosophila* Genomics Resource Centre (DGRC, #1358). Transgenics were balanced, screened using mini-white as a selectable marker and validated using qPCR. Following primers (5'-> 3' direction) were used: *CERT* cDNA- *ATGGACACGAACGCTGGGGAG* (forward), *TCAGAACATGATCGGCTTGTCCTT* (reversed). For cloning in pUASp-attB vector: *GGATCAGATCCGCGGCCGCATGGACACGAACGCTGGGGAG* (forward), *CCACTAGTGGCCTATGCGGCCGCTCAGAACATGATCGGCTTGTC* (reversed) and for *pUASp-CERT* DNA sequencing: *GGCAAGGGTCGAGTCGATAG* (forward) and *AGGTTTAACCAGGGGATGCT* (reversed), for FF>AA DNA sequencing: *GGACCAAAGCAAAAAGCTCAA* (forward) and *GCGATCGATCTCCGGCCACAG* (reversed).

**4.6.4 Real Time PCR:** mRNA was extracted from 10-day-old male flies (10 flies per genotype) using the Abcam manual extraction protocol. A total of 1µg RNA was used for cDNA synthesis using the High-Capacity cDNA reverse transcriptase Kit (4368814) by Invitrogen. Then qPCR was performed using gene specific primers along with iTaq Universal SyBr Green Supermix (Biorad, #1725124) in qTOWER3 778 Series Real Time PCR 779 Thermal Cycler. The relative fold change for each genotype was calculated by normalizing to housekeeping gene *rp49*. Experiment was performed for three replicates per genotype. Following primer pairs (5'->3') were used: *rp49: GACGCTTCAAGGGACAGTATC* (forward); *AAACGCGGTTCTGCATGAG* (reverse), *CERT: ATCGATTTCAAGGGCGAATCCATC* (forward); *TCCTTGAGCTTTTTGCTTTGGTCC* (reverse), FFAT: *ACATTGCCCGAGGATGAGTTCTTC* (forward) and *GCGATCGATCTCCGGCCACAG* (reverse).

**4.6.5 Drug feeding:** (100µM myriocin, M1177-SIGMA ALDRICH) and (20µM Avasimibe, PZ0190-SIGMA ALDRICH) both in 2% DMSO were added to the regular food of the flies and DMSO was used as control solvent. Media was changed after every 3 days.

**4.6.6 Statistical tests:** For lipid species, multiple unpaired t-test was used for comparisons between lipid species followed by FDR of Benjamin and Hochberg with p value using APA style. For climbing assays, Two way ANOVA followed by Tukey's test was used for multiple comparisons between genotypes using APA style for p values.

**4.6.7 Software/ Applications:** Snapgene software was used to design primers, Graphpad for statistical tests, Powerpoint for image representation, Biorender for schematic diagrams,

**4.7 Contributions:** Senthilkumar Deivasigamani from the lab generated *UAS-CERT* transgenic fly lines with the assistance of Dr. Anuradha Ratnaparkhi. Shweta from the lab prepared the lipid samples of adult brains for wildtype and *ALS8* flies. Prof. Siddhesh Kamat provided technical assistance for LC-MS lipid profiling and data analysis.

**4.8 Acknowledgements:** Aparna helped in brain dissections for lipid profiling experiments. The fly facility at the National Centre for Biological Sciences (NCBS), Bangalore, for injecting *CERT* constructs into *Drosophila* embryos.

## 4.9 References

Agrawal, I., Lim, Y. S., Ng, S. Y., & Ling, S. C. (2022). Deciphering lipid dysregulation in ALS: from mechanisms to translational medicine. *Transl Neurodegener*, *11*(1), 48. https://doi.org/10.1186/s40035-022-00322-0

Anna B. Ziegler , C. W., Konstantin Beckschäfer,Anna-Lena Wulf,Neena Dhiman,Peter Soba,Christoph Thiele,Reinhard Bauer,Gaia Tavosanis (2025). Individual lipid alterations at the origin of neuronal Ceramide Synthase defects. *PloS Genetics*, *21*(9). https://doi.org/https://doi.org/10.1371/journal.pgen.1011880

Bohnert, M., & Schrul, B. (2024). Lipid droplets in health and disease. *FEBS Lett*, *598*(10), 1113-1115. https://doi.org/10.1002/1873-3468.14900

Carreira, A. C., Santos, T. C., Lone, M. A., Zupančič, E., Lloyd-Evans, E., de Almeida, R. F. M., Hornemann, T., & Silva, L. C. (2019). Mammalian sphingoid bases: Biophysical, physiological and pathological properties. *Progress in Lipid Research*, *75*(100988). https://doi.org/10.1016/j.plipres.2019.100988

Carter, H. E., Haines, W. J., Ledyard, W. E., & Norris, W. P. (1947). Biochemistry of the sphingolipides: i. Preparation of sphingolipides from beef brain and spinal cord. *Journal of Biological Chemistry*, *169*(1), 77-82. https://doi.org/https://doi.org/10.1016/S0021-9258(17)35063-9

Chaplot, K. (2019). *Regulation of VAP(P58S) neuroaggregation in a Drosophila model of Amyotrophic Lateral Sclerosis* IISER Pune]. http://dr.iiserpune.ac.in:8080/xmlui/handle/123456789/2922

Chaplot, K., Pimpale, L., Ramalingam, B., Deivasigamani, S., Kamat, S. S., & Ratnaparkhi, G. S. (2019). SOD1 activity threshold and TOR signaling modulate VAP(P58S) aggregation via reactive oxygen species-induced proteasomal degradation in a Drosophila model of amyotrophic lateral sclerosis. *Dis Model Mech*, *12*(2). https://doi.org/10.1242/dmm.033803

Chaves-Filho, A. B., Pinto, I. F. D., Dantas, L. S., Xavier, A. M., Inague, A., Faria, R. L., Medeiros, M. H. G., Glezer, I., Yoshinaga, M. Y., & Miyamoto, S. (2019). Alterations in lipid metabolism of spinal cord linked to amyotrophic lateral sclerosis. *Sci Rep*, *9*(1), 11642. https://doi.org/10.1038/s41598-019-48059-7

Cheng, D., Jenner, A. M., Shui, G., Cheong, W. F., Mitchell, T. W., Nealon, J. R., Kim, W. S., McCann, H., Wenk, M. R., Halliday, G. M., & Garner, B. (2011). Lipid Pathway Alterations in Parkinson's Disease Primary Visual Cortex. *PLoS One*, *6*(2), e17299. https://doi.org/10.1371/journal.pone.0017299

Crivelli, S. M., Giovagnoni, C., Zhu, Z., Tripathi, P., Elsherbini, A., Quadri, Z., Pu, J., Zhang, L., Ferko, B., Berkes, D., Spassieva, S. D., Martinez-Martinez, P., & Bieberich, E. (2022). Function of ceramide transfer protein for biogenesis and sphingolipid composition of extracellular vesicles. *J Extracell Vesicles*, *11*(6), e12233. https://doi.org/10.1002/jev2.12233

Cutler, R. G., Pedersen, W. A., Camandola, S., Rothstein, J. D., & Mattson, M. P. (2002). Evidence that accumulation of ceramides and cholesterol esters mediates oxidative stress-induced death of motor neurons in amyotrophic lateral sclerosis. *Ann Neurol*, *52*(4), 448-457. https://doi.org/10.1002/ana.10312

Farmer, B. C., Walsh, A. E., Kluemper, J. C., & Johnson, L. A. (2020). Lipid Droplets in Neurodegenerative Disorders. *Front Neurosci*, *14*, 742. https://doi.org/10.3389/fnins.2020.00742

Girard, V., Goubard, V., Querenet, M., Seugnet, L., Pays, L., Nataf, S., Dufourd, E., Cluet, D., Mollereau, B., & Davoust, N. (2020). Spen modulates lipid droplet content in adult Drosophila glial cells and protects against paraquat toxicity. *Sci Rep*, *10*(1), 20023. https://doi.org/10.1038/s41598-020-76891-9

Goyal, G., Zheng, J., Adam, E., Steffes, G., Jain, M., Klavins, K., & Hummel, T. (2019). Sphingolipid-dependent Dscam sorting regulates axon segregation. *Nat Commun*, *10*(1), 813. https://doi.org/10.1038/s41467-019-08765-2

Hanada, K. (2014). Co-evolution of sphingomyelin and the ceramide transport protein CERT. *Biochim Biophys Acta*, *1841*(5), 704-719. https://doi.org/10.1016/j.bbalip.2013.06.006

Hannun, Y. A., & Obeid, L. M. (2018). Sphingolipids and their metabolism in physiology and disease. *Nat Rev Mol Cell Biol*, *19*(3), 175-191. https://doi.org/10.1038/nrm.2017.107

Hartmann, H., Ho, W. Y., Chang, J. C., & Ling, S. C. (2022). Cholesterol dyshomeostasis in amyotrophic lateral sclerosis: cause, consequence, or epiphenomenon? *FEBS J*, *289*(24), 7688-7709. https://doi.org/10.1111/febs.16175

Haynes, P. R., Pyfrom, E. S., Li, Y., Stein, C., Cuddapah, V. A., Jacobs, J. A., Yue, Z., & Sehgal, A. (2024). A neuron-glia lipid metabolic cycle couples daily sleep to mitochondrial homeostasis. *Nat Neurosci*, *27*(4), 666-678. https://doi.org/10.1038/s41593-023-01568-1

He, X., Huang, Y., Li, B., Gong, C.-X., & Schuchman, E. H. (2010). Deregulation of sphingolipid metabolism in Alzheimer's disease. *Neurobiology of Aging*, *31*(3), 398-408. https://doi.org/https://doi.org/10.1016/j.neurobiolaging.2008.05.010

Hebbar, S., Sahoo, I., Matysik, A., Argudo Garcia, I., Osborne, K. A., Papan, C., Torta, F., Narayanaswamy, P., Fun, X. H., Wenk, M. R., Shevchenko, A., Schwudke, D., & Kraut, R. (2015). Ceramides And Stress Signaling Intersect With Autophagic Defects In Neurodegenerative Drosophila blue cheese (bchs) Mutants. *Sci Rep*, *5*, 15926. https://doi.org/10.1038/srep15926

Henriques, A., Croixmarie, V., Bouscary, A., Mosbach, A., Keime, C., Boursier-Neyret, C., Walter, B., Spedding, M., & Loeffler, J. P. (2017). Sphingolipid Metabolism Is Dysregulated at Transcriptomic and Metabolic Levels in the Spinal Cord of an Animal Model of Amyotrophic Lateral Sclerosis. *Front Mol Neurosci*, *10*, 433. https://doi.org/10.3389/fnmol.2017.00433

Hussain, G., Wang, J., Rasul, A., Anwar, H., Imran, A., Qasim, M., Zafar, S., Kamran, S. K. S., Razzaq, A., Aziz, N., Ahmad, W., Shabbir, A., Iqbal, J., Baig, S. M., & Sun, T. (2019). Role of

cholesterol and sphingolipids in brain development and neurological diseases. *Lipids Health Dis*, *18*(1), 26. https://doi.org/10.1186/s12944-019-0965-z

Ioannou, M. S., Jackson, J., Sheu, S. H., Chang, C. L., Weigel, A. V., Liu, H., Pasolli, H. A., Xu, C. S., Pang, S., Matthies, D., Hess, H. F., Lippincott-Schwartz, J., & Liu, Z. (2019). Neuron-Astrocyte Metabolic Coupling Protects against Activity-Induced Fatty Acid Toxicity. *Cell*, *177*(6), 1522-1535 e1514. https://doi.org/10.1016/j.cell.2019.04.001

Islam, M. N., Mandal, N., Khanom, N. I., Spivey, A. L., Patel, A. S., Ahmed, T., Islam, R., & Bhuiyan, M. I. H. (2025). Sphingolipid Signaling and Metabolism in Neuronal and Glial Cells: Implications for Cerebrovascular and Neurodegenerative Disorders. *Aging Dis*. https://doi.org/10.14336/AD.2025.1024

Jana, A., Hogan, E. L., & Pahan, K. (2009). Ceramide and neurodegeneration: Susceptibility of neurons and oligodendrocytes to cell damage and death. *Journal of the Neurological Sciences*, *278*(1), 5-15. https://doi.org/https://doi.org/10.1016/j.jns.2008.12.010

Kawano, M., Kumagai, K., Nishijima, M., & Hanada, K. (2006). Efficient trafficking of ceramide from the endoplasmic reticulum to the Golgi apparatus requires a VAMP-associated protein-interacting FFAT motif of CERT. *J Biol Chem*, *281*(40), 30279-30288. https://doi.org/10.1074/jbc.M605032200

Kentaro Hanada, K. K., Satoshi Yasuda, Yukiko Miura, Miyuki Kawano, Masayoshi Fukasawa & Masahiro Nishijima. (2003). Molecular machinery for non-vesicular trafficking of ceramide. *Nature*, *426*, 803-809.

Kors, S., Costello, J. L., & Schrader, M. (2022). VAP Proteins - From Organelle Tethers to Pathogenic Host Interactors and Their Role in Neuronal Disease. *Front Cell Dev Biol*, *10*, 895856. https://doi.org/10.3389/fcell.2022.895856

Kraut, R. (2011). Roles of sphingolipids in Drosophila development and disease. *J Neurochem*, *116*(5), 764-778. https://doi.org/10.1111/j.1471-4159.2010.07022.x

Kumagai, K., & Hanada, K. (2019). Structure, functions and regulation of CERT, a lipid-transfer protein for the delivery of ceramide at the ER-Golgi membrane contact sites. *FEBS Lett*, *593*(17), 2366-2377. https://doi.org/10.1002/1873-3468.13511

Kumagai, K., Kawano-Kawada, M., & Hanada, K. (2014). Phosphoregulation of the ceramide transport protein CERT at serine 315 in the interaction with VAMP-associated protein (VAP) for inter-organelle trafficking of ceramide in mammalian cells. *J Biol Chem*, *289*(15), 10748-10760. https://doi.org/10.1074/jbc.M113.528380

Layalle, S., They, L., Ourghani, S., Raoul, C., & Soustelle, L. (2021). Amyotrophic Lateral Sclerosis Genes in Drosophila melanogaster. *Int J Mol Sci*, *22*(2). https://doi.org/10.3390/ijms22020904

Liu, L., MacKenzie, K. R., Putluri, N., Maletic-Savatic, M., & Bellen, H. J. (2017). The Glia-Neuron Lactate Shuttle and Elevated ROS Promote Lipid Synthesis in Neurons and Lipid Droplet

Accumulation in Glia via APOE/D. *Cell Metab*, *26*(5), 719-737 e716. https://doi.org/10.1016/j.cmet.2017.08.024

Liu, L., Zhang, K., Sandoval, H., Yamamoto, S., Jaiswal, M., Sanz, E., Li, Z., Hui, J., Graham, B. H., Quintana, A., & Bellen, H. J. (2015). Glial lipid droplets and ROS induced by mitochondrial defects promote neurodegeneration. *Cell*, *160*(1-2), 177-190. https://doi.org/10.1016/j.cell.2014.12.019

Long, J., Liu, S., Shi, Y., Zhang, C., Qin, L., & Ai, Q. (2026). Targeting lipid metabolism in neurodegenerative diseases: From experimental to clinical. *Metabolism*, *175*, 156436. https://doi.org/10.1016/j.metabol.2025.156436

McBenedict, B., Hauwanga, W. N., Nezam, U., Ko Oo, A., Eapi, S., Pradhan, S., Dang, N. B., Cher, P. W., Orsini, M. A., & Lima Pessoa, B. (2025). Amyotrophic Lateral Sclerosis (ALS) Type 8: A Narrative Review. *Cureus*, *17*(1), e76717. https://doi.org/10.7759/cureus.76717

McCluskey, G., Donaghy, C., Morrison, K. E., McConville, J., Duddy, W., & Duguez, S. (2022). The Role of Sphingomyelin and Ceramide in Motor Neuron Diseases. *J Pers Med*, *12*(9). https://doi.org/10.3390/jpm12091418

McInnis, J. J., Sood, D., Guo, L., Dufault, M. R., Garcia, M., Passaro, R., Gao, G., Zhang, B., & Dodge, J. C. (2024). Unravelling neuronal and glial differences in ceramide composition, synthesis, and sensitivity to toxicity. *Commun Biol*, *7*(1), 1597. https://doi.org/10.1038/s42003-024-07231-0

Mencarelli, C., & Martinez-Martinez, P. (2013). Ceramide function in the brain: when a slight tilt is enough. *Cell Mol Life Sci*, *70*(2), 181-203. https://doi.org/10.1007/s00018-012-1038-x

Mesmin, B., Kovacs, D., & D'Angelo, G. (2019). Lipid exchange and signaling at ER-Golgi contact sites. *Curr Opin Cell Biol*, *57*, 8-15. https://doi.org/10.1016/j.ceb.2018.10.002

Mishra, S., Manohar, V., Chandel, S., Manoj, T., Bhattacharya, S., Hegde, N., Nath, V. R., Krishnan, H., Wendling, C., Di Mattia, T., Martinet, A., Chimata, P., Alpy, F., & Raghu, P. (2024). A genetic screen to uncover mechanisms underlying lipid transfer protein function at membrane contact sites. *Life Sci Alliance*, *7*(6). https://doi.org/10.26508/lsa.202302525

Moulton, M. J., Barish, S., Ralhan, I., Chang, J., Goodman, L. D., Harland, J. G., Marcogliese, P. C., Johansson, J. O., Ioannou, M. S., & Bellen, H. J. (2021). Neuronal ROS-induced glial lipid droplet formation is altered by loss of Alzheimer's disease-associated genes. *Proc Natl Acad Sci U S A*, *118*(52). https://doi.org/10.1073/pnas.2112095118

Moustaqim-Barrette, A., Lin, Y. Q., Pradhan, S., Neely, G. G., Bellen, H. J., & Tsuda, H. (2014). The amyotrophic lateral sclerosis 8 protein, VAP, is required for ER protein quality control. *Hum Mol Genet*, *23*(8), 1975-1989. https://doi.org/10.1093/hmg/ddt594

Oswald, M. C., West, R. J., Lloyd-Evans, E., & Sweeney, S. T. (2015). Identification of dietary alanine toxicity and trafficking dysfunction in a Drosophila model of hereditary sensory and

autonomic neuropathy type 1. *Hum Mol Genet*, *24*(24), 6899-6909. https://doi.org/10.1093/hmg/ddv390

Pan, X., Dutta, D., Lu, S., & Bellen, H. J. (2023). Sphingolipids in neurodegenerative diseases. *Front Neurosci*, *17*, 1137893. https://doi.org/10.3389/fnins.2023.1137893

Pant, D. C., Aguilera-Albesa, S., & Pujol, A. (2020). Ceramide signaling in inherited and multifactorial brain metabolic diseases. *Neurobiol Dis*, *143*, 105014. https://doi.org/10.1016/j.nbd.2020.105014

Pant, D. C., Dorboz, I., Schluter, A., Fourcade, S., Launay, N., Joya, J., Aguilera-Albesa, S., Yoldi, M. E., Casasnovas, C., Willis, M. J., Ruiz, M., Ville, D., Lesca, G., Siquier-Pernet, K., Desguerre, I., Yan, H., Wang, J., Burmeister, M., Brady, L., . . . Pujol, A. (2019). Loss of the sphingolipid desaturase DEGS1 causes hypomyelinating leukodystrophy. *J Clin Invest*, *129*(3), 1240-1256. https://doi.org/10.1172/JCI123959

Peretti, D., Dahan, N., Shimoni, E., Hirschberg, K., & Lev, S. (2008). Coordinated lipid transfer between the endoplasmic reticulum and the Golgi complex requires the VAP proteins and is essential for Golgi-mediated transport. *Mol Biol Cell*, *19*(9), 3871-3884. https://doi.org/10.1091/mbc.e08-05-0498

Perry, R. J., & Ridgway, N. D. (2006). Oxysterol-binding protein and vesicle-associated membrane protein-associated protein are required for sterol-dependent activation of the ceramide transport protein. *Mol Biol Cell*, *17*(6), 2604-2616. https://doi.org/10.1091/mbc.e06-01-0060

Rachakonda, V., Pan Th Fau - Le, W. D., & Le, W. D. (2004). Biomarkers of neurodegenerative disorders: how good are they? *Cell research*, *14*(5), 349-360.

Rao, R. P., Scheffer, L., Srideshikan, S. M., Parthibane, V., Kosakowska-Cholody, T., Masood, M. A., Nagashima, K., Gudla, P., Lockett, S., Acharya, U., & Acharya, J. K. (2014). Ceramide transfer protein deficiency compromises organelle function and leads to senescence in primary cells. *PLoS One*, *9*(3), e92142. https://doi.org/10.1371/journal.pone.0092142

Rao, R. P., Yuan, C., Allegood, J. C., Rawat, S. S., Edwards, M. B., Wang, X., Merrill, A. H., Jr., Acharya, U., & Acharya, J. K. (2007). Ceramide transfer protein function is essential for normal oxidative stress response and lifespan. *Proc Natl Acad Sci U S A*, *104*(27), 11364-11369. https://doi.org/10.1073/pnas.0705049104

Slee, J. A., & Levine, T. P. (2019). Systematic prediction of FFAT motifs across eukaryote proteomes identifies nucleolar and eisosome proteins with the predicted capacity to form bridges to the endoplasmic reticulum. *Contact (Thousand Oaks)*, *2*, 1-21. https://doi.org/10.1177/2515256419883136

Smolic, T., Tavcar, P., Horvat, A., Cerne, U., Haluzan Vasle, A., Tratnjek, L., Kreft, M. E., Scholz, N., Matis, M., Petan, T., Zorec, R., & Vardjan, N. (2021). Astrocytes in stress accumulate lipid droplets. *Glia*, *69*(6), 1540-1562. https://doi.org/10.1002/glia.23978

Tendulkar, S., Hegde, S., Garg, L., Thulasidharan, A., Kaduskar, B., Ratnaparkhi, A., & Ratnaparkhi, G. S. (2022). Caspar, an adapter for VAPB and TER94, modulates the progression of ALS8 by regulating IMD/NFkappaB-mediated glial inflammation in a Drosophila model of human disease. *Hum Mol Genet*, *31*(17), 2857-2875. https://doi.org/10.1093/hmg/ddac076

Theisen, E. K., Rivas-Serna, I. M., Lee, R. J., Jay, T. R., Kunduri, G., Nguyen, T. T., Mazurak, V., Clandinin, M. T., Clandinin, T. R., & Vaughen, J. P. (2025). Glia phagocytose neuronal sphingolipids to infiltrate developing synapses. *bioRxiv*. https://doi.org/10.1101/2025.04.14.648777

Thulasidharan, A., Garg, L., Tendulkar, S., & Ratnaparkhi, G. S. (2024). Age-dependent dynamics of neuronal VAPB(ALS) inclusions in the adult brain. *Neurobiol Dis*, *196*, 106517. https://doi.org/10.1016/j.nbd.2024.106517

Tracey, T. J., Kirk, S. E., Steyn, F. J., & Ngo, S. T. (2021). The role of lipids in the central nervous system and their pathological implications in amyotrophic lateral sclerosis. *Semin Cell Dev Biol*, *112*, 69-81. https://doi.org/10.1016/j.semcdb.2020.08.012

Tracey, T. J., Steyn, F. J., Wolvetang, E. J., & Ngo, S. T. (2018). Neuronal Lipid Metabolism: Multiple Pathways Driving Functional Outcomes in Health and Disease. *Front Mol Neurosci*, *11*, 10. https://doi.org/10.3389/fnmol.2018.00010

Vaughen, J. P., Theisen, E., Rivas-Serna, I. M., Berger, A. B., Kalakuntla, P., Anreiter, I., Mazurak, V. C., Rodriguez, T. P., Mast, J. D., Hartl, T., Perlstein, E. O., Reimer, R. J., Clandinin, M. T., & Clandinin, T. R. (2022). Glial control of sphingolipid levels sculpts diurnal remodeling in a circadian circuit. *Neuron*, *110*(19), 3186-3205 e3187. https://doi.org/10.1016/j.neuron.2022.07.016

Voelzmann, A., & Bauer, R. (2010). Ceramide synthases in mammalians, worms, and insects: emerging schemes. *Biomol Concepts*, *1*(5-6), 411-422. https://doi.org/10.1515/bmc.2010.028

Vos, M., Dulovic-Mahlow, M., Mandik, F., Frese, L., Kanana, Y., Haissatou Diaw, S., Depperschmidt, J., Bohm, C., Rohr, J., Lohnau, T., Konig, I. R., & Klein, C. (2021). Ceramide accumulation induces mitophagy and impairs beta-oxidation in PINK1 deficiency. *Proc Natl Acad Sci U S A*, *118*(43). https://doi.org/10.1073/pnas.2025347118

Walther, T. C., & Farese, R. V., Jr. (2012). Lipid droplets and cellular lipid metabolism. *Annu Rev Biochem*, *81*, 687-714. https://doi.org/10.1146/annurev-biochem-061009-102430

Wang, X., Rao, R. P., Kosakowska-Cholody, T., Masood, M. A., Southon, E., Zhang, H., Berthet, C., Nagashim, K., Veenstra, T. K., Tessarollo, L., Acharya, U., & Acharya, J. K. (2009). Mitochondrial degeneration and not apoptosis is the primary cause of embryonic lethality in ceramide transfer protein mutant mice. *J Cell Biol*, *184*(1), 143-158. https://doi.org/10.1083/jcb.200807176

Weber-Boyvat, M., Kentala, H., Peranen, J., & Olkkonen, V. M. (2015). Ligand-dependent localization and function of ORP-VAP complexes at membrane contact sites. *Cell Mol Life Sci*, *72*(10), 1967-1987. https://doi.org/10.1007/s00018-014-1786-x

Yamaji, T., Kumagai, K., Tomishige, N., & Hanada, K. (2008). Two sphingolipid transfer proteins, CERT and FAPP2: their roles in sphingolipid metabolism. *IUBMB Life*, *60*(8), 511-518. https://doi.org/10.1002/iub.83

Yang, D., Wang, X., Zhang, L., Fang, Y., Zheng, Q., Liu, X., Yu, W., Chen, S., Ying, J., & Hua, F. (2022). Lipid metabolism and storage in neuroglia: role in brain development and neurodegenerative diseases. *Cell Biosci*, *12*(1), 106. https://doi.org/10.1186/s13578-022-00828-0

Zhu, Y., Cho, K., Lacin, H., Zhu, Y., DiPaola, J. T., Wilson, B. A., Patti, G., & Skeath, J. B. (2025). Loss of dihydroceramide desaturase drives neurodegeneration by disrupting endoplasmic reticulum and lipid droplet homeostasis in glial cells. *Elife*, *13*. https://doi.org/10.7554/eLife.99344

# Chapter V

# Glial ceramide orchestrates LD homeostasis and motor function in *Drosophila*

## 5.1 Abstract

Glia cells have emerged as equal partners to neurons in the development and maintenance of the nervous system. Glia provide structural, metabolic and regulatory support for neuronal function. In this study, we examine glial roles in the context of adult motor function. Specifically, we find that genes in the ceramide pathway, which produce and transport ceramides from the endoplasmic reticulum, affect age-dependent adult motor function; *e.g., schlank* activity in glia is critical, whereas *lace*, but not *schlank*, is critical in neurons. Further, reduction of CERT in glia also affects age-dependent motor function, highlighting the importance of targeted, efficient non-vesicular ceramide transfer at the endoplasmic reticulum/ Golgi interface in glial cells. Additionally, we find that the density and size of Lipid Droplets in glial cells are sensitive to ceramide production and transfer, with motor function correlating to a drop in glial Lipid Droplets. Our findings link the ceramide pathway, Lipid Droplets and adult motor activity into an interconnected physiological network.

In summary, our research links Lipid Droplet dynamics, ceramide production and ceramide transfer to vulnerability in the adult motor neuronal circuit, with Glial cells playing key metabolic roles.

## 5.2 Introduction

**5.2.1 Ceramides and their roles:** Ceramides are bioactive lipids which contain a long-chain sphingoid base that is connected with a fatty acyl chain via an amide bond. Ceramides are quite diverse in nature in terms of different chain lengths, hydroxylations, and saturated bonds of both the base as well as fatty acid moieties (Bikman & Summers, 2011; Islam et al., 2025; Pan et al., 2023). Ceramides are the substrates for the formation of the more complex sphingolipids and glycosphingolipids. Ceramide metabolism is essential to maintain cellular homeostasis (Bikman & Summers, 2011; Pant et al., 2020) (Mencarelli & Martinez-Martinez, 2013). Ceramide dysregulation is linked to several disorders like type-II diabetes, fatty liver disease and neurodegenerative disorders (Cutler et al., 2002; Hebbar et al., 2015; Henriques et al., 2017; islam et al., 2025; Jeon et al., 2023; Pant et al., 2020; Pant et al., 2019). Within cells, Ceramides are at the center of a sphingolipid

metabolic network connecting multiple pathways of synthesis, recycling and breakdown. Ceramides are synthesized through *de novo* pathway that occurs at the cytosolic leaflet of ER membrane through a series of enzymes that are conserved across species (Jeon et al., 2023; Mccluskey et al., 2022; Mencarelli & Martinez-Martinez, 2013; Pant et al., 2020). *Drosophila melanogaster* is also able to generate ceramide from scratch using a similar set of enzymes and substrates (Kraut, 2011; Pan et al., 2023) and unlike vertebrates, usually has one paralog at each step of synthesis. For example, *Drosophila* has a single Ceramide synthase (CERS), *schlank*, as compared to six *CERS* genes in *H. sapiens* (Bauer et al., 2009; Pathak et al., 2018; Voelzmann & Bauer, 2010).

**5.2.2 Ceramide dysregulation in the brain:** Perturbation in ceramide pathway genes can lead to a host of neurological disorders, including Hereditary Sensory and Autonomous Neuropathy 1 (HSAN1), Hereditary Spastic Paraplagia (HSP), ALS, and Parkinson's (Agrawal et al., 2022; Cutler et al., 2002; Hebbar et al., 2015; Hussain et al., 2019; Islam et al., 2025; Liping wang, 2022; Pan et al., 2023; Pant et al., 2020; Tracey et al., 2021; Vos et al., 2021). Studies also underscore the importance of ceramide production in the development of the brain (Ghosh et al., 2013; Goyal et al., 2019; Oswald et al., 2015). Moreover, glial CPE, also plays a crucial role in the wrapping of neuronal axons and can affect the circadian rhythm of the flies (Chen et al., 2022; Ghosh et al., 2013; Theisen et al., 2025). Alterations in ceramide levels affect ER structure as well, which can thus lead to disruption in ER function, LD formation (Pant et al., 2019; Rao et al., 2014; Robles-Martinez et al., 2025), which originates at the ER membrane. Generally, glia is the major hub for LD formation in the brain and LD dynamics are known to be modulated in neurodegenerative disorders (Goodman et al., 2024; Liu et al., 2015; Pennetta & Welte, 2018; Zhang et al., 2025). Interestingly, ceramide-synthesizing enzymes like *schlank* and *infertile crescent (ifc)* in the flies have been shown to affect LD homeostasis in the larvae (Bauer et al., 2009; Sociale et al., 2018; Zhu et al., 2025). But how it is correlated to motor function is not explored very well**.**

**5.2.3 CERT role in *Drosophila* physiology:** CERT sole function is to transfer ceramide from ER to *trans*-Golgi in the cell. Ravi Acharya's laboratory (Rao et al., 2007) report that CERT null flies have age-dependent motor dysfunction. *Drosophila* CERT is essential for maintaining the integrity of other cellular membranes, including the plasma membrane. The absence of *CERT* impairs mitochondrial function, shortening the fly lifespan to 30 days. Lack of ceramide transfer also leads to changes in ER network, ER stress and increased autophagy (Rao et al., 2014). *Drosophila CERT*

null embryos eclose normally, whereas mouse embryos die from cardiac failure (Rao et al., 2007; Wang et al., 2009). Recently, *CERT1* gain-of-function mutants have been found in human patients as well (Gehin et al., 2023). However, tissue specific functions of ceramide and CERT have not been explored very well in both mammals and flies. Recent studies suggest a diverse set of functions of ceramide synthesis enzymes with respect to production of ceramides in neurons vs glia, but how these changes can influence behavioral outcomes is poorly understood. (Theisen et al., 2025).

Our interest in CERT stems from its interaction with VAPB. In the Chapter IV, we found that *CERT* was showing tissue specific roles in the brain of *ALS8* model as neuronal KD of CERT showed improvement in the motor activity but not in glial cells. Similarly, *schlank* KD showed the same results. Interestingly, glial KD of *schlank* and *CERT* showed worsening of *ALS8* motor function suggesting glia specific functions of ceramide and ceramide transfer. We have found a differential role of ceramides in the brain for motor function, which led us to a strong correlation between glial ceramide production and its anterograde transfer from the ER to both LD formation and motor function.

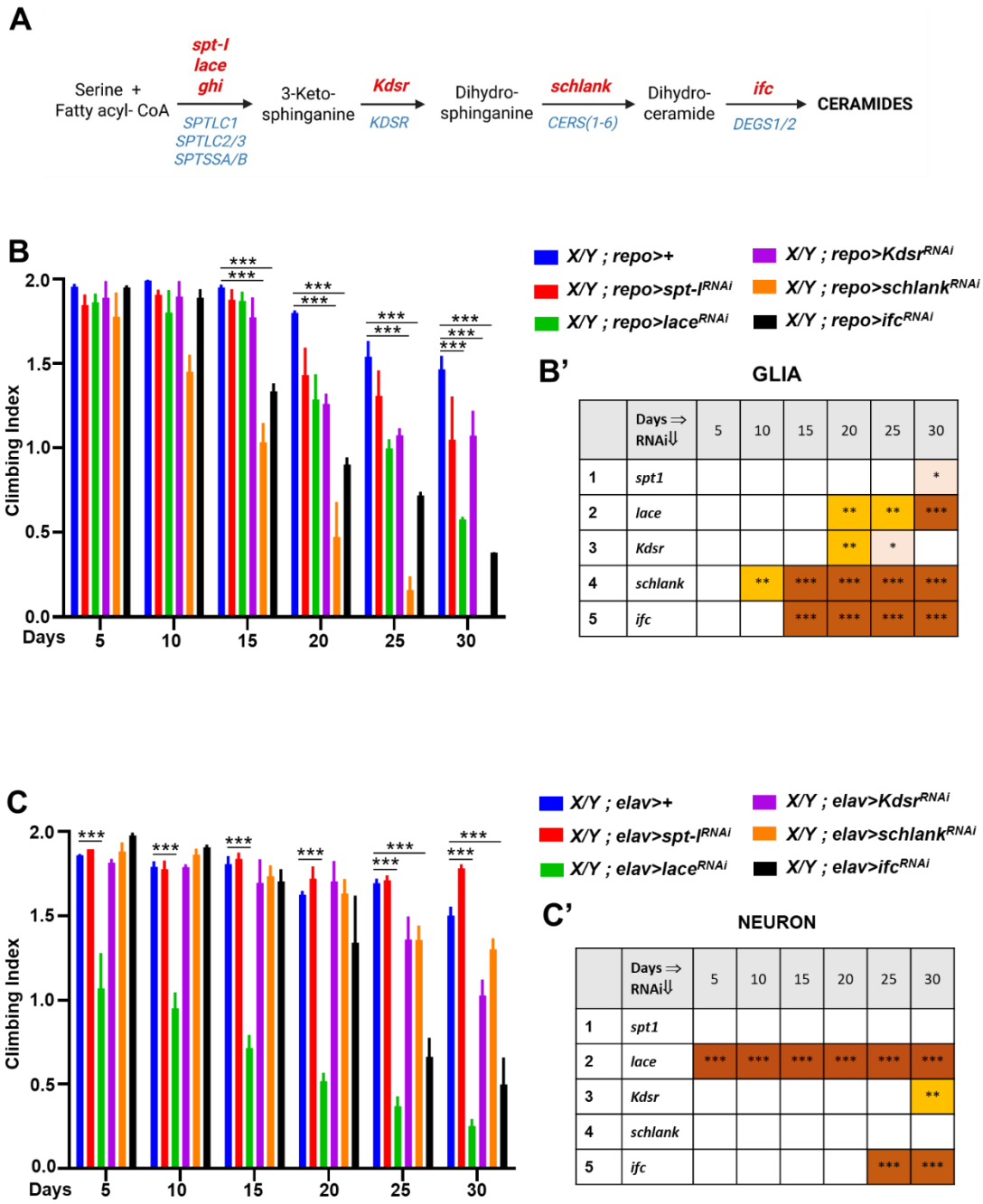
## 5.3 Results

**5.3.1 A reverse genetic screen for motor function in the Ceramide pathway:** To establish a relationship between ceramide formation and motor function, we procured RNA interference (RNAi) lines targeting enzymes involved in *de novo* ceramide synthesis, based on the genes listed by (Kraut, 2011). The genes targeted, and their functions, are listed in Table 1, while their Bloomington *Drosophila* Stock Centre (BDSC) identifiers are listed in Materials and Methods.

The schematic in Fig. 5.1A shows the *de novo* ceramide synthesis pathway at the ER membrane, which is conserved from yeast to mammals as reported in (Pan et al., 2023). We knocked down each gene (Table 5.1) using a pan-glial driver (*repo-Gal4*), and F1 males were evaluated for motor function using the 'Startle Induced Negative Geotaxis' assay. The statistical significance of the individual genes from the screening is shown in the summary table (Fig. 5.1B') whereas the bar graph of the climbing assay is plotted in Fig. 5.1B. KD of each gene is expected to reduce the overall flux of ceramides produced by the ER, with the extent of the reduction determined by the KD efficiency and the gene's individual role. The data (Fig. 5.1B, B') suggest that the absence of ceramides in the glia leads to an age-dependent decline in motor function, with *schlank* emerging as the prominent player in the glia where its KD displayed the most substantial loss of climbing ability, followed by *ifc, lace, Kdsr and spt-I.*

**Table 5.1: Genes of the *Drosophila* Ceramide pathway screened for adult motor function.**

| Gene (Flybase Computed Gene #) | Gene name/Enzyme name | Function | References |
|---|---|---|---|
| *spt-I/CG4016* | Serine palmitoyltransferase subunit-I, serine C-palmitoyltransferase | Sphingolipid biosynthetic process | (Ghosh et al., 2013) (Oswald et al., 2015) (Goyal et al., 2019) |
| *lace/CG4162* | Lace, serine C-palmitoyltransferase | Sphingolipid biosynthetic process | (Ghosh et al., 2013) (Goyal et al., 2019) (Theisen et al., 2025) |
| *Kdsr/CG10425* | 3-ketodihydrosphingosine reductase, 3-dehydrosphinganine reductase | Sphingolipid biosynthetic process | (Pan et al., 2023) |
| *schlank/CG3576* | Schlank, Sphingosine N-acyltransferase | Ceramide synthesis and TAG metabolism | (Bauer et al., 2009) |
| *ifc/CG9078* | Infertile crescent, sphingolipid 4-desaturase | Sphingolipid biosynthetic process, negative regulation of lipophagy | (Zhu et al., 2025) |




| | Days ⇒ RNAi⇓ | 5 | 10 | 15 | 20 | 25 | 30 |
|---|---|---|---|---|---|---|---|
| 1 | *spt1* | | | | | | * |
| 2 | *lace* | | | | ** | ** | *** |
| 3 | *Kdsr* | | | | ** | * | |
| 4 | *schlank* | | ** | *** | *** | *** | *** |
| 5 | *ifc* | | | *** | *** | *** | *** |

| | Days ⇒ RNAi⇓ | 5 | 10 | 15 | 20 | 25 | 30 |
|---|---|---|---|---|---|---|---|
| 1 | *spt1* | | | | | | |
| 2 | *lace* | *** | *** | *** | *** | *** | *** |
| 3 | *Kdsr* | | | | | | ** |
| 4 | *schlank* | | | | | | |
| 5 | *ifc* | | | | | *** | *** |

**Figure 5.1: Motor assay screen for enzymes involved in *de novo* ceramide synthesis.**

(A) Schematic diagram of *de-novo* ceramide synthesis pathway at the ER membrane. *H. sapiens* genes are marked in blue and *D. melanogaster* genes in red.

(B) Climbing Index after KD of Glial ceramide synthesis genes in *Drosophila* males, plotted in the form of bar graphs. X-axis represents days post-eclosion (B') Summary table for climbing assay for male flies with statistical significance shown at each day interval (5, 10, 15, 20, 25, 30) compared to the control.

(C) Climbing Index after KD of Neuronal ceramide synthesis genes in *Drosophila* males, plotted in the form of bar graphs. (C') Summary table for the climbing assay for male flies with statistical significance shown at each day interval (5, 10, 15, 20, 25, 30). n=25-30 males, N=3 biological replicates per genotype. P<0.001(***), <0.001(**) and <0.05(*). Blank spaces in the tables indicate statistical non-significance (ns).

As a counterpoint, we also tested KD of the same set of genes in neurons, using *elav-Gal4* as the driver. *lace* KD in neurons affected motor function the most, as the climbing ability was significantly reduced on day 5 itself, with *ifc* affecting climbing day 25 onwards (Fig. 5.1C, C'). Intriguingly, *schlank* KD did not affect climbing ability (Fig. 5.1C). This suggests that the regulation of ceramide dynamics in glia differs from that in neurons. Although these genes have been shown to play differential roles in neurodevelopment (Table 5.1), this is the first study in the sphingolipid field to report tissue-specific differential roles of ceramides in age-dependent motor function.

**5.3.2 LD homeostasis in Glia is sensitive to ceramide levels:** We measured the status of LDs in 5-day adult brains after glial KD of the set of genes (Table 5.1) involved in ceramide synthesis. We find (Fig. 5.2A-F) that average LD density decreases on KD of ceramide pathway genes, with *schlank* KD showing the most substantial decrease, followed by *ifc* and *spt-I*. Additionally, *lace* and *Kdsr* KD also showed a slight decline in LD density as well. The data are displayed as bar graphs in Fig 5.2G & H. Fig. 5.2G quantifies LD density (number of LDs per $\mu m^3$) while Fig. 5.2H shows variation in LD size (Individual LD volume in $\mu m^3$) with KD for all genes leading to a reduction in average LD size and the disappearance of larger LDs, except for the case of *ifc* KD.

Thus, a decrease in ceramide synthesis in the ER leads to fewer and smaller LDs, and this broadly correlates with age-dependent loss of motor function, with *schlank* KD having the most substantial effect on both LD formation and age-dependent decrease of motor function.

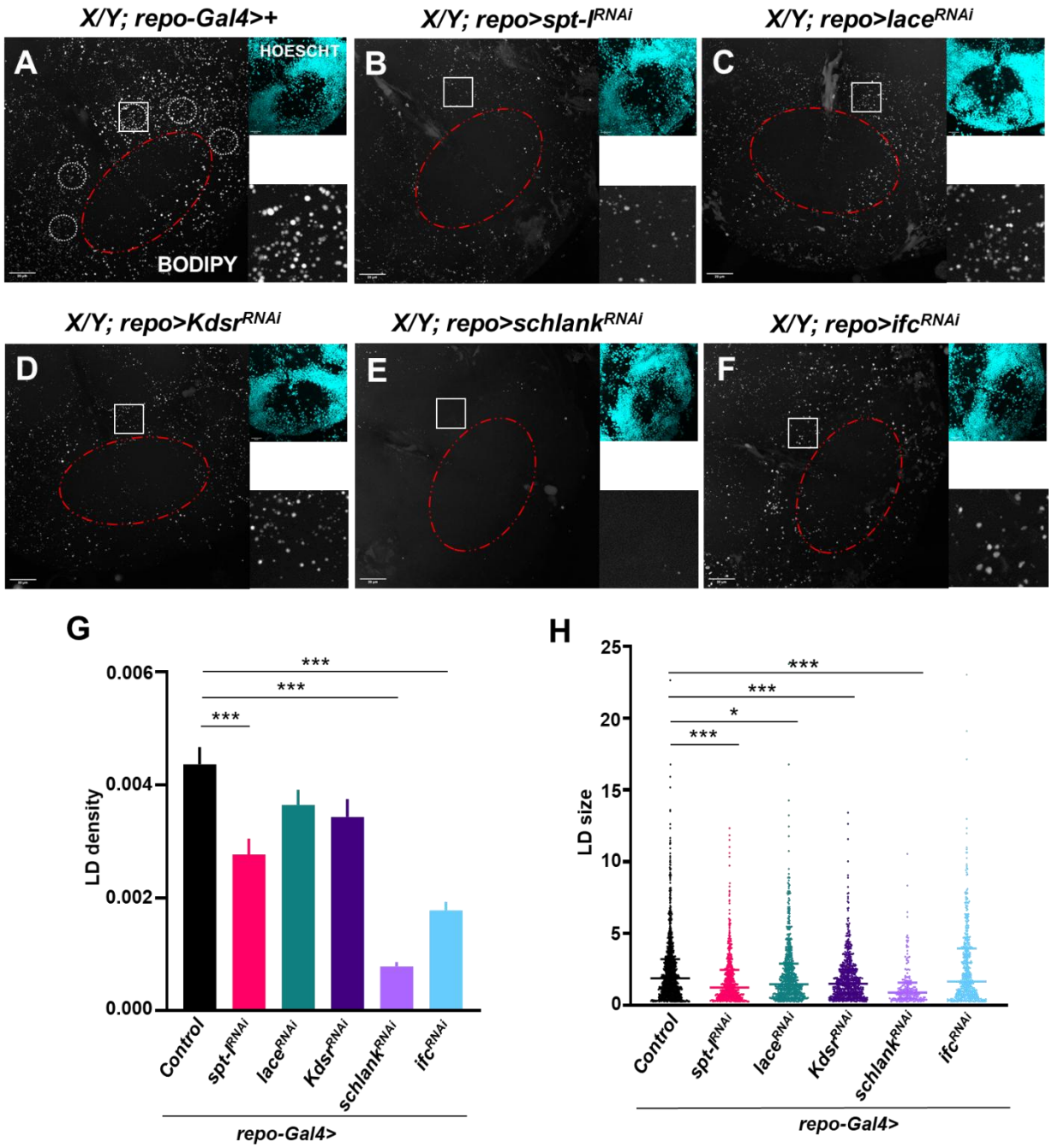



**Figure 5.2: Effect of glial ceramide pathway gene KD on LD distribution in the *Drosophila* adult brain.**

(A-F) represents MIP projections (20% brightness, zoom 1X) of BODIPY-stained LDs in the SEZ (Subesophageal zone) of 5-day-old male adult brains. Glial KD of *de novo* ceramide synthesis pathway genes (B) *spt-I*, (C) *lace*, (D) *Kdsr*, (E) *schlank*, (F) *ifc* showed differential effect on LDs, with *schlank* KD showing the strongest decrease compared to control (A). Nuclei staining of the

adult brain is shown at the right top corner of the LD images. Zoomed image of the inset is shown at the right bottom corner of the individual images. Scale bar length is 20µm.
(G) and (H) Quantitative analysis for LD density and LD size were performed using five ROIs at the periphery of the SEZ region, marked as a red outline in (A). All genes showed a reduction in LD density with *spt-I, schlank,* and *ifc* KD being statistically significant, whereas, in terms of LD size, all genes showed a significant reduction, except for *ifc.*
LD density (number of LDs per $\mu m^3$) are plotted as Mean±SEM in the bar graph with statistical significance. For LD size ($\mu m^3$), scattered dot plot with all the lipid droplets from five ROIs of all brain samples from each genotype is represented with median and interquartile range. *p* value is shown as <0.001(***), <0.05(*). n=5 ROIs per brain, N=5-6 adult brains per genotype.

**5.3.3 Lack of Ceramide Transfer leads to age-dependent motor dysfunction:** In the previous section, we have established that the role of ceramide synthesis in the glia is essential for motor function as well as LD homeostasis. We were interested in whether ceramide transfer from the ER, by CERT, post synthesis, also affects these functions. A schematic of CERT function (Fig. 5.3A) and its domain structure (Fig. 5.3B) highlights its location in the MCS and its interaction with the ER-based MCS architecture protein VAPB (Kumagai & Hanada, 2019; Mishra et al., 2024; Perry & Ridgway, 2006; Slee & Levine, 2019). The Acharya lab generated a CERT null line, $dCERT^1$ (Rao et al., 2007) and were the first to demonstrate that these mutants had reduced lifespan, metabolic dysfunction, reduced thermal tolerance, and locomotor defects (Rao et al., 2007). (Gehin et al., 2023) also reported loss of motor activity because of lack of *CERT* function in flies. Here, we first reproduced the $dCERT^1$ (called $CERT^{\Delta}$ henceforth) motor phenotype, confirming that $CERT^{\Delta}$ homozygotes cannot climb efficiently in 'startle-induced negative geotaxis assays', showing a reduced climbing index on day 5, with further decline with age. At day 25, $CERT^{\Delta}$ animals could not climb. The *CERT* allele was haplosufficient for climbing ability, with $CERT^{\Delta}$/+ animals showing no reduction in climbing ability over 25 days of ageing. $CERT^{\Delta}$/Df animals had a stronger climbing phenotype and shorter lifespan, dying by day 15 (Fig. 5.3C).

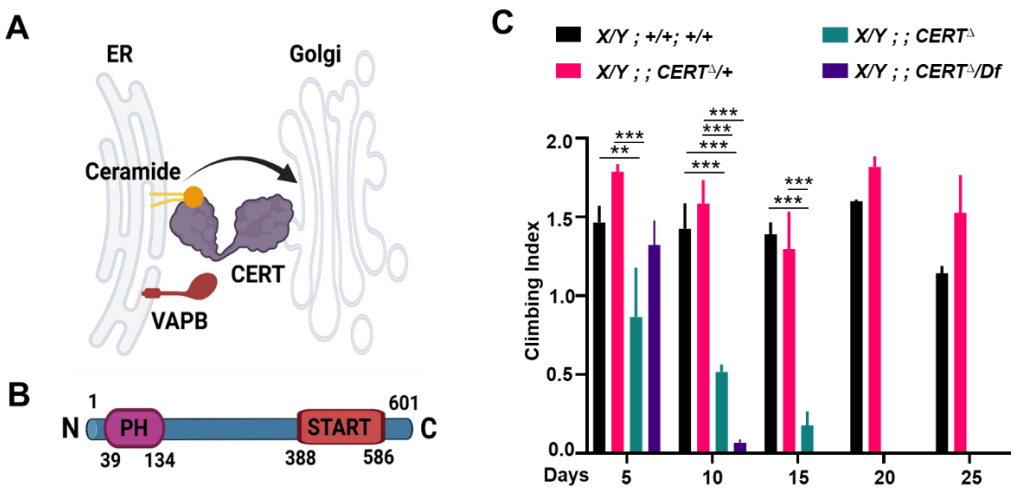



**Figure 5.3: *CERT* loss in *Drosophila* has age dependent motor dysfunction.**

(A) Schematic representation of ceramide transfer from ER to *trans*-Golgi mediated by CERT with the help of ER resident VAPB.

(B) Domain architecture of *Drosophila* CERT.

(C) Homozygous *CERT* null mutant (*CERT*$^{\Delta}$) exhibit significant motor defects at day 5 itself, which worsen with age. However, the heterozygous mutant climbs at par with wild-type flies. *CERT*$^{\Delta}$/Df showed progressive motor impairment and completely stopped climbing after day 10. Mean±SEM values are plotted in the graph representing climbing index on Y- axis with number of days on X-axis with statistical significance as p<0.001(***). n=25-30 males, N=3 replicates per genotype.

**5.3.4 Lack of Ceramide Transfer perturbs LD homeostasis:** The *CERT*$^{\Delta}$ line showed an age-dependent loss of motor function (Fig. 5.3C), with 30% climbing ability lost on Day 5 post eclosion (Fig. 3C, Green Bar). We were interested in whether ceramide transfer can also affect LD dynamics. On probing LDs for *CERT*$^{\Delta}$ mutant brain samples at day 5, we found wild-type LD density was 0.0032/µm$^3$ and for *CERT*$^{\Delta}$/+, 0.0037/µm$^3$, indicating that *CERT* is haplo-sufficient in terms of LD density (Fig. 5.4A-D). Interestingly, LD density dropped by 40% to 0.002/µm$^3$ on day 5 in *CERT*$^{\Delta}$ adult brains (Fig. 5.4E). *CERT*$^{\Delta}$*/Df* showed a 60% decrease in LD density to 0.001/µm$^3$ (Fig. 5.4E), validating the reduction in overall LD density in the absence of CERT. Both *CERT*$^{\Delta}$ and *CERT*$^{\Delta}$*/Df* showed a reduced average LD size, with *CERT*$^{\Delta}$*/Df* having the lowest median LD size in this experimental set. Intriguingly, *CERT*$^{\Delta}$ and *CERT*$^{\Delta}$/+ had similar average LD size, suggesting that LD size determination requires a full CERT allelic dose (Fig. 5.4F).

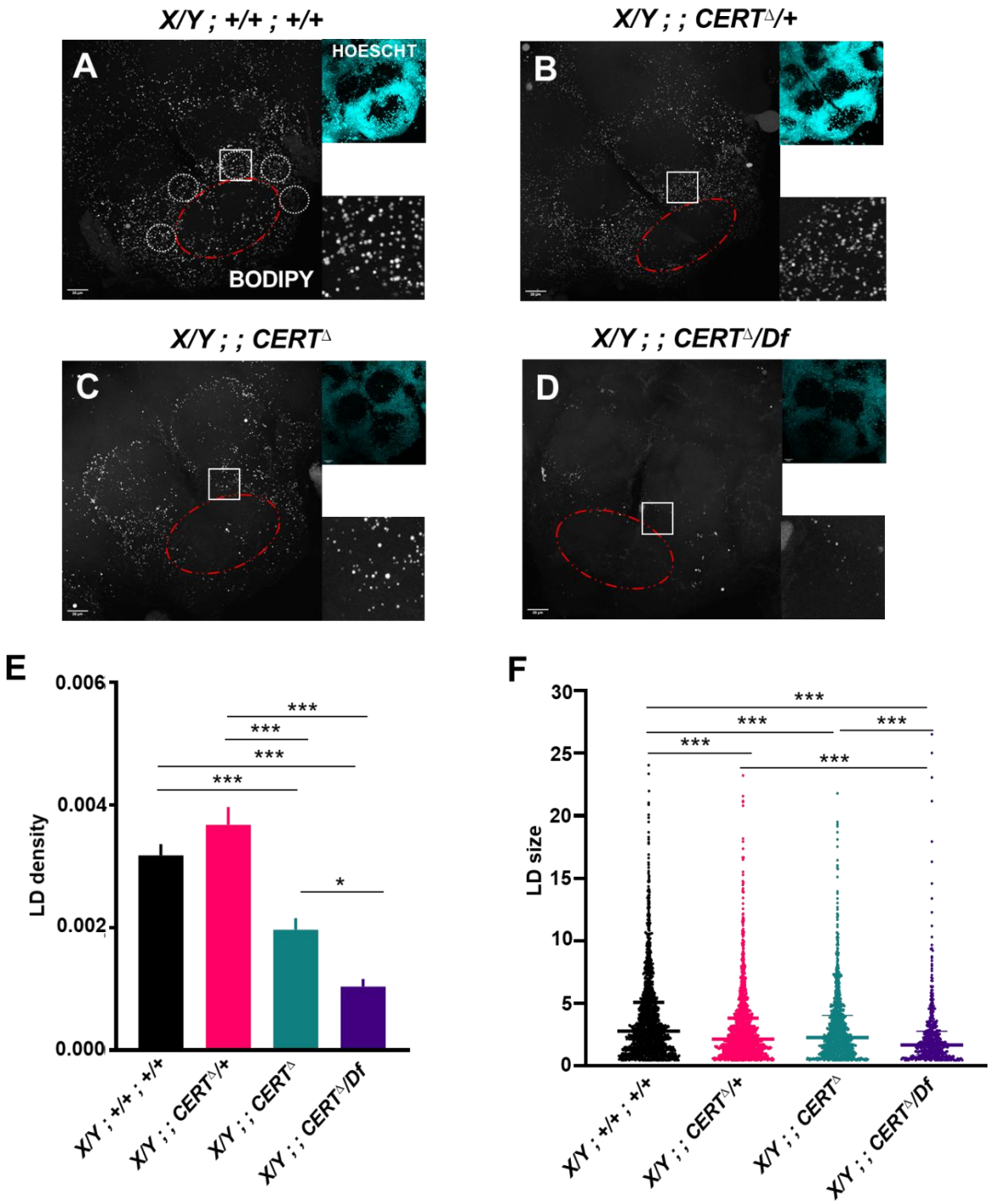



**Figure 5.4: *CERT* loss in *Drosophila* perturbs LD homeostasis in the adult brain.**

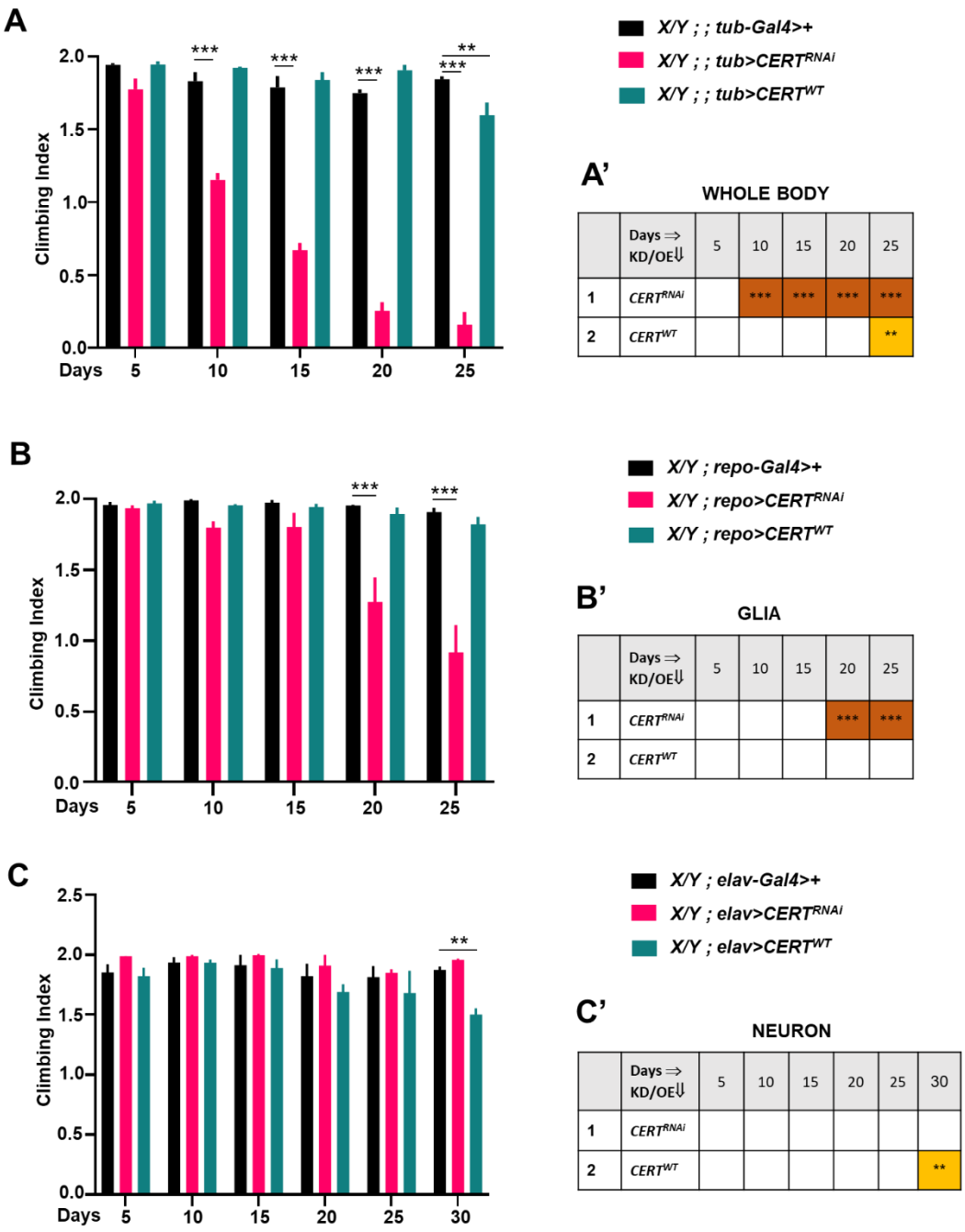
(A-D) shows representative MIPs (20% brightness) of BODIPY-stained LDs in 5-day-old male adult brains. *CERT*$^{\Delta}$ (C) and *CERT*$^{\Delta}$*/Df* (D) have fewer LDs compared to wildtype (A) and *CERT*$^{\Delta}$/+ (B). Nuclei staining of the adult brain is shown at the right top corner of the LD images. Zoomed image of the inset is shown at the right bottom corner of the individual images. Scale bar length is 20µm.

(E) and (F) shows quantitative analysis of LDs with LD density and LD size as parameters analyzed using five ROIs around SEZ region (depicted with red outline in panel D). For LD density (number of LDs per $\mu m^3$), Mean±SEM values are plotted in the graph with p<0.001(***), <0.01(**), <0.05(*). For LD size ($\mu m^3$), scattered dot plot with all the lipid droplets from five ROIs is represented with median and interquartile range and p<0.001(***), <0.01(**), <0.05(*). n=5 ROIs for each brain, N=5 adult brains of each genotype.

**5.3.5 Lack of glial *CERT* leads to age-dependent motor defects in *Drosophila:*** Earlier (Fig. 5.1) we uncovered a correlation between glial ceramide production and motor function. CERT null animals (Fig. 5.3) also showed age-dependent loss of climbing ability. To dissect tissue-specific roles for CERT, we both OE and KD *CERT* via RNAi using a set of tissue-specific drivers and subsequently evaluated climbing ability in the adult F1 fly over 25-30 days post-eclosion. First, we used a ubiquitous driver, *tubulin-Gal4* (*tub-Gal4*), to modulate *CERT* and assessed fly motor activity. The ubiquitous *CERT* KD (Fig. 5.5A, A') recapitulated, though to a lesser extent, the whole-body loss-of-function (Fig. 5.3C), confirming that loss of *CERT* led to age-dependent motor deterioration. *CERT* OE did not lead to climbing defects, with a mild decrease in climbing index seen on day 25.

Next, in order to test the tissue-specificity of CERT function, we OE and KD *CERT* in both glia (*repo-Gal4*) and neurons (*elav-Gal4*) (Fig. 5.5). Interestingly, glial KD led to a loss of climbing ability from day 20 onward, whereas neuronal knockdown did not. OE of *CERT* did not show any climbing defects over age, with a mild reduction in the climbing index for neuronal OE on day 30 (Fig. 5.5B-C).

Our data suggests that the transfer of glial ceramide by CERT from the ER is important for the animal to maintain its motor function, viz its climbing ability, with the neuronal role being less important, vis-à-vis motor function. We also used an alternative neuronal driver *nSyb-Gal4* to KD *CERT* in neurons (Fig. 5.6A, A'). Here, again, we see that climbing ability is normal till day 20 and *CERT-KD* and OE flies start showing major motor defects after day 25 onwards. Interestingly, male flies OE $CERT^{EAAD}$ in both neurons and glia (Fig.5.6 A-B) did not show any climbing defects, although flies were sluggish in the case of glia OE.




| | Days ⇒ KD/OE⇓ | 5 | 10 | 15 | 20 | 25 |
|---|---|---|---|---|---|---|
| 1 | $CERT^{RNAi}$ | | *** | *** | *** | *** |
| 2 | $CERT^{WT}$ | | | | | ** |

| | Days ⇒ KD/OE⇓ | 5 | 10 | 15 | 20 | 25 |
|---|---|---|---|---|---|---|
| 1 | $CERT^{RNAi}$ | | | | *** | *** |
| 2 | $CERT^{WT}$ | | | | | |

| | Days ⇒ KD/OE⇓ | 5 | 10 | 15 | 20 | 25 | 30 |
|---|---|---|---|---|---|---|---|
| 1 | $CERT^{RNAi}$ | | | | | | |
| 2 | $CERT^{WT}$ | | | | | | ** |

**Figure 5.5: Tissue-specific *CERT* role in motor function.**

(A) Climbing Index is plotted for whole body modulation of *CERT* using *tub-Gal4* in male flies with statistical significance. *CERT KD* showed progressive motor defects with age, whereas OE caused mild defects observed at day 25. (A') Summary table for statistical significance for each day interval (5, 10, 15, 20, 25) compared to control.

(B) Climbing Index is plotted for glial modulation of *CERT* using *repo-Gal4* in male flies with statistical significance. Glial KD of *CERT* in *Drosophila* led to motor defects by day 20 and kept on worsening with age, whereas *CERT* OE did not cause any detectable motor impairment. (B') Summary table for statistical significance for each day interval (5, 10, 15, 20, 25) compared to the control.
(C) Climbing Index is plotted for neuronal modulation of *CERT* using *elav-Gal4* in male flies with statistical significance. Neuronal KD of *CERT* showed no defect in motor activity whereas overexpressing *CERT* led to mild motor defects on day 25. (C') Summary table for statistical significance for each day interval (5, 10, 15, 20, 25, 30) compared to control.
Mean±SEM values are plotted in the graph. p<0.001(***), <0.01(**). n=25-30 males, N=3 replicates per genotype.

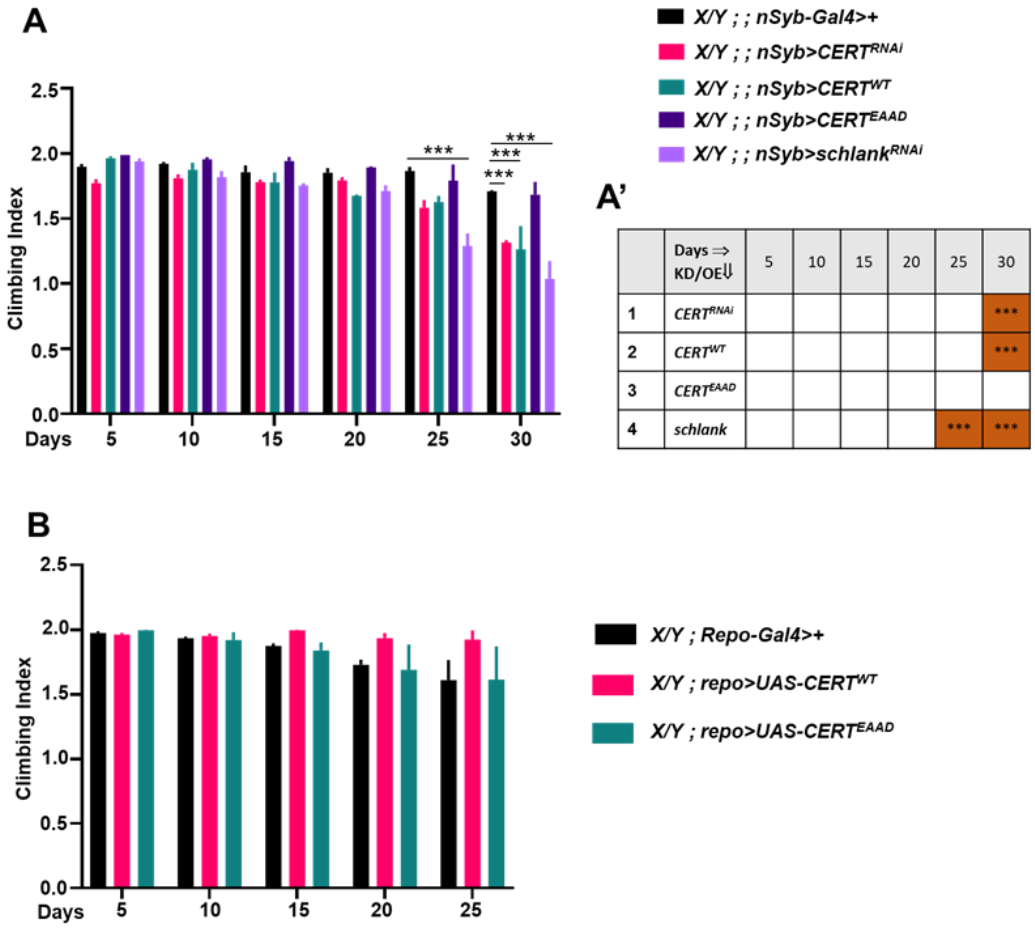



**Figure 5.6: *CERT*$^{EAAD}$ OE in neurons and glia does not affect motor function of *Drosophila.***

(A) *CERT* KD and OE using *nSyb-Gal4* showed motor defects after day 25 onwards however, *CERT*$^{EAAD}$ in neurons did not show defects at all. Also, pan-neuronal *schlank* knockdown led to

motor defects at day 25 only. (A') Summary table of the genes modulation with statistical significance shown for each day compared to control.
(B) OE of $CERT^{EAAD}$ in glia showed no change in motor activity of male flies.
Mean±SEM values are plotted in the graph with $p<0.001$(***), climbing Index is represented on Y-axis with number of days after eclosion on X-axis. n=25-30 males, N=3 biological replicates for each genotype.

**5.3.6 Lack of glial Ceramide Transfer leads to LD defects in the adult brain:** Since ceramide transfer by glial CERT is important for motor function, does *CERT* KD also affect LD dynamics? *CERT* KD in glia (Fig. 5.7A-C, F-G) led to a ~60% reduction in LD density. The drop was stronger when a more efficient Valium 20 RNAi line was used rather than the maternal Valium22 RNAi line (Mishra et al., 2024). The reduction in LD density was of the same order as seen in *schlank* (80%) and *ifc* (50%) KDs (Fig. 5.2) as well as $CERT^{\Delta}/Df$ (Fig. 5.3H). *CERT* KD also led to a change in distribution of LD size, with larger LDs not observed, much like in the case of *schlank* KD and $CERT^{\Delta}/Df$ (Fig. 5.2H, Fig 5.3I).

Excess *CERT* did not appear to affect LD dynamics, with both LD density and size in the brain similar to wild-type (Fig. 5.7D, F& G.) Intriguingly, glial OE of the $CERT^{EAAD}$ line led to a significant reduction in LD density but no change in LD size (Fig. 5.7E-G). This suggests that an excess of CERT that does not bind VAPB efficiently can perturb LD density, but not LD size.

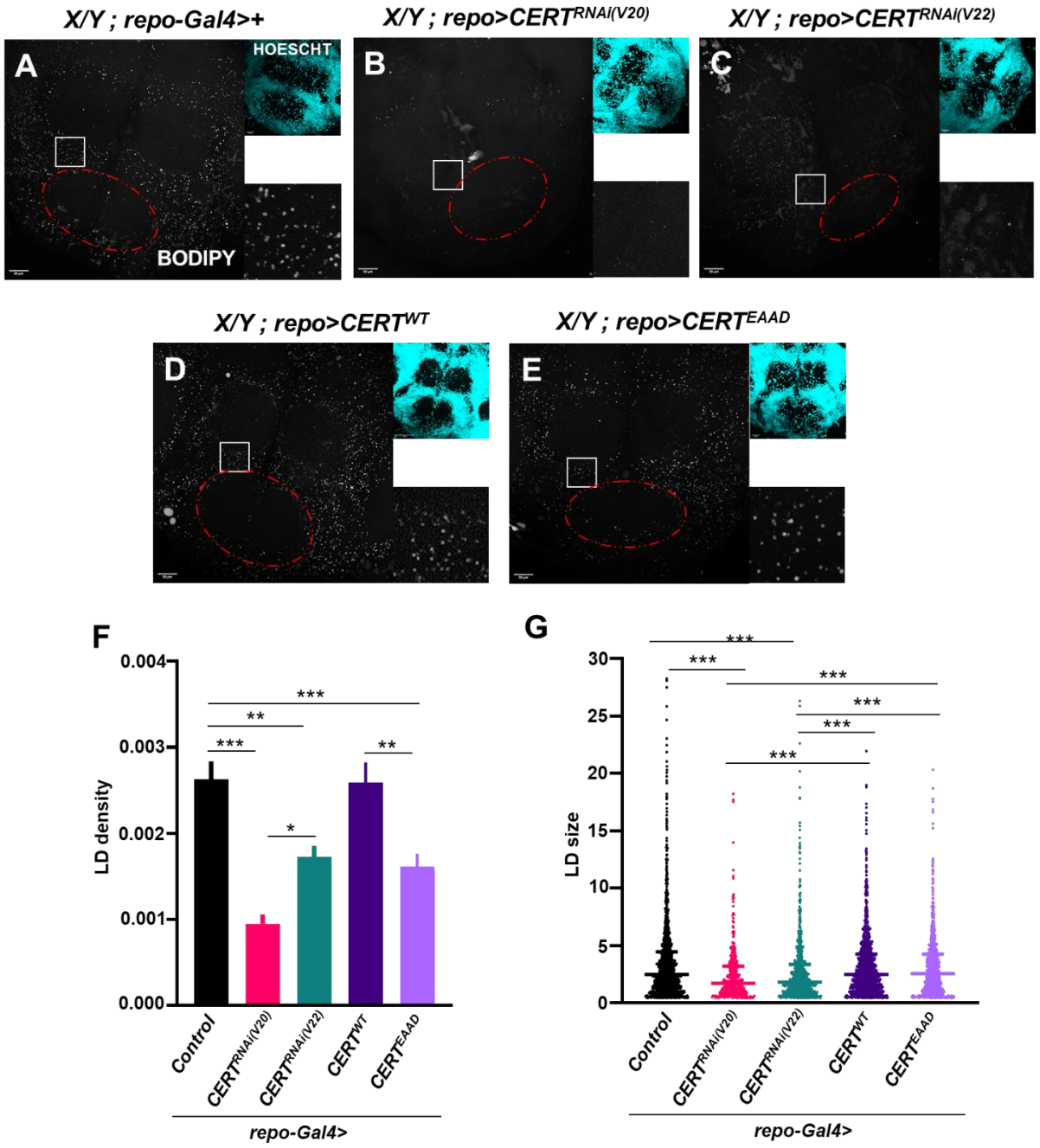



**Figure 5.7: Glial *CERT* affects LD dynamics in the *Drosophila* adult brain.**

(A-E) Representative MIPs (20% brightness) of LDs stained with BODIPY in 5-day-old male adult brains. *CERT* KD in glia using Valium 20 (B) and Valium 22 (C) RNAi lines led to fewer LDs with a smaller size compared to control (A). However, $CERT^{WT}$ OE (D) showed no change at all compared to the control. (E) $CERT^{EAAD}$ OE shows a significant reduction in LDs but no change in size. Nuclei staining of the adult brain is shown at the right top corner of the LD images. Zoomed image of the inset is shown at the right bottom corner of the individual images. Scale bar length is 20µm.

(F) and (G) Quantitative analysis of LDs with LD density and LD size as parameters analyzed using five ROIs around SEZ region (depicted with red outline in panel A).
Mean±SEM values are plotted for LD density (number of LDs per $\mu m^3$) in the graph. For LD size ($\mu m^3$), scattered dot plot with all the individual lipid droplets from five ROIs of all brain samples is represented with median and interquartile range. Statistical significance is shown as $p<0.001$(***), $<0.01$(**), $<0.05$(*). n=5 ROIs per adult brain, N=5 brains for each genotype.

**5.3.7 Motor function can be rescued by transgenic glial CERT:** (GEHIN ET AL., 2023) generated transgenic $CERT^{WT}$ and $CERT^{SL}$ lines expressed under genomic promotors referred as $gCERT^{WT}$ and $gCERT^{SL}$. $gCERT^{SL}$ corresponds to expression of *CERT* with Ser to Leu mutation at 149$^{th}$ position (132$^{th}$ position in humans). $gCERT^{SL}$ is a hyperactive allele which shows CerTra syndrome-like phenotypes in flies. Briefly, *CERT* gain of function led to the production of more ceramides, dihydroceramide, CPE, as well as di-CPE in the heads of the flies (GEHIN ET AL., 2023). Interestingly, both genotypes do not show any climbing defects under normal conditions but have climbing defects under mechanical stress. We find that the climbing index is substantially improved when we balance either $gCERT^{WT}$ and $gCERT^{SL}$ with $CERT^{\Delta}$ (Fig. 5.8A). The rescue improves the climbing index two-fold when compared to $CERT^{\Delta}$, up to day 20, but does not achieve the climbing index of wild-type flies. Intriguingly, glial OE of $CERT^{WT}$ (Fig. 5.8B) shows a more substantial rescue of motor function, with the climbing index being at par with wild-type flies on days 5 and 10, and a 3-fold improvement in climbing index in older flies (days 15, 20 and 25). OE of $CERT^{EAAD}$ also rescues motor function in an age-dependent manner, with the rescue at par with wild-type $CERT^{WT}$ (Fig. 5.8B) for days 5, 10 and 15, with a slight fall in average climbing index on days 20 and 25.

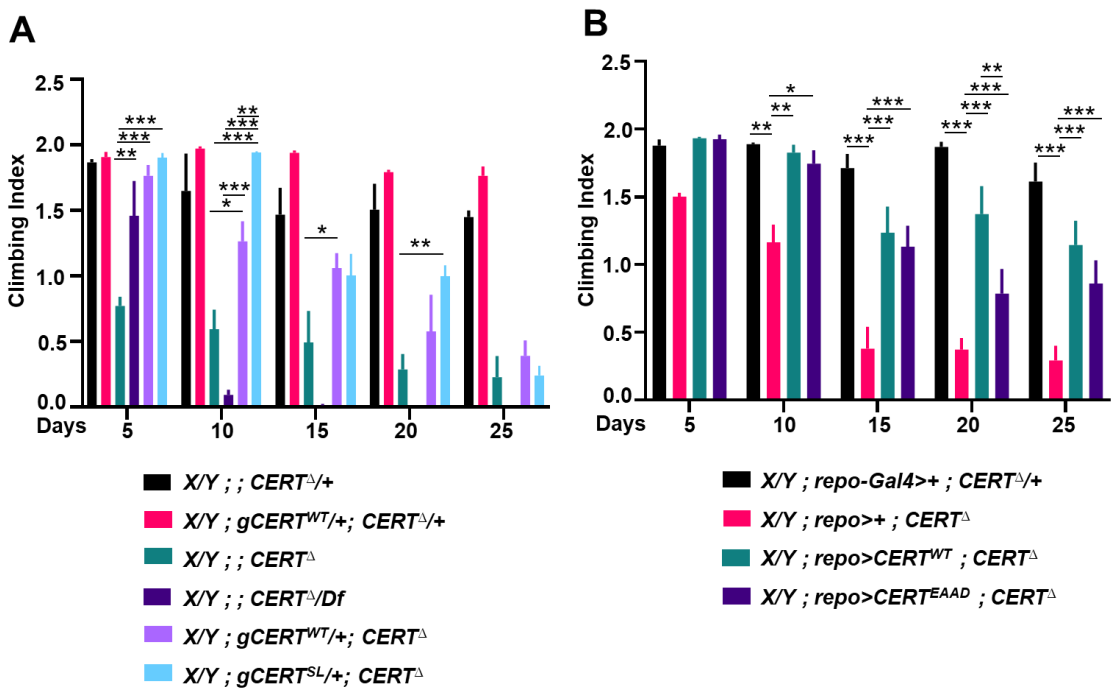



**Figure 5.8: Glial expression of *CERT* rescues motor dysfunction in *CERT*$^{\Delta}$.**

(A) Introducing a genomic copy of *CERT*$^{WT}$ in *CERT*$^{\Delta}$ resulted in partial rescue of motor activity, and it behaved completely normally in a heterozygous *CERT*$^{\Delta}$ mutant. Adding a genomic copy of the hyperactive allele *CERT*$^{SL}$ in the *CERT*$^{\Delta}$ background showed stronger rescue than *CERT*$^{WT}$.
(B) Glia-specific expression of *CERT*$^{WT}$ in the background of *CERT*$^{\Delta}$ rescued motor defects significantly, as well as *CERT*$^{EAAD}$.
Mean±SEM values of climbing index are plotted in the graph with p<0.001(***) <0.01(**), <0.05(*). n=25-30 males, N=3 biological replicates per genotype.

**5.3.8 LD dynamics can be rescued by glial expression of CERT.** Both ceramide synthesis and transfer appear to be important in the glia for motor function. Next, we expressed *CERT*$^{WT}$ in the glia of 5-day-old *CERT*$^{\Delta}$ animals (Fig.5.9C) to examine if glial expression of *CERT*$^{WT}$ could rescue LD dynamics. Intriguingly, LD density was completely rescued in the presence of excess glial CERT (Fig. 5.9F), however, the *CERT*$^{EAAD}$ was not as efficient in rescuing in the *repo* domain, with its overexpression not rescuing either LD density or size significantly (Fig. 5.9E-G).

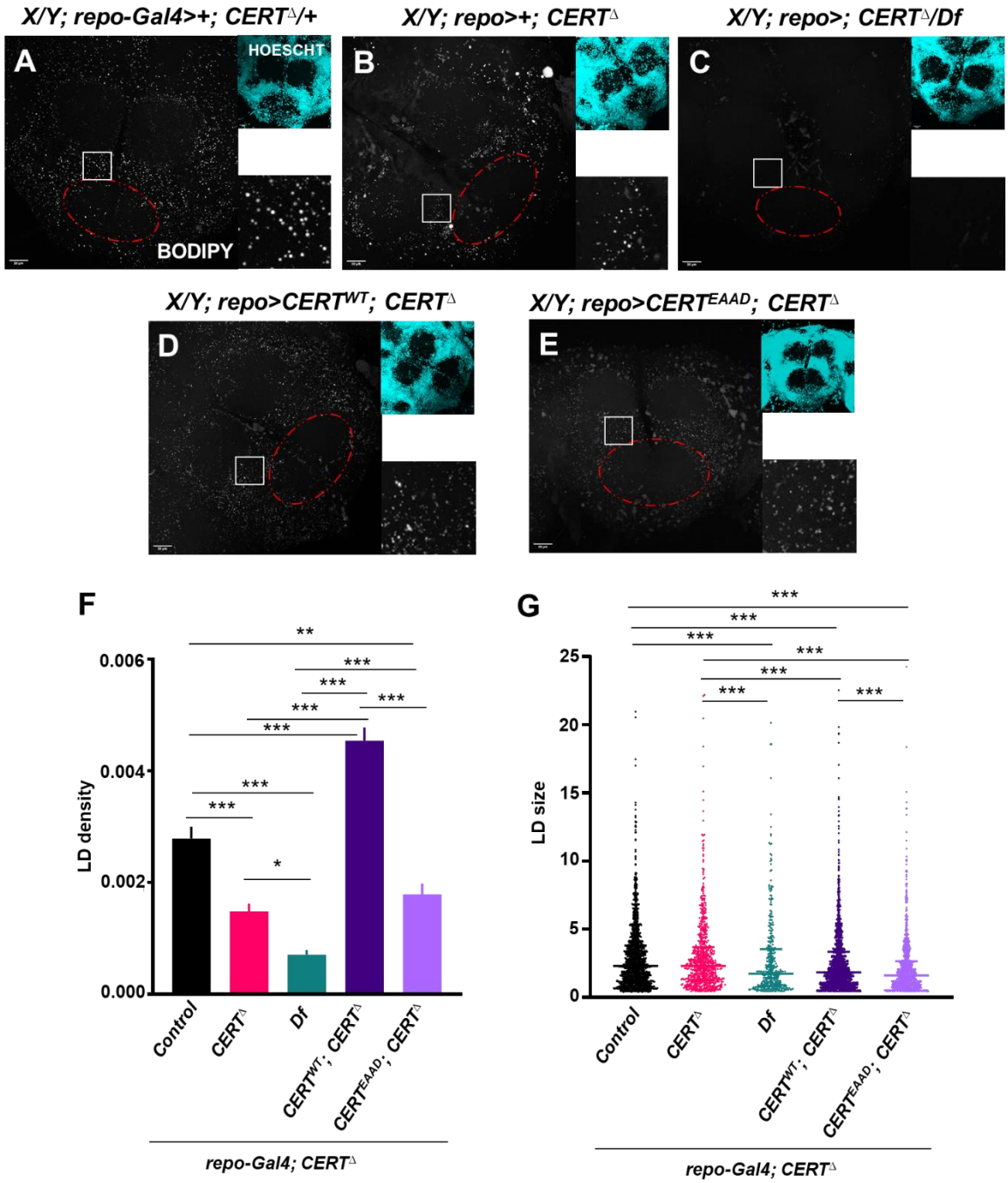



**Figure 5.9: Glial expression of *CERT* rescues LD defects seen in *CERT*$^{\Delta}$.**

(A-E) represents MIP projections (20% brightness) of BODIPY stained LDs in the brain of 5 day old males. *CERT*$^{WT}$ OE (D) in glia of *CERT*$^{\Delta}$ showed rescue with more LDs compared to (B) and (C) although LDs were smaller in size. However, *CERT*$^{EAAD}$ OE leads to fewer and smaller LDs compared to (A) but more LDs compared to (C) with no change in size. Nuclei staining of the adult brain is shown at the right top corner of the LD images. Zoomed image of the inset is shown at the right bottom corner of the individual images. Scale bar length is 20µm.

(F-G) Quantitative analysis of LD density (number of LDs per $\mu m^3$) and LD size ($\mu m^3$) were performed on five ROIs surrounding SEZ region. For LD density, data is represented as Mean±SEM in the graph with statistical significance as $p<0.001$(***). LD size is shown as scattered dot plot with all the lipid droplets from five ROIs of all brain samples of each genotype $p<0.001$(***). n= 5 ROIs, N=5 adult brains per genotype.

**5.3.9: Glial ceramide in *Drosophila* development regulates adult motor function:** We have so found so far that *schlank, ifc* and *CERT* shows LD defects as early as day 5 itself. We wanted to see if there is any development role of these genes which is leading to motor defects in the flies as other studies also suggest *schlank* and *ifc* play active role in the development. So, we knocked down *CERT, schlank* and *ifc* at the adult stage only, basically, $Gal80^{ts}$ was introduced into the system so that it can inhibit Gal4 activity during the development phase by keeping the eggs at 18℃ and shift them to 29℃ after the flies have eclosed. We did not detect any motor defects for all three genes even at 20 days which was quite interesting as *schlank* gives early phenotypes by day 10 only (Fig. 5.10A). Similarly, we performed second experiment where flies were kept at 25℃ after eclosion so that *Gal80* works at the adult stage also. This was a control experiment to see if *Gal80* was working at 25℃ as well (Fig. 5.10B).

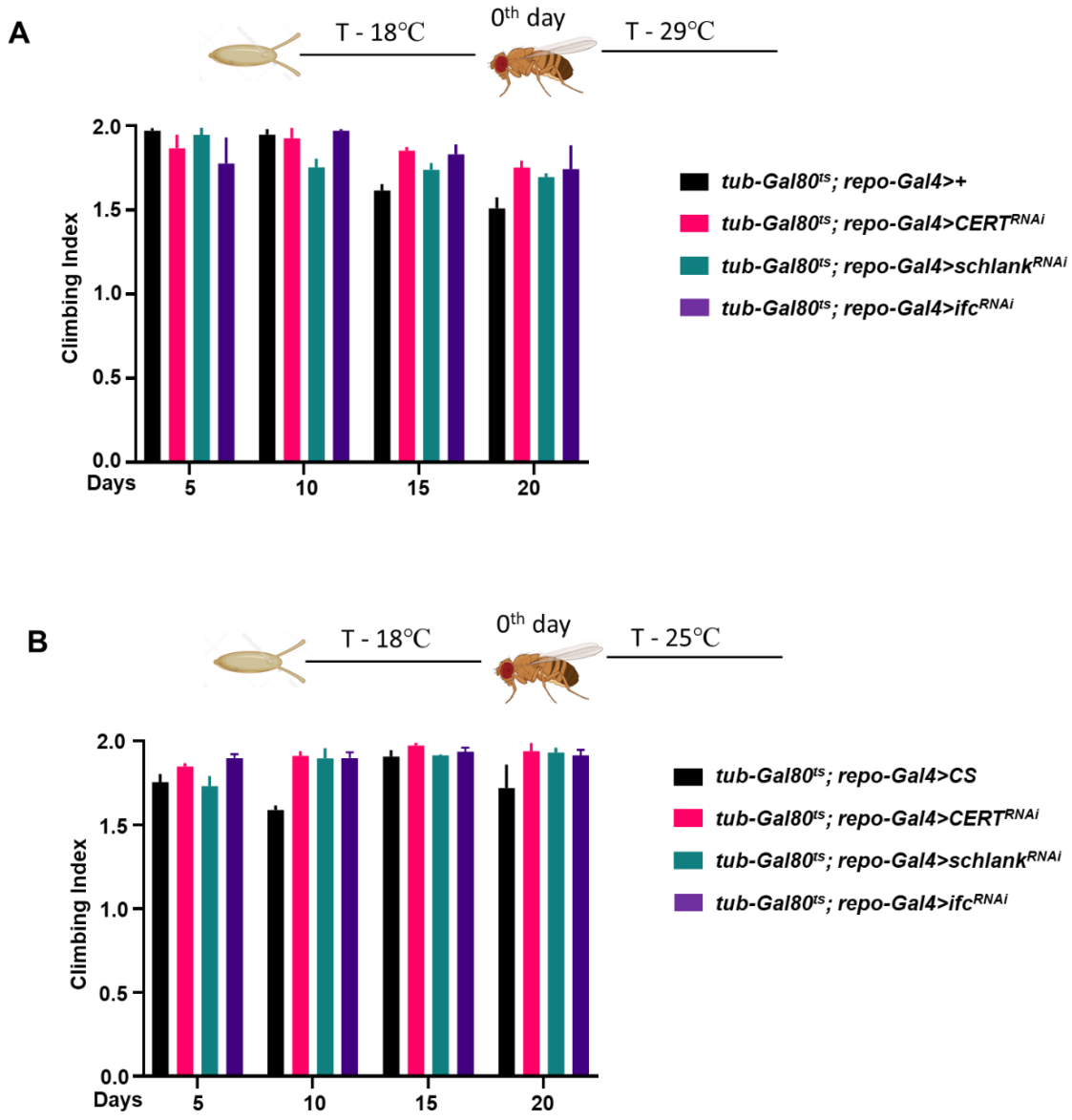



**Figure 5.10: Developmental role of glial ceramide in regulation of motor activity of *Drosophila*.**
(A) panel shows climbing activity of male flies when *CERT*, *schlank* and *ifc* were knocked down in the glial cells at the adult stage and kept the flies at 29℃ to activate the Gal4 expression. No change was found in the climbing index of tested genes compared to control.
(B) Climbing Index of the male flies when same genes were knocked down at the adult stage and kept the flies at 25℃ to inhibit Gal4 expression. No change was found in the motor activity of the flies.
n=25-30 males, N=3. Mean±SEM values are plotted in the graph with p values represented as ***(<0.001), climbing Index is represented on Y-axis with number of days after eclosion on X-axis. Motor assays were performed at 25℃.

## 5.4 Discussion

**5.4.1 Lipid homeostasis in Motor neuron disorders:** Motor function in animals is regulated by the neuromuscular system. The brain plans, initiates and coordinates voluntary movements using specific neuronal circuits with motor neurons carrying signals to the muscles that execute the action. Feedback systems fine-tune motor actions. Motor function is affected when neurons, their glial partners, or muscle cells lose their ability to perform a function. Loss of motor function is seen in motor neuron diseases, which are often progressive (Gunay et al., 2021; Ilieva et al., 2009; Rachakonda et al., 2004; Tendulkar et al., 2022). Increasingly, MNDs are linked to changes in lipid homeostasis, with lipid dynamics significantly altered in disease; phospholipids, ceramides, and cholesterol show major alterations and serve as biomarkers of disease progression (Agrawal et al., 2022; Byrns et al., 2024; Cutler et al., 2002; Henriques et al., 2017; Hussain et al., 2019; Liu et al., 2020; McCluskey et al., 2022; Oswald et al., 2015; Pan et al., 2023; Pant et al., 2020; Schmitt et al., 2014; Tracey et al., 2021; Vos et al., 2021; Wanikawa et al., 2020; Yang et al., 2022). One major pathway that is altered in MNDs is the Ceramide pathway. An increase or decrease in ceramide species can lead to mitochondrial dysfunction, ER stress, and inflammation, and can result in neuronal or glial cell death. This makes the various enzymes in the ceramide pathway important therapeutic targets, as each enzyme works to convert one metabolite to another, maintaining levels across the ceramide/sphingolipid metabolic network (Agrawal et al., 2022; Cutler et al., 2002; Goyal et al., 2019; Hebbar et al., 2015; Henriques et al., 2017; Islam et al., 2025; Jung et al., 2017; McCluskey et al., 2022; Pan et al., 2023; Pant et al., 2019; Vos et al., 2021).

**5.4.2 Differential role of ceramides in neurons and glia:** Our work highlights several important features of motor neuron function and dysfunction. First, from our screen of ceramide pathway enzymes, it is clear that Neurons and Glia differ significantly in their ability to handle ceramide. This is supported by (McInnis et al., 2024), who report differential levels of ceramide species in neurons and glia, which may be linked to the animal's motor function. Glia appear to be more sensitive to sphingolipid levels, as alterations at multiple steps in the ceramide pathway lead to motor dysfunction in the adult flies. Interestingly, in our experiments, *schlank* KD in neurons, which would lead to the accumulation of dihydrosphinganine or reduction in dihydroceramides, did not have any effect on motor function. In contrast, reduction of dihydrosphinganine following neuronal knockdown of *lace* results in severe motor neuron dysfunction. Recently, it is shown that loss of

ceramide synthase leads to accumulation of sphinganines in neurons which affect dendritic arborization suggesting sphinganine levels has to keep in check in the neurons (Anna B. Ziegler 2025). Several studies report differential roles of *spt-I, lace, schlank* and *ifc* in neurodevelopment, with neuronal knockdown of *spt-I* and *lace* affecting mushroom body development, suggesting that sphinganine formation is essential for neuronal function (Goyal et al., 2019; Oswald et al., 2015). Recently, it has been shown that ceramide synthase is quite important in the developmental phase. Moreover, fatty acids accumulate in neurons in the absence of these enzymes, leading to oxidative stress (Liu et al., 2017; Tang et al., 2024). In the case of *schlank* and *ifc*, studies point to their developmental roles in glia (Chen et al., 2022; Ghosh et al., 2013; Islam et al., 2025; Theisen et al., 2025; Zhu et al., 2025) as the nervous system forms in the animal. We find that in the case of *ifc*, loss in both neurons and glia affects motor function, suggesting that dihydroceramide levels have a toxic impact on both cell types. Interestingly, glial loss of *ifc is* more potent than in neurons, as seen in our motor assay screen and recently reported by (Zhu et al., 2025).

**5.4.3 CERT function in the glia:** *CERT* KD in glia alone approaches, in terms of penetrance, the age-dependent motor dysfunction seen in whole-body KD or a CERT null animal. This suggests a more important role for CERT in glia than in neurons, especially in the context of adult motor function. Broadly, our data indicate that the generation of complex sphingolipids (CPE/SM, GSLs), which are biochemical steps downstream of ER-based ceramide production and transfer, is a critical requirement for motor function. The absence or reduction of these species perturbs the glial-neuronal metabolic equilibrium and disrupts the motor circuit. This hypothesis is supported by recent studies (Byrns et al., 2024; Chen et al., 2022; Islam et al., 2025; Liping Wang, 2022; Theisen et al., 2025; Vaughen et al., 2022; Zhu et al., 2025).

From figure 5.10, it becomes quite clear that CERT is playing a developmental role in the glial cells of the *Drosophila.* However, in chapter IV, neuronal knockdown of *CERT* in the *ALS8* flies throughout development did not show any rescue in the motor dysfunction. So, a possibility cannot be rule out that CERT may be playing an important role in the neurons as well during the larval brain development. Also, expression of CERT in the neurons and glia during the different life cycle stages of the flies can tell us more about its role in terms of its functioning. It is highly possible that ceramides are more sensitive in the glia compared to neurons because of which glial knockdown of *CERT* or *schlank* leads to motor impairment but not in the neurons.

**5.4.4 Ceramide connection to LD homeostasis:** Perturbing both ceramide production and their transfer affects LD dynamics. This finding is intriguing, as LD formation has no direct relationship with the ceramide synthesis pathway aside from the fact that both processes occur at the ER membrane (Bikman & Summers, 2011; Walther & Farese, 2012). Recently, LDs have been shown to contain acylceramides and small amounts of dihydroceramides (Robles-Martinez et al., 2025; Senkal et al., 2017). Consistent with this, ceramide production or its transfer from the ER results in smaller, less dense LDs. *A priori*, LD formation would depend on the availability of TAG, which in turn would depend on fatty acid availability and the normal functioning of TAG-generating enzymes, namely Glycerol-3-phosphate Acyltransferase (GPAT), 1-Acylglycerol-3-phosphate Acyltransferase (AGPAT), and Diacylglycerol Acyltransferase (DGAT), which are present on ER and mitochondrial membranes. The formation of CEs depends on Acyl CoA Cholesterol Acyltransferase, an ER protein which would again be affected by ER architecture (Henne et al., 2025; Smolic et al., 2021).

Thus, a drop in LD density or size may result from one or more of the following. (i) A lack of ceramide production, which affects ER structure and thus influences LD formation. Earlier studies have suggested that ceramide depletion leads to ER expansion and compromised plasma membrane integrity (Rao et al., 2014; Rao et al., 2007; Zhu et al., 2025). (ii) Increase in various ceramide intermediates within the ER, and subsequent diversion of the flux to other metabolic pathways (iii) Limited production of complex sphingolipids due to a reduction of ceramide either being produced or being transferred from the ER (iv) Lipolysis – a drop in lipid density and size could be a result of an upswing in LD utilization for membrane maintenance. One possible reason for the requirement for extra membranes would be Glial roles in phagocytosis and axonal ensheathment, which would be affected in the absence of sphingolipids (Ghosh et al., 2013; Kunduri et al., 2025; Theisen et al., 2025; Vaughen et al., 2022). (v) Acharya's paper shows that mitochondria is completely comprised in *CERT* loss of function mutant which is attributed to low ATP production, low glucose utilization and altered morphology. Also, ER-mitochondria contact sites are quite essential for lipid transfer. Ceramides are known to present near membrane associated mitochondria (MAM) contact sites. It is highly possible altered ceramides will affect these sites which can thus perturb lipid balance as well between ER-mitochondria. This imbalance of lipids can affect LD homeostasis as well.

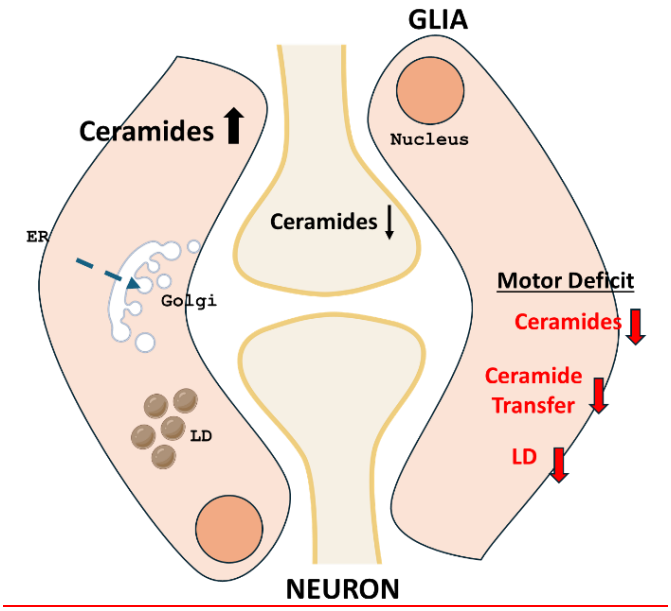



**Figure 5.11: Schematic model of ceramide and CERT roles in neurons and glia.**

Our current understanding of differential roles for the Ceramide pathway in glia *vs* neurons suggests that the flux of ceramide synthesis from the ER to the Golgi is higher in glial cells, especially those with higher membrane turnover. In contrast, neurons appear to require more complex signaling sphingolipids e.g., Sphingosine-1-phosphate, for function, while keeping basal Ceramide synthesis in check. In glia, we find that a drop in glial Ceramide synthesis or a cessation of its transfer to the Golgi, both of which are required for the generation of complex sphingolipids, leads to motor neuron deficits. The reduction of flux through the ceramide pathway also affects LD dynamics, suggesting cross-communication between the LD and sphingolipid pathways.

**5.5 Conclusion:** In summary, our data points to a direct link between ceramide production and/or its transfer to vulnerability in the motor neuronal circuit. Glial cells appear to be major players in maintaining motor function, with LDs serving as a useful readout of glial ceramide status and markers of motor dysfunction.

## 5.6 Materials and Methods

**5.6.1 *Drosophila* husbandry, fly stocks and reagents:** All the experimental stocks were maintained and crossed on a standard corn agar media in 12 hr Light: 12hr Dark cycle at 25 ℃ and F1 male progeny were used for experiments, which were performed at 25℃. *w1118* is used as wild-type control in the experiments. *dCERT$^{1}$ (CERT$^{\Delta}$)* was a kind gift from Ravi Acharya Lab (RAO ET AL., 2007). Genomic *CERT$^{WT}$* and *CERT$^{SL}$* lines were acquired from Charlotte Gehin & Giovanni D'Angelo (GEHIN ET AL., 2023). *UASp-CERT$^{WT}$* and *UASp-CERT$^{EAAD}$* transgenic lines are described in chapter IV. *repo-Gal4* and *elav-Gal4* are described in chapter III. For *CERT* KD, Valium 20 Trip RNAi line was used unless specified. Bloomington fly Stocks: *w1118* (BL_3605), *Df(3L)Exel6112* (BL_7591), *tub-Gal4*(BL_5138), *nSyb-Gal4*(BL_51635), *CERT$^{RNAi}$* (BL_60080), *CERT$^{RNAi}$* (BL_35579), *spt-I$^{RNAi}$* (BL_55685), *lace$^{RNAi}$* (BL_51475), *Kdsr$^{RNAi}$* (BL_64494), *schlank$^{RNAi}$* (BL_29340), *ifc$^{RNAi}$* (BL_32514), *tub-Gal80$^{ts}$* (BL_7016) were used for experiments.

**5.6.2 Statistical tests:** Two way ANOVA was used for climbing assays followed by Tukey's test for multiple comparisons. For LD density, ordinary one-way ANOVA was used and then multiple comparisons were done using Tukey's test. For LD size, one-way ANOVA was performed using the Kruskal-Wallis test followed by Dunn's test for multiple comparison correction.

**5.6.3 Software/Applications:** Graphpad Prism 10.4.1(532) was used for statistical tests and graphs. Image J is used for image analysis and representative images. Biorender and Microsoft PowerPoint for schematic diagrams.

**5.7 Contributions:** Karthik H, Master's student in the lab dissected adult brains and performed LD staining for the ceramide pathway enzymes screening. He also analyzed the images for LD quantitation using the same protocol for LDs as described in chapter III.

**5.8 Acknowledgements:** We thank Prof. Jairaj Acharya, NIH for providing the *dCERT$^{1}$* line. We also acknowledge Charlotte Gehin from Prof. Angelo's Lab, EPFL for providing the genomic *CERT* transgenic lines.

## 5.9 References

Agrawal, I., Lim, Y. S., Ng, S. Y., & Ling, S. C. (2022). Deciphering lipid dysregulation in ALS: from mechanisms to translational medicine. *Transl Neurodegener*, *11*(1), 48. https://doi.org/10.1186/s40035-022-00322-0

Anna B. Ziegler , C. W., Konstantin Beckschäfer,Anna-Lena Wulf,Neena Dhiman,Peter Soba,Christoph Thiele,Reinhard Bauer,Gaia Tavosanis (2025). Individual lipid alterations at the origin of neuronal Ceramide Synthase defects. *PloS Genetics*, *21*(9). https://doi.org/https://doi.org/10.1371/journal.pgen.1011880

Bauer, R., Voelzmann, A., Breiden, B., Schepers, U., Farwanah, H., Hahn, I., Eckardt, F., Sandhoff, K., & Hoch, M. (2009). Schlank, a member of the ceramide synthase family controls growth and body fat in Drosophila. *EMBO J*, *28*(23), 3706–3716. https://doi.org/10.1038/emboj.2009.305

Bikman, B. T., & Summers, S. A. (2011). Ceramides as modulators of cellular and whole-body metabolism. *J Clin Invest*, *121*(11), 4222–4230. https://doi.org/10.1172/JCI57144

Byrns, C. N., Perlegos, A. E., Miller, K. N., Jin, Z., Carranza, F. R., Manchandra, P., Beveridge, C. H., Randolph, C. E., Chaluvadi, V. S., Zhang, S. L., Srinivasan, A. R., Bennett, F. C., Sehgal, A., Adams, P. D., Chopra, G., & Bonini, N. M. (2024). Senescent glia link mitochondrial dysfunction and lipid accumulation. *Nature*, *630*(8016), 475–483. https://doi.org/10.1038/s41586-024-07516-8

Chen, X., Li, J., Gao, Z., Yang, Y., Kuang, W., Dong, Y., Chua, G. H., Huang, X., Jiang, B., Tian, H., Wang, Y., Huang, X., Li, Y., Lam, S. M., & Shui, G. (2022). Endogenous ceramide phosphoethanolamine modulates circadian rhythm via neural-glial coupling in Drosophila. *Natl Sci Rev*, *9*(12), nwac148. https://doi.org/10.1093/nsr/nwac148

Cutler, R. G., Pedersen, W. A., Camandola, S., Rothstein, J. D., & Mattson, M. P. (2002). Evidence that accumulation of ceramides and cholesterol esters mediates oxidative stress-induced death of motor neurons in amyotrophic lateral sclerosis. *Ann Neurol*, *52*(4), 448–457. https://doi.org/10.1002/ana.10312

Gehin, C., Lone, M. A., Lee, W., Capolupo, L., Ho, S., Adeyemi, A. M., Gerkes, E. H., Stegmann, A. P., Lopez-Martin, E., Bermejo-Sanchez, E., Martinez-Delgado, B., Zweier, C., Kraus, C., Popp, B., Strehlow, V., Grafe, D., Knerr, I., Jones, E. R., Zamuner, S.,…Gennarino, V. A. (2023). CERT1 mutations perturb human development by disrupting sphingolipid homeostasis. *J Clin Invest*, *133*(10). https://doi.org/10.1172/JCI165019

Ghosh, A., Kling, T., Snaidero, N., Sampaio, J. L., Shevchenko, A., Gras, H., Geurten, B., Gopfert, M. C., Schulz, J. B., Voigt, A., & Simons, M. (2013). A global in vivo Drosophila RNAi screen identifies a key role of ceramide phosphoethanolamine for glial ensheathment of axons. *PLoS Genet*, *9*(12), e1003980. https://doi.org/10.1371/journal.pgen.1003980

Goodman, L. D., Ralhan, I., Li, X., Lu, S., Moulton, M. J., Park, Y. J., Zhao, P., Kanca, O., Ghaderpour Taleghani, Z. S., Jacquemyn, J., Shulman, J. M., Ando, K., Sun, K., Ioannou, M. S., & Bellen, H. J. (2024). Tau is required for glial lipid droplet formation and resistance to neuronal oxidative stress. *Nat Neurosci*, *27*(10), 1918–1933. https://doi.org/10.1038/s41593-024-01740-1

Goyal, G., Zheng, J., Adam, E., Steffes, G., Jain, M., Klavins, K., & Hummel, T. (2019). Sphingolipid-dependent Dscam sorting regulates axon segregation. *Nat Commun*, *10*(1), 813. https://doi.org/10.1038/s41467-019-08765-2

Gunay, A., Shin, H. H., Gozutok, O., Gautam, M., & Ozdinler, P. H. (2021). Importance of lipids for upper motor neuron health and disease. *Semin Cell Dev Biol*, *112*, 92–104. https://doi.org/10.1016/j.semcdb.2020.11.004

Hebbar, S., Sahoo, I., Matysik, A., Argudo Garcia, I., Osborne, K. A., Papan, C., Torta, F., Narayanaswamy, P., Fun, X. H., Wenk, M. R., Shevchenko, A., Schwudke, D., & Kraut, R. (2015). Ceramides And Stress Signalling Intersect With Autophagic Defects In Neurodegenerative Drosophila blue cheese (bchs) Mutants. *Sci Rep*, *5*, 15926. https://doi.org/10.1038/srep15926

Henne, W. M., Reynolds, E., & Prinz, W. A. (2025). Lipid droplets: Open questions and conceptual advances around a unique organelle. *J Cell Biol*, *224*(10). https://doi.org/10.1083/jcb.202406019

Henriques, A., Croixmarie, V., Bouscary, A., Mosbach, A., Keime, C., Boursier-Neyret, C., Walter, B., Spedding, M., & Loeffler, J. P. (2017). Sphingolipid Metabolism Is Dysregulated at Transcriptomic and Metabolic Levels in the Spinal Cord of an Animal Model of Amyotrophic Lateral Sclerosis. *Front Mol Neurosci*, *10*, 433. https://doi.org/10.3389/fnmol.2017.00433

Hussain, G., Wang, J., Rasul, A., Anwar, H., Imran, A., Qasim, M., Zafar, S., Kamran, S. K. S., Razzaq, A., Aziz, N., Ahmad, W., Shabbir, A., Iqbal, J., Baig, S. M., & Sun, T. (2019). Role of cholesterol and sphingolipids in brain development and neurological diseases. *Lipids Health Dis*, *18*(1), 26. https://doi.org/10.1186/s12944-019-0965-z

Ilieva, H., Polymenidou, M., & Cleveland, D. W. (2009). Non-cell autonomous toxicity in neurodegenerative disorders: ALS and beyond. *J Cell Biol*, *187*(6), 761–772. https://doi.org/10.1083/jcb.200908164

Islam, M. N., Mandal, N., Khanom, N. I., Spivey, A. L., Patel, A. S., Ahmed, T., Islam, R., & Bhuiyan, M. I. H. (2025). Sphingolipid Signaling and Metabolism in Neuronal and Glial Cells: Implications for Cerebrovascular and Neurodegenerative Disorders. *Aging Dis*. https://doi.org/10.14336/AD.2025.1024

Jeon, S., Scorletti, E., Dempsey, J., Buyco, D., Lin, C., Saiman, Y., Bayen, S., Harkin, J., Martin, J., Hooks, R., Ogretmen, B., Argemi, J., Melo, L., Bataller, R., & Carr, R. M. (2023). Ceramide synthase 6 (CerS6) is upregulated in alcohol-associated liver disease and exhibits sex-based differences in the regulation of energy homeostasis and lipid droplet accumulation. *Mol Metab*, *78*, 101804. https://doi.org/10.1016/j.molmet.2023.101804

Jung, W. H., Liu, C. C., Yu, Y. L., Chang, Y. C., Lien, W. Y., Chao, H. C., Huang, S. Y., Kuo, C. H., Ho, H. C., & Chan, C. C. (2017). Lipophagy prevents activity-dependent neurodegeneration due to dihydroceramide accumulation in vivo. *EMBO Rep*, *18*(7), 1150–1165. https://doi.org/10.15252/embr.201643480

Kraut, R. (2011). Roles of sphingolipids in Drosophila development and disease. *J Neurochem*, *116*(5), 764–778. https://doi.org/10.1111/j.1471-4159.2010.07022.x

Kumagai, K., & Hanada, K. (2019). Structure, functions and regulation of CERT, a lipid-transfer protein for the delivery of ceramide at the ER-Golgi membrane contact sites. *FEBS Lett*, *593*(17), 2366–2377. https://doi.org/10.1002/1873-3468.13511

Kunduri, G., Godenschwege, T. A., Sankey, K., Abhilasha, K. V., Acharya, U. R., & Acharya, J. K. (2025). Light and temperature sensitive seizures are regulated by spatially distinct cortex glial populations in the central nervous system. *bioRxiv*. https://doi.org/10.1101/2025.06.27.661959

Liping Wang, G. L., Zhongyuan Zuo, Yarong Li, Seul Kee Byeon, Akhilesh Pandey, Hugo J. Bellen. (2022). Neuronal activity induces glucosylceramide that is secreted via exosomes for lysosomal degradation in glia. *Science Advances*.

Liu, J., Luo, X., Chen, X., & Shang, H. (2020). Lipid Profile in Patients With Amyotrophic Lateral Sclerosis: A Systematic Review and Meta-Analysis. *Front Neurol*, *11*, 567753. https://doi.org/10.3389/fneur.2020.567753

Liu, L., MacKenzie, K. R., Putluri, N., Maletic-Savatic, M., & Bellen, H. J. (2017). The Glia-Neuron Lactate Shuttle and Elevated ROS Promote Lipid Synthesis in Neurons and Lipid Droplet Accumulation in Glia via APOE/D. *Cell Metab*, *26*(5), 719–737 e716. https://doi.org/10.1016/j.cmet.2017.08.024

Liu, L., Zhang, K., Sandoval, H., Yamamoto, S., Jaiswal, M., Sanz, E., Li, Z., Hui, J., Graham, B. H., Quintana, A., & Bellen, H. J. (2015). Glial lipid droplets and ROS induced by mitochondrial defects promote neurodegeneration. *Cell*, *160*(1-2), 177–190. https://doi.org/10.1016/j.cell.2014.12.019

McCluskey, G., Donaghy, C., Morrison, K. E., McConville, J., Duddy, W., & Duguez, S. (2022). The Role of Sphingomyelin and Ceramide in Motor Neuron Diseases. *J Pers Med*, *12*(9). https://doi.org/10.3390/jpm12091418

McInnis, J. J., Sood, D., Guo, L., Dufault, M. R., Garcia, M., Passaro, R., Gao, G., Zhang, B., & Dodge, J. C. (2024). Unravelling neuronal and glial differences in ceramide composition, synthesis, and sensitivity to toxicity. *Commun Biol*, *7*(1), 1597. https://doi.org/10.1038/s42003-024-07231-0

Mencarelli, C., & Martinez-Martinez, P. (2013). Ceramide function in the brain: when a slight tilt is enough. *Cell Mol Life Sci*, *70*(2), 181–203. https://doi.org/10.1007/s00018-012-1038-x

Mishra, S., Manohar, V., Chandel, S., Manoj, T., Bhattacharya, S., Hegde, N., Nath, V. R., Krishnan, H., Wendling, C., Di Mattia, T., Martinet, A., Chimata, P., Alpy, F., & Raghu, P. (2024). A genetic screen to uncover mechanisms underlying lipid transfer protein function at membrane contact sites. *Life Sci Alliance*, *7*(6). https://doi.org/10.26508/lsa.202302525

Oswald, M. C., West, R. J., Lloyd-Evans, E., & Sweeney, S. T. (2015). Identification of dietary alanine toxicity and trafficking dysfunction in a Drosophila model of hereditary sensory and autonomic neuropathy type 1. *Hum Mol Genet*, *24*(24), 6899–6909. https://doi.org/10.1093/hmg/ddv390

Pan, X., Dutta, D., Lu, S., & Bellen, H. J. (2023). Sphingolipids in neurodegenerative diseases. *Front Neurosci*, *17*, 1137893. https://doi.org/10.3389/fnins.2023.1137893

Pant, D. C., Aguilera-Albesa, S., & Pujol, A. (2020). Ceramide signalling in inherited and multifactorial brain metabolic diseases. *Neurobiol Dis*, *143*, 105014. https://doi.org/10.1016/j.nbd.2020.105014

Pant, D. C., Dorboz, I., Schluter, A., Fourcade, S., Launay, N., Joya, J., Aguilera-Albesa, S., Yoldi, M. E., Casasnovas, C., Willis, M. J., Ruiz, M., Ville, D., Lesca, G., Siquier-Pernet, K., Desguerre, I., Yan, H., Wang, J., Burmeister, M., Brady, L.,…Pujol, A. (2019). Loss of the sphingolipid desaturase DEGS1 causes hypomyelinating leukodystrophy. *J Clin Invest*, *129*(3), 1240–1256. https://doi.org/10.1172/JCI123959

Pathak, D., Mehendale, N., Singh, S., Mallik, R., & Kamat, S. S. (2018). Lipidomics Suggests a New Role for Ceramide Synthase in Phagocytosis. *ACS Chem Biol*, *13*(8), 2280–2287. https://doi.org/10.1021/acschembio.8b00438

Pennetta, G., & Welte, M. A. (2018). Emerging Links between Lipid Droplets and Motor Neuron Diseases. *Dev Cell*, *45*(4), 427–432. https://doi.org/10.1016/j.devcel.2018.05.002

Perry, R. J., & Ridgway, N. D. (2006). Oxysterol-binding protein and vesicle-associated membrane protein-associated protein are required for sterol-dependent activation of the ceramide transport protein. *Mol Biol Cell*, *17*(6), 2604–2616. https://doi.org/10.1091/mbc.e06-01-0060

Rachakonda, V., Pan Th Fau - Le, W. D., & Le, W. D. (2004). Biomarkers of neurodegenerative disorders: how good are they? *Cell research*, *14*(5), 349–360.

Rao, R. P., Scheffer, L., Srideshikan, S. M., Parthibane, V., Kosakowska-Cholody, T., Masood, M. A., Nagashima, K., Gudla, P., Lockett, S., Acharya, U., & Acharya, J. K. (2014). Ceramide transfer protein deficiency compromises organelle function and leads to senescence in primary cells. *PLoS One*, *9*(3), e92142. https://doi.org/10.1371/journal.pone.0092142

Rao, R. P., Yuan, C., Allegood, J. C., Rawat, S. S., Edwards, M. B., Wang, X., Merrill, A. H., Jr., Acharya, U., & Acharya, J. K. (2007). Ceramide transfer protein function is essential for normal oxidative stress response and lifespan. *Proc Natl Acad Sci U S A*, *104*(27), 11364–11369. https://doi.org/10.1073/pnas.0705049104

Robles-Martinez, L., Morin, K. H., & Nikolova-Karakashian, M. (2025). Ceramide homeostasis in hepatic lipid droplets. *Biochemical Society Transactions*, *53*(02), 509–518. https://doi.org/10.1042/bst20253042

Schmitt, F., Hussain, G., Dupuis, L., Loeffler, J. P., & Henriques, A. (2014). A plural role for lipids in motor neuron diseases: energy, signaling and structure. *Front Cell Neurosci*, *8*, 25. https://doi.org/10.3389/fncel.2014.00025

Senkal, C. E., Salama, M. F., Snider, A. J., Allopenna, J. J., Rana, N. A., Koller, A., Hannun, Y. A., & Obeid, L. M. (2017). Ceramide Is Metabolized to Acylceramide and Stored in Lipid Droplets. *Cell Metab*, *25*(3), 686–697. https://doi.org/10.1016/j.cmet.2017.02.010

Slee, J. A., & Levine, T. P. (2019). Systematic prediction of FFAT motifs across eukaryote proteomes identifies nucleolar and eisosome proteins with the predicted capacity to form bridges to the endoplasmic reticulum. *Contact (Thousand Oaks)*, *2*, 1–21. https://doi.org/10.1177/2515256419883136

Smolic, T., Zorec, R., & Vardjan, N. (2021). Pathophysiology of Lipid Droplets in Neuroglia. *Antioxidants (Basel)*, *11*(1). https://doi.org/10.3390/antiox11010022

Sociale, M., Wulf, A. L., Breiden, B., Klee, K., Thielisch, M., Eckardt, F., Sellin, J., Bulow, M. H., Lobbert, S., Weinstock, N., Voelzmann, A., Schultze, J., Sandhoff, K., & Bauer, R. (2018). Ceramide Synthase Schlank Is a Transcriptional Regulator Adapting Gene Expression to Energy Requirements. *Cell Rep*, *22*(4), 967–978. https://doi.org/10.1016/j.celrep.2017.12.090

Tang, Y., Majewska, M., Less, B., Mehmeti, I., Wollnitzke, P., Semleit, N., Levkau, B., Saba, J. D., van Echten-Deckert, G., & Gurgul-Convey, E. (2024). The fate of intracellular S1P regulates lipid droplet turnover and lipotoxicity in pancreatic beta-cells. *J Lipid Res*, *65*(8), 100587. https://doi.org/10.1016/j.jlr.2024.100587

Tendulkar, S., Hegde, S., Garg, L., Thulasidharan, A., Kaduskar, B., Ratnaparkhi, A., & Ratnaparkhi, G. S. (2022). Caspar, an adapter for VAPB and TER94, modulates the progression of ALS8 by regulating IMD/NFkappaB-mediated glial inflammation in a Drosophila model of human disease. *Hum Mol Genet*, *31*(17), 2857–2875. https://doi.org/10.1093/hmg/ddac076

Theisen, E. K., Rivas-Serna, I. M., Lee, R. J., Jay, T. R., Kunduri, G., Nguyen, T. T., Mazurak, V., Clandinin, M. T., Clandinin, T. R., & Vaughen, J. P. (2025). Glia phagocytose neuronal sphingolipids to infiltrate developing synapses. *bioRxiv*. https://doi.org/10.1101/2025.04.14.648777

Tracey, T. J., Kirk, S. E., Steyn, F. J., & Ngo, S. T. (2021). The role of lipids in the central nervous system and their pathological implications in amyotrophic lateral sclerosis. *Semin Cell Dev Biol*, *112*, 69–81. https://doi.org/10.1016/j.semcdb.2020.08.012

Vaughen, J. P., Theisen, E., Rivas-Serna, I. M., Berger, A. B., Kalakuntla, P., Anreiter, I., Mazurak, V. C., Rodriguez, T. P., Mast, J. D., Hartl, T., Perlstein, E. O., Reimer, R. J., Clandinin, M. T., & Clandinin, T. R. (2022). Glial control of sphingolipid levels sculpts diurnal remodeling in a circadian circuit. *Neuron*, *110*(19), 3186–3205 e3187. https://doi.org/10.1016/j.neuron.2022.07.016

Voelzmann, A., & Bauer, R. (2010). Ceramide synthases in mammalians, worms, and insects: emerging schemes. *Biomol Concepts*, *1*(5-6), 411–422. https://doi.org/10.1515/bmc.2010.028

Vos, M., Dulovic-Mahlow, M., Mandik, F., Frese, L., Kanana, Y., Haissatou Diaw, S., Depperschmidt, J., Bohm, C., Rohr, J., Lohnau, T., Konig, I. R., & Klein, C. (2021). Ceramide accumulation induces mitophagy and impairs beta-oxidation in PINK1 deficiency. *Proc Natl Acad Sci U S A*, *118*(43). https://doi.org/10.1073/pnas.2025347118

Walther, T. C., & Farese, R. V., Jr. (2012). Lipid droplets and cellular lipid metabolism. *Annu Rev Biochem*, *81*, 687–714. https://doi.org/10.1146/annurev-biochem-061009-102430

Wang, X., Rao, R. P., Kosakowska-Cholody, T., Masood, M. A., Southon, E., Zhang, H., Berthet, C., Nagashim, K., Veenstra, T. K., Tessarollo, L., Acharya, U., & Acharya, J. K. (2009). Mitochondrial degeneration and not apoptosis is the primary cause of embryonic lethality in ceramide transfer protein mutant mice. *J Cell Biol*, *184*(1), 143–158. https://doi.org/10.1083/jcb.200807176

Wanikawa, M., Nakamura, H., Emori, S., Hashimoto, N., & Murayama, T. (2020). Accumulation of sphingomyelin in Niemann-Pick disease type C cells disrupts Rab9-dependent vesicular trafficking of cholesterol. *J Cell Physiol*, *235*(3), 2300–2309. https://doi.org/10.1002/jcp.29137

Yang, D., Wang, X., Zhang, L., Fang, Y., Zheng, Q., Liu, X., Yu, W., Chen, S., Ying, J., & Hua, F. (2022). Lipid metabolism and storage in neuroglia: role in brain development and neurodegenerative diseases. *Cell Biosci*, *12*(1), 106. https://doi.org/10.1186/s13578-022-00828-0

Zhang, L., Zhou, Y., Yang, Z., Jiang, L., Yan, X., Zhu, W., Shen, Y., Wang, B., Li, J., & Song, J. (2025). Lipid droplets in central nervous system and functional profiles of brain cells containing lipid droplets in various diseases. *J Neuroinflammation*, *22*(1), 7. https://doi.org/10.1186/s12974-025-03334-5

Zhu, Y., Cho, K., Lacin, H., Zhu, Y., DiPaola, J. T., Wilson, B. A., Patti, G., & Skeath, J. B. (2025). Loss of dihydroceramide desaturase drives neurodegeneration by disrupting endoplasmic reticulum and lipid droplet homeostasis in glial cells. *Elife*, *13*. https://doi.org/10.7554/eLife.99344

# Future Directions

This study employed an integrative experimental framework combining biochemistry, genetics and confocal imaging to investigate lipid metabolism in the context of Amyotrophic Lateral Sclerosis which is modelled in *Drosophila.* By focusing on *ALS8* in *D. melanogaster*, this work establishes a solid platform for lipid dysregulation in the pathogenesis of *ALS8* which remained largely unexplored for quite some time. Importantly, how lipid homeostasis is perturbed in cell specific manner shows the need of this field to explore it further in terms of neuron-glia cross talk as contributor in the disease progression.

Although the findings presented in the thesis establish a strong connection of cell specific lipid imbalance in *ALS8* model of *Drosophila*, extending these observations to neuronal and glial cell culture systems would be the next crucial step. Cell type specific studies will allow us to study the autonomous and non-cell autonomous roles of lipids in the neurological disorder. Moreover, comparing lipid phenotypes across in vivo and in vitro systems would strengthen the relevance of these findings and clarify the cell centric roles to lipid dysregulation.

A central finding of this work is the perturbation of lipid droplet homeostasis in the ALS8 disease which is in contrast to other ALS models suggesting VAPB specific roles in LD regulation. It will be interesting to see the roles of other ALS loci in the background of *ALS8* in the regulation of LD homeostasis. VAPB is known to interact with lipid transfer proteins that interact with LDs. Therefore genetic manipulation of such genes in the *ALS8* background represents an important direction. Next, what is the significance of LD homeostasis in the progression of ALS? Knockdown of *spen* showed increased in LD density but did not improve the motor performance suggesting LD accumulation may have threshold which glia can accommodate or it will become detrimental. This highlights the importance of LD composition in determining cellular outcomes. Future lipidomic studies will benefit to understand these results better. Such studies will help to understand the glial roles in terms of LD regulation and their impact on animal physiology.

The results of this work point towards active neuron-glia lipid cross-talk in the *ALS8* model although the precise mechanisms are still unclear. Neurons and glia are known to exchange metabolites and lipids under both physiological and pathological conditions. Targeting specific lipid carrier proteins or transporters followed by experimental analysis in terms of motor behavior

or lipid distribution will elucidate how this communication is involved in the progression of the disease.

Lactate metabolism has been shown to play major role as a critical regulator for neuronal survival. Lactate shuttling between neurons and glia plays an important role in meeting neuronal energy demands especially under metabolic stress. Investigating lactate metabolism in the context of *ALS8* could provide useful insights about the neuron and glia dependence on each other. Previous studies from the lab have demonstrated genetic interactions between *ALS8, ALS1* and *ALS14*. We have established that these loci interact with each other and can modulate lifespan and aggregate dynamics. It will be informative to examine the lipid levels and LD homeostasis in this case and their contribution to the progression of the disease.

Lipid homeostasis is tightly linked to mitochondrial activity of the cell. In other *ALS8* models like yeast and cell lines, mitochondrial dysfunction is reported so replicating those results in *Drosophila* will be really useful. In this thesis, we saw modulating ceramide related genes improves motor activity of *ALS8* flies suggesting ceramide signaling may influence mitochondrial function, protein aggregation and ER stress based on existing literature. In the Chapter II, a list of potential VAP interactors is generated which contain FFAT motif in *Drosophila*. Detailed characterization of these genes including their interaction with VAP and their impact on ALS8 model in terms of lifespan, motor performance, aggregate dynamics and lipid metabolism would further expand our knowledge about VAP roles in the cell.

Finally, this study reveals unexplored roles of glial ceramides in regulating LD homeostasis. We Preliminary data from the lab indicates abnormal mitochondrial morphology in the brain upon reduction of ceramide transfer in the glia. This suggests a critical intersection between ceramide metabolism, LD dynamics and mitochondria function. Further studies could intergrate cell specific lipidomics, organelle imaging and behavioral assays to determine how ceramides are coordinating LD homeostasis and mitochondrial function. Such insights may prove valuable for the therapeutic interventions in the human diseases.

# Appendix – I

# Balancing and validation of fly reagents

## I.1 Introduction

*Drosophila melanogaster* has remain a powerful model organism for a long time because of the genetic tools available to manipulate and maintain genetic variation (Duffy, 2002; Gratz et al., 2015; Layalle et al., 2021; Liguori et al., 2021). One of the most prominent features of *Drosophila* genetics is the use of balancer chromosomes, which leads to stabilization of deleterious or lethal mutations. Balancer chromosomes carry multiple inversions that suppress recombination, along with dominant visible markers and recessive lethal alleles (Casci & Pandey, 2015; Hegde & Srivastava, 2022; Venken et al., 2011). This design makes sure that homologous chromosomes do not exchange genetic material and only heterozygous individuals survive, effectively balancing the gene of interest across generations (Braems et al., 2021).

In the earlier studies, to understand the effect of $VAP^{P58S}$ allele on the organism, overexpression system was used using UAS-Gal4 system where it used to be expressed under neuronal Gal4 (Deivasigamani et al., 2014; Ratnaparkhi et al., 2008). Although, it leads to the production of mutant protein 10-15 times more than the endogenous protein and also it did not show any ALS like phenotypes apart from aggregation phenotype (Chaplot et al., 2019). Then, a genomic model of *ALS8* was developed where $VAP^{P58S}$ is expressed under genomic promotor of endogenous *VAP* and the wild-type *VAP* allele was functional null (Moustaqim-Barrette et al., 2014; Tsuda et al., 2008). This model mimics ALS8 like phenotypes and has been used extensively for multiple studies and in this thesis work as well (Tendulkar et al., 2022; Thulasidharan et al., 2024). However, due to complicated genetics, some of the experiments was not possible and it does not completely replicates the genetics of human *ALS8* allele. So, in our lab endogenous *VAP* was mutated to $VAP^{P58S}$ using CRISPR-Cas9 technology and characterized in the lab (Thulasidharan, 2023). However, to study the modifiers of *VAP* in the CRISPR model of ALS, tissue specific Gal4 had to be introduced. In this appendix, I have described the methodology and shared the genetics of balancing tissue specific Gal4s in the CRISPR *ALS8.* Along with that, I have also recombined $Gal80^{ts}$ with the CRISPR $VAP^{P58S}$ allele so that temperature shift experiments can be performed (Duffy, 2002). Apart from that, I have made a list of the fly lines which I

balanced and validated in the lab for the other projects. All the fly lines listed here have been deposited to the stock center of the lab.

**I.2 Results and Discussion:**

**I.2.1 Addition of balancers and tissue specific Gal4s in CRISPR *VAP$^{P58S}$* fly line:** I used CRISPR *VAP$^{P58S}$* (279.1) fly line to add the balancer chromosomes as it was well characterized in the lab by the previous student (Thulasidharan, 2023). I have drawn a schematic diagram of the crosses as shown in (Fig. I.1) where male balancer line was used to cross homozygous CRISPR *VAP$^{P58S}$* allele and after two crosses, final stable line was generated where yellow body, vermilion eye were visible along with *Pin* as a marker and *Cyo* balancer. After adding the balancers on second chromosomes, then I proceeded with different tissue specific Gal4 to the *VAP$^{P58S}$* balanced line as shown for glial specific Gal4 (*repo-Gal4*) in (Fig. I.2). Similarly, I introduced pan-neuronal specific Gal4 (*elav-Gal4*), muscle specific Gal4 (*MHC-Gal4*) and motor neuron specific Gal4 (*vGlut-Gal4*) in the CRISPR mutant of *ALS8.* I randomly picked three males from the mentioned genotypes, y-v-*VAP$^{P58S}$*/Y; +/+; +/+, y-v-*VAP$^{P58S}$/Y; repo-Gal4/Cyo* and y-v-*VAP$^{P58S}$/Y; elav-Gal4/Cyo* and performed genomic DNA extraction along with restriction digestion to validate the presence of *VAP$^{P58S}$* allele as described in (Thulasidharan, 2023). In the design of CRISPR mutant, 5'-TACGTA-3' site is there which gets cleaved under appropriate restriction enzyme only in the *VAP$^{P58S}$* allele (Fig. I.3). To validate the Gal4s expression, UAS-GFP was used to express in the flies under tissue specific manner and observed under epifluorescence microscope.

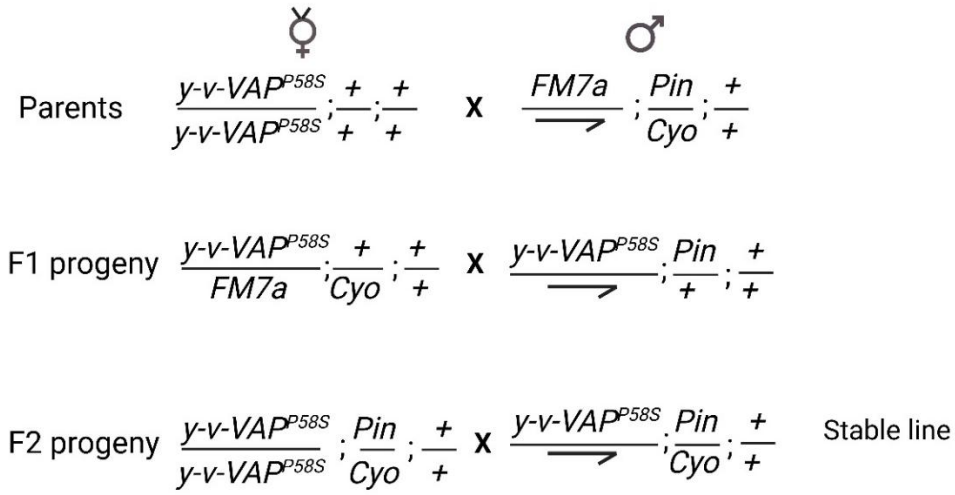



**Figure I.1: Schematic diagram of adding balancer chromosomes to the CRISPR *VAP$^{P58S}$*.**

Male balancer line was crossed to the female virgin flies of CRISPR *VAP*$^{P58S}$ then F1 virgin females were self-crossed to male flies which gave a stable *VAP*$^{P58S}$ line with balancers on second chromosome.

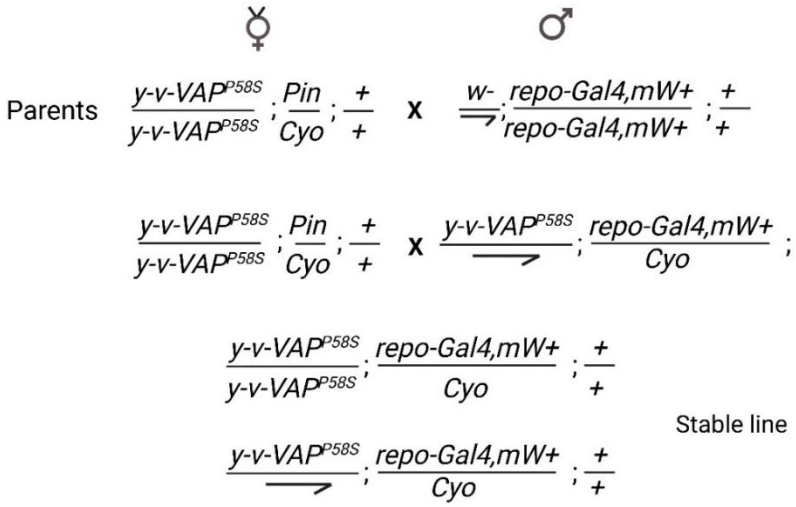



**Figure I.2: Schematic diagram of adding tissue specific Gal4 drivers to the CRISPR *VAP*$^{P58S}$.**

Glial specific Gal4 (*repo-Gal4)* males were crossed to the virgin females of CRISPR *VAP*$^{P58S}$ balanced line then F1 males were back crossed to parent virgin females which gave a stable *VAP*$^{P58S}$ line with glial specific Gal4 on second chromosome.

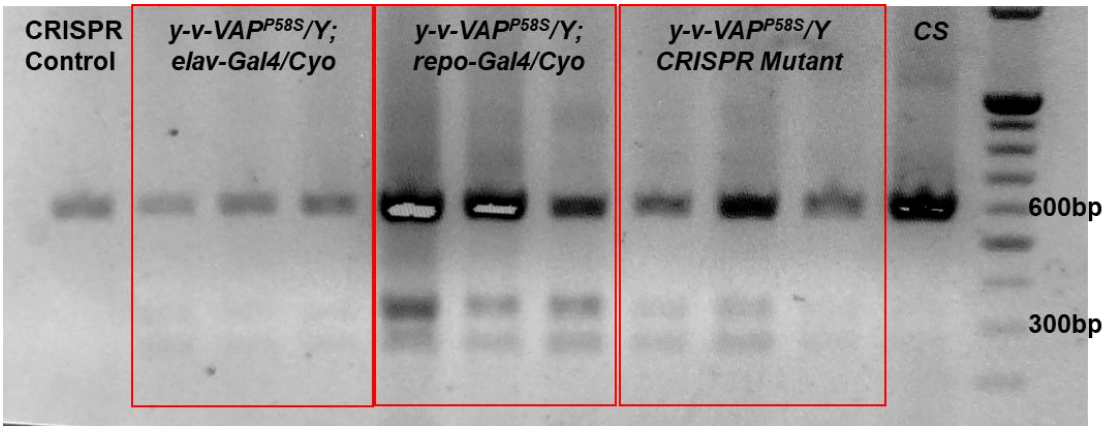



**Figure I.3: Validation of CRISPR *VAP*$^{P58S}$ fly line containing tissue specific Gal4 drivers.**

Starting from the right side to the left, DNA ladder, *CantonS (CS)* control, next three lanes for CRISPR *VAP*$^{P58S}$ flies, next three for y-v-*VAP*$^{P58S}$*/Y; repo-Gal4/Cyo*, next three for y-v-*VAP*$^{P58S}$*/Y; elav-Gal4/Cyo* and last lane CRISPR control DNA was loaded after restriction digestion with SnaB1. 1 male fly for each well was used to extract DNA. Lower two bands at 300 bp shows restriction digestion happened for *VAP*$^{P58S}$ allele but not for controls.

**I.2.2: Recombination of *Gal80$^{ts}$* to the *VAP$^{P58S}$*fly line and its validation:** I used the CRISPR *VAP$^{P58S}$* balanced line (yellow body) to recombine *Gal80$^{ts}$* (BL_7016) in the background. Firstly, in the F1 generation, I picked up 50 female flies (normal body color) from the parent cross and set up individual crosses with the male balancer line. From the F1 cross, I picked up females with kidney shaped eyes because of the presence of *FM7a* balancer. Then, I let it grow for few generations and generated stable balanced lines represented in (Fig. I.4). As *Gal80$^{ts}$* fly line is homozygous lethal in females due to its insertion in *sxl* gene, if *Gal80* is there, it will always show kidney shaped eyes in females. However, males with *Gal80* are viable. But due to the presence of *VAP$^{P58S}$* allele male will show yellow body color. Then, I selected the lines and performed genomic PCR described earlier in (Thulasidharan, 2023)for checking the presence of *VAP$^{P58S}$* allele as shown in (Fig. I.5). Flies which did not have yellow body but had kidney shaped eyes were used as *Gal80* fly line control. On the other hand, flies with yellow body but normal eyes were picked up as *VAP$^{P58S}$* balanced line without *Gal80* (Fig. I.5). All the fly lines were allotted numbers based on the vial number.

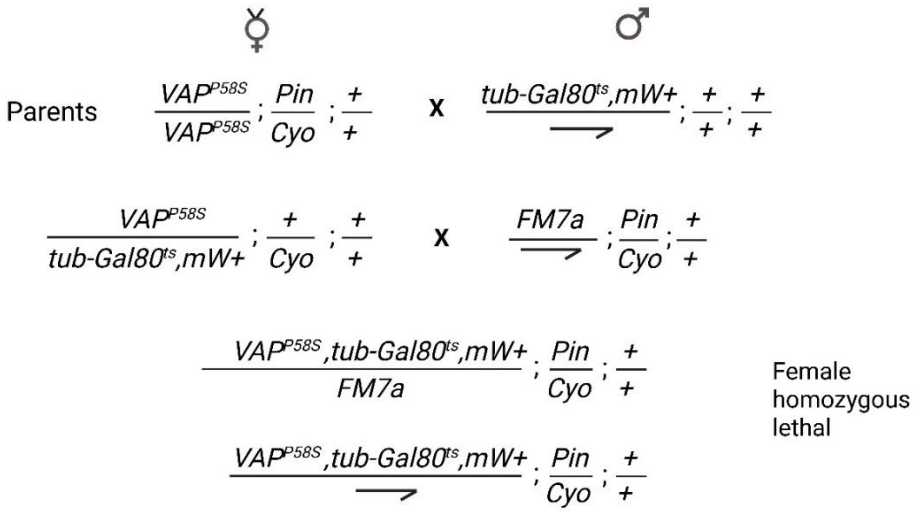



**Figure I.4: Schematic diagram of recombining *Gal80$^{ts}$* to the CRISPR *VAP$^{P58S}$*.**

Males with *Gal80$^{ts}$* on X chromosome (BL_7016) was crossed to the female virgin flies of CRISPR *VAP$^{P58S}$* balanced line then F1 virgin females (50) were individually crossed to male balancer line, then from F2 generation, virgin females balanced with *FM7a* back crossed to male parent balancer line which gave a stable *VAP$^{P58S}$* line recombined with *Gal80$^{ts}$* on the X chromosome.

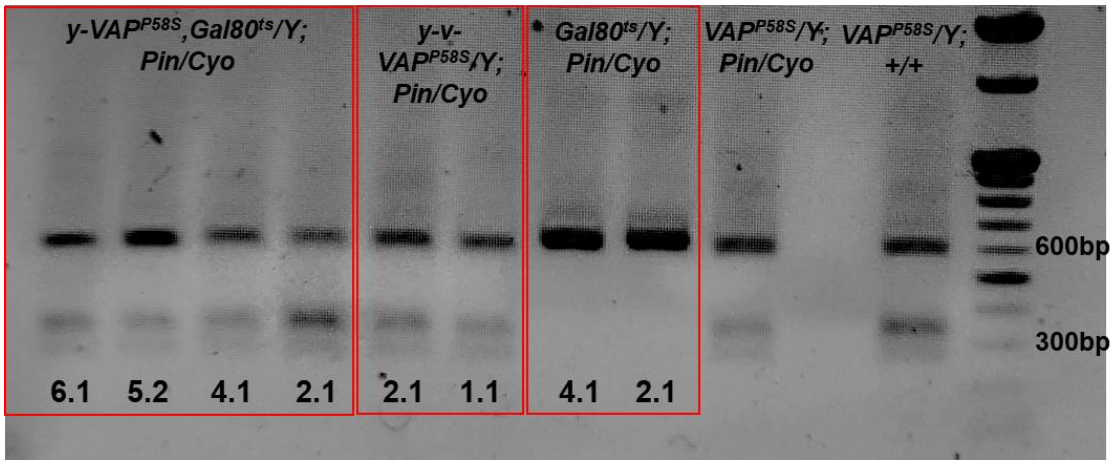



**Figure I.5: Validation of CRISPR *VAP$^{P58S}$* fly line recombined with *Gal80$^{ts}$*.**

Starting from the right side to the left, DNA ladder, *VAP$^{P58S}$* as control, third lane empty, fourth lane for CRISPR *VAP$^{P58S}$* balanced line, next two lanes for *Gal80$^{ts}$; Pin/Cyo* (2.1, 4.1), next two lanes for y-v-*VAP$^{P58S}$/Y; Pin/Cyo* (1.1, 2.1) and last four lanes for y-v-*VAP$^{P58S}$,Gal80$^{ts}$/Y; Pin/Cyo* (2.1, 4.1, 5.2, 6.1) were loaded after restriction digestion with SnaB1. 1 male fly for each well was used to extract DNA. Lower two bands at 300 bp shows restriction digestion happened for *VAP$^{P58S}$* allele but not for controls.

**I.2.3 Addition of Tissue specific Gal4 lines to *Gal80$^{ts}$, VAP$^{P58S}$ Drosophila*:** After the successful validation of the recombined balanced line, I added various tissue specific Gal4s such as *elav-Gal4* (pan-neuronal expression), *repo-Gal4* (glial expression), *vGlut-Gal4* (motor neuronal expression) and *MHC-Gal4* (muscle expression). For simplicity, schematic diagram is shown for introducing Gal4s in (Fig. I.6). Similarly, I balanced these *Gal4s* with *Gal80$^{ts}$* fly line as well which are listed in the Table I.1.

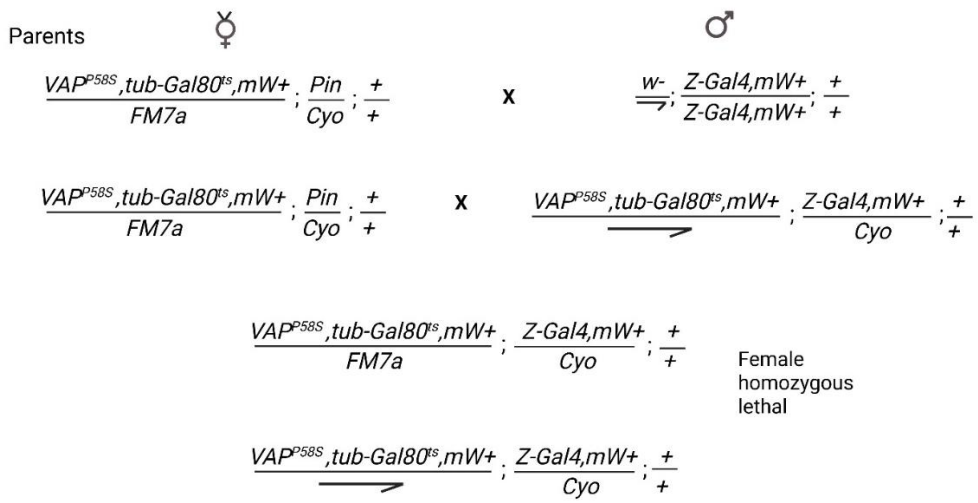



**Figure I.6: Schematic diagram of adding tissue specific Gal4 drivers to the *VAP$^{P58S}$*, *Gal80$^{ts}$*.**

Tissue specific Gal4 males were crossed to the virgin females of *Gal80* recombined *VAP$^{P58S}$* balanced line then F1 males were back crossed to parent virgin females which gave a stable *VAP$^{P58S}$* line with tissue specific Gal4 on second chromosome.

**Table I.1: List of the fly lines balanced and recombined in the lab.**

| S.No. | Genotype | Lines used | Source | Remarks |
|---|---|---|---|---|
| 1. | *y-v-VAP$^{P58S}$;Pin/Cyo* | *y-v-VAP$^{P58S}$- 279.1 FM7a; Pin/Cyo* | CRISPR *VAP* mutant in house | Yellow body vermilion eyes |
| 2. | *y-v-VAP$^{P58S}$;BL38464-Gal4/Cyo* | *y-v-VAP$^{P58S}$- 279.1 FM7a; Pin/Cyo BL38464-MHC-Gal4* | BDSC MHC line | MHC-RFP is present |
| 3. | *y-v-VAP$^{P58S}$;vGlut-Gal4/Cyo* | *y-v-VAP$^{P58S}$- 279.1 FM7a; Pin/Cyo BL26160-vGlut-Gal4* | BDSC BL26160 – Dr. Aurnab Ghose | v-Glut-Gal4 has red color eyes |
| 4. | *y-v-VAP$^{P58S}$;elav-Gal4/Cyo* | *y-v-VAP$^{P58S}$- 279.1 FM7a; Pin/Cyo elav-Gal4/Cyo-GFP* | *elav-Gal4/Cyo-GFP* (Ratnaparkhi et al., 2008) | *elav-Gal4* has mini white, homozygous lethal |
| 5. | *y-v-VAP$^{P58S}$;repo-Gal4/Cyo* | *y-v-VAP$^{P58S}$- 279.1 FM7a; Pin/Cyo repo-Gal4* | *repo-Gal4* (Tendulkar et al., 2022) | *repo-Gal4* has mini white, homozygous viable |
| 6. | *VAP$^{P58S}$;gCERT$^{WT}$/Cyo* | *y-v-VAP$^{P58S}$- 279.1 FM7a; Pin/Cyo gCERT$^{WT}$, mW+* | *w-;gCERT$^{WT}$, mW+* (Gehin et al., 2023) | Homozygous viable, red color eyes |

| | | | | |
|---|---|---|---|---|
| 7. | *VAP$^{P58S}$;gCERT$^{SL}$/Cyo* | *y-v-VAP$^{P58S}$- 279.1 FM7a; Pin/Cyo gCERT$^{SL}$, mW+* | *w-;gCERT$^{SL}$, mW+* (Gehin et al., 2023) | Homozygous viable, red color eyes |
| 8. | *y-v-VAP$^{P58S}$;BL81100/Cyo* | *y-v-VAP$^{P58S}$- 279.1 FM7a; Pin/Cyo BL81100-NPC1a null* | BDSC- BL81100 | Homozygous lethal, it has GFP present |
| 9. | *y-v-VAP$^{P58S}$;BL81101/Cyo* | *y-v-VAP$^{P58S}$- 279.1 FM7a; Pin/Cyo BL81101-NPC1a(I1060T)* | BDSC- BL81101 | |
| 10. | *y-v-VAP$^{P58S}$;BL81102/Cyo* | *y-v-VAP$^{P58S}$- 279.1 FM7a; Pin/Cyo BL81102-NPC1a(V890M)* | BDSC- BL81102 | |
| 11. | *y-v-VAP$^{P58S}$;BL81103/Cyo* | *y-v-VAP$^{P58S}$- 279.1 FM7a; Pin/Cyo BL81103-NPC1a(A1015T)* | BDSC- BL81103 | |
| 12. | *VAP$^{P58S}$,Gal80$^{ts}$mW+/FM7a;vGlut-Gal4/Cyo* | *y-v-VAP$^{P58S}$- 279.1 FM7a; Pin/Cyo BL26160-vGlut-Gal4 BL7016-Gal80$^{ts}$* | BL26160 – Dr. Aurnab Ghose BDSC- BL7016 | *Gal80$^{ts}$* females homozygous lethal, male viable |
| 13. | *VAP$^{P58S}$,Gal80$^{ts}$mW+/FM7a; BL38464-Gal4/Cyo* | *y-v-VAP$^{P58S}$- 279.1 FM7a; Pin/Cyo BL38464-MHC-Gal4 BL7016-Gal80$^{ts}$* | BDSC- BL38464, BL7016 | MHC-RFP is present, females homozygous lethal |
| 14. | *VAP$^{P58S}$,Gal80$^{ts}$mW+/FM7a;elav-Gal4/Cyo* | *y-v-VAP$^{P58S}$- 279.1 FM7a; Pin/Cyo elav-Gal4/Cyo-GFP BL7016-Gal80$^{ts}$* | *elav-Gal4/Cyo-GFP* described above | Females homozygous lethal |
| 15. | *VAP$^{P58S}$,Gal80$^{ts}$mW+/FM7a;repo-Gal4/Cyo* | *y-v-VAP$^{P58S}$- 279.1 FM7a; Pin/Cyo repo-Gal4, BL7016-Gal80$^{ts}$* | | Females homozygous lethal, male viable |
| 16. | *Gal80$^{ts}$mW+/FM7a; repo-Gal4/Cyo* | *FM7a; Pin/Cyo repo-Gal4 BL7016-Gal80$^{ts}$* | | *Gal80$^{ts}$* females homozygous lethal, male viable, yellow to orange eyes |
| 17. | *Gal80$^{ts}$mW+/FM7a; elav-Gal4/Cyo* | *FM7a; Pin/Cyo elav-Gal4/Cyo-GFP BL7016-Gal80$^{ts}$* | | Homozygous lethal, yellow to orange eyes |
| 18. | *Gal80$^{ts}$mW+/FM7a; vGlut-Gal4/Cyo* | *FM7a; Pin/Cyo BL26160-vGlut-Gal4* | | Females homozygous lethal, male viable, yellow to orange eyes |

| | | | | |
|---|---|---|---|---|
| | | *BL7016-Gal80$^{ts}$* | | |
| 19. | *Gal80$^{ts}$mW+/FM7a; Pin/Cyo* | *FM7a; Pin/Cyo*<br>*BL7016-Gal80$^{ts}$* | | *Gal80$^{ts}$* females homozygous lethal, male viable |
| 20. | *X/X; gCERT$^{WT}$/Cyo; MKRS/Ser* | *w-; gCERT$^{WT}$, mW+*<br>*If/Cyo; MKRS/Ser* | | Homozygous viable, red color eyes because of *Ser* |
| 21. | *X/X; gCERT$^{SL}$/Cyo; MKRS/Ser* | *w-;gCERT$^{SL}$, mW+*<br>*If/Cyo; MKRS/Ser* | | Homozygous viable, red color eyes because of *Ser* |
| 22. | *X/X; gCERT$^{WT}$/Cyo; CERT$^{\Delta}$/Ser* | *w-; gCERT$^{WT}$, mW+*<br>*If/Cyo; MKRS/Ser*<br>*w-;dCERT$^{1}$(CERT$^{\Delta}$)* | *w-;dCERT$^{1}$*<br>(Rao et al., 2007) | Homozygous lethal, red color eyes because of *Ser* |
| 23. | *X/X; gCERT$^{SL}$/Cyo; CERT$^{\Delta}$/Ser* | *w-; gCERT$^{SL}$, mW+*<br>*If/Cyo; MKRS/Ser*<br>*w-;dCERT$^{1}$* | | Homozygous lethal, red color eyes because of *Ser* |
| 24. | *X/X; repo-Gal4;MKRS/Ser* | *repo-Gal4*<br>*If/Cyo; MKRS/Ser* | | Homozygous viable, red color eyes because of *Ser* |
| 25. | *X/X; repo-Gal4; CERT$^{\Delta}$/Ser* | *w-; gCERT$^{SL}$, mW+*<br>*If/Cyo; MKRS/Ser*<br>*w-;dCERT$^{1}$* | | Homozygous viable (yellow eyes), heterozygous- red color eyes because of *Ser* |
| 26. | *X/X; elav-Gal4/Cyo;MKRS/Ser* | *elav-Gal4*<br>*If/Cyo; MKRS/Ser* | | Homozygous lethal, red color eyes because of *Ser* |
| 27. | *C155-Gal4/FM7a;; MKRS/Tb* | *C155-Gal4*<br>*FM7a; MKRS/Tb* | | Homozygous viable |
| 28. | *C155-Gal4/FM7a;; CERT$^{\Delta}$* | *C155-Gal4*<br>*FM7a; MKRS/Tb*<br>*w-;dCERT$^{1}$* | | Homozygous viable |
| 29. | *X/X; UAS-CERT(4C)/Cyo;MKRS/Ser* | *UAS-CERT(4C)/Cyo*<br>*If/Cyo; MKRS/Ser* | *UAS-CERT(4C)/Cyo*<br>In house | Homozygous lethal |
| 30. | *X/X; UAS-CERT(4C)/Cyo; CERT$^{\Delta}$/Ser* | *UAS-CERT(4C)/Cyo*<br>*If/Cyo; MKRS/Ser*<br>*w-;dCERT$^{1}$* | | Homozygous lethal |
| 31. | *X/X; UAS-CERT(5A)/Cyo; CERT$^{\Delta}$/Ser* | *UAS-CERT(5A)/Cyo*<br>*If/Cyo; MKRS/Ser*<br>*w-;dCERT$^{1}$* | *UAS-CERT(5A)/Cyo*<br>In house | Homozygous lethal |
| 32. | *X/X; UAS-CERT4A (FF>AA)/Cyo;MKRS/Ser* | *UAS-CERT4A(FF>AA)*<br>*If/Cyo; MKRS/Ser* | *UAS-CERT4A(FF>AA)*<br>In house, may have Sb | Homozygous viable |
| 33. | *X/X; UAS-CERT4A (FF>AA)/Cyo; CERT$^{\Delta}$/Ser* | *UAS-CERT(4A)*<br>*If/Cyo; MKRS/Ser*<br>*w-;dCERT$^{1}$* | | Homozygous viable |

| | | | | |
|---|---|---|---|---|
| 34. | *X/X; UAS-GFP/Cyo; CERT$^{\Delta}$/Ser* | *If/Cyo; MKRS/Ser UAS-GFP w-;dCERT$^{1}$* | BDSC-BL_32186 *UAS-GFP* | |
| 35. | *X/X; VAP$^{RNAi}$; CERT$^{\Delta}$/Ser* | *BL77440- VAP$^{RNAi}$ If/Cyo; MKRS/Ser w-;dCERT$^{1}$* | BDSC-BL_77440 | |
| 36. | *X/X; myc-VAP$^{WT}$; CERT$^{\Delta}$/Ser* | *UAS-myc-VAP$^{WT}$ If/Cyo; MKRS/Ser w-;dCERT$^{1}$* | *UAS-myc-VAP$^{WT}$* (Ratnaparkhi et al., 2008) | |
| 37. | *y-v-VAP$^{P58S}$;mex-Gal4/Cyo* | *y-v-VAP$^{P58S}$- 279.1 FM7a; Pin/Cyo Mex-Gal4/Cyo* | *Mex-Gal4/Cyo* Dr. Irene Miguel | |
| 38. | *X/X;BL85769;Gal80$^{ts}$dCas9/Tb* | *BL85769-CG10907 gRNA TOE line Gal80$^{ts}$dCas9* taken from BL67067 | BDSC BL85769, BL67067 | PPIase project, homozygous lethal |
| 39. | *X/X;BL68125;Gal80$^{ts}$dCas9/Tb* | *BL68125- Cyp1* gRNA TOE line *Gal80$^{ts}$dCas9* taken from BL67067 | BDSC BL68125, BL67067 | PPIase project, homozygous lethal |

**I.3 References:**

Braems, E., Tziortzouda, P., & Van Den Bosch, L. (2021). Exploring the alternative: Fish, flies and worms as preclinical models for ALS. *Neuroscience Letters*, *759*, 136041. https://doi.org/https://doi.org/10.1016/j.neulet.2021.136041

Casci, I., & Pandey, U. B. (2015). A fruitful endeavor: Modeling ALS in the fruit fly. *Brain Research*, *1607*, 47-74. https://doi.org/https://doi.org/10.1016/j.brainres.2014.09.064

Chaplot, K., Pimpale, L., Ramalingam, B., Deivasigamani, S., Kamat, S. S., & Ratnaparkhi, G. S. (2019). SOD1 activity threshold and TOR signalling modulate VAP(P58S) aggregation via reactive oxygen species-induced proteasomal degradation in a Drosophila model of amyotrophic lateral sclerosis. *Dis Model Mech*, *12*(2). https://doi.org/10.1242/dmm.033803

Deivasigamani, S., Verma, H. K., Ueda, R., Ratnaparkhi, A., & Ratnaparkhi, G. S. (2014). A genetic screen identifies Tor as an interactor of VAPB in a Drosophila model of amyotrophic lateral sclerosis. *Biol Open*, *3*(11), 1127-1138. https://doi.org/10.1242/bio.201410066

Duffy, J. B. (2002). GAL4 system in Drosophila: a fly geneticist's Swiss army knife. *Genesis*, *34*(1-2), 1-15. https://doi.org/10.1002/gene.10150

Gehin, C., Lone, M. A., Lee, W., Capolupo, L., Ho, S., Adeyemi, A. M., Gerkes, E. H., Stegmann, A. P., Lopez-Martin, E., Bermejo-Sanchez, E., Martinez-Delgado, B., Zweier, C., Kraus, C., Popp, B., Strehlow, V., Grafe, D., Knerr, I., Jones, E. R., Zamuner, S., . . . Gennarino, V. A. (2023). CERT1 mutations perturb human development by disrupting sphingolipid homeostasis. *J Clin Invest*, *133*(10). https://doi.org/10.1172/JCI165019

Gratz, S. J., Rubinstein, C. D., Harrison, M. M., Wildonger, J., & O'Connor-Giles, K. M. (2015). CRISPR-Cas9 Genome Editing in Drosophila. *Current Protocols in Molecular Biology*, *111*(1), 31.32.31-31.32.20. https://doi.org/https://doi.org/10.1002/0471142727.mb3102s111

Hegde, K. N., & Srivastava, A. (2022). Drosophila melanogaster as a Tool for Amyotrophic Lateral Sclerosis Research. *J Dev Biol*, *10*(3). https://doi.org/10.3390/jdb10030036

Layalle, S., They, L., Ourghani, S., Raoul, C., & Soustelle, L. (2021). Amyotrophic Lateral Sclerosis Genes in Drosophila melanogaster. *Int J Mol Sci*, *22*(2). https://doi.org/10.3390/ijms22020904

Liguori, F., Amadio, S., & Volonté, C. (2021). Where and Why Modeling Amyotrophic Lateral Sclerosis. *International Journal of Molecular Sciences*, *22*(8), 3977.

Moustaqim-Barrette, A., Lin, Y. Q., Pradhan, S., Neely, G. G., Bellen, H. J., & Tsuda, H. (2014). The amyotrophic lateral sclerosis 8 protein, VAP, is required for ER protein quality control. *Hum Mol Genet*, *23*(8), 1975-1989. https://doi.org/10.1093/hmg/ddt594

Rao, R. P., Yuan, C., Allegood, J. C., Rawat, S. S., Edwards, M. B., Wang, X., Merrill, A. H., Jr., Acharya, U., & Acharya, J. K. (2007). Ceramide transfer protein function is essential for normal

oxidative stress response and lifespan. *Proc Natl Acad Sci U S A, 104*(27), 11364-11369. https://doi.org/10.1073/pnas.0705049104

Ratnaparkhi, A., Lawless, G. M., Schweizer, F. E., Golshani, P., & Jackson, G. R. (2008). A Drosophila model of ALS: human ALS-associated mutation in VAP33A suggests a dominant negative mechanism. *PLoS One*, *3*(6), e2334. https://doi.org/10.1371/journal.pone.0002334

Tendulkar, S., Hegde, S., Garg, L., Thulasidharan, A., Kaduskar, B., Ratnaparkhi, A., & Ratnaparkhi, G. S. (2022). Caspar, an adapter for VAPB and TER94, modulates the progression of ALS8 by regulating IMD/NFkappaB-mediated glial inflammation in a Drosophila model of human disease. *Hum Mol Genet*, *31*(17), 2857-2875. https://doi.org/10.1093/hmg/ddac076

Thulasidharan, A. (2023). *Age-dependent VAP$^{P58S}$ aggregation in a Drosophila model of Amyotrophic Lateral Sclerosis* IISER Pune]. http://dr.iiserpune.ac.in:8080/xmlui/handle/123456789/8576

Thulasidharan, A., Garg, L., Tendulkar, S., & Ratnaparkhi, G. S. (2024). Age-dependent dynamics of neuronal VAPB(ALS) inclusions in the adult brain. *Neurobiol Dis*, *196*, 106517. https://doi.org/10.1016/j.nbd.2024.106517

Tsuda, H., Han, S. M., Yang, Y., Tong, C., Lin, Y. Q., Mohan, K., Haueter, C., Zoghbi, A., Harati, Y., Kwan, J., Miller, M. A., & Bellen, H. J. (2008). The amyotrophic lateral sclerosis 8 protein VAPB is cleaved, secreted, and acts as a ligand for Eph receptors. *Cell*, *133*(6), 963-977. https://doi.org/10.1016/j.cell.2008.04.039

Venken, K. J. T., Schulze, K. L., Haelterman, N. A., Pan, H., He, Y., Evans-Holm, M., Carlson, J. W., Levis, R. W., Spradling, A. C., Hoskins, R. A., & Bellen, H. J. (2011). MiMIC: a highly versatile transposon insertion resource for engineering Drosophila melanogaster genes. *Nature Methods*, *8*(9), 737-743. https://doi.org/10.1038/nmeth.1662

# Appendix- II

# Role of Peptidyl Prolyl Isomerases in the aggregate dynamics of *ALS8* model

## II.1 Introduction

VAPB is one of ALS related genetic loci which is known to cause motor neurodegeneration in the human patients (Nishimura et al., 2004). A missense mutation from Proline to Serine at 56$^{th}$ position in the MSP domain of VAPB (*VAP*$^{P56S}$) has been found to cause misfolding of the protein and is the most prominent mutation associated with ALS8 disease (Teuling et al., 2007). Interestingly, in *Drosophila* models of *ALS8/VAP*$^{P58S}$, it is shown that this mutation leads to the formation of cellular aggregates and recruits wildtype VAPB also to these aggregates eliciting a dominant negative effect (Chaplot et al., 2019). These aggregates are present at ER membrane as well as in cytosol and also ubiquitinated (Moustaqim-Barrette et al., 2014; Teuling et al., 2007). The proline residue at the 56$^{th}$ position in human VAPB is in *cis*-conformation (Bashar et al., 2025). Interestingly, Proline is the only amino acid known to present in both *cis* and *trans*-confirmation apart from glycine. There are three prolines present in *cis*-confirmation whereas four are in *trans*-confirmation in the MSP domain (Chaplot, 2019). The mutation in the *ALS8* model is from Proline to Serine which may affect the proper folding of the protein as Proline *cis*-confirmations are often found at the turns of protein structure and helps in stabilizing α-helices and β-sheets (Bashar et al., 2025; Stump et al., 2023).

The interconversion between *cis* and *trans*-confirmation is a rate limiting step and often requires chaperone molecules known as peptidyl-prolyl *cis-trans* isomerases (PPIases) in biological systems (Chaplot, 2019). Three different classes of PPIase are known and classified on the basis of their response to immunosuppressive drugs - Cyclosporine A (CsA), FK506 Binding Proteins (FKBPs) (Ghartey-Kwansah et al., 2018; Pasetto et al., 2017). Parvulins are another class of PPIases which do not play role in immunity. Around 30 PPIases are known to be conserved between humans and *Drosophila* (Ghartey-Kwansah et al., 2018; Ondek et al., 1992). PPIases are generally present at various locations of the cell and play significant roles in the folding, regulation and degradation of the proteins (Ondek et al., 1992). PPIases have been associated with different ALS models such as SOD1, TARDBP, however there role in ALS8 is still not known (Chaplot, 2019; Y. Manabe 2002). From the previous study done in the lab, we identified three prolines to

be in *cis*-confirmation in humans ($12^{th}$, $21^{th}$, $56^{th}$ position in VAPB) which corresponds to ($14^{th}$, $23^{th}$, $58^{th}$ position) in *Drosophila.* In addition, Prolines in *trans*-confirmation ($49^{th}$, $77^{th}$, $96^{th}$, $111^{th}$ position) in humans corresponds to ($51^{st}$, $77^{th}$, $98^{th}$, $115^{th}$ position) in *Drosophila.* We found that point mutation from Proline present in *cis*-confirmation to Serine led to the aggregation of the protein whereas Prolines present in *trans*-confirmation mutated to Serine did not induce aggregate formation in S2R+ insect cell line. Moreover, mutation of *cis*-Proline present at $58^{th}$ position to any amino acid led to aggregation suggesting the *cis*-confirmation of the Prolines is crucial for the stability of the protein. To check the role of PPiase in VAP folding, overexpression model of $VAP^{P58S}$ was used which is expressed using neuronal Gal4 driver and induce aggregation in the neurons of $3^{rd}$ instar larval brain. Then, a screening of PPIase proteins was performed by knocking each PPIase and check its effect on the $VAP^{P58S}$ aggregation (Chaplot, 2019).

In this study, we performed a FRAP (Fluorescence Recovery After Photobleaching) experiment to understand the aggregate dynamics of VAP protein. Then, we continued with the previous PPIase screening done in the lab by knocking down various PPIase using BDSC RNAi lines or VDRC RNAi lines which were not previously checked and came up with a list of potential targets which we are currently exploring in the lab.

## II.2 Results and Discussion

**II.2.1 Differential aggregate dynamics of *cis-trans* Proline present in VAP protein:** We performed a screening for different prolines present in VAP protein by transfecting S2R+ cell line with the plasmid containing *VAP-GFP* with individual proline to serine mutation (P14S, P23S, P51S, P58S, P77S, P98S and P115S) and imaged the live cells containing GFP fluorescent VAP aggregates after 24 hours of induction. We used FRAP technique by bleaching the protein aggregate using 100% intensity laser for 3 iterations and then let it recover for 150 continuous frames (Fig. II.1). Interestingly, we found that fluorescent signal with mutated prolines of *cis*-confirmation (P14S, P23S and P58S) could not recover properly whereas GFP signal for aggregates containing mutated prolines of *trans*-confirmation (P51S, P77S and P115S) started recovering in 4 seconds only. Surprisingly, $VAP^{WT}$ expression leads to recovery of the GFP signal in between *cis-trans* mutations. This experiment suggests that *cis*-proline are quite important for VAP folding and can restrict movement of VAP protein due to immobile aggregation whereas *trans*-proline mutations are mobile in nature and leads to less aggregation of the protein.

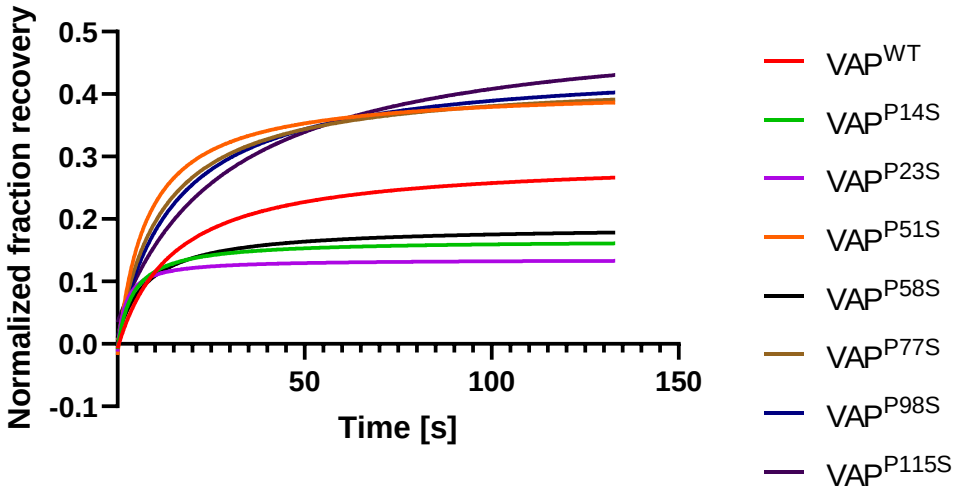



**Figure II.1: FRAP experiment for understanding protein movement in VAP proline mutations.**

*VAP-GFP* plasmids with Pro to Ser mutations were transfected in S2R+ cell line and imaged after 24 hrs of induction. FRAP assay was performed where Proline in *cis*-confirmation mutated to Serine (P14S, P23S, P58S) shows less recovery of fluorescence compared to Proline in *trans*-confirmation (P51S, P77S, P98S, P115S).

**II.2.2 PPIase screening for identifying potential modifiers involved in VAP$^{P58S}$ folding:** To check the effect of PPIase role in aggregate dynamics of VAP$^{P58S}$, PPIase screening was done in the lab where VAP$^{P58S}$ was overexpressed with neuronal Gal4 driver and change in aggregate density was observed in the 3$^{rd}$ instar larval brain. However, only 13 genes were tested out of 30 PPIases, I continued that screening by knocking down remaining PPIases using different RNAi lines and come up with a list of modifiers. Overexpression of VAP$^{P58S}$ in the neurons leads to the formation of big aggregates compared to genomic model of *ALS8* and it also sequesters wild-type VAP protein. When we knocked down these genes (*CG15767*, *CG4735*, *CG3492*, *CG14715*, *CG5808*, *CG11777*, *CG32236*, *CG2852*, *CG10907*, *CG4886*, *CG17051*, *CG1866*, *CG17266* and *CG5071*), interesting hits came up in the screen. Knockdown of *CG4735*, *CG5071* led to significant reduction in the aggregate density as visible in (Fig. II.2).

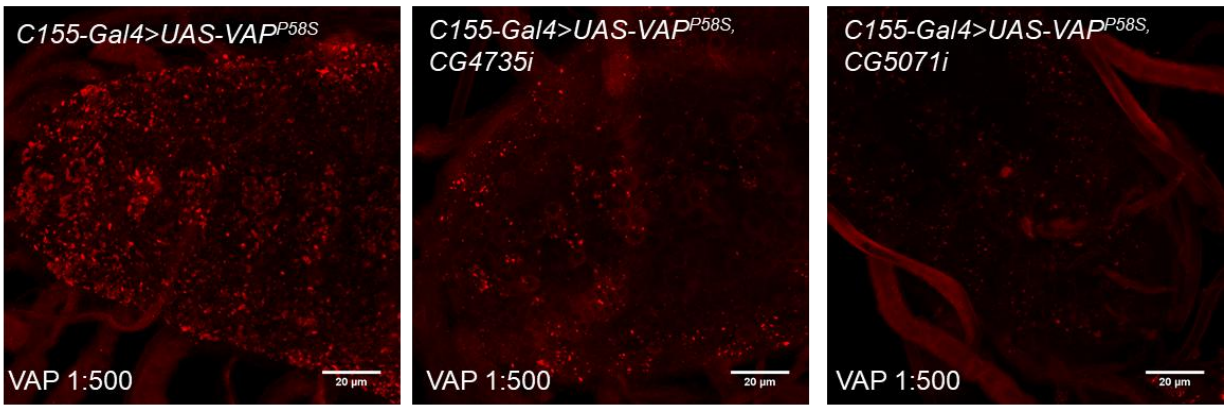



**Figure II.2: Modulating PPIase affects VAP$^{P58S}$ aggregates in 3$^{rd}$ instar larval brain.**

Representative MIPs of overexpressed VAP$^{P58S}$ in the neurons of 3$^{rd}$ instar larval brain which leads to aggregate formation in the ventral nerve cord. Knocking down *shutdown (CG4735)* and *CG5071* leads to reduction of aggregate density in the larval brain. N=5-6 brains for each genotype.

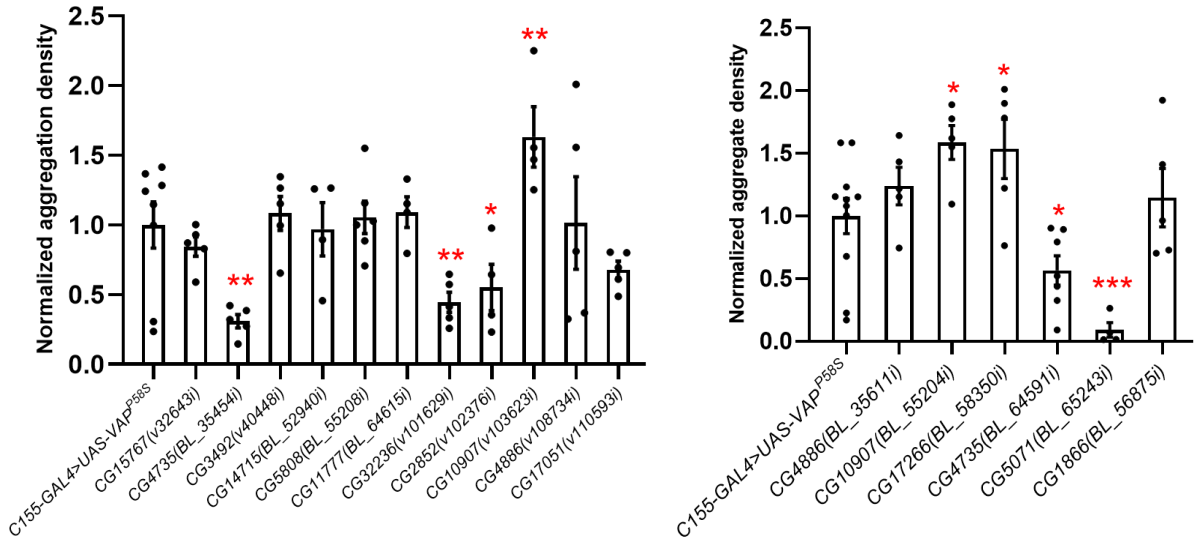



**Figure II.3: Quantitation for aggregate density on modulation of PPIases in *VAP$^{P58S}$*.**

Quantitative analysis for aggregate density was performed using Huygens software. Knockdown of PPIases show change in aggregate density of overexpression model of *ALS8* marked with statistical significance p<0.001(***), <0.01(**), <0.05(*). Normalized aggregate density is plotted on Y axis with gene name along with RNAi number mentioned on X axis. One way ANOVA was used followed by Bonferroni test for comparison to control line. n=5 ROIs, N=4-8 brains per genotype.

Other hits include *CG32236, CG2852* which showed reduction in the aggregates (Fig. II.3). Interestingly, *CG10907* knockdown led to increase in aggregate density verified using two

different lines (Fig. II.3). Similarly, *CG17266* knockdown also showed more aggregates compared to control (Fig. II.3). Based on the current screening and previous screening, We have made a list of all the PPIases tested and the change observed in aggregate density (Table II.1). Some of PPIases could not be tested because of unavailability of reagents. Currently, we picked up two potential targets based on the resource availability i.e. *CG10907, Cyclophillin-1(Cyp-1)*. Cyp-1 is known to play role in other neurodegenerative disorders as well (Pasetto et al., 2017). CG10907 plays role in mRNA splicing and is not well characterized. We are modulating these genes by overexpressing and knocking down in the same $VAP^{P58S}$ background and looking at the change in aggregates.

**Table II.1: List of PPIases along with Gene ID and KD/OE line used for the study.**

| | PPIase | Name | Symbol | RNAi line | Aggregate change | Insert line | Aggregate change | OE lines | Aggregate change |
|---|---|---|---|---|---|---|---|---|---|
| 1 | Cyclophillin | | CG5808 | 55208 | 0 | | | UAS line | 0 |
| 2 | | | CG5071 | 65243 | ↓↓↓ | | | | |
| 3 | | CypL | CG13892 | v104316 | ↓↓ | | | | |
| 4 | | Cyp1 | CG7768 | v35266 | 0 | | | UAS line | ↑↑ |
| 5 | | Cyp1 | CG9916 | 33950 | ↓↓↓↓ | | | | |
| 6 | | | CG7747 | 56975 | 0 | | | | |
| 7 | | | CG3492 | v40448 | 0 | | | | |
| 8 | | | CG32236 | v101629 | ↓↓ | | | | |
| 9 | | | CG17266 | 58350 | ↑ | | | | |
| 10 | | | CG11777 | 64615 | 0 | | | | |
| 11 | | | CG3511 | 50597 | not done yet | | | UAS line | 0 |
| 12 | | nina[A] | CG3966 | 3533 | not done yet | | | | |
| 13 | | | CG15767 | v32643 | 0 | | | | |
| 14 | | moca-cyp | CG1866 | 56875 | 0 | 16389 | 0 | | |
| 15 | | Cyp40 | CG8336 | v23729 | – | 24728 | ↓↓↓ | | |
| 16 | | | CG2852 | v102376 | ↓ | | | | |
| | | | | 55196 | not done yet | | | | |
| 17 | | Cyp33 | CG4886 | v108374 | 0 | | | | |
| | | Cyp33 | | 35611 | 0 | | | | |
| 18 | | | CG10907 | v103623 | ↑↑ | | | | |
| | | | | 55204 | ↑↑ | | | | |
| 19 | | | CG30350 | x | – | | | | |
| 20 | FKBPs | FKBP2 | CG14715 | 52940 | 0 | 32608 | ↓↓ | | |
| 21 | | FKBP6 | CG4735 | 35454 | ↓↓ | | | | |
| | | | | 64591 | ↓ | | | | |
| 22 | | FKBP8 | CG5482 | v4991 | 0 | | | UAS line | 0 |
| | | | | 64622 | not done yet | | | | |
| 23 | | FKBP12 | CG11001 | 58245 | 0 | | | | |
| 24 | | FKBP14 | CG9847 | 67224 | ↓↓ | | | | |
| 25 | | FKBP39 | CG6226 | 32348 | ↓↓↓↓ | | | | |
| 26 | | FKBP59 | CG4535 | 19999 | 0 | | | | |
| | | | | 28349 | ↓ | | | | |
| 27 | | | CG1847 | 44490 | – | | | | |
| 28 | Parvulins | dod | CG17051 | v110593 | 0 | | | | |
| 29 | | | CG11858 | v106769 | – | | | | |
| 30 | | | CG32845 | x | – | | | | |

Red arrow represents decrease in density, blue arrow represents increase in aggregate density, 0 means no change, - represents line not available. Number of arrows represents statistical significance with each arrow as one star. Previous screening data is also plotted as shown in (Chaplot, 2019).

## II.3 Materials and methods

**II.3.1 Fluorescent Recovery After Photobleaching:** Firstly, 500µl of S2R+ cells were seeded into 24 well plate and kept it for 24 hours incubation at 23°C. DNA mix was prepared with Serum free media containing 1µg of plasmid DNA and Mirus TransIT (2020) and 20 minute incubation was given. After the settling of cells, DNA mix was added to the cells after the removal of media and kept it for 2 hours so that cells can take up the mix because of starvation. After two hours incubation, Serum containing media was added along with Copper Sulphate solution (500µM) for each well to induce the metallothionein promotor of pRM plasmid vector. Cells were incubated for 24 hours so that protein can be expressed and leads to the aggregate formation. 200µl cell volume was taken after the suspension in the Lab-Tech chamber and live cells were imaged on 20X objective lens of Zeiss Multiphoton microscope. Images were captured at 16 bit resolution with 1X zoom. 8-10 cells of each plasmid sample were selected from each well and 50% laser was used to bleach the single aggregate in each cell for 3 iterations. Then, single cell was imaged along with cell containing aggregate with no bleaching and a background region for noise reduction for 150 continuous frames. Following formula was used to calculate the fraction recovery of the intensity which was averaged for each sample and plotted in the graphical form.

Fluorescence Intensity Recovery = [({A-B}-C)/(D-B)] x [E/F]

A= Aggregate Intensity, B= Background Intensity, C= Aggregate Intensity at bleaching point, D= Cell Intensity, E= Average [D-B] intensity of 3 iterations before bleaching, F= Average aggregate [(A-B)-C] intensity of 3 iterations before bleaching

**II.3.2 Larval brain immunostaining and aggregate analysis:** Late 3$^{rd}$ instar larval brains were dissected in ice cold 1X PBS and processed for immunostaining assay. 4% PFA containing 0.3% Triton-X-100 was used for fixation followed by washes with 1X PBS. 2% BSA containing 0.3% Triton-X-100 was used as blocking reagent and three washes of 20 minutes each were given before antibody staining. Brains were stained with 1:500 diluted anti-VAP antibody and 1:1000 anti-rabbit secondary (Invitrogen) was used. Z-stacks of four-eight brains for each sample were imaged under 63X oil objective of Ziess LSM 710 or 780 Confocal Microscope. Aggregate density was quantified using Huygens Professional Software. A constant threshold value was set for controls as well as for test samples. An object filter was used to remove objects of size greater than 1000

voxels and garbage size smaller than 10 voxels was excluded. Five 3D region of interests of fixed size were drawn along the tip of the ventral nerve cord and number of objects were counted and averaged for each animal. The volume (in cubic micron) of ROI depicting the thickness of the brain tissue was measured as the range of the z-stack of the image. The aggregation density obtained for each brain is normalized to the mean of the control group. Graphpad Prism is used for plotting the data and performing statistical analysis.

**II.4 Contributions:** Kriti Chaplot has contributed significantly in this project which involves plasmid cloning, introducing mutations in *VAP-GFP*, balancing *C155-Gal4;UAS-VAP$^{P58S}$/Cyo-GFP* line and performing the PPIase screen as mentioned in the result section.

**II.5 References**

Bashar, M. A., Dash, N., Mitra, S., & Dash, R. (2025). Disclosing Pathogenic Variant Effects on the Structural Dynamics of the VAPB MSP Domain Causing Familial ALS. *Int J Mol Sci*, *26*(13). https://doi.org/10.3390/ijms26136489

Chaplot, K. (2019). *Regulation of VAP(P58S) neuroaggregation in a Drosophila model of Amyotrophic Lateral Sclerosis* IISER Pune]. http://dr.iiserpune.ac.in:8080/xmlui/handle/123456789/2922

Chaplot, K., Pimpale, L., Ramalingam, B., Deivasigamani, S., Kamat, S. S., & Ratnaparkhi, G. S. (2019). SOD1 activity threshold and TOR signalling modulate VAP(P58S) aggregation via reactive oxygen species-induced proteasomal degradation in a Drosophila model of amyotrophic lateral sclerosis. *Dis Model Mech*, *12*(2). https://doi.org/10.1242/dmm.033803

Ghartey-Kwansah, G., Li, Z., Feng, R., Wang, L., Zhou, X., Chen, F. Z., Xu, M. M., Jones, O., Mu, Y., Chen, S., Bryant, J., Isaacs, W. B., Ma, J., & Xu, X. (2018). Comparative analysis of FKBP family protein: evaluation, structure, and function in mammals and Drosophila melanogaster. *BMC Dev Biol*, *18*(1), 7. https://doi.org/10.1186/s12861-018-0167-3

Moustaqim-Barrette, A., Lin, Y. Q., Pradhan, S., Neely, G. G., Bellen, H. J., & Tsuda, H. (2014). The amyotrophic lateral sclerosis 8 protein, VAP, is required for ER protein quality control. *Hum Mol Genet*, *23*(8), 1975-1989. https://doi.org/10.1093/hmg/ddt594

Nishimura, A. L., Mitne-Neto, M., Silva, H. C. A., Richieri-Costa, A., Middleton, S., Cascio, D., Kok, F., Oliveira, J. R. M., Gillingwater, T., Webb, J., Skehel, P., & Zatz, M. (2004). A Mutation in the Vesicle-Trafficking Protein VAPB Causes Late-Onset Spinal Muscular Atrophy and Amyotrophic Lateral Sclerosis. *The American Journal of Human Genetics*, *75*(5), 822-831. https://doi.org/10.1086/425287

Ondek, B., Hardy, R. W., Baker, E. K., Stamnes, M. A., Shieh, B. H., & Zuker, C. S. (1992). Genetic dissection of cyclophilin function. Saturation mutagenesis of the Drosophila cyclophilin

homolog ninaA. *Journal of Biological Chemistry*, *267*(23), 16460-16466. https://doi.org/10.1016/s0021-9258(18)42025-x

Pasetto, L., Pozzi, S., Castelnovo, M., Basso, M., Estevez, A. G., Fumagalli, S., De Simoni, M. G., Castellaneta, V., Bigini, P., Restelli, E., Chiesa, R., Trojsi, F., Monsurro, M. R., Callea, L., Malesevic, M., Fischer, G., Freschi, M., Tortarolo, M., Bendotti, C., & Bonetto, V. (2017). Targeting Extracellular Cyclophilin A Reduces Neuroinflammation and Extends Survival in a Mouse Model of Amyotrophic Lateral Sclerosis. *J Neurosci*, *37*(6), 1413-1427. https://doi.org/10.1523/JNEUROSCI.2462-16.2016

Stump, A. L., Rioux, D. J., Albright, R., Melki, G. L., & Prosser, D. C. (2023). Yeast Models of Amyotrophic Lateral Sclerosis Type 8 Mimic Phenotypes Seen in Mammalian Cells Expressing Mutant VAPB(P56S). *Biomolecules*, *13*(7). https://doi.org/10.3390/biom13071147

Teuling, E., Ahmed, S., Haasdijk, E., Demmers, J., Steinmetz, M. O., Akhmanova, A., Jaarsma, D., & Hoogenraad, C. C. (2007). Motor neuron disease-associated mutant vesicle-associated membrane protein-associated protein (VAP) B recruits wild-type VAPs into endoplasmic reticulum-derived tubular aggregates. *J Neurosci*, *27*(36), 9801-9815. https://doi.org/10.1523/JNEUROSCI.2661-07.2007

Y. Manabe , H. W., T. Murakami, M. Shiote, T. Hayashi, N. Omori, I. Nagano, M. Shoji, K. Abe. (2002). Early decrease of the immunophilin FKBP 52 in the spinal cord of a transgenic model for amyotrophic lateral sclerosis. *Brain Research*, *935*, 124-128.

# Appendix – III

# Role of autophagy in the pathogenesis of *ALS8* model of *Drosophila*

## III.1 Introduction

Autophagy has been instrumental in the nervous system as it has well established roles in the neurons where proteins associated with autophagy plays crucial role in the degradation of proteins through autophagosomes (Gomez-Suaga et al., 2017; Hebbar et al., 2015; Nguyen & Olzmann, 2017; Zhao et al., 2018). VCP is a type II AAA ATPase complex present in the cytosol which is involved in the segregation of misfolded proteins and send it for degradation (Baron et al., 2014; Casci & Pandey, 2015). It plays essential role in the recognition and removal of ubiquitinated proteins from the membranes, aggregates and organelles. VCP is expressed ubiquitously and can modulate several pathways such as ER associated degradation, autophagy or proteosomal degradation (Zhao et al., 2018). VCP is also known to cause ALS and identified as *ALS14* locus (Casci & Pandey, 2015). It belongs to the familial cases of ALS where point mutations from Arg to His at 152$^{th}$ positon (R152H) and Ala to Glu at 229$^{th}$ position (A229E) are identified in ALS patients (Ajroud-Driss & Siddique, 2015). *Drosophila has* conserved *VCP* gene also known as *TER94* (Transitional Endoplasmic Reticulum 94). From our previous papers and other lab studies, it has been shown that *TER94* is a genetic interactor of *VAP* and regulate its function via intermediate protein FAF1/Caspar (Tendulkar et al., 2022). We have shown that glial modulation of *TER94* worsens the lifespan of *ALS8* flies whereas neuronal modulation affects aggregate dynamics of VAP$^{P58S}$ protein (Tendulkar et al., 2022; Thulasidharan et al., 2024). Also, we showed that *Atg1* which is a homolog of *ULK1* regulates aggregate density of VAP$^{P58S}$ protein and is crucial for its clearance in *ALS8* model of *Drosophila* (Thulasidharan et al., 2024).

Here, I have modulated *TER94* and *Atg1* in the neurons of *ALS8* flies and performed motor function assays in an age dependent manner. During the behavioral experiments, I have also identified a novel role of TER94 in the neurons where its removal shows a wing phenotype in the *ALS8* flies.

### III.2 Results and Discussion

**III.2.1 *ALS14/TER94* modulation in neurons enhances the motor phenotype of *ALS8:*** To check the genetic interaction between *TER94* and *VAP*, we modulated *TER94* in the neurons of genomic model of *ALS8* and performed motor assays in an age dependent manner. Interestingly, *TER94* KD (BL_32869) significantly enhanced the motor defects of *ALS8* male flies whereas overexpression of *TER94* (BL_95268) did not show any change in the flies (Fig. III.1). When I overexpressed human *ALS14* locus $TER94^{R152H}$ (BL_95266) in the neurons, it also enhanced the climbing defects in *ALS8* males (Fig. III.1). This data suggests *TER94* plays a crucial role in the neurons and dictates motor activity of the flies. Moreover, it seems VAP is important for TER94 to function as more TER94 did not show any change whereas dominant allele of *TER94* worsens the phenotype.

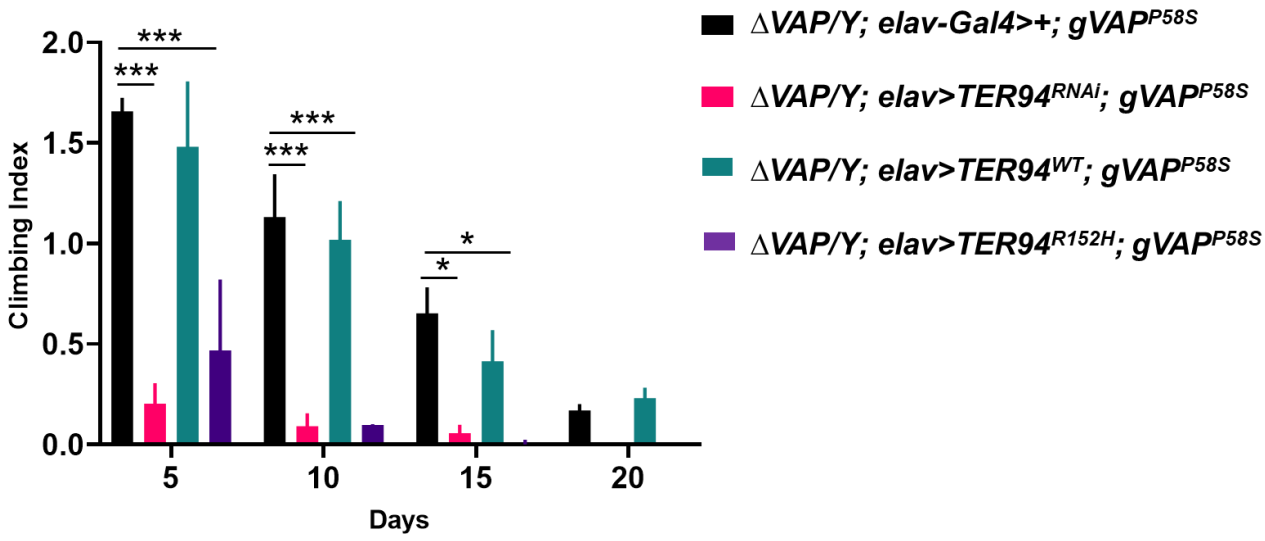



**Figure III.1: Impact of modulating *TER94* in the neurons on the motor function of *ALS8* flies.**

Climbing Index is plotted in the graphical form where *TER94* KD using BL_32869 RNAi line enhanced motor defects at day 5 itself whereas *TER94* overexpression (BL_95268) showed no change. Similarly like *TER94* KD, $TER94^{R152H}$ OE (BL_95266) enhanced motor phenotype at day 5 itself. Mean±SEM values are plotted with statistical significance where climbing index is on Y axis, number of days are on X-axis. Two way ANOVA was performed for statistical significance followed by Tukey's test for multiple comparison using APA style of p value. n=25-30 males, N=3 biological replicates per genotype. Experiment was performed at 25°C.

**III.2.2 *TER94* KD in neurons shows a novel upward halt wing phenotype in *Drosophila:*** While performing motor assays for *TER94* modulated flies in *ALS8* background, I observed an unusual phenotype in the wings when *TER94* was knocked down in the neurons of *ALS8* males. They had "upward halt wing" phenotype immediately after the eclosion of the flies (III.2B). However, *TER94* OE did not show the same phenotype as visible in (Fig. III.2C). We knocked down *TER94* in the neurons of wild-type flies and saw similar phenotype 3-5 days after the eclosion of the flies although it needs to be checked again. Interestingly, knocking down *TER94* in the motor neurons do not replicate the same phenotype. These crosses need to be performed again to verify the results and understand the role of TER94 in the neurons. Also, it tells us that *TER94* phenotype in the wings is independent of *ALS8* mutant and may be connected to neuronal degeneration.

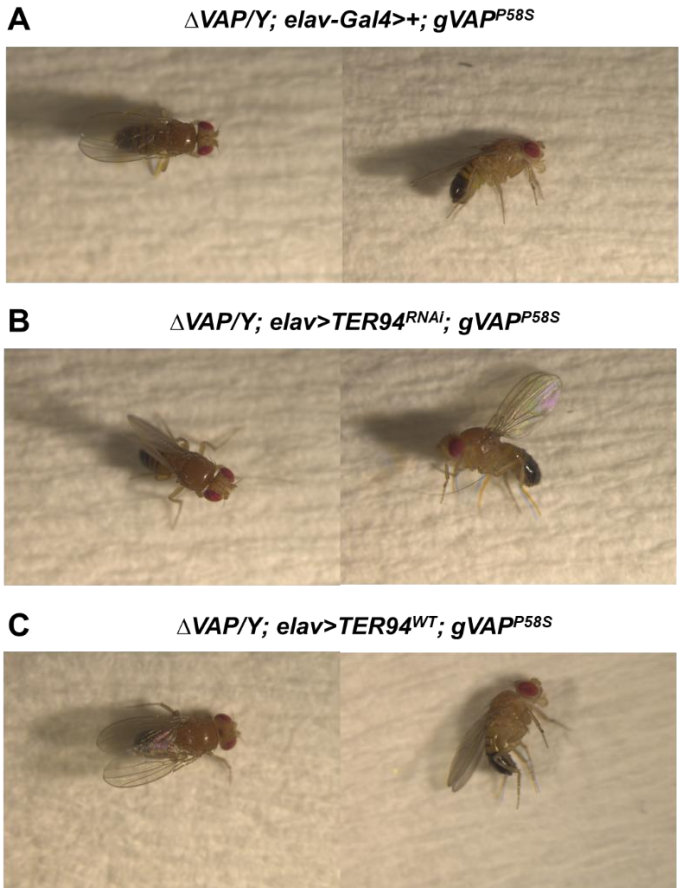



**Figure III.2: Knockdown of *TER94* in neurons of *ALS8* shows upward halt wing phenotype.**

(A) Genomic model of *ALS8* male fly have normal wings on day 5 from both dorsal (left) and lateral (right) sides.

(B) Knocking down *TER94* shows upward halt wing phenotype from both angles of dorsal (left) and lateral (right) sides.
(C) Overexpression of *TER94* shows no change in the wings of *ALS8* flies.
n=3 male flies per genotype. Experiment was performed at 25℃. Video of the phenotype is also available in lab drive.

**III.2.3 *Atg1* KD in neurons impairs motor function of rescued *ALS8* flies*:*** Previous studies from the lab established Atg1 role in the aggregate dynamics of *ALS8* flies. As already discussed single copy of VAP is enough to rescue motor phenotype of *ALS8* flies, so we knocked down *Atg1* (BL_44034) in the neurons of female flies of *ALS8.* Interestingly, removal of Atg1 led to age dependent motor defects in *ALS8* flies with severe motor defects at day 5 itself (Fig. III.3). This suggests even in the presence of VAP, *ALS8* phenotype cannot be rescued and makes Atg1 crucial for proper neuronal functioning. Surprisingly, *TER94* knockdown in neurons leads to reduction in aggregate density whereas *ALS14* OE shows more *VAP* mutant aggregates. Similarly, Atg1 removal also leads to more aggregates suggesting no correlation between aggregates and the motor function of the flies. However, further studies need to be done to comment on the relation between aggregate dynamics and motor function of *ALS8* flies.

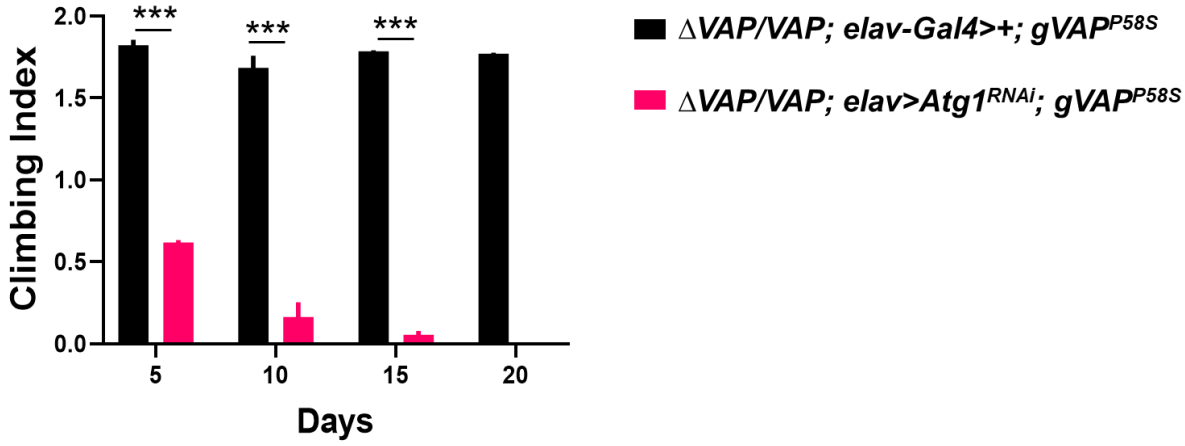



**Figure III.3: Removal of *Atg1* in the neurons of rescued *ALS8* females leads to motor impairment.**

Climbing Index is plotted in the graphical form where *Atg1* KD using BL_44034 RNAi line showed motor defects in age dependent manner even though VAP copy was present in *ALS8* background. Mean±SEM data is plotted with statistical significance where climbing index is on Y axis, number of days are on X-axis. Two way ANOVA was performed for statistical significance followed by Tukey's test for multiple comparison using APA style of p value. n=25-30 females, N=2 biological replicates per genotype. Experiment was performed at 25℃.

## III.3 References

Ajroud-Driss, S., & Siddique, T. (2015). Sporadic and hereditary amyotrophic lateral sclerosis (ALS). *Biochimica et Biophysica Acta (BBA) - Molecular Basis of Disease*, *1852*(4), 679-684. https://doi.org/https://doi.org/10.1016/j.bbadis.2014.08.010

Baron, Y., Pedrioli, P. G., Tyagi, K., Johnson, C., Wood, N. T., Fountaine, D., Wightman, M., & Alexandru, G. (2014). VAPB/ALS8 interacts with FFAT-like proteins including the p97 cofactor FAF1 and the ASNA1 ATPase. *BMC Biol*, *12*, 39. https://doi.org/10.1186/1741-7007-12-39

Casci, I., & Pandey, U. B. (2015). A fruitful endeavor: Modeling ALS in the fruit fly. *Brain Research*, *1607*, 47-74. https://doi.org/https://doi.org/10.1016/j.brainres.2014.09.064

Gomez-Suaga, P., Paillusson, S., Stoica, R., Noble, W., Hanger, D. P., & Miller, C. C. J. (2017). The ER-Mitochondria Tethering Complex VAPB-PTPIP51 Regulates Autophagy. *Curr Biol*, *27*(3), 371-385. https://doi.org/10.1016/j.cub.2016.12.038

Hebbar, S., Sahoo, I., Matysik, A., Argudo Garcia, I., Osborne, K. A., Papan, C., Torta, F., Narayanaswamy, P., Fun, X. H., Wenk, M. R., Shevchenko, A., Schwudke, D., & Kraut, R. (2015). Ceramides And Stress Signalling Intersect With Autophagic Defects In Neurodegenerative Drosophila blue cheese (bchs) Mutants. *Sci Rep*, *5*, 15926. https://doi.org/10.1038/srep15926

Nguyen, T. B., & Olzmann, J. A. (2017). Lipid droplets and lipotoxicity during autophagy. *Autophagy*, *13*(11), 2002-2003. https://doi.org/10.1080/15548627.2017.1359451

Tendulkar, S., Hegde, S., Garg, L., Thulasidharan, A., Kaduskar, B., Ratnaparkhi, A., & Ratnaparkhi, G. S. (2022). Caspar, an adapter for VAPB and TER94, modulates the progression of ALS8 by regulating IMD/NFkappaB-mediated glial inflammation in a Drosophila model of human disease. *Hum Mol Genet*, *31*(17), 2857-2875. https://doi.org/10.1093/hmg/ddac076

Thulasidharan, A., Garg, L., Tendulkar, S., & Ratnaparkhi, G. S. (2024). Age-dependent dynamics of neuronal VAPB(ALS) inclusions in the adult brain. *Neurobiol Dis*, *196*, 106517. https://doi.org/10.1016/j.nbd.2024.106517

Zhao, Y. G., Liu, N., Miao, G., Chen, Y., Zhao, H., & Zhang, H. (2018). The ER Contact Proteins VAPA/B Interact with Multiple Autophagy Proteins to Modulate Autophagosome Biogenesis. *Curr Biol*, *28*(8), 1234-1245 e1234. https://doi.org/10.1016/j.cub.2018.03.002